NEW SERVICE TO READERS

VOLUME 39 SECOND SERIES NUMBER 1

THE PHYSICAL REVIEW

A JOURNAL OF EXPERIMENTAL AND THEORETICAL PHYSICS

CONDUCTED BY

THE AMERICAN PHYSICAL SOCIETY

BOARD OF EDITORS

Managing Editor, JOHN T. TATE, University of Minnesota, Minneapolis
Assistant Editor, J. W. BUCHTA, University of Minnesota, Minneapolis
K. F. HERZFELD, A. W. HULL, F. W. LOOMIS, A. J. DEMPSTER, DAVID M. DENNISON,
J. C. SLATER, G. E. M. JAUNCEY, E. O. LAWRENCE, J. H. VAN VLECK

JANUARY 1, 1932

X-ray Wave-Lengths by the Dispersion in Quartz – – – – – – J. A. Bearden 1
Spectra of Two-and-Three-Valence-Electron Atoms, Si II, P III, S IV, P IV and S V – – – – – –

THE AMERICAN PHYSICAL SOCIETY

OFFICERS OF THE SOCIETY

President:	W. F. G. Swann	Bartol Research Foundation, Philadelphia, Pa.
Vice-President:	Paul D. Foote	The Gulf Companies, Pittsburgh, Pa.
Secretary:	W. L. Severinghaus	Columbia University, New York City
Treasurer:	G. B. Pegram	Columbia University, New York City
Editor:	John T. Tate	University of Minnesota, Minneapolis, Minn.
Local Secretary for the Pacific Coast:	L. B. Loeb	University of California, Berkeley, Calif.

THE PHYSICAL REVIEW

Published by the American Physical Society. Executive office: University of Minnesota, Minneapolis, Minn. Two volumes annually, twelve issues per volume.

First series. From July 1, 1893, to January 1, 1913, the Review was conducted by Edward L. Nichols, Ernest Merritt and Frederick Bedell, with the financial support of Cornell University. The first four volumes were issued annually; subsequent volumes, semi-annually; thirty-five volumes in all.

Second series. On January 1, 1913, the Review was transferred to the American Physical Society as announced on the first page of the new series which was then begun. Since then it has been conducted by a Board of Editors elected by the Society. Semi-annual volumes begin in January and July. Since July 1, 1929, the Review has been issued twice a month.

Contributors are referred to page 2 of the advertisements for further information.

Annual subscription, throughout the Postal Union, $12.00 in advance.

General index, 1893-1920, $4.00 in advance.

Back Volumes, $9.00 per volume; Back Numbers, $1.50 per copy for issues prior to July 1, 1929 (Vols. 1-33), $.75 per copy for issues subsequent thereto. Postage is free if remittance accompanies order; otherwise postage is extra. No bound volumes can be supplied. The Review offers to purchase a limited number of First Series, Vol. 1, No. 1 (at $2.00 each); Second Series, Vol. 7, No. 1, January 1916; Vol. 7, No. 2, February 1916; Vol. 7, No. 4, April 1916; and Vol. 7, No. 5, May 1916 (at $2.00 each).

Advertisements. Rates will be supplied by the Editor on request. Copy for each number must be received at Minneapolis two weeks prior to the dates of issue; old copy is used until new copy is received. Send electrotypes direct to the printers, George Banta Publishing Co., Menasha, Wis.

Discount of ten percent is allowed to members of the American Physical Society on purchase of back numbers.

Changes of Address and Complaints of failure to receive the Review, in the case of members of the Physical Society, should be addressed to the Treasurer; in the case of other subscribers, to the Editor. New copies can be sent free in response to complaints of non-delivery only if notice of non-delivery is received within three months of date of issue.

Editorial Correspondence should be addressed to the Physical Review, University of Minnesota, Minneapolis, Minn.

Entered at the post office at Menasha, Wis., as second class matter.
Acceptance for mailing at special rate of postage provided for in section 1103, Act of October 3, 1917, authorized September 6, 1926.

Physics
Library
9-1-37
531

PHYSICAL REVIEW

PREPARATION OF PRELIMINARY ABSTRACTS

An article will not be accepted for publication in THE PHYSICAL REVIEW unless the manuscript is accompanied by an adequate abstract for publication at the beginning of the article. This abstract is intended to aid the reader by furnishing an index and a brief summary of the contents of the article. Besides serving these purposes it should also be suitable for reproduction in abstract journals so as to make it unnecessary for the editors of these journals to have another abstract prepared.

As *an index* it should be complete; all the subjects, major and minor, concerning which new information is presented, should each be given, with sufficient precision so that any reader can tell from the abstract whether the article contains anything of interest to him. The subject indexes of abstract journals are fundamental in reference work. These indexes are prepared exclusively from the abstracts and whatever is omitted from the abstracts cannot be included in the index and may thus be lost. The writer of an abstract should therefore feel himself under an important obligation to his scientific colleagues to make sure that the abstract is accurate and complete, at least as an index.

As *a summary* the abstract should give briefly the conclusions of the article, important advances in experimental technique and theory, and all numerical results of general interest that may be conveniently given including all that might belong in a handbook and table of contents. It should give all the information that readers who are not specialists in the particular field involved might desire to know about the article thus saving them the time and trouble in referring to the article itself. Experience has shown that in general the length of the abstract should be from four to eight percent of the length of the article.

THE PHYSICAL REVIEW, 1923-1925, contains many examples of adequate abstracts. Most of these contain paragraph titles and subtitles which indicate the subjects concerning which new information is given and it is required that authors include such subtitles when all the information contained in the article does not refer to the subject indicated by the title of the article. Such subtitles may be frequently avoided by rewording the title so as to make it more precise.

Are you interested in another improvement?

We have sold a great deal of the 5-inch base log paper. At last a customer comes forward with a request that we print it on our 13 lb. stock which does not have a watermark. It costs more because the paper is better. Do you blue print your curves?

CORNELL CO-OP. SOCIETY

BARNES HALL **ITHACA, N. Y.**

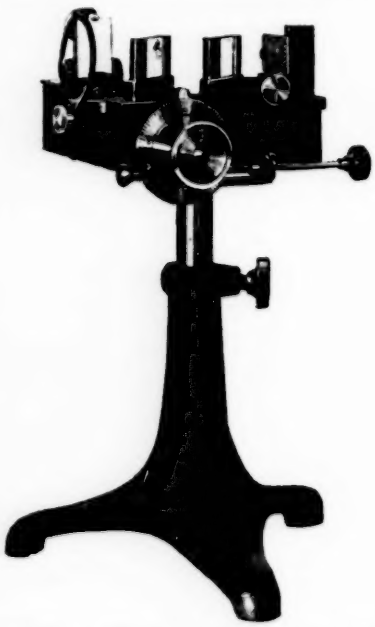

I-1010 INTERFEROMETER

THIS small Interferometer is of the Michelson type, for use in research work or for students. It contains many new improvements adding to its accuracy and convenience in operation. Prompt delivery can be made from stock.

Write for catalog I, listing our complete line of Interferometers and Accessories.

***The* GAERTNER SCIENTIFIC CORP.**

1201 Wrightwood Ave. **Chicago, U.S.A.**

Second Series *January 1, 1932* *Vol. 39, No. 1*

THE

PHYSICAL REVIEW

X-RAY WAVE-LENGTHS BY THE DISPERSION IN QUARTZ

By J. A. Bearden

The Department of Physics, Johns Hopkins University

(Received November 24, 1931)

Abstract

It has been shown that the quantum theory of dispersion accounts satisfactorily for the measured refraction of x-rays. Since the x-ray wave-lengths as determined by crystals and by ruled gratings differ by 0.25 percent, the dispersion may be used to indicate which of these values is correct. Thus the quantum theory of dispersion may be written

$$\lambda=\delta^{1/2}\left[\frac{\rho}{W}\cdot\frac{e}{m}\cdot\frac{F}{2\pi}\sum_{1}^{s}N_s\left\{1+\frac{\log(x^2-1)}{x^2}-\frac{2\pi q}{x^3}\right\}\right]^{-1/2}$$

where $\delta=1-\mu$, ρ the density, W the molecular weight, e/m the ratio of the electronic charge to mass, F the Faraday constant, N_s the number of electrons per molecule of frequency ν_s, $x=\nu/\nu_s$, ν the frequency of the incident radiation, $q=h/\nu_s$, k the damping factor which can be obtained from the atomic absorption coefficient. Precise measurements of the refraction of the copper and molybdenum K series in crystal quartz have been made. Both possible methods of using a prism were used. The 90° edge of the prism was very carefully prepared. The results obtained are given in the following table.

Method	$\delta\times10^6$	λ (Dispersion)	λ (Crystal)	λ(Grating)
1	8.553	1.536A	1.538A	1.542A
1	6.971	1.388	1.389	1.392
2	8.560	1.537	1.538	1.542
2	6.976	1.388	1.389	1.392
1 and 2	1.805	0.7089	0.7093	0.7109
1 and 2	1.432	0.6315	0.6314	0.6328

It is difficult to believe that such an agreement between the wave-lengths as determined by dispersion and by crystals is entirely fortuitous. The apparent precision obtained in the ruled grating measurements is so high that the above results must indicate a failure of the optical diffraction theory when applied to x-ray wave-lengths.

THE measured index of refraction of x-rays affords one of the most accurate tests of any theory of dispersion. Thus recent x-ray measurements[1] have shown that the quantum theory of dispersion as developed by Kronig,[2] Kramers, Kallman and Mark[3] more accurately accounts for the ob-

[1] A. Larsson, Inaugurald Dissertation, Uppsala (1929).
[2] R. de L. Kronig, Journal Opt. Soc. Am. **12**, 547 (1926).
[3] H. Kallman and H. Mark, Ann. d. Physik **82**, 585 (1927).

served values than does the classical theory. The well-known classical theory as developed by Drude and Lorentz may be written

$$\mu = 1 - \delta = \frac{e^2}{2\pi m} \sum_1^s \frac{n_s}{\nu^2_s - \nu^2} \tag{1}$$

or

$$\frac{\delta}{\lambda^2} = \frac{\rho}{W} \cdot \frac{e}{m} \cdot \frac{F}{2\pi} \sum_1^s \frac{N_s}{\lambda_s^2 - 1/\lambda^2} \tag{2}$$

where μ is the index of refraction, e the charge on the electron, m the mass, n_s the number of electrons per unit volume of natural frequency ν_s or wave-length λ_s, ν the frequency or λ the wave-length of the incident x-rays, ρ the density of the refracting medium, W the molecular weight, F the Faraday constant, and N_s the number of electrons per molecule of frequency ν_s. Eq. (2) has been used[4] to determine the value of e/m from the measured value of δ. Since there is now very little question about the real value of e/m we can get some information concerning the real wave-length of the x-rays λ. Thus Eq. (2) may be solved for λ

$$\lambda = \delta^{1/2}\left(\frac{\rho}{W} \cdot \frac{e}{m} \cdot \frac{E}{2\pi} \sum_1^s \frac{N_s}{\lambda_s^2 - 1/\lambda^2}\right)^{-1/2}. \tag{3}$$

The approximate values of λ and λ_s are known. It has been shown that the x-ray wave-lengths obtained by using crystal gratings differ by about 0.25 percent from those obtained by using ruled gratings. While Eq. (3) cannot be expected to give precise wave-lengths, it should indicate which of the two existing values is correct. It was pointed out above that Eq. (1) does not agree as well with the experimental facts as does the quantum theory, but it was thought best to indicate the method of determining λ in this simpler equation, although all later calculations have been made using the quantum theory.

The quantum theory has been put in a very convenient form by Prins.[5] The index of refraction may be written

$$\mu = 1 - \sum_1^s \alpha_s - \sum_1^s \beta_s i \tag{4}$$

where α and β are given by:

For the region $\nu_s > \nu$

$$\alpha_k = \frac{e^2}{2\pi m} \cdot \frac{n_k}{\nu^2}\left[1 + \frac{\log (1 - x^2)}{x^2}\right] \tag{5}$$

$$\beta_k = \frac{e^2}{2\pi m} \cdot \frac{n_k \nu_k}{\nu^3}\left[\frac{2 - x^2}{1 - x^2} + \frac{2 \log (1 - x^2)}{x^2}\right]. \tag{6}$$

[4] J. A. Bearden, Phys. Rev. **38,** 835 (1931).

[5] J. A. Prins, Zeits. f. Physik **47,** 479 (1928).

For the region $\nu > \nu_s$

$$\alpha_k = \frac{e^2}{2\pi m} \cdot \frac{n_k}{\nu^2}\left[1 + \frac{\log (x^2 - 1)}{x^2} - \frac{2\pi q}{x^2}\right] \tag{7}$$

$$\beta_k = \frac{e^2}{2\pi m} \cdot \frac{n_k}{\nu_k^2}\left[\left\{\frac{x^2 - 2}{x^2 - 1} + \frac{2 \log (x^2 - 1)}{x^2}\right\}\frac{q}{x^3} + \frac{\pi}{4}\right] \tag{8}$$

where $x = \nu/\nu_k$, q is the damping factor divided by ν_k and e and m are the same as in Eq. (1). The $\sum_1^s \alpha_s$ corresponds to the δ used in Eqs. (1), (2) and (3), and the imaginary term $\sum_1^s \beta_s i$ is proportional to the absorption of the x-rays. The value of q in Eq. (7) can be obtained from Eq. (8) by substituting for β its value as obtained from the measured atomic absorption coefficient. Since we are primarily interested in the region $\nu > \nu_s$ we can obtain from Eqs. (4) and (7) a value of λ similar in form to that given in Eq. (3) or

$$\lambda = \delta^{1/2}\left[\frac{\rho}{W} \cdot \frac{e}{m} \cdot \frac{F}{2\pi} \sum_1^s N_s\left\{1 + \frac{\log (x^2 - 1)}{x^2} - \frac{2\pi q}{x^3}\right\}\right]^{-1/2} \tag{9}$$

Experiment

There are three methods by which the index of refraction of x-rays may be measured. First, the deviation from the Bragg law, second the total reflection of x-rays, and third the prism method. Since the prism method is the most direct and precise, it has been used in the present experiments.

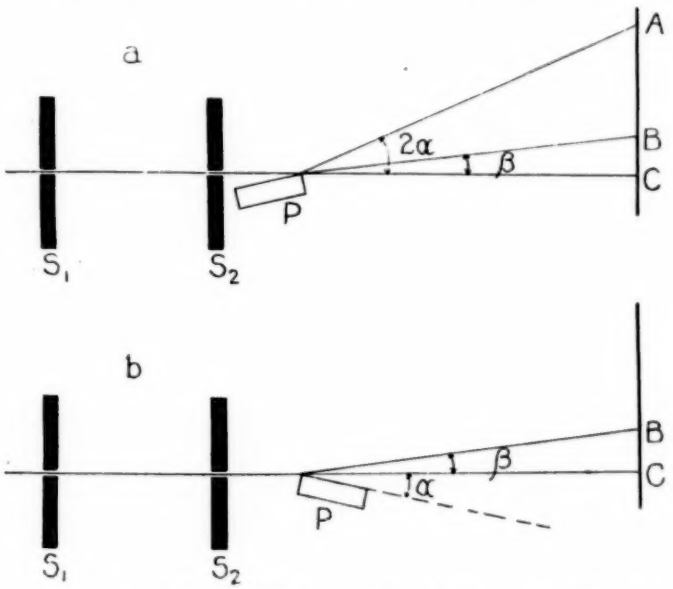

Fig. 1. Apparatus. Slits S_1 and S_2 were 0.015 mm wide and 40 cm apart. The distance from the prism P to the plate was about 200 cm.

The two methods of using a prism for determining the index of refraction

can be easily explained by reference to Fig. 1a and b. In Fig. 1a the x-ray beam struck the first face of the 90° prism at a glancing angle slightly larger than the critical angle of total reflection for the copper $K\alpha$ line. The continuous spectrum of longer wave-length was reflected from this face of the prism and was used to determine the angle between the direction of the x-ray beam and the surface of the prism. The reflected beam was recorded on a photographic plate at A, at the same time the refracted beam was recorded at B. The direct beam was recorded at C. Thus the angles α and β needed for determining μ can be obtained from the separations of the lines on the photographic plate, and the distance R from the edge of the prism to the plate. The index of refraction μ can be calculated from the equation

$$\mu = 1 - \delta = \frac{\cos \alpha}{\cos (\alpha - \beta)} \tag{10}$$

and for small angles α and β this may be written (11)

$$\delta = \beta(\alpha - \beta/2).$$

In the second method (Fig. 1b) the x-ray beam struck the second face internally at almost zero glancing angle and left at nearly the critical angle of total reflection. Stauss[6] has shown that the refracted beam should be less divergent than the incident beam in this case, and all wave-lengths should suffer maximum deviation simultaneously. This method, however, necessitates the precise measurement of a small angular rotation of the prism in order to determine the angle α. It is obvious from Fig. 1b that δ can be obtained from Eqs. (10) and (11).

Since the absorption of the x-rays in the prism limits the useful portion to a region very close to the edge of the prism it is very necessary that the edge be carefully prepared. In order to obtain as sharp an edge as possible a crystal quartz plate 33×65 mm was polished optically flat and then cut into two pieces 33×32 mm. These pieces were cleaned and worked together until the central white light interference fringe showed that the two polished surfaces were in practically perfect contact. These pieces were then placed in a rigid clamp, and the edges which were produced when the large plate was cut into were ground off until the line of demarcation between the plates practically disappeared. This edge was then polished and when the plates were separated a microscopic examination of the 90° edge showed it to be very sharp.

The precise adjustments of the slits, prism and plate holder were made by the method described by the writer[7] in the measurements of x-ray wave-lengths by ruled grating. The location of the edge of the prism on the axis of rotation of the prism table was made with the aid of a Michelson interferometer. The slits were about 0.015 mm wide and 40 cm apart. The distance of the plate holder from the edge of the prism was about 2 meters. The source of x-rays was a water-cooled copper or molybdenum target Coolidge tube

[6] H. E. Stauss, Phys. Rev. **36**, 1101 (1930).
[7] J. A. Bearden, Phys. Rev. **37**, 1217 (1931).

with a small focal spot. The tube was operated at about 10 m.a. and 30 kv peak. In order to reduce the exposure time to a minimum, a simple calculation shows what fraction of the primary beam should be absorbed. The adjustment of the prism to absorb this fraction was easily made with the aid of an ionization chamber.

The exposures varied from 30 min. to three hours, depending upon the angular deviation of the refracted beam. Eastman x-ray plates were used for recording the positions of the various x-ray lines. The separations of these lines were measured with a calibrated comparator. Measurements were made on both the unresolved $K\alpha$ doublets and the $K\beta$ lines. The average wave-length of the $K\alpha$ doublet was obtained from the equation

$$\lambda = \tfrac{1}{3}(2\lambda_1 + \lambda_2)$$

where λ_1 is the wave-length of the $K\alpha_1$ line and λ_2 the $K\alpha_2$ line. The wave-lengths as obtained with crystal gratings are

copper $K\alpha = 1.538$A	molybdenum $K\alpha = 0.7093$A
copper $K\beta = 1.389$	molybdenum $K\beta = 0.6314$

The corresponding wave-lengths as obtained from ruled gratings[7] are

copper $K\alpha = 1.542$A	molybdenum $K\alpha = 0.7109$
copper $K\beta = 1.392$	molybdenum $K\beta = 0.6328$

The density of the quartz prism was determined by the method described in a recent issue of this Journal.[8] The density was

$$\rho = 2.6485 \pm 0.0002 \text{ gr/cm}^3.$$

Results

The first measurements[4] were made with the prism as shown in Fig. 1a using the copper K radiation. The angle α was varied from 16′30″ to 27′57″ in the different exposures. Eighteen measurable exposures were obtained by this method. Fig. 2a shows a typical plate. The results were

$$\delta_\alpha = 8.553 \pm 0.006 \times 10^{-6}$$

$$\delta_\beta = 6.971 \pm 0.005 \times 10^{-6}.$$

The probable error was calculated from the variations in the results by the method of least squares. The alignment of the apparatus and the measurement of the distance from the edge of the prism to the plate holder have been so carefully made that the writer believes the maximum error in δ from these sources is less than $\pm 0.002 \times 10^{-6}$. It should be pointed out, however, that an indeterminate error may arise from the fact that it is necessary to measure to the edge of the reflected beam. The length of the exposures was varied over a wide range in order to reduce this possible error to a minimum. The agreement between the present results and those obtained by Larsson[1] indicate that this error must be negligible.

[8] J. A. Bearden, Phys. Rev. **38**, 2089 (1931).

The next measurements were made with the some wave-length as above but with the prism as shown in Fig. 1b. This method should have given a refracted line narrower than was obtained in the first method.[6] A comparison

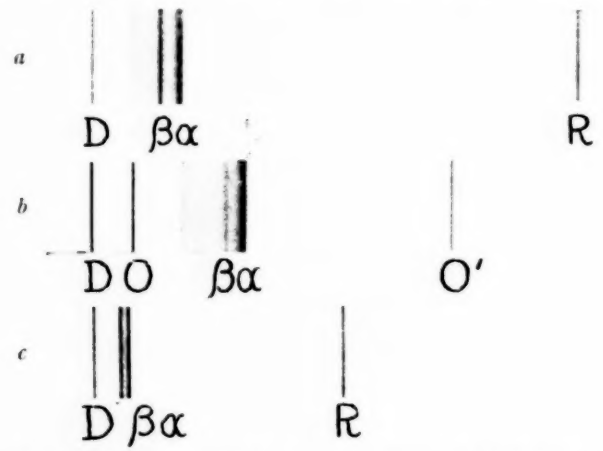

Fig. 2. Three-fold enlargements of typical plates. D is the direct beam, β and α are the refracted $K\beta$ and $K\alpha$ lines, R is the reflected beam, O and O' are reflected lines used for determining the angles with method 2.

of a typical plate shown in Fig. 2b with the plate in Fig. 2a shows that there is very little if any difference in the widths of the refracted lines. The results from 11 plates taken under various conditions gave

$$\delta_\alpha = 8.560 \pm 0.008 \times 10^{-6}$$
$$\delta_\beta = 6.976 \pm 0.007 \times 10^{-6}$$

where the probable error was calculated as above.

After the above results had been obtained, the copper target x-ray tube was replaced by a molybdenum tube and a series of measurements similar to those above were made. Fig. 2c shows a typical photograph. The deviation of the refracted ray from the direct beam was much less in this case than above, but appeared sharper. Thus the results are just about as precise as those for the copper radiation. The average of all the results obtained with the molybdenum K series gives

$$\delta_\alpha = 1.805 \pm 0.001 \times 10^{-6}$$
$$\delta_\beta = 1.432 \pm 0.001 \times 10^{-6}.$$

Calculations of Wave-Lengths and Discussion

As was pointed out above, the bracket term of Eq. (9) is a constant for slight variations of λ. Thus the wave-lengths used in this term may be changed by ± 0.25 percent and the value of the bracket will be changed by less than one part in 5000. The results given in Table I have been calculated assuming wave-lengths which were the average of the wave-lengths as given

TABLE I.

Method	$\delta \times 10^{-6}$	λ (Dispersion)	λ (Crystal)	λ (Grating)
1	8.553	1.536A	1.538A	1.542A
1	6.971	1.388	1.389	1.392
2	8.560	1.537	1.538	1.542
2	6.976	1.388	1.389	1.392
1 and 2	1.805	0.7089	0.7093	0.7109
1 and 2	1.432	0.6315	0.6314	0.6328

by the crystal and grating methods. The wave-lengths calculated from Eq. (9) with the measured δ are given in the column headed λ (dispersion). The agreements between the wave-lengths as obtained from dispersion and those with crystal gratings are not perfect, but it appears to the writer that the agreement is entirely too close to be fortuitous. Larsson[1] has also reported seven determinations of δ for the copper $K\alpha$ line refracted by a quartz prism using essentially method 1. His results when used as above give

$$\lambda = 1.536\text{A}$$

which is in exact agreement with the writer's result for method 1, Table I. Stauss[6] has measured δ for the molybdenum $K\alpha_1$ and $K\beta$ lines in quartz by using method 1. His results are slightly higher than those obtained by the writer and give

$$\lambda_\alpha = 0.7087\text{A}$$
$$\lambda_\beta = 0.6325$$

which are in some better agreement with the grating wave-lengths than the crystal values. Stauss[6] apparently did not take into account the natural width of the refracted beam and this may account for the difference of his results and those obtained by the writer.

These results thus indicate that the grating measurements of x-ray wave-lengths are definitely in error. Considering the precautions taken in the grating measurements[7] and the general agreement between various observers, the cause of the difference in the two methods must be due to a failure of the ruled grating diffraction theory when applied to x-ray wave-lengths.

THE SPECTRA OF TWO AND THREE-VALENCE-ELECTRON ATOMS, Si II, P III, S IV, Si III, P IV AND S V

By I. S. Bowen
Norman Bridge Laboratory of Physics
California Institute of Technology

(Received November 20, 1931)

Abstract

New measurements of the vacuum spark spectra of silicon, phosphorus and sulphur have been made with a vacuum spectrograph. With the aid of these data it has been possible to analyse a large number of hitherto unclassified lines. In Si III and P IV the stronger singlet lines have been classified, while in these ions and in S V a large number of lines involving terms in which both electrons are excited have been identified. In Si II, P III and S IV many of the important quartet lines have been located.

I. Introduction

FOWLER,[1] in his monumental analysis of the silicon spectrum, classified a large number of doublet lines in Si II and a group of triplet lines in Si III which are emitted when only one of the electrons is excited. Later Saha[2] called attention to two quartet multiplets in Si II, and Bowen[3] added a few quartet and doublet lines. The doublets of phosphorus III and sulphur IV were orginally classified by Millikan and Bowen.[4] Miss Saltmarsh[5] independently analysed the P III lines of wave-length greater than 1600A. Additional doublet lines and one quartet multiplet in each atom were later classified by Bowen[3]. The strong triplet lines of P IV and S V, emitted when a single electron is excited, were first arranged by Bowen and Millikan.[6] Again Miss Saltmarsh[5] independently listed a few of the multiplets of P IV.

In the course of the present investigation, new spectra of these elements have been obtained with a vacuum spark between metallic silicon electrodes or between magnesium electrodes containing compounds of phosphorus or sulphur. Many of the lines have been observed in all orders up to the third or fourth of a one meter grating. By the introduction of self induction in the spark circuit it was possible partially to differentiate the various stages of ionization.

II. Two Electron Atoms

The lines that have been classified in Si III, P IV and S V are given in Tables I, III and V, while the terms deduced from them are listed in Tables

[1] A. Fowler, Phil. Trans. **225,** 1 (1925).
[2] M. Saha, Nature **116,** 644 (1925).
[3] I. S. Bowen, Phys. Rev. **31,** 34 (1928).
[4] R. A. Millikan and I. S. Bowen, Phys. Rev. **25,** 600 (1925).
[5] M. O. Saltmarsh, Proc. Roy. Soc. **A108,** 332 (1925).
[6] I. S. Bowen and R. A. Millikan, Phys. Rev. **25,** 591 (1925).

II, IV and VI. For the sake of completeness all previously identified lines have been included as well as the new classifications. The wave-lengths below 2000A are new determinations which, it is hoped, have a somewhat higher

TABLE I. *Classified lines in Si III.*

Int.	λ Vac.	ν	Series Designation
3	566.54	176510	$(3s)^2\ {}^1S-3s4p\ {}^1P$
2	651.65	153457	$3s3p\ {}^3P_0-3s5s\ {}^3S$
3	652.21	153325	$3s3p\ {}^3P_1-3s5s\ {}^3S$
3	653.33	153062	$3s3p\ {}^3P_2-3s5s\ {}^3S$
1	672.29	148745	$3s3p\ {}^3P_1-3s4d\ {}^3D$
1	673.43	148494	$3s3p\ {}^3P_2-3s4d\ {}^3D$
1	800.06	124991	$3s3p\ {}^1P-3s5s\ {}^1S$
3	823.42	121445	$3s3p\ {}^1P-3s4d\ {}^1D$
4	993.54*	100650	$3s3p\ {}^3P_0-3s4s\ {}^3S$
5	994.82*	100521	$3s3p\ {}^3P_1-3s4s\ {}^3S$
5	997.40*	100261	$3s3p\ {}^3P_2-3s4s\ {}^3S$
3	1031.09	96984.7	$(3p)^2\ {}^3P_1-3p4s\ {}^3P_2$
3	1032.89	96815.7	$(3p)^2\ {}^3P_0-3p4s\ {}^3P_1$
4	1033.92	96719.3	$(3p)^2\ {}^3P_2-3p4s\ {}^3P_2$
2	1034.25	96688.4	$(3p)^2\ {}^3P_1-3p4s\ {}^3P_1$
2	1035.63	96559.6	$(3p)^2\ {}^3P_1-3p4s\ {}^3P_0$
4B	1037.02	96430.2	$(3p)^2\ {}^3P_2-3p4s\ {}^3P_1$
7	1108.35*	90224.2	$3s3p\ {}^3P_0-3s3d\ {}^3D_1$
8	1109.95*	90094.1	$3s3p\ {}^3P_1-3s3d\ {}^3D_{1,2}$
9	1113.20*	89831.1	$3s3p\ {}^3P_2-3s3d\ {}^3D_{1,2,3}$
4	1140.56	87676.2	$(3p)^2\ {}^2P_0-3p3d\ {}^3D_1$
4	1141.58	87597.9	$(3p)^2\ {}^3P_1-3p3d\ {}^3D_2$
4	1142.30	87542.7	$(3p)^2\ {}^3P_1-3p3d\ {}^3D_1$
5	1144.31	87388.9	$(3p)^2\ {}^3P_2-3p3d\ {}^3D_3$
4	1144.99	87337.0	$(3p)^2\ {}^3P_2-3p3d\ {}^3D_2$
3	1155.01	86579.3	$(3p)^2\ {}^3P_0-3p3d\ {}^3P_1$
3	1155.96	86508.2	$(3p)^2\ {}^3P_1-3p3d\ {}^3P_0$
3	1156.80	86445.4	$(3p)^2\ {}^3P_1-3p3d\ {}^3P_1$
3	1158.11	86347.6	$(3p)^2\ {}^3P_1-3p3d\ {}^3P_2$
3	1160.27	86186.8	$(3p)^2\ {}^3P_2-3p3d\ {}^3P_1$
3	1161.60	86088.2	$(3p)^2\ {}^3P_2-3p3d\ {}^3P_2$
10	1206.52*	82883.0	$(3s)^2\ {}^1S-3s3p\ {}^1P$
7	1294.55*	77246.9	$3s3p\ {}^3P_1-(3p)^2\ {}^3P_2$
7	1296.72*	77117.7	$3s3p\ {}^3P_0-(3p)^2\ {}^3P_1$
8	1298.90*	76988.2	$3s3p\ {}^3P_{2,1}-(3p)^2\ {}^3P_{2,1}$
7	1301.12*	76856.9	$3s3p\ {}^3P_1-(3p)^2\ {}^3P_0$
7	1303.30*	76728.3	$3s3p\ {}^3P_2-(3p)^2\ {}^3P_1$
4	1312.61	76184.1	$3s3p\ {}^1P-3s4s\ {}^1S$
4	1341.46	74545.6	$3s3d\ {}^3D-3p3d\ {}^3D_3$
3	1342.39	74494.0	$3s3d\ {}^3D-3p3d\ {}^3D_2$
3	1343.41	74437.4	$3s3d\ {}^3D-3p3d\ {}^3D_1$
3	1361.59	73443.5	$3s4s\ {}^3S-3p4s\ {}^3P_2$
2	1362.36	73402.0	$3s3d\ {}^3D_1-3p3d\ {}^3P_0$
3	1363.47	73342.3	$3s3d\ {}^3D_{1,2}-3p3d\ {}^3P_1$
3	1365.26	73246.1	$3s3d\ {}^3D_{1,2,3}-3p3d\ {}^3P_2$
3	1367.04	73150.7	$3s4s\ {}^3S-3p4s\ {}^3P_1$
2	1369.44	73022.5	$3s4s\ {}^3S-3p4s\ {}^3P_0$
1	1371.61	72907.0	$3s4p\ {}^3P_1-3p4p\ {}^3P_2$
1	1372.99	72833.7	$3s4p\ {}^3P_2-3p4p\ {}^3P_2$
1	1375.05	72724.6	$3s4p\ {}^3P_0-3p4p\ {}^3P_1$
1	1375.65	72692.9	$3s4p\ {}^3P_1-3p4p\ {}^3P_1$
2	1377.06	72618.5	$3s4p\ {}^3P_{2,1}-3p4p\ {}^3P_{1,0}$
5	1417.20	70561.7	$3s3p\ {}^1P-(3p)^2\ {}^1S$
4	1500.18*	66658.7	$3s3d\ {}^3D_3-3s4f\ {}^3F_4$
4	1501.16*	66615.2	$3s3d\ {}^3D_{3,2}-3s4f\ {}^3F_3$
3	1501.87*	66583.7	$3s3d\ {}^3D_{1,2,3}-3s4f\ {}^3F_2$
0	1833.42	54542.9	$(3p)^2\ {}^1D-3s4p\ {}^1P$
3	1842.54	54272.9	$3s3d\ {}^1D-3s3p\ {}^1P$
2	1895.46	52757.6	$(3s)^2\ {}^1S-3s4p\ {}^3P_1$
	λ Air		
10	2541.83	39329.9	$3s3p\ {}^1P-3s3d\ {}^1D$
7	2559.22	39062.7	$3s3p\ {}^1P-(3p)^2\ {}^1D$
1	3034.74*	32942.2	$3s4f\ {}^3F_3-3s6g\ {}^3G$
1	3037.26*	32914.9	$3s4f\ {}^3F_3-3s6g\ {}^3G$
1	3040.93*	32875.1	$3s4f\ {}^3F_4-3s6g\ {}^3G$
7	3086.225*	32392.7	$3s3d\ {}^3D_3-3s4p\ {}^3P_2$
3	3086.429*	32390.5	$3s3d\ {}^3D_2-3s4p\ {}^3P_2$
1	3086.620*	32388.5	$3s3d\ {}^3D_1-3s4p\ {}^3P_2$
6	3093.423*	32317.3	$3s3d\ {}^3D_3-3s4p\ {}^3P_1$
3	3093.613*	32315.3	$3s3d\ {}^3D_1-3s4p\ {}^3P_1$
4	3096.786*	32282.2	$3s3d\ {}^3D_1-3s4p\ {}^3P_0$
0	3126.25	31978.0	$3p3d\ {}^3P_2-3p4p\ {}^3P_2$
0	3147.38	31763.3	$3p3d\ {}^3P_2-3p4p\ {}^3P_1$
3	3185.16	31386.6	$3s4p\ {}^1P-3s5s\ {}^1S$
3	3230.55*	30945.6	$3s4p\ {}^3P_0-3s5s\ {}^3S$
5	3234.00*	30912.6	$3s4p\ {}^3P_1-3s5s\ {}^3S$
6	3241.67*	30839.4	$3s4p\ {}^3P_2-3s5s\ {}^3S$
00	3253.44	30727.9	$3p3d\ {}^3D_3-3p4p\ {}^3P_2$
1	3258.67	30678.6	$3p3d\ {}^3D_3-3p4p\ {}^3P_2$
1	3276.25	30513.9	$3p3d\ {}^3D_3-3p4p\ {}^3P_1$
0	3279.25	30486.0	$3p3d\ {}^3D_1-3p4p\ {}^3P_0$
8	3590.46	27843.7	$3s4p\ {}^1P-3s4d\ {}^1D$
3	3791.41*	26368.0	$3s4p\ {}^3P_0-3s4d\ {}^3D$
4	3796.11*	26335.3	$3s4p\ {}^3P_1-3s4d\ {}^3D$
5	3806.56*	26263.0	$3s4p\ {}^3P_2-3s4d\ {}^3D$
1	4338.52	23042.9	$(3p)^2\ {}^1S-3s4p\ {}^1P$
9	4552.654*	21959.2	$3s4s\ {}^3S-3s4p\ {}^3P_2$
7	4567.872*	21886.0	$3s4s\ {}^3S-3s4p\ {}^3P_1$
4	4574.777*	21853.0	$3s4s\ {}^3S-3s4p\ {}^3P_0$
1	4638.12	21554.4	$3p4s\ {}^3P_0-3p4p\ {}^3P_1$
0	4665.87	21426.3	$3p4s\ {}^3P_1-3p4p\ {}^3P_1$
2B	4683.774	21344.4	$3p4s\ {}^3P_1-3p4p\ {}^3P_0$
2B	4683.018	21347.8	$3p4s\ {}^3P_2-3p4p\ {}^3P_2$
2	4813.290*	20770.0	$3s4f\ {}^3F_3-3s5g\ {}^3G$
3	4819.740*	20742.2	$3s4f\ {}^3F_3-3s5g\ {}^3G$
4	4828.923*	20702.8	$3s4f\ {}^3F_4-3s5g\ {}^3G$
8	5739.762	17417.5	$3s4s\ {}^1S-3s4p\ {}^1P$

* Previously classified by Fowler (reference 1).
B Blend.

accuracy than previous measurements. In silicon the wave-lengths above 2000A are taken from Fowler[1], and in phosphorus from Geuter.[7]

[7] Geuter, Zeits. f. wiss. Photographie **5**, 1 (1907).

TABLE II. *Term values in Si III.*

		$3s3p\,^3P_0$ 217311	$3s3d\,^3D_1$ 127088.9				
		$3s3p\,^3P_1$ 217183	$3s3d\,^3D_2$ 127090.9				
		$3s3p\,^3P_2$ 216922	$3s3d\,^3D_3$ 127093.0				
$(3s)^2\,^1S$	269940.6	$3s3p\,^1P$ 187057.6	$3s3d\,^1D$ 147727.6				
$3s4s\,^3S$	116659.6	$3s4p\,^3P_0$ 94806.6	$3s4d\,^3D$ 68438.1	$3s4f\,^3F_2$ 60503.9			
		$3s4p\,^3P_1$ 94773.6		$3s4f\,^3F_3$ 60476.3			
		$3s4p\,^3P_2$ 94700.4		$3s4f\,^3F_4$ 60436.8			
$3s4s\,^1S$	110872.2	$3s4p\,^1P$ 93454.7	$3s4d\,^1D$ 65611.0				
$3s5s\,^3S$	63861.0					$3s5g\,^3G$	39734.0
$3s5s\,^1S$	62068.1					$3s6g\,^3G$	27561.6
			$(3p)^2\,^3P_0$ 140326.	$3p3d\,^3P_0$ 53686.			
			$(3p)^2\,^3P_1$ 140194.	$3p3d\,^3P_1$ 53748.			
			$(3p)^2\,^3P_2$ 139935.	$3p3d\,^3P_2$ 53846.			
			$(3p)^2\,^1S$ 116497.6	$3p3d\,^3D_1$ 52651.			
				$3p3d\,^3D_2$ 52597.			
			$(3p)^2\,^1D$ 147995.	$3p3d\,^3D_3$ 52546.			
		$3p4s\,^3P_0$ 43636.	$3p4p\,^3P_0$ 22165.				
		$3p4s\,^3P_1$ 43509.	$3p4p\,^3P_1$ 22082.				
		$3p4s\,^3P_2$ 43214.	$3p4p\,^3P_2$ 21868.				

TABLE III. *Classified lines in P IV.*

Int.	λ Vac.	ν	Series Designation
5	628.983	158987.	$3s3p\,^3P_0-3s4s\,^3S$
6	629.914	158752.	$3s3p\,^3P_1-3s4s\,^3S$
7	631.765*	158287.	$3s3p\,^3P_2-3s4s\,^3S$
2	652.79	153189.	$(3p)^2\,^3P_1-3p4s\,^3P_2$
2	653.51	153020.	$(3p)^2\,^3P_0-3p4s\,^3P_1$
1	654.54	152779.	$(3p)^2\,^3P_1-3p4s\,^3P_1$
3	654.86	152704.	$(3p)^2\,^3P_2-3p4s\,^3P_2$
2	655.78	152490.	$(3p)^2\,^3P_1-3p4s\,^3P_0$
2	656.55	152311.	$(3p)^2\,^3P_2-3p4s\,^3P_1$
3	776.340	128809.5	$3s3p\,^1P-3s4s\,^1S$
6	823.177*	121480.6	$3s3p\,^3P_0-3s3d\,^3D$
7	824.733*	121251.4	$3s3p\,^3P_1-3s3d\,^3D$
8	827.932*	120782.9	$3s3p\,^3P_2-3s3d\,^3D$
3	845.964	118208.3	$(3p)^2\,^3P_0-3p3d\,^3D_1$
3	846.999	118063.9	$(3p)^2\,^3P_1-3p3d\,^3D_2$
4*B*	847.660	117971.8	$(3p)^2\,^3P_1-3p3d\,^3D_1$
4	849.799	117674.9	$(3p)^2\,^3P_2-3p3d\,^3D_3$
2	850.390	117593.1	$(3p)^2\,^3P_2-3p3d\,^3D_2$
1	851.094	117495.8	$(3p)^2\,^3P_2-3p3d\,^3D_1$
1	860.48	116214.	$(3p)^2\,^3P_1-3p3d\,^3P_0$
2	861.517	116074.3	$(3p)^2\,^3P_1-3p3d\,^3P_1$
2	863.288	115836.2	$(3p)^2\,^3P_1-3p3d\,^3P_2$
1	865.018	115604.5	$(3p)^2\,^3P_2-3p3d\,^3P_1$
2	866.820	115364.2	$(3p)^2\,^3P_2-3p3d\,^3P_2$
10	950.669*	105189.1	$(3s)^2\,^1S-3s3p\,^1P$
4	1006.237	99380.1	$3s3d\,^1D-3s4p\,^1P$
7	1025.579*	97505.9	$3s3p\,^3P_1-(3p)^2\,^3P_2$
7	1028.131*	97263.9	$3s3p\,^3P_0-(3p)^2\,^3P_1$
8	1030.545*	97036.0	$3s3p\,^3P_{2,1}-(3p)^2\,^3P_{2,1}$
7	1033.135*	96792.8	$3s3p\,^3P_1-(3p)^2\,^3P_0$
7	1035.542*	96567.8	$3s3p\,^3P_2-(3p)^2\,^3P_1$
3	1064.60	93932.	$3s3d\,^3D-3p3d\,^3D_3$
3	1065.554	93847.9	$3s3d\,^3D-3p3d\,^3D_2$
2	1066.640	93752.3	$3s3d\,^3D-3p3d\,^3D_1$
2	1086.943	92001.1	$3s3d\,^3D-3p3d\,^3P_0$
3	1088.608	91860.4	$3s3d\,^3D-3p3d\,^3P_1$
4	1091.442	91621.9	$3s3d\,^3D-3p3d\,^3P_2$
2	1093.318	91464.7	$3s4s\,^3S-3p4s\,^3P_2$
2	1098.183	91059.5	$3s4s\,^3S-3p4s\,^3P_1$
1	1101.65	90773.0	$3s4s\,^3S-3p4s\,^3P_0$
4	1484.508*	67362.4	$3s3d\,^3D-3s4p\,^3P_2$
4	1487.793*	67213.7	$3s3d\,^3D-3s4p\,^3P_1$
3	1489.093*	67155.0	$3s3d\,^3D-3s4p\,^3P_0$
8	1888.55	52950.7	$3s3p\,^1P-3s3d\,^1D$
1	1904.80*	52499.0	$3s4p\,^3P_1-3s5s\,^3S$
1	1910.18*	52351.1	$3s4p\,^3P_2-3s5s\,^3S$
		λ Air	
4	2724.96*	36688.4	$3s4p\,^3P_0-3s4d\,^3D_1$
4	2728.90*	36635.4	$3s4p\,^3P_1-3s4d\,^3D_2$
3	2729.29*	36630.2	$3s4p\,^3P_1-3s4d\,^3D_1$
5	2739.42*	36494.6	$3s4p\,^3P_2-3s4d\,^3D_3$
3	2740.00*	36486.9	$3s4p\,^3P_2-3s4d\,^3D_2$
6	3347.85*	29862.6	$3s4s\,^3S-3s4p\,^3P_2$
6	3364.57*	29714.2	$3s4s\,^3S-3s4p\,^3P_1$
5	3371.24*	29655.5	$3s4s\,^3S-3s4p\,^3P_0$
6	4249.73	23525.2	$3s4s\,^1S-3s4p\,^1P$

* Previously classified by Bowen and Millikan (reference 6).
B Blend.

Most of the new triplet terms arise from electron configurations in which both electrons are excited. In general, these terms combine with so many other terms, both old and new, to give observed lines that there can be little doubt as to the existence of the levels. Furthermore the irregular doublet law relationships, displayed in Table VII, confirm the assignment of the levels to

TABLE IV. *Term values in P IV.*

		$3s3p\ ^3P_0$	346659	$3s3d\ ^3D$	225174.6		
		$3s3p\ ^3P_1$	346427				
		$3s3p\ ^3P_2$	345960				
$(3s)^2\ ^1S$	414247	$3s3p\ ^1P$	309058	$3s3d\ ^1D$	256105.		
$3s4s\ ^3S$	187675	$3s4p\ ^3P_0$	158019.5	$3s4d\ ^3D_1$	121330.9		
		$3s4p\ ^3P_1$	157960.8	$3s4d\ ^3D_2$	121325.5		
		$3s4p\ ^3P_2$	157812.4	$3s4d\ ^3D_3$	121317.8		
$3s4s\ ^1S$	180250.0	$3s4p\ ^1P$	156724.8				
$3s5s\ ^3S$	105461.6						
				$(3p)^2\ ^3P_0$	249634.	$3p3d\ ^3P_0$	133176
				$(3p)^2\ ^3P_1$	249393.	$3p3d\ ^3P_1$	133317
				$(3p)^2\ ^3P_2$	248922.	$3p3d\ ^3P_2$	133556
						$3p3d\ ^3D_1$	131425
						$3p3d\ ^3D_2$	131328
						$3p3d\ ^3D_3$	131245
		$3p4s\ ^3P_0$	96902.				
		$3p4s\ ^3P_1$	96615.				
		$3p4s\ ^3P_2$	96210.				

TABLE V. *Classified lines in S V.*

Int.	λ Vac.	ν	Series Designation	Int.	λ Vac.	ν	Series Designation
1	437.37*	228639.	$3s3p\ ^3P_0-3s4s\ ^3S$	1	691.74	144563	$(3p)^2\ ^3P_1-3p3d\ ^3P_1$
1	438.19*	228212.	$3s3p\ ^3P_1-3s4s\ ^3S$	2	693.522	144192	$(3p)^2\ ^3P_1-3p3d\ ^3P_2$
1	439.65*	227454.	$3s3p\ ^3P_2-3s4s\ ^3S$	8	786.476*	127149.4	$(3s)^2\ ^1S-3s3p\ ^1P$
3	658.262*	151915.	$3s3p\ ^3P_0-3s3d\ ^3D$	6	849.241*	117752.2	$3s3p\ ^3P_1-(3p)^2\ ^3P_2$
4	659.853*	151549.	$3s3p\ ^3P_1-3s3d\ ^3D$	5	852.185*	117345.4	$3s3p\ ^3P_0-(3p)^2\ ^3P_1$
5	663.155*	150794.	$3s3p\ ^3P_2-3s3d\ ^3D$	7	854.792*	116987.5	$3s3p\ ^3P_{1,2}-(3p)^2\ ^3P_{1,2}$
1	676.21	147883.	$(3p)^2\ ^3P_0-3p3d\ ^3D_1$	5	857.872*	116567.5	$3s3p\ ^3P_1-(3p)^2\ ^3P_0$
1	677.342	147636.	$(3p)^2\ ^3P_1-3p3d\ ^3F_2$	5	860.462*	116216.6	$3s3p\ ^3P_2-(3p)^2\ ^3P_1$
2	678.08	147475.	$(3p)^2\ ^3P_1-3p3d\ ^3D_1$				
3	680.326	146988.	$(3p)^2\ ^3P_2-3p3d\ ^3D_2$	2	883.59	113175.	$3s3d\ ^3D-3p3d\ ^3D_3$
5B	680.940	146856.	$(3p)^2\ ^3P_2-3p3d\ ^3D_3$	2	884.46	113063.	$3s3d\ ^3D-3p3d\ ^3D_2$
3B	681.565	146721.	$(3p)^2\ ^3P_2-3p3d\ ^3D_1$	1	885.77	112896.	$3s3d\ ^3D-3p3d\ ^3D_1$
1	686.150	145741.	$(3p)^2\ ^3P_0-3p3d\ ^3P_1$	2	900.93	110996.	$3s3d\ ^3D-3p3d\ ^3P_0$
1	686.93	145575.	$(3p)^2\ ^3P_1-3p3d\ ^3P_0$	1	902.80	110767.	$3s3d\ ^3D-3p3d\ ^3P_1$
0	688.04	145340.	$(3p)^2\ ^3P_1-3p3d\ ^3P_1$	2	905.92	110385.	$3s3d\ ^3D-3p3d\ ^3P_2$
1	689.838	144962.	$(3p)^2\ ^3P_1-3p3d\ ^3P_2$				

* Previously classified by Bowen and Millikan (reference 6).
B Blend

TABLE VI. *Term values in S V.*

		$3s3p\ ^3P_0$	501629	$3s3d\ ^3D$	349713		
		$3s3p\ ^3P_1$	501267				
		$3s3p\ ^3P_2$	500500				
$3s4s\ ^3S$	273030						
				$(3p)^2\ ^3P_0$	384700	$3p3d\ ^3P_0$	238713
				$(3p)^2\ ^3P_1$	384283	$3p3d\ ^3P_1$	238950
				$(3p)^2\ ^3P_2$	383514	$3p3d\ ^3P_2$	239324
						$3p3d\ ^3D_1$	236817
						$3p3d\ ^3D_2$	236649
						$3p3d\ ^3D_3$	236532

TABLE VII. *Irregular doublet law relationships in two electron-systems.*

	$3s3d\ ^3D_3-3p3d\ ^3P_2$		$3s3d\ ^3D_3-3p3d\ ^3D_3$		$(3p)^2\ ^3P_2-3p3d\ ^3P_2$		$(3p)^2\ ^3P_2-3p3d\ ^3D_3$	
	ν	Diff.	ν	Diff.	ν	Diff.	ν	Diff.
Si III	73246.1		74545.6		86088.2		87388.9	
		18375.8		19386.4		29276.0		30286.0
P IV	91621.9		93932.		115364.2		117674.9	
		18763.1		19243.		28827.8		29313.1
S V	110385.		113175.		144192.		146988.	
	$3s4s\ ^3S-3p4s\ ^3P_2$		$3s3p\ ^1P-3s3d\ ^1D$		$3s4s\ ^1S-3s4p\ ^1P$		$(3s)^2\ ^1S-3s3p\ ^3P_1$	
Mg I			11351.8		5843.6		21870.7	
				14277.5		5726.2		15583.1
Al II	54686.4		25629.3		11569.8		37453.8	
		18757.1		13700.6		5847.7		15303.8
Si III	73443.5		39329.9		17417.5		52757.6	
		18021.2		13620.8		6107.7		
P IV	91464.7		52950.7		23525.2			

configurations. Table VII includes these relationships for the newly identified lines only, as previous articles gave similar tables for the lines classified in them. Additional evidence for the correctness of the assignments is found in the comparison of the observed multiplet separations with the predictions of the theory developed by Goudsmit and Humphreys.[8] The comparison is shown in Table XIV and discussed in section IV.

Tables VII and XIV show at once that the P'' term in Al II, found by Sawyer and Paschen,[9] satisfies the predictions completely for the ^3P term of the $3p4s$ configuration, but definitely cannot be assigned to the $3p3d$ configuration as originally suggested by these authors.

TABLE VIII. *Quartet lines in Si II.*

Int.	λ Vac.	ν	Series Designation	Int.	λ Vac.	ν	Series Designation
3	1246.73	80209.8	$3p\ ^4P_1-(3p)^3\ ^4S$	0	5540.74*	18043.1	$4s\ ^4P_1-4p\ ^4S$
3	1248.40	80102.5	$3p\ ^4P_2-(3p)^3\ ^4S$	1	5576.61*	17927.1	$4s\ ^4P_2-4p\ ^4S$
4	1251.16	79925.8	$3p\ ^4P_3-(3p)^3\ ^4S$	2	5639.492*	17727.2	$4s\ ^4P_3-4p\ ^4S$
3	1346.92	74243.5	$3p\ ^4P_3-4s\ ^4P_3$	1	5800.48*	17235.2	$4s\ ^4P_3-4p\ ^4P_3$
3	1348.55	74153.7	$3p\ ^4P_1-4s\ ^4P_1$	2	5806.75*	17216.6	$4s\ ^4P_1-4p\ ^4P_2$
4	1350.07	74070.2	$3p\ ^4P_3-4s\ ^4P_3$	0	5827.80*	17154.4	$4s\ ^4P_1-4p\ ^4P_1$
3	1350.58	74042.3	$3p\ ^4P_3-4s\ ^4P_2$	0	5846.12*	17100.6	$4s\ ^4P_2-4p\ ^4P_2$
3	1352.68	73927.3	$3p\ ^4P_2-4s\ ^4P_1$	1	5867.497*	17038.4	$4s\ ^4P_2-4p\ ^4P_1$
3	1353.75	73868.9	$3p\ ^4P_2-4s\ ^4P_2$	3	5868.404*	17035.7	$4s\ ^4P_2-4p\ ^4P_2$
				1	5915.266*	16900.7	$4s\ ^4P_2-4p\ ^4P_2$

* Previously classified by Saha (reference 2).

TABLE IX. *Quartet term values in Si II.*

		$3s(3p)^2\ ^4P_1$	87737.7	$(3p)^3\ ^4S$	7526.8
		$3s(3p)^2\ ^4P_2$	87627.1		
		$3s(3p)^2\ ^4P_3$	87453.6		
$3s3p4s\ ^4P_1$	13700.0	$3s3p4p\ ^4S$	−4343.1		
$3s3p4s\ ^4P_2$	13584.0				
$3s3p4s\ ^4P_3$	13384.1	$3s3p4p\ ^4P_1$	−3454.4		
		$3s3p4p\ ^4P_2$	−3516.6		
		$3s3p4p\ ^4P_3$	−3651.4		

[8] S. Goudsmit and C. J. Humphreys, Phys. Rev. **31**, 960 (1928).

[9] R. A. Sawyer and F. Paschen, Ann. d. Physik **84**, 1 (1927).

In the singlet system it is, of course, impossible to make all of the tests of the classification such as those discussed above. This naturally makes the assignment of singlet lines somewhat less certain. In most of the cases, however, the great strength of the lines and the irregular doublet law relationships shown in Table VII leave little doubt as to the reality of most of the levels. However the assignment of the levels to configurations is quite uncertain for the terms tentatively ascribed to the $3s3d$, $3s4d$ and $(3p)^2$ configurations. In fact due to the overlapping of the $3s3d$ and $(3p)^2$ configurations the terms due to them are doubtless much disturbed and any attempt to assign these terms to a definite configuration may have little significance.

The identification of the intercombination line $(3s)^2\ {}^1S-3s3p^3P_1$ in Si III is also doubtful. However the term values of the singlets and triplets can be independently determined with an accuracy which precludes any large shift in the relative position of the two systems regardless of this identification.

The term values listed correspond to an ionization potential of 33.30 volts for Si III and 51.1 volts for P IV.

III. Three-Electron Atoms

The lines that have been classified in the quartet systems of Si II, P III and S IV, including those identified by previous authors, are given in Tables VIII, X and XII, while the terms deduced from them are listed in Tables

TABLE X. *Quartet lines in P III.*

Int.	λ Vac.	ν	Series Designation	Int.	λ Air.	ν	Series Designation
2	781.728	127921.7	$3p\ {}^4P_3-4s\ {}^4P_3$	5B	2739.42	36494.6	$3d\ {}^4P_3-4p\ {}^4P_3$
2B	782.965	127719.6	$3p\ {}^4P_1-4s\ {}^4P_2$	2	2752.81	36317.2	$3d\ {}^4P_2-4p\ {}^4P_2$
3B	783.739	127593.5	$3p\ {}^4P_2-4s\ {}^4P_2$	4	2758.62	36240.7	$3d\ {}^4P_2-4p\ {}^4P_2$
1	784.10	127535.	$3p\ {}^4P_1-4s\ {}^4P_1$	0	2771.93	36066.7	$3d\ {}^4P_2-4p\ {}^4P_2$
1	784.25	127510.	$3p\ {}^4P_2-4s\ {}^4P_2$				
2	785.383	127326.4	$3p\ {}^4P_2-4s\ {}^4P_1$	0	2779.9	35963.3	$3d\ {}^4D_3-4p\ {}^4S$
2	786.239	127187.8	$3p\ {}^4P_3-4s\ {}^4P_2$				
				3	2780.89	35950.5	$3d\ {}^4P_{2,1}-4p\ {}^4P_{1,0}$
4	844.644	118393.1	$3p\ {}^4P_1-3d\ {}^4D_2$	1	2790.09	35831.9	$3d\ {}^4P_1-4p\ {}^4P_1$
4	845.029	118339.1	$3p\ {}^4P_1-3d\ {}^4D_1$				
4	845.665	118250.1	$3p\ {}^4P_2-3d\ {}^4D_3$	2	2857.07	34992.0	$3d\ {}^4D_2-4p\ {}^4P_3$
3	846.120	118186.5	$3p\ {}^4P_2-3d\ {}^4D_2$	3	2862.17	34929.6	$3d\ {}^4D_3-4p\ {}^4P_3$
2	846.477	118136.7	$3p\ {}^4P_2-3d\ {}^4D_1$	4	2866.25	34879.9	$3d\ {}^4D_4-4p\ {}^4P_3$
4B	847.660	117971.8	$3p\ {}^4P_3-3d\ {}^4D_4$	1	2873.27	34794.7	$3d\ {}^4D_1-4p\ {}^4P_2$
3	848.017	117922.2	$3p\ {}^4P_3-3d\ {}^4D_3$	3	2877.64	34741.9	$3d\ {}^4D_3-4p\ {}^4P_2$
1	848.150	117862.0	$3p\ {}^4P_3-3d\ {}^4D_2$	1	2882.86	34679.0	$3d\ {}^4D_{1,2}-4p\ {}^4P_{1,2}$
				1	2887.40	34624.5	$3d\ {}^4D_2-4p\ {}^4P_1$
2	853.355	117184.5	$3p\ {}^4P_1-3d\ {}^4P_1$				
3	854.228	117064.8	$3p\ {}^4P_1-3d\ {}^4P_2$	5B	3717.77	26891.3	$4s\ {}^4P_1-4p\ {}^4S$
3	854.831	116982.2	$3p\ {}^4P_2-3d\ {}^4P_1$	5	3744.36	26700.3	$4s\ {}^4P_2-4p\ {}^4S$
3	856.980	116688.8	$3p\ {}^4P_2-3d\ {}^4P_3$	6	3802.22	26294.1	$4s\ {}^4P_3-4p\ {}^4S$
3	858.133	116532.1	$3p\ {}^4P_3-3d\ {}^4P_2$				
3	859.403	116359.8	$3p\ {}^4P_3-3d\ {}^4P_3$	6	3895.17	25666.6	$4s\ {}^4P_3-4p\ {}^4P_3$
				6	3904.93	25602.4	$4s\ {}^4P_1-4p\ {}^4P_2$
3	972.830	102792.9	$3p\ {}^4P_1-(3p)^3\ {}^4S$	4	3922.86	25485.4	$4s\ {}^4P_1-4p\ {}^4P_1$
4	974.768	102588.5	$3p\ {}^4P_2-(3p)^3\ {}^4S$	4	3933.52	25416.3	$4s\ {}^4P_2-4p\ {}^4P_2$
4	977.890	102261.0	$3p\ {}^4P_3-(3p)^3\ {}^4S$	5	3951.65	25299.7	$4s\ {}^4P_3-4p\ {}^4P_1$
	λ Air			6	3957.77	25260.6	$4s\ {}^4P_3-4p\ {}^4P_2$
3	2664.09	37526.6	$3d\ {}^4P_3-4p\ {}^4S$	5	3997.31	25010.8	$4s\ {}^4P_2-4p\ {}^4P_2$
2	2685.08	37233.1	$3d\ {}^4P_1-4p\ {}^4S$				

B Blend

IX, XI and XIII. Since the present investigation has yielded no new doublet or intercombination lines no doublet lines or terms have been included. The wave-lengths in silicon and phosphorus above 2000A are taken from Fowler[1] and Geuter[7] respectively. Since no intercombinations are known, the quartet term values cannot be fixed accurately with respect to those of the doublets.

TABLE XI. *Quartet terms in P III.*

		$3s(3p)^2\,{}^4P_1$	185423.6	$(3p)^3\,{}^4S$	82630.6
		$3s(3p)^2\,{}^4P_2$	185219.2		
		$3s(3p)^2\,{}^4P_3$	184891.4	$3s3p3d\,{}^4P_1$	68238.5
				$3s3p3d\,{}^4P_2$	68356.3
				$3s3p3d\,{}^4P_3$	68531.2
				$3s3p3d\,{}^4D_1$	67084.0
				$3s3p3d\,{}^4D_2$	67031.1
				$3s3p3d\,{}^4D_3$	66968.9
				$3s3p3d\,{}^4D_4$	66919.2
$3s3p4s\,{}^4P_1$	57891.7	$3s3p4p\,{}^4S$	31005.7		
$3s3p4s\,{}^4P_2$	57705.8				
$3s3p4s\,{}^4P_3$	57300.0	$3s3p4p\,{}^4P_1$	32406.2		
		$3s3p4p\,{}^4P_2$	32289.3		
		$3s3p4p\,{}^4P_3$	32039.3		

TABLE XII. *Quartet lines in S IV.*

Int.	λ Vac.	ν	Series Designation	Int.	λ Vac.	ν	Series Designation
2	519.30	192567.	$3p\,{}^4P_2-4s\,{}^4P_3$	4	655.553	152543.	$3p\,{}^4P_3-3d\,{}^4D_4$
2	520.11	192267.	$3p\,{}^4P_1-4s\,{}^4P_2$	2	655.887	152465.	$3p\,{}^4P_2-3d\,{}^4D_3$
3	520.83	192001.	$3p\,{}^4P_3-4s\,{}^4P_3$	1	656.30	152369.	$3p\,{}^4P_3-3d\,{}^4D_3$
1	521.13	191891.	$3p\,{}^4P_2-4s\,{}^4P_2$				
2	521.99	191575.	$3p\,{}^4P_3-4s\,{}^4P_1$	3	660.945	151299.	$3p\,{}^4P_1-3d\,{}^4P_2$
2	522.54	191373.	$3p\,{}^4P_2-4s\,{}^4P_2$	3	663.707	150669.	$3p\,{}^4P_2-3d\,{}^4P_3$
				3	664.822	150416.	$3p\,{}^4P_3-3d\,{}^4P_2$
3	652.523	153251.	$3p\,{}^4P_1-3d\,{}^4D_2$	4	666.114	150124.	$3p\,{}^4P_2-3d\,{}^4P_1$
3	653.000	153139.	$3p\,{}^4P_1-3d\,{}^4D_1$				
4	653.560	153008.	$3p\,{}^4P_2-3d\,{}^4D_2$	3	798.277	125270.	$3p\,{}^4P_1-(3p)^3\,{}^4S$
3	653.988	152908.	$3p\,{}^4P_2-3d\,{}^4D_3$	4	800.477	124926.	$3p\,{}^4P_2-(3p)^3\,{}^4S$
1	654.37	152819.	$3p\,{}^4P_3-3d\,{}^4D_1$	4	803.996	124379.	$3p\,{}^4P_3-(3p)^3\,{}^4S$

TABLE XIII. *Quartet terms in S IV.*

		$3s(3p)^2\,{}^4P_1$	309701	$(3p)^3\,{}^4S$	184431
		$3s(3p)^2\,{}^4P_2$	309357		
		$3s(3p)^2\,{}^4P_3$	308810	$3s3p3d\,{}^4P_2$	158398
				$3s3p3d\,{}^4P_3$	158687
				$3s3p3d\,{}^4D_1$	156550
				$3s3p3d\,{}^4D_2$	156447
				$3s3p3d\,{}^4D_3$	156347
				$3s3p3d\,{}^4D_4$	156267
$3s3p4s\,{}^4P_1$	117782				
$3s3p4s\,{}^4P_2$	117436				
$3s3p4s\,{}^4P_3$	116800				

However the relative positions of the two systems can be determined approximately by assuming that the $3s3p4s\,{}^4P$ term of the quartet system differs from the $(3s)^2 4s^2S$ term of the doublet system by an amount equal to the difference between the terms in the next ion on which these terms are respectively based, namely, $(3s)^2\,{}^1S-3s3p^3P$. The tabulated values of the terms are fixed in this way.

With one exception in each element all the terms found are due to configurations having a $3s$ and a $3p$ electron plus an excited electron whose transitions cause the emission of the observed lines. This makes it feasible to simplify the notation for the series designation of the lines by the omission of the $3s3p$.

TABLE XIV. *Multiplet separations.*

Triplets									Quartets								
	Al II		Si III		P IV		S V			Si II		P III		S IV	
	Calc.	Obs.	Calc.	Obs.	Calc.	Obs.	Calc.	Obs.		Calc.	Obs.	Calc.	Obs.	Calc.	Obs.
$3p4s\,^3P$	156	127	308	295	530	405	845		$3s3p4s\,^4P$	216	199.9	388	405.8	627	636
	78	58	154	127	265	287	423			130	116.0	233	185.9	376	346
$3p4p\,^3P$	78		154	214	265		423		$3s3p4p\,^4P$	108	134.8	194	250.0	314	
	39		77	83	133		211			65	62.2	117	117.1	188	
$3p4p\,^3D$	117		231		398		634		$3s3p4p\,^4D$	151		272		439	
	78		154		265		423			108		194		314	
										65		117		188	
$3p3d\,^3P$	−78		−154	−98	−265	−239	−423	−374	$3s3p3d\,^4P$	−108		−194	−174.9	−314	−289
	−39		−77	−62	−133	−141	−211	−237		−65		−117	−117.8	−188	
$3p3d\,^3D$	39		77	51	133	83	211	117	$3s3p3d\,^4D$	50		91	49.7	146	80
	26		51	54	88	97	141	168		36		65	62.2	104	100
										22		39	52.9	63	103

The results of this analysis of the quartets were checked with the predictions of the theory of Goudsmit and Humphreys[8] with the very satisfactory results shown in Table XIV.

IV. General Considerations

This analysis has brought to light a large number of multiplet separations, whose value can also be predicted by the theory of Goudsmit and Humphreys[8]. Table XIV gives a comparison of the predicted and observed values. The predicted values are calculated on the assumption that the a_2 of their Eq. (3) is small enough to be neglected in comparison with A'. This is probably justified in cases such as these where the electron to which the a_2 applies is much less tightly bound than the electrons to which the A' refers. As is at once seen, the theory predicts the observed values with surprising accuracy, particularly when one considers the various approximations made in the calculation.

One other regularity that is brought out by this analysis is the uniformity of arrangement of the terms arising from a given configuration in isoelectronic ions of this row of the periodic system. Thus in every atom where the terms arising from the $3p4p$ configuration of a two-electron system, the $3s3p4p$ configuration of a three-electron system or the $(3s)^2 3p4p$ configuration of a four-electron system have been observed, the order of increasing term values is S, P, D. Likewise for the terms of the $3p3d$, $3s3p3d$ and the $(3s)^2 3p3d$ configurations the order is D, P, F for all cases except Si I and P II. In both of these cases other irregularities throw great doubt on the published identifications of the terms that are not in agreement with this arrangement. As might be expected from the symmetry of the eigenfunctions of s electrons, this indicates that the addition of s electrons has little effect on the relative positions of these levels. A similar regularity is found in the first row of the periodic table. In this case, however, the $2p3p$, $2s2p3p$ and $(2s)^2 2p3p$ configurations give uniformly the order P, S, D, while the $2p3d$, $2s2p3d$ and $(2s)^2 2p3d$ configurations yield P, D, F.

THE RED CN BAND SYSTEM

By F. A. Jenkins, Department of Physics
University of California

Yale K. Roots, Department of Physics
Findlay College

and

Robert S. Mulliken, Ryerson Physical Laboratory
University of Chicago

(Received November 17, 1931)

Abstract

Rotational structure of red CN bands. The rotational structure of the (4,1), (5,2), (6,1), (6,2), (7,2), (7,3) and (8,3) bands of this system is measured on plates from the first order of a 21-foot grating. To excite the spectrum, carbon tetrachloride vapor was mixed with active nitrogen. The lines of each band are arranged in eight branches, giving a structure characteristic of a $^2\Pi \rightarrow {}^2\Sigma$ transition in which the spin doubling in $^2\Sigma$ is small. Missing lines show the $^2\Pi$ state to be inverted. Good agreement is obtained for the constants of the lower state with those of the violet CN system. The rotational constants of the $^2\Pi$ state are: $A=-52.2$ cm^{-1}, $B_v=1.6990-0.01746\ (v+\frac{1}{2})$ cm^{-1}, $D_v=-[6.133+0.0127\ (v+\frac{1}{2})]\times 10^{-6}$ cm^{-1}, $I_e=16.28\times 10^{-40}$ g cm^2, $r_e=1.236\times 10^{-8}$ cm. The $^2\Pi$ terms are represented accurately by the Hill and Van Vleck formula. Microphotometer measurements of photographic densities in the 8,3 band are given, and agree qualitatively with the theory. They show the $^2\Pi_{3/2} \rightarrow {}^2\Sigma$ band to be stronger than the $^2\Pi_{1/2} \rightarrow {}^2\Sigma$ band.

Spin doubling and Λ-doubling. A rough evaluation of the difference $F_1''(K)-F_2''(K)=\gamma_0\ (K+\frac{1}{2})$ is possible, and gives $\gamma_0=+0.0071$ and 0.0082 and for $v''=3$ and 2, respectively. For the states $v'=4$, 5 and 8, the Λ-doubling is regular, and of the form recently discussed by Mulliken and Christy. We find $p_0=0.00621$, 0.00853, 0.01872, $q_0=-0.000252$, -0.000365 and -0.000435 for $v'=4$, 5 and 8.

Perturbations. Three strong perturbations are found in $v'=6$, in T_{1c} at $J=13\frac{1}{2}$, in T_{1d} at $J=25\frac{1}{2}$ and in T_{2d} at $J=27\frac{1}{2}$. These are exactly as expected theoretically from the three corresponding perturbations found in the violet system by Rosenthal and Jenkins, and from an extrapolation of the unperturbed levels. An anomalous Λ-doubling in $^2\Pi_{1/2}{}^{(7)}$ is explained as a perturbation, with the difference that here the perturbing levels of $^2\Pi_{1/2}{}^{(7)}$ and $a^2\Sigma^{(1^c)}$ do not cross, but merely approach closely.

Vibrational structure. From measurements of the R_2 heads of 17 other bands, and correction to origins, the following expression is obtained for band origins:

$$\nu=11{,}043.20+1788.66\ (v'+\tfrac{1}{2})-12.883\ (v'+\tfrac{1}{2})^2-2068.79\ (v''+\tfrac{1}{2})+13.176\ (v''+\tfrac{1}{2})^2.$$

Perturbations of the band origins by 1 or 2 cm^{-1} occur for $v'=6$ and 7, and are evidently of similar origin to the rotational perturbations in these states. The vibrational numbering used here for the $^2\Pi$ state is that of Asundi and Ryde. This numbering, hitherto in doubt, has now been definitely established by a comparison of the observed vibrational intensity relations with those predicted by the wave mechanics with the method of Condon.

Introduction

THE extensive system of "cyanogen" bands which has its maximum intensity in the orange and red was first measured in vacuum-tube spectra of compounds containing carbon and nitrogen.[1] In the first studies of Ray-

[1] H. Kayser, "Handbuch der Spectroscopie," Vol. 7, pp. 135–7.

leigh[2] and of Rayleigh and Fowler[3] on the spectra excited by active nitrogen, it was discovered that carbon compounds produce a bright cyanogen spectrum exceptionally free from impurities. The intensity of the red CN system relative to the violet system varies greatly with the compound used. In particular, the halogen compounds, such as chloroform and carbon tetrachloride, were found to give the red system such predominance that the glow produced is orange, instead of the usual lilac color. Since the bands of the red system are sharp and strong with this mode of excitation, Fowler and Shaw[4] used active nitrogen as a source in obtaining the first accurate measurements of the heads of these bands. The system was also identified in the carbon arc in air, where it is responsible for most of the luminosity in the longer wave-length part of the visible spectrum. The appearance of the bands, however, is very different in this source. The heads are weak and masked by a great deal of overlapping rotational structure from adjacent bands. On the contrary, in the vacuum-tube and particularly in active nitrogen a large number of distinctly separated bands are seen, extending from the blue to the extreme red. The system has been traced as far as λ8134 by Croze[5], and to λ9400 by Asundi and Ryde.[5] Probably it extends far into the infrared. Each band shows four heads, degraded toward the red, that of shortest wave-length being very weak relative to the others.

As part of his pioneer work on the vibrational structure of band spectra, Heurlinger[6] assigned vibrational quantum numbers to the red system, and gave an equation for heads. The constants of the lower state agreed with those of the lower state of the violet CN bands, showing that these two band systems result from transitions to a common electronic configuration. Recently the vibrational numbering of the upper state of the red system has been changed as a result of the work of Asundi and Ryde.[5] The rotational structure of the violet system, for which accurate measurements[7] have been available since the early work of Kayser and Runge, was one of the first to which Heurlinger applied the quantum theory, and its interpretation is now well understood through the work of Kratzer, Dieke, Birge, and Mulliken.[8,9,10] The electronic transition is designated $^2\Sigma \rightarrow {}^2\Sigma$. The lower state of the red bands is therefore $^2\Sigma$, and is in all probability the normal state of CN. Evidence for this appears in the fact that the violet system can be self-reversed in the electric furnace.[11] The upper state of the red system is known to be $^2\Pi$, from various considerations including a study of the gross structure of the bands. The rotational analysis of the red system has not hitherto been

[2] R. J. Strutt, Proc. Roy. Soc. **85A,** 219 (1911); **88A,** 539 (1913).

[3] R. J. Strutt and A. Fowler, Proc. Roy. Soc. **86A,** 105 (1912).

[4] A. Fowler and H. Shaw, Proc. Roy. Soc. **86A,** 118 (1912).

[5] F. Croze, Comptes Rendus **150,** 1672 (1910). R. K. Asundi and J. W. Ryde, Nature **124,** 57 (1929).

[6] T. Heurlinger, Zeits. f. Physik **1,** 82 (1920).

[7] W. Jevons, Proc. Roy. Soc. **112A,** 407 (1926). Summary.

[8] A. Kratzer, Ann. d. Physik **71,** 72 (1923).

[9] R. T. Birge, Bull. Nat. Res. Council, No. 57, pp. 181–6.

[10] R. S. Mulliken, Phys. Rev. **30,** 138 (1927).

[11] A. S. King, Astrophys. J. **53,** 161 (1921).

attempted, perhaps because of the extreme complexity with which it is developed in the arc, from which high-dispersion spectra are most easily obtained. The analysis is nevertheless desirable, in order to study the properties and constants of the $^2\Pi$ state. A particular feature of this state requiring further investigation is the perturbation of the rotational levels $^2\Pi^{(6)}(J)$, which was discovered by Miss J. E. Rosenthal and one of the writers[12] in one of the first verifications of Kronig's theory of perturbations in band spectra. The present paper[13] contains the results of our analysis of the rotational structure, which was made possible by the use of grating plates of the red system as produced by active nitrogen.

Spectrograms

The source of light was the bright orange-colored flame obtained when carbon tetrachloride vapor is introduced slowly into a continuously flowing stream of active nitrogen. The rate of introduction was adjusted by a capillary leak to obtain the best intensity. Purification of the nitrogen previous to its activation was necessary, and consisted primarily in the removal of oxygen by passage through a tube of moist white phosphorous, and subsequent thorough drying. The form of the discharge tube and reaction chamber was smilar to that used in previous work with this type of excitation,[14] as were the conditions of pressure, rate of flow of nitrogen, etc. A detailed description of these will therefore be omitted here. As dispersing apparatus, the 21-foot Harvard grating was used in the first and second orders. Four sets of plates were obtained, covering the region 3500–8000A, each with two iron arc comparison spectra to eliminate the possibility of false shifts. Eastman Speedway plates were used for the region 3500–4900, Astronomical Green Sensitive plates for 4900–5800, Ilford panchromatic plates hypersensitized in ammonia for 5800–6850, and Speedway plates bathed in dicyanin for still longer wavelengths. Exposures were from 4 to 10 hours, constant temperature being maintained in the grating room.

Only the first order plates, with a dispersion varying from 1.91 to 1.95A per mm, were strong enough for satisfactory measurement.[15] The wavelengths were measured with reference to the international iron arc standards, from plates showing no relative shift of the two iron spectra. The complete rotational structure in seven of the strongest bands was measured, and also the band heads in 17 fainter ones. The agreements later obtained in the application of the combination principle indicate an accuracy of somewhat better than 0.01A for the measurements of the sharper lines.

[12] J. E. Rosenthal and F. A. Jenkins, Proc. Nat. Acad. Sci. **15,** 381 (1929).

[13] Preliminary report: F. A. Jenkins, Y. K. Roots and R. S. Mulliken, Phys. Rev. **38,** 1075 (1931). In this Letter we unfortunately used an incorrect v numbering in the $^2\Pi$ state, having overlooked the work of Asundi and Ryde.[5] We are indebted to Dr. W. Jevons for calling our attention to this. In the present account we have used the correct v numbering (cf. last paragraph of this paper.)

[14] For example, F. A. Jenkins and H. de Laszló, Proc. Roy. Soc. **122A,** 103 (1929).

[15] The (6,1), (6,2), and (7,3) bands were measured by the second writer (Y.K.R.) with a comparator at New York University, and the (4,1), (5,2), (6,2), and (8,3) bands with a Société Génévoise comparator at the University of California by the first writer (F.A.J.).

Rotational Structure

Term-formulas and permitted transitions

The spectral terms involved in $^2\Pi \rightarrow {}^2\Sigma$ bands, with an inverted $^2\Pi$ state intermediate between case (*a*) and case (*b*), are essentially as given by the following equations:[16]

$$\left.\begin{aligned}
{}^2\Pi_{3/2}: T_1'(J) &= T_e' + G' + B_v'\left\{(J+\tfrac{1}{2})^2 - 1 - \tfrac{1}{2}\left[4(J+\tfrac{1}{2})^2 - 4A/B_v' + A^2/B_v'^2\right]^{1/2} + \overline{G^2}\right\} + \Phi_i(J) + D_v'J^4 + \cdots \\
{}^2\Pi_{1/2}: T_2'(J) &= T_e' + G' + B_v'\left\{(J+\tfrac{1}{2})^2 - 1 + \tfrac{1}{2}\left[4(J+\tfrac{1}{2})^2 - 4A/B_v' + A^2/B_v'^2\right]^{1/2} + \overline{G^2}\right\} + \Phi_i(J) + D_v'(J+1)^4 + \cdots \\
{}^2\Sigma,\ J = K+\tfrac{1}{2}: T_1''(J) &= T_e'' + G'' + \tfrac{1}{2}\gamma K + B_v''(K+\tfrac{1}{2})^2 + D_v''(K+\tfrac{1}{2})^4 + \cdots \\
&= T_e'' + G'' + \tfrac{1}{2}\gamma(J-\tfrac{1}{2}) + B_v''J^2 + D_v''J^4 + \cdots \\
{}^2\Sigma,\ J = K-\tfrac{1}{2}: T_2''(J) &= T_e'' + G'' - \tfrac{1}{2}\gamma(K+1) + B_v''(K+\tfrac{1}{2})^2 + D_v''(K+\tfrac{1}{2})^4 + \cdots \\
&= T_e'' + G'' - \tfrac{1}{2}\gamma(J+\ ) + B_v''(J+1)^2 + D_v''(J+1)^4 + \cdots.
\end{aligned}\right\} \quad (1)$$

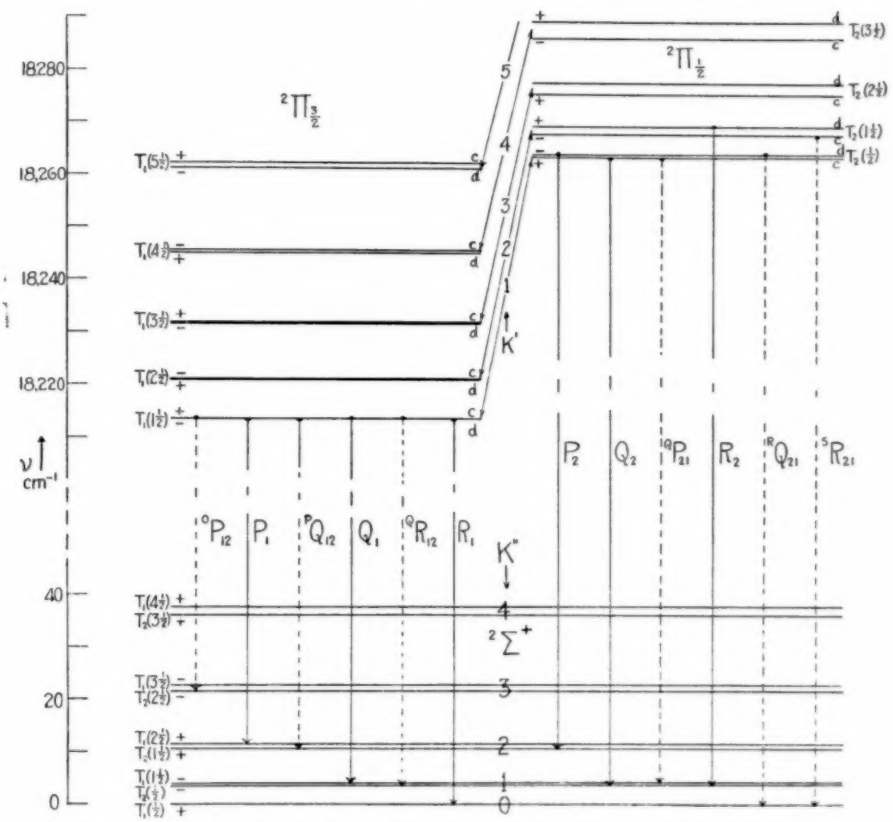

Fig. 1. Term-scheme for the 8,3 red CN band. The transition giving the first line in each branch is indicated by a vertical arrow. Satellite branches ($\Delta K \neq \Delta J$), and those with $\Delta K = 2$, are shown by dashed arrows. The spin doubling in $^2\Sigma$, and the Λ-doubling in $^2\Pi$, are magnified 50 times.

[16] **R. S. Mulliken,** Rev. Mod. Phys. **3,** 130 (1931); **2,** 109 (1930), with $\Lambda = 1$ for the $^2\Pi$ state.

For the $^2\Pi$ terms, A is the spin coupling constant, which in doublet states represents the electronic doublet separation for zero rotation. The small uncoupling term $\Phi_i(J)$ represents the splitting of each of the $^2\Pi$ rotational levels into two, designated T_c and T_d. Explicit equations of a somewhat complicated form can be given[17] for this term; they will be used below in the discussion of Λ-*doubling*. The additive constants $B_v(\overline{G}^2-1)$ cannot be found from the spectrum, since one can only evaluate the differences between terms. In the equation for the $^2\Sigma$ terms, the small constant γ measures the interaction of the electron spin with the magnetic field developed by the rotation of the molecule. It gives rise to a small separation of the two levels with $J=K\pm\frac{1}{2}$ associated with each value of K. Evidence for this in the present case will be considered later, under *spin doubling*.

The positive and negative symmetry properties of the terms $T(J)$ are important in determining the allowed transitions. The lower state in the present case is probably $^2\Sigma^+$, requiring a $+$ designation for the lowest rotational level ($K=0$).[18] Applying the two selection rules $+\rightleftarrows-$ and $J\rightleftarrows J$, $J\pm1$, the $+$ and $-$ character of all the $^2\Pi$ rotational levels is easily found.[18] As shown in Fig. 1, there are twelve types of transitions allowed, giving rise to twelve branches in any one band. These are

$$
\begin{array}{cc}
^2\Pi_{3/2}\rightarrow{}^2\Sigma & ^2\Pi_{1/2}\rightarrow{}^2\Sigma \\
R_1(J)=T_{1d}'(J+1)-T_1''(J) & {}^SR_{21}(J)=T_{2c}'(J+1)-T_1''(J) \\
{}^QR_{12}(J)=T_{1c}'(J+1)-T_2''(J) & R_2(J)=T_{2d}'(J+1)-T_2''(J) \\
Q_1(J)=T_{1c}'(J)-T_1''(J) & {}^RQ_{21}(J)=T_{2d}'(J)-T_1''(J) \\
{}^PQ_{12}(J)=T_{1d}'(J)-T_2''(J) & Q_2(J)=T_{2c}'(J)-T_2''(J) \\
P_1(J)=T_{1d}'(J-1)-T_1''(J) & {}^QP_{21}(J)=T_{2c}'(J-1)-T_1''(J) \\
{}^OP_{12}(J)=T_{1c}'(J-1)-T_2''(J) & P_2(J)=T_{2d}'(J-1)-T_2''(J).
\end{array}
\qquad (2)
$$

In the bands under consideration, the 3/2-form branches ${}^SR_{21}$ and ${}^OP_{12}$, having $\Delta K=2$, are very weak, and could be measured only for the strongest bands. Also, since the separation of the terms $T_1''(K)$ and $T_2''(K)$ is very small, the $\frac{1}{2}$-form satellite branches could not be resolved from the corresponding main branches. As a result, the branches coalesce in pairs, as indicated by the brackets of Eqs. (2). Only eight branches are therefore measured for the strong bands, and six for the weaker ones.

Wave-numbers of band-lines

Table I contains the wave-numbers in vacuum of all the measured lines assigned to the band structure. For each branch which forms a head, the wave-length in I.A. of the head is given at the top of the appropriate column. In designating the branches in which coalescence occurs, the symbol of the satellite branch is omitted for brevity, although at low values of K it may

[17] R. S. Mulliken and A. Christy, Phys. Rev. **38**, 87 (1931).

[18] Reference 17, p. 103.

TABLE I

	4, 1 band λ 6332.159			λ6347.036	λ6355.126	
K''	R_2	Q_2	P_2	R_1	Q_1	P_1
0	15,785.52	—	—		—	—
1	786.77	15,781.69	—		15,731.00	—
2	787.64	779.04		15,742.35	731.22	
3	788.04	776.40	15,768.03	745.38	731.00	15,719.79
4	788.04	773.00	761.39	747.63	730.24	716.06
5	787.64	769.27	754.33	749.35	728.84	711.48
6	786.77	765.12	746.86	750.47	726.83	706.33
7	785.52	760.52	738.86	751.05	724.27	700.64
8	783.80	755.50	730.60	751.05	721.09	694.28
9	781.69	750.08	721.84	750.47	717.35	687.38
10	779.04	744.15	712.67	749.35	713.07	679.90
11	776.01	737.79	702.99	747.63	708.20	671.84
12	772.46	731.00	692.96	745.38	702.78	663.26
13	768.53	723.78	682.46	742.61	696.82	654.10
14	764.04	716.06	671.44	739.26	690.25	644.33
15	759.19	707.88	660.04	735.37	683.23	634.24
16	753.76	699.26	648.06	731.00	675.60	623.30
17	747.90	690.25	635.75	725.99	667.47	611.95
18	741.60	680.61	622.92	720.44	658.78	600.14
19	734.76	670.57	609.60	714.37	649.54	587.68
20	727.46	660.04	595.82	707.88	639.76	574.68
21	719.79	649.06	581.55	700.64	629.56	561.20
22	711.48	637.63	566.96	692.78	618.73	
23	702.78	625.63	551.74		607.40	
24	693.45	613.13			595.53	
25		600.14			583.18	
26		586.84			570.29	
27					566.88	

	5, 2 band λ6478.422			λ6494.103	λ6502.318	
K''	R_2	Q_2	P_2	R_1	Q_1	P_1
0	15,428.94	—	—		—	—
1	430.25	15,425.44	—	15,382.32	15,374.70	—
2	431.10	422.94		385.75	374.89	15,367.50
3	431.55	422.03	15,411.74	388.74	374.70	363.86
4	431.55	416.72	405.19	390.86	373.90	359.81
5	431.10	412.96	398.19	392.58	372.48	355.33
6	430.25	408.80	390.86	393.76	370.45	350.19
7	428.94	404.22	382.88	394.35	367.86	344.48
8	427.17	399.21	374.70	394.35	364.73	338.18
9	424.99	393.76	365.89	393.76	360.96	331.30
10	422.34	387.86	356.68	392.58	356.68	323.89
11	419.26	381.51	347.12	390.99	351.81	315.86
12	415.72	374.70	337.05	388.58	346.40	307.26
13	411.74	367.50	326.54	385.75	340.41	298.15
14	407.24	359.81	315.67	382.32	333.89	288.49
15	402.26	351.65	304.23	378.38	326.83	278.22
16	396.89	343.00	292.37	373.90	319.22	267.45
17	390.86	333.89	280.06	368.94	311.07	256.16
18	384.65	324.31	267.26	363.39	302.42	244.32
19	377.85	314.30	254.03	357.28	293.18	231.92
20	370.45	303.77	240.25	350.66	283.45	219.02
21	362.70	292.77	226.04	343.56	273.17	205.51
22	354.32	281.29	211.37	335.86	262.36	191.55
23	345.54	269.32	196.19	327.64	251.06	177.09
24	336.28	256.87	180.54	318.94	239.22	162.12
25	326.54	243.97		309.67	226.85	146.53
26		230.58		299.93	214.00	
27		216.62			200.63	
28		202.18			186.75	
29		187.27			172.51	

TABLE I. (*Continued*).

6, 1 band

K''	λ5232.629 $^{S}R_{21}$	λ5239.288 R_2	Q_2	P_2	λ5250.017 R_1	λ5254.869 Q_1	P_1	$^{O}P_{12}$
0			—	—	19,028.50	—	—	
1		19,080.52	19,075.67	—	032.33	19,024.69	—	
2		081.27	072.99	19,068.50	035.74	024.69	19,017.18	*Not*
3	19,095.99	081.27	069.89	061.75	038.44	024.69	013.61	*Observed*
4	098.77	081.27	066.60	055.23	040.40	023.36	009.53	
5	101.25	080.17	062.28	047.67	041.63	021.59	004.61	
6	103.24	078.88	057.66	039.92	042.27	019.17	18,999.13	
7	104.98	077.06	052.60	031.51	042.27	016.10	992.96	
8	105.55	074.70	047.02	022.48	041.63	012.39	986.05	
9	105.55	071.86	040.93	013.09	040.40	007.99	978.65	
10	105.55	068.50	034.34	003.15	038.44	003.15	970.55	
11	104.98	064.58	027.22	18,992.96	036.00	18,997.72	961.78	
12	103.75	060.19	019.63	982.46	032.33	*p* 991.98 986.43	952.49	
13	102.14	055.25	011.46	971.09	029.10	*p* 987.45 982.46	942.45	
14	099.56	049.79	002.86	959.34	024.69	976.18	931.82	
15	096.85	043.73	18,993.58	946.79	019.63	968.01	920.63	
16	093.67	037.22	983.78	934.02	014.14	960.06	908.82	
17		030.10	973.50	920.63	007.99	950.13	896.25	
18		022.48	962.69	906.49	001.17	940.24	883.33	
19		014.14	951.31	891.88	18,993.58	929.08	869.67	
20		005.48	939.38		986.05	918.56	855.48	
21		18,996.27	926.88		976.18	906.81	840.59	
22		986.43	913.88			894.45	825.37	
23			900.31			881.54		
24			886.19			868.01		
25			871.47					
26			856.24					
27			840.59					
28			824.08					

6, 2 band

K''	λ5849.347 $^{S}R_{21}$	λ5858.170 R_2	Q_2	P_2	λ5871.329 R_1	λ5877.643 Q_1	P_1	$^{O}P_{12}$
0	17,068.25	17,063.37	—	—	17,012.36	—	—	—
1	072.57	064.49	17,059.57	—	016.24	17,008.62	—	—
2	076.45	065.27	057.06	17,052.23	019.48	008.92	17,001.02	—
3	080.06	065.46	054.04	045.95	022.44	008.62	16,997.61	16,990.39
4	083.10	065.27	050.64	039.28	024.48	007.65	993.58	983.26
5	085.66	064.65	046.80	031.94	025.97	006.06	989.02	975.12
6	087.79	063.55	042.38	024.48	026.87	003.82	983.88	966.85
7	089.41	061.98	037.49	016.39	027.21	001.02	977.84	957.92
8	090.56	059.91	032.21	007.88	026.87	16,997.61	971.29	948.08
9	091.20	057.40	026.48	16,998.91	025.97	993.58	964.16	938.04
10	091.38	054.35	020.23	989.48	024.48	989.02	956.37	927.17
11	091.20	050.89	013.50	979.48	022.44	983.88	948.08	915.75
12	090.38	046.80	006.31	969.12	019.48	*p* 978.63 973.78	939.10	903.84
13	089.02	042.38	16,998.58	958.20	016.24	*p* 974.53 969.60	929.51	891.35
14	087.24	037.49	990.39	946.83	012.36	963.53	919.44 *p*	878.63
15	084.93	031.94	981.72	934.84	007.88	956.19	908.75 *p*	862.44
16	082.12	025.97	972.53	922.54	002.83	948.08	897.49	
17	078.79	019.48	962.83	909.80	16,997.26	939.41	885.60	
18	074.87	012.36	952.62	896.45	991.09	930.13	873.25	
19	070.53	004.93	941.91	882.51	984.41	920.26	860.27	
20	065.46	16,996.90	930.69	868.13	977.22	909.80	846.73	
21	060.94	988.39	918.98	853.21 *p*	969.60	898.86	832.67	
22		979.48	906.72	837.72 *p*	961.51	887.30	818.14	
23		969.86	893.95	*p*	954.66	875.19		
24		*p* 959.93	880.70			862.44		
25		*p* 949.81	866.85			849.21		
26			852.54			835.37		
27			837.72			820.93		

TABLE I. (*Continued*).

	7, 2 band							
	λ5347.480	λ5354.103			λ5365.018	λ5369.919		
K''	$^SR_{21}$	R_2	Q_2	P_2	R_1	Q_1	P_1	$^cP_{12}$
0	18,674.35	18,669.77	—	—	18,620.92	—	—	
1	678.89	671.08	18,666.10	—	624.60	18,616.72	—	
2	682.75	671.86	663.48	18,659.48	627.62	617.09	18,609.57	*Not*
3	686.11	672.09	660.35	652.63	630.23	616.72	605.98	*Observed*
4	688.89	671.86	656.73	646.14	632.14	615.56	601.78	
5	691.20	671.08	652.63	638.71	633.46	613.74	596.98	
6	693.07	669.77	648.01	631.19	634.10	611.31	591.48	
7	694.35	667.96	642.93	622.81	634.10	608.17	585.31	
8	595.21	665.64	637.31	614.08	633.46	604.47	578.48	
9	695.21	662.83	631.19	604.95	632.14	600.04	571.04	
10	695.21	659.48	624.60	595.09	630.23	595.09	562.97	
11	694.35	655.55	617.50	584.91	627.61	589.43	554.24	
12	693.07	651.15	609.89	574.23	624.35	583.16	544.87	
13	691.20	646.14	601.78	562.96	620.50	576.31	534.88	
14	688.89	640.70	593.13	551.10	616.02	568.69	524.27	
15		634.62	583.94	538.74	610.94	560.61	513.03	
16		628.04	574.23	525.88	605.21	551.86	501.20	
17		620.92	564.02	512.45	598.98	542.52	488.73	
18		613.25	553.24	498.50	592.09	532.56	475.66	
19		604.95	541.94	483.95	584.57	521.99	461.99	
20		596.21	530.06	468.90	576.31	510.81	447.74	
21		586.89	517.62	453.33	567.80	499.04	432.78	
22		576.97	504.67	437.14	558.48	486.69	417.36	
23		566.59	491.14	420.42	548.55	473.73	401.31	
24		555.52	477.06	403.16	538.06	460.17		
25		543.89	462.42		526.94	446.01		
26		531.72	447.52		515.26	431.34		
27		518.97	431.34		502.92	415.93		
28		505.66	415.09		490.11	400.04		
29		491.67			476.61			
30					462.41			

	7, 3 band					
	λ5992.645			λ6006 053	λ6012.472	
K''	R_2	Q_2	P_2	R_1	Q_1	P_1
0	16,680.21	—	—	—	—	—
1	681.45	16,676.51	—	16,634.86	16,627.19	—
2	682.37	673.90		638.18	627.50	16,620.29
3	682.51	670.86		640.83	627.19	616.48
4	682.37	667.36	16,656.60	643.06	626.18	611.90
5	681.87	663.41	649.14	644.35	624.57	607.76
6	680.77	659.05	642.33	645.03	622.31	602.46
7	679.19	654.17	633.97	645.27	619.46	596.55
8	677.16	648.88	625.46	645.03	615.99	589.97
9	674.61	643.06	616.70	643.93	611.90	582.84
10	671.63	636.85	607.19	642.33	607.19	575.10
11	668.13	630.07	597.52	640.14	601.98	566.83
12	664.13	622.92	587.23	637.32	596.13	557.91
13	659.65	615.25	576.31	633.97	589.67	548.28
14	654.64	607.19	565.01	630.07	582.69	538.18
15	649.14	598.42	553.17	625.46	575.10	527.49
16	643.06	589.29	540.88	620.29	566.83	516.19
17	636.60	579.60	528.03	614.63	558.11	504.35
18	629.59	569.47	514.67	608.30	548.75	491.90
19	621.97	558.82	500.90		538.88	
20	613.87	547.66	486.50		528.41	
21	605.30	535.97			517.37	
22		523.77			505.78	
23		511.04			493.63	
24		497.83			480.90	

TABLE I. (*Continued*).

	8, 3 band							
	λ5466.306	λ5473.289			λ5484.921	λ5489.950		
K''	$^{S}R_{21}$	R_2	Q_2	P_2	R_1	Q_1	P_1	$^{O}P_{12}$
0	18,268.45	18,263.65	—	—	18,213.58	—	—	—
1	272.63	264.76	18,259.95	—	217.45	18,209.61	—	—
2	276.44	265.49	257.36		220.59	210.06	18,202.61	—
3	279.74	265.49	254.30	18,246.52	223.17	209.61	199.07	
4	282.55	265.15	250.74	239.65	225.03	208.43	194.91	18,184.26
5	284.86	264.28	246.70	232.44	226.24	206.65	190.08	176.67
6	286.58	262.91	242.13	224.65	226.75	204.25	184.61	167.83
7	287.82	261.03	237.07	216.57	226.75	201.09	178.51	158.87
8	288.57	258.64	231.51	207.82	225.99	197.29	171.69	149.11
9	288.82	255.72	225.44	198.60	224.65	192.96	164.23	138.64
10	288.57	252.28	218.85	188.80	222.64	187.92	156.17	127.57
11	287.82	248.34	211.73	178.51	220.01	182.26	147.49	115.83
12	286.37	243.85	204.07	167.83	216.75	175.98	138.12	103.55
13	284.45	238.84	195.97	156.55	212.86	169.08	128.16	090.52
14	281.94	233.28	187.27	144.68	208.43	161.55	117.57	076.86
15	279.03	227.18	178.03	132.37	203.27	153.40	106.39	062.59
16	275.51	220.59	168.28	119.48	197.50	144.68	094.60	047.84
17	271.36	213.36	157.98	106.10	191.20	135.29	082.14	032.40
18	266.77	205.61	147.15	092.08	184.26	125.31	069.08	016.28
19		197.29	135.77	077.62	176.67	114.76	055.42	17,999.73
20		188.44	123.83	062.59	168.53	103.55	041.23	982.66
21		179.03	111.32	047.02	159.77	091.78	026.37	964.64
22		169.08	098.28	030.87	150.43	079.41	010.95	946.31
23		158.53	084.68	014.19	140.46	066.45	17,994.96	927.11
24		147.49	070.55	17,996.94	129.90	052.89	978.29	907.48
25		135.77	055.84	979.13	118.77	038.76	961.07	
26		123.58	040.59	960.85	107.01	024.02	943.27	
27		110.77	024.77	941.89	094.60	008.64	924.85	
28		097.39	008.36	922.42	081.74	17,992.74	905.88	
29		083.47	17,991.42	902.40	068.23	976.25	886.26	
30		069.08	973.93	881.75	18,054.12	959.15	866.09	
31		053.93	955.83	860.66	039.40	941.43		
32		038.30	937.20		024.02	923.16		
33		022.07	917.96		008.36	904.29		
34		005.26	898.17			884.85		
35		17,987.83	877.89			864.82		
36		969.69						

contribute a considerable part of the intensity. The first wave-number in the column headed R_2 should be denoted $^{R}Q_{21}(0)$, since the line $R_2(0)$ is missing (cf. Fig. 1). Each branch in the stronger bands has been found to begin with the value of K'' expected from Fig. 1, with the possible exception of the P_2 branch, the first lines of which are extremely weak. Thus in the 8,3 band, the line $P_2(2)$ was not found, although its expected position is free from other lines. On the whole, however, the evidence from the missing lines is definite, and shows that the $^2\Pi$ state must be inverted, since there is a greater number of missing lines in the low-frequency sub-band.

The appearance of the bands under high dispersion is shown in Fig. 2, in which one typical regular band, 8,3, and one which shows marked perturba-

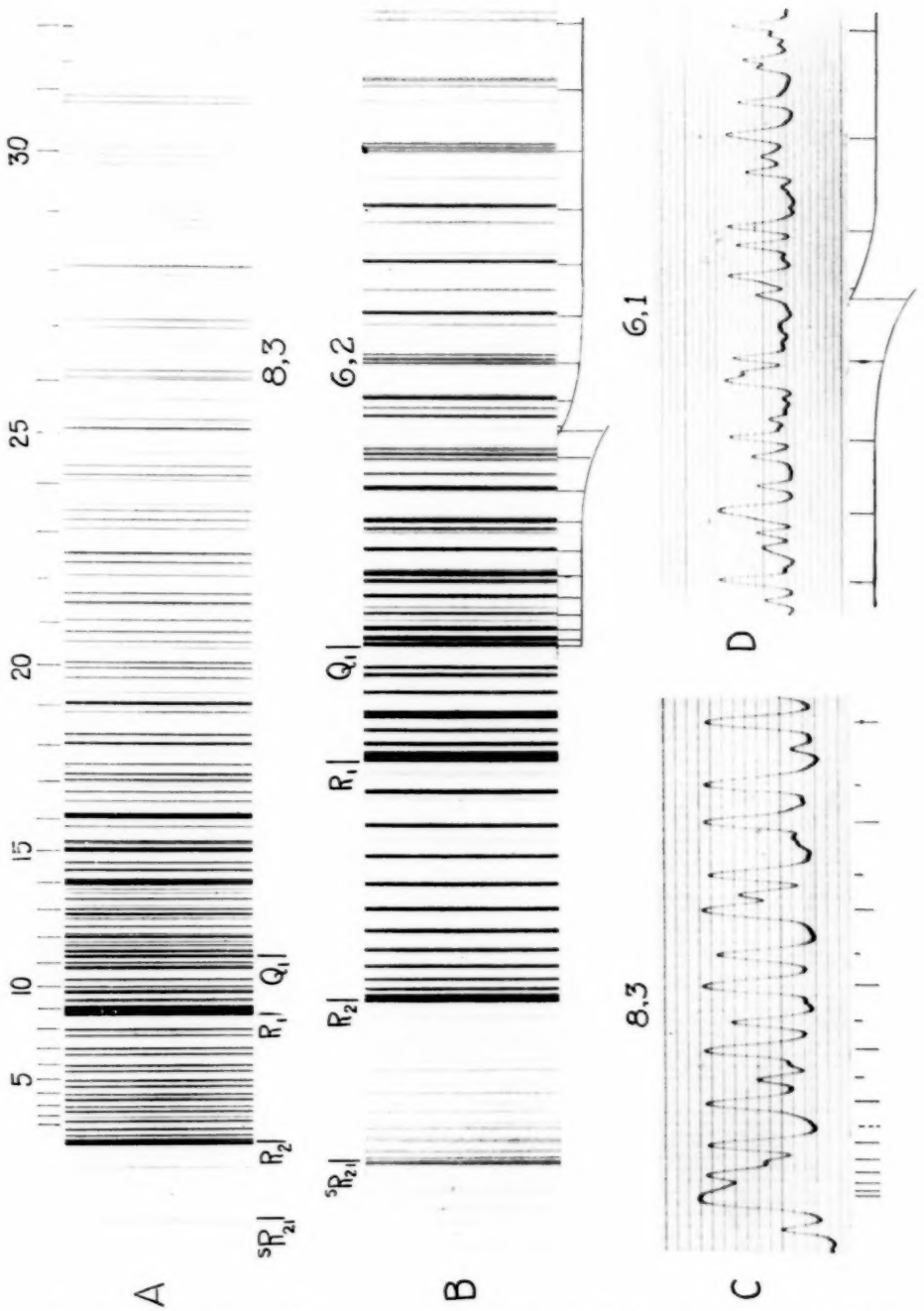

Fig. 2. Bands of the red CN system. *A*. The 8,3 band. The four heads are marked below. Above, the Q_2 lines are designated, and numbered with the values of K''. Wave-lengths increase to the right. *B*. The 6,2 band, enlarged somewhat more than the 8,3 band in *A*. The perturbed branch Q_1 is marked below. Displacements of the lines toward the red or toward the violet are indicated by a rise or fall of the otherwise horizontal connecting line. *C*. Microphotometer curve of the first part of the 8,3 band. The position of the single missing line between the two strong branches R_2 (long lines) and Q_2 (short lines) is indicated by the dotted line. *D*. Microphotometer curve of the main perturbation in the 6,1 band, corresponding to that shown in *B* for the 6,2 band.

tions, 6,2, are reproduced. The irregularities and "extra" lines which occur in the regions of perturbations are designated in Table I by p and will be considered in detail below. In Fig. 2c, a microphotometer trace is given of the first part of the 8,3 band, to show the single missing line occurring between ${}^{R}Q_{21}(0)$ and $Q_2(1)$. A Fortrat diagram of this band is given in Fig. 3. The 8,3 band was chosen as a representative strong band in which there is a minimum of overlapping, and which contains no perturbations.

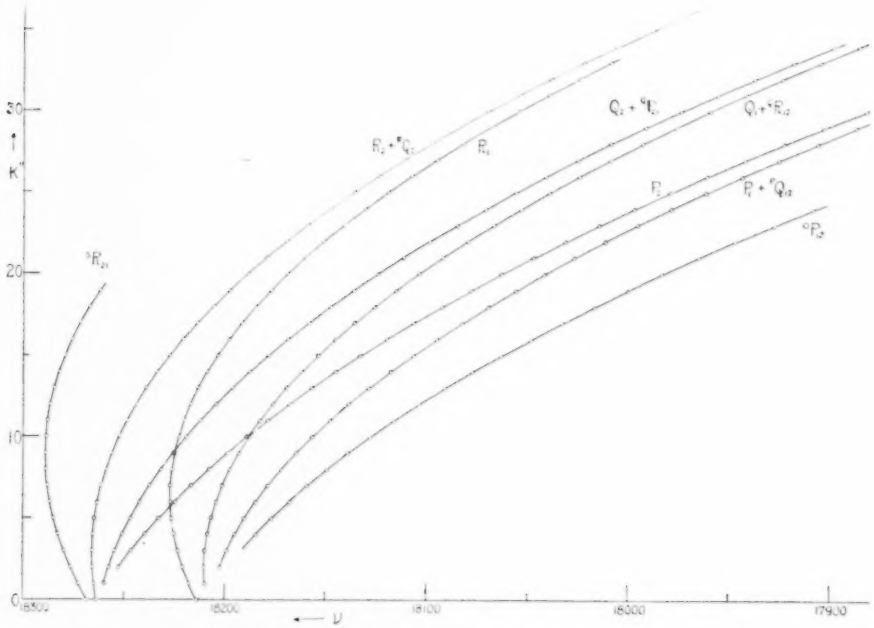

Fig. 3. Fortrat diagram of the 8,3 band. The circles are experimental values, while the curves have been drawn according to the theoretical Eq. (1), using the constants given in Table IV. The largest deviation from experiment is one-tenth the diameter of one of the small circles, hence less than the accuracy of drawing the curves.

Line intensities

Instead of giving visual intensity estimates of all the lines, as is usual, we have preferred to study the intensity relations in the typical 8,3 band in a more quantitative way. The original plates were not calibrated with density marks, and since they were color-sensitized the form of the characteristic curves is very uncertain. Considerable information can, however, be obtained from a study of the photographic densities of the lines, since this at least gives the proper order of intensities. Fig. 4 gives the density, or logarithm of the opacity, of every unblended line in the 8,3 band, measured on a green sensitive plate which was developed about 4 minutes in metol-hydroquinone. The opacities of the line centers were obtained with a Zeiss-Koch recording microphotometer, having the slit much narrower than the width of a line.

The intensities of the several branches should be given by the theoretical

formulas derived by Hill and Van Vleck.[19] Qualitatively, the observed relations are those to be expected if the superposition of the satellite branches on the corresponding main branches is taken into account. The $^2\Pi$ state is intermediate between Hund's case (*a*) and case (*b*), with the result that for very low J the case (*a*) intensity relations are approximated, while for large rotation, we have very nearly case (*b*). In strict case (*a*) the twelve branches of Eqs. (2) are of comparable intensities, the order being $Q_i > R_i > P_i$. In case (*b*), however, the $^SR_{21}$ and $^OP_{12}$ branches, with $\Delta K = 2$, are strictly forbidden, and the satellites $^QR_{12}$, $^PQ_{12}$, $^RQ_{21}$ and $^QP_{21}$ with $\Delta K \neq \Delta J$, are very weak. In Fig. 4 it will be seen that the $^SR_{21}$ and $^OP_{12}$ branches are weakest of all, and

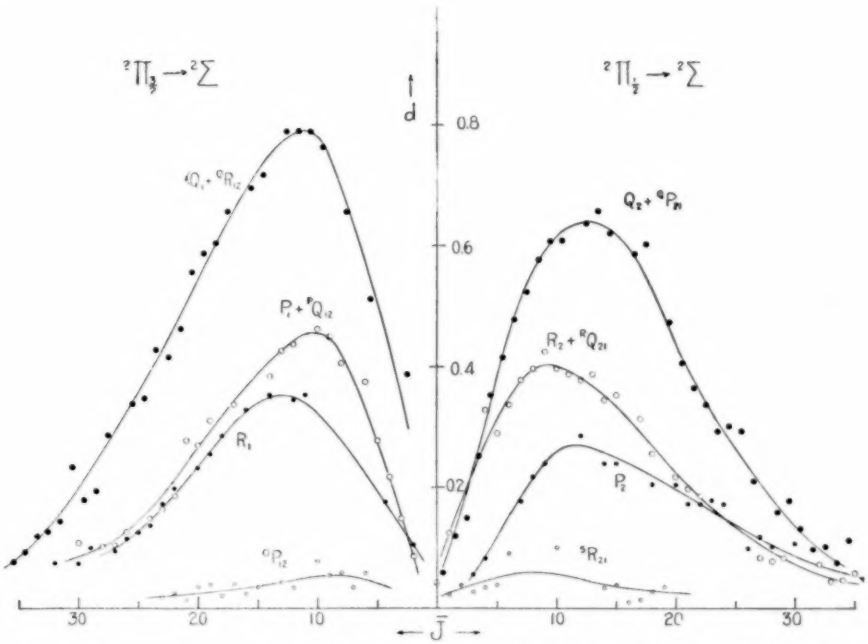

Fig. 4. Photographic densities in the 8,3 band. The densities d of all lines which are not known to be blended are plotted against $\bar{J}$, the mean J in the upper and lower states.

fade out very soon with increasing J. However, at the lowest values of J, the $^SR_{21}$ branch is fairly strong, and in several bands its first line, $^SR_{21}(0)$ could easily be measured. This results from the fact that for very small rotation case (*a*) is approached. In the branches in which coalescence with a satellite occurs, we find at first a very rapid rise of intensity, where the satellite branch is strong, then a more gradual falling off after the satellite has decreased to the very low intensity characteristic of case (*b*). The R_1 and P_2 branches, on the other hand, are weaker at first, but at the highest J have become practically equal to R_2 and P_1, respectively, as the intensity formulas for case (*b*) require. Fig. 4 shows that the total intensity of $^2\Pi_{3/2} \rightarrow {}^2\Sigma$ is distinctly greater

[19] E. L. Hill and J. H. Van Vleck, Phys. Rev. **32**, 267 (1928). Cf. also the review by R. S. Mulliken, Rev. Mod. Phys. **3**, 94 (1931), sections *J2c*, *J2d*, *J3*, and Fig. 29.

than that of $^2\Pi_{1/2} \rightarrow {}^2\Sigma$. This appears to be in agreement with the intensity equations of Hill and VanVleck if the $^2\Pi_{1/2}$ and $^2\Pi_{1\ 1/2}$ levels are initially about equally populated.[19]

Rotational terms of the $^2\Sigma$ state

Because of the double character of all the rotational terms in $^2\Pi$ and $^2\Sigma$ states, the combination principle as applied within any one band does not yield more than a single value for a given term-difference. Exact agreements are expected only when an identical term-difference is evaluated from two bands with a common vibrational state. This requirement will be found to be fulfilled for all of the bands in Table I. As an example, we quote in Table II the values of the differences

$$R_1(K-1) - P_1(K+1) = \Delta_2 F_1''(K),$$

TABLE II. *Combination differences $\Delta_2 F_1''$ for the $^2\Sigma$ state.*

K	$^2\Pi \rightarrow {}^2\Sigma$ 4, 1	6, 1	$^2\Sigma \rightarrow {}^2\Sigma$ 1, 1, (U &P)	0, 1(H)	$^2\Pi \rightarrow {}^2\Sigma$ 5, 2	6, 2	$^2\Sigma \rightarrow {}^2\Sigma$ 1, 2 (H)
3	—	18.72	18.85	18.74	18.46	18.63	18.82
4	26.29	26.21	26.04	26.21	25.94	26.25	26.09
5	33.90	33.83	33.63	33.74	33.41	33.42	33.42
6	41.30	41.27	41.21	41.21	40.67	40.60	40.84
7	48.71	48.67	48.76	48.69	48.10	48.13	48.26
8	56.19	56.22	56.22	56.21	55.58	55.58	55.64
9	63.67	63.62	63.58	63.60	63.05	63.05	62.98
10	71.15	71.08	71.17	71.15	70.46	70.50	70.42
11	78.63	78.62	78.53	78.62	77.90	77.89	77.80
12	86.09	85.95	86.23	86.18	85.32	85.38	85.16
13	93.53	93.55	93.69	93.61	92.84	92.93	92.57
14	101.05	100.51	101.01	101.06	100.09	100.04	99.92
15	108.37	108.47	108.55	—	107.53	107.49	107.41
16	115.96	115.87	115.85	116.08	114.87	114.87	114.81
17	123.42	123.38	123.38	—	122.22	122.28	122.06
18	130.86	130.81	130.81	—	129.58	129.58	129.71

as found from the bands with $v'' = 1$ and 2. The violet CN bands, having the same lower state, also give values of $\Delta_2 F''$ for $v = 1$ and 2, and these are given in the table for comparison.[20] Data for the violet bands are from Heurlinger,[21] and from Uhler and Patterson.[22]

Since the rotational terms of the lower state are identical with those already known from the violet bands, no new information about them can be derived from the red bands, except in regard to the spin doubling, as discussed below. Our data include bands with $v'' = 1$, 2 and 3, and the rotational constants have been computed, with the hope of improving the accuracy for states 2 and 3, for which the data from the violet bands are poor. Treating the

[20] Since the spin doublets in the violet bands are not resolved for low K, the combination differences represent the mean of $\Delta_2 F_1$ and $\Delta_2 F_2$. This should differ from $\Delta_2 F_1$ itself only slightly.

[21] T. Heurlinger, Dissertation, Lund (1918).

[22] H. S. Uhler and R. A. Patterson, Astrophys. J. **42**, 434 (1915).

combination differences in the usual manner by the method of least squares, we find the following values of B_v'': $B_1'' = 1.8731$, $B_2'' = 1.8558$, $B_3'' = 1.8384$, from which we obtain

$$B_v'' = 1.8991 - 0.01735(v'' + \tfrac{1}{2}).$$

This agrees well with the equation obtained from the violet bands by Heurlinger[21]:

$$B_v'' = 1.9002 - 0.0173(v'' + \tfrac{1}{2}).$$

The slight difference in B_e'' is probably due to different methods of evaluation. In our computation, the term in D_v'' was corrected for by using the values from the equation

$$D_v'' = -6.401 \times 10^{-6} - 0.00949(v'' + \tfrac{1}{2}) \times 10^{-6},$$

which results from the theoretical relations between D_e, β, ω_e, α_e, and x_e.[23] Further information about the constants of the $^2\Sigma$ state could be obtained by measuring other bands with higher v'', but we have not undertaken to do this.

Spin doubling in the $^2\Sigma$ state

The violet bands permit us to determine only the difference between the spin doublings, i.e., the separations of $F_1(K)$ and $F_2(K)$, in the upper and lower $^2\Sigma$ states. From $^2\Sigma \rightarrow {}^2\Sigma$ bands, the absolute value of the spin doubling cannot be found in either state, because only $F_1 \rightarrow F_1$ and $F_2 \rightarrow F_2$ transitions occur. The red bands should yield the actual doubling in the lower state. It is extremely small, however, and the satellite branches are in no case resolved from the main branches. Evidence for the doubling is found, however, in the fact that at high values of K a slight difference is found in the combination differences, such that

$${}^SR_{21}(K-1) - \begin{Bmatrix} Q_2 \\ {}^QP_{21} \end{Bmatrix}(K+1) < \begin{Bmatrix} R_2 \\ {}^RQ_{21} \end{Bmatrix}(K-1) - P_2(K+1)$$

and

$$\begin{Bmatrix} Q_1 \\ {}^QR_{12} \end{Bmatrix}(K-1) - {}^OP_{12}(K+1) < R_1(K-1) - \begin{Bmatrix} P_1 \\ {}^PQ_{12} \end{Bmatrix}(K+1).$$

Since all of the lines in each inequality come from the same upper state, this can only result from a doubling in the lower state. We can assume that the satellites are of negligible intensity at high K, where the inequality is appreciable. The doubling is then found from the relations

$$\begin{aligned} &[R_1(K-2) - P_1(K)] - [Q_1(K-2) - {}^OP_{12}(K)] \\ &= [R_2(K) - P_2(K+2)] - [{}^SR_{21}(K) - Q_2(K+2)] \\ &= F_1''(K) - F_2''(K) = \gamma_0(K + \tfrac{1}{2}). \end{aligned}$$

On plotting these differences, they appear to be linear in K within experimental error, and the resulting values of γ_0 are, for $v'' = 3$, $\gamma_0 = +0.0071$, for

[23] E. C. Kemble, Jour. Opt. Soc. Am. **12**, 1 (1926). Cf. also F. A. Jenkins, Phys. Rev. **35**, 327 (1930).

$v''=2$, $\gamma_0=+0.0082$. Hence $F_1>F_2$, as usually occurs, and the splitting is of the same order of magnitude as the actual doubling of the lines in the violet bands, which in the 0,0 band amounts to 0.0090 $(K''+\frac{1}{2})$ for low K.[24] Unfortunately do data are available for the doubling in the violet bands with $v''=2$ and 3, so that the term-splitting in the upper $^2\Sigma$ state cannot be evaluated.

Rotational terms of the $^2\Pi$ state

The combination relations yield term differences Δ_2F_i' which refer either to the T_c or to the T_d terms, as will be evident from the energy levels of Fig. 1. The differences Δ_2F_{ic}', obtained by using the $^SR_{21}$ and $^OP_{12}$ branches, are slightly less than the true values, because of the spin doubling in the lower state. Hence only the values of Δ_2F_{id}', obtained from the main branches, have been used in calculating the constants. These are also more accurate because of the greater intensity of the lines involved. In every case the application of the combination principle gives term-differences showing the proper relations if it is assumed that in the $^2\Pi$ states $T_{2d}>T_{2c}$ and $T_{1c}>T_{1d}$ for low J, and in the $^2\Sigma$ state $T_1>T_2$ throughout. An example of the agreement of combination differences in the upper state is given in Table III, derived from the 6,1 and 6,2 bands.

TABLE III. *Exact and approximate combination differences Δ_2F_i' for the $^2\Pi$ state, $v'=6$.*

J	*6, 1 band* $R_2(J)$ $-P_2(J)$	$R_1(J)$ $-P_1(J)$	$^SR_{21}(J)$ $-Q_2(J-1)$	*6, 2 band* $R_2(J)-$ $P_2(J)$	$R_1(J)$ $-P_1(J)$	$^SR_{21}(J)$ $-Q_2(J-1)$	$Q_1(J+1)$ $^OP_{12}(J)$
$1\frac{1}{2}$	12.77			13.04		13.00	
$2\frac{1}{2}$	19.52	18.56		19.51	18.46	19.39	18.23
$3\frac{1}{2}$	26.04	24.83	26.10	25.99	24.83	26.02	24.39
$4\frac{1}{2}$	32.50	30.87	32.17	32.71	31.25	32.46	30.84
$5\frac{1}{2}$	38.96	37.02	38.97	39.07	36.95	38.86	36.97
$6\frac{1}{2}$	45.55	43.14	45.58	45.59	42.99	45.41	43.10
$7\frac{1}{2}$	52.22	49.31	52.38	52.03	49.37	51.92	49.53
$8\frac{1}{2}$	58.25	55.58	58.53	58.49	55.58	58.35	55.54
$9\frac{1}{2}$	65.35	61.75	64.62	64.87	61.81	64.72	61.85
$10\frac{1}{2}$	71.62	67.89	71.21	71.41	68.11	71.15	68.13
$11\frac{1}{2}$	77.73	74.22	77.76	77.68	74.36	77.70	74.79*p*
$12\frac{1}{2}$	84.16	79.84	84.12	84.18	80.38	84.07	78.25*p*
$13\frac{1}{2}$	90.45	86.65	90.68	90.66	86.73	90.44	84.90*p*
$14\frac{1}{2}$	96.94	92.87	96.70	97.10	92.92	96.85	93.75*p*
$15\frac{1}{2}$	103.20	99.00	103.27	103.43	99.13	103.21	
$16\frac{1}{2}$	109.47	105.32	109.89	109.68	105.34	109.59	
$17\frac{1}{2}$	115.99	111.74		115.91	111.66	115.96	
$18\frac{1}{2}$	122.26	117.84		122.42	117.84	122.25	
$19\frac{1}{2}$		123.91		128.77	124.14	128.62	
$20\frac{1}{2}$		130.57		135.18	130.49		

In determining the constants we have used the fact that for low values of J, the following term-formulas are approximately valid:[25]

[24] R. T. Birge, Astrophys. J. **55**, 280 (1922).

[25] R. S. Mulliken, Rev. Mod. Phys. **3**, 116 (1931), and Eqs. (47), (46) in **2**, 113–4 (1930).

$$
\begin{aligned}
{}^2\Pi_{3/2}: T_1(J) &= C + B^*_{v,+1/2}[(J+\tfrac{1}{2})^2 - (\tfrac{3}{2})^2] + D^*_{v,+1/2}(J+\tfrac{1}{2})^4 + \cdots \\
{}^2\Pi_{1/2}: T_2(J) &= C + B^*_{v,-1/2}[(J+\tfrac{1}{2})^2 - (\tfrac{1}{2})^2] + D^*_{v,-1/2}(J+\tfrac{1}{2})^4 + \cdots,
\end{aligned} \tag{3}
$$

where C is a constant depending on the value of v. In these expressions $B_{v,\Sigma}{}^*$ is the "apparent" value of B_v which is obtained by assuming that the low rotational terms have the form characteristic of case (a). It is connected[25] with the true value of B_v by the relation

$$B^*_{v,\pm 1/2} = B_v(1 \pm B_v/A\Lambda). \tag{4}$$

To evaluate $B^*_{v\,\Sigma}$, for the various values of v, we investigate the quantities

$$
\begin{aligned}
\Delta_2 F_i'(J) &= F_i'(J+1) - F_i'(J-1) \\
&= 4B^*_{v,\Sigma}(J+\tfrac{1}{2}) + 8D^*_{v,\Sigma}(J+\tfrac{1}{2})^3 + \cdots.
\end{aligned}
$$

Since the second term is small, we can assume without appreciable error that $D^*_{v,\Sigma} = D_v = D_e + \beta(v+\frac{1}{2})$, where D_e is given by the well-known relation[23]

$$D_e = -4B_e{}^3/\omega_e{}^2.$$

Using preliminary values of B_e, ω_e, and of the quantities required for calculating β, one can compute the term $8D_v(J+\frac{1}{2})^3$, subtract from the quantities $\Delta_2 F_1'(J)$, and, dividing by $J+\frac{1}{2}$, obtain

$$[\Delta_2 F_i'(J) - 8D_v(J+\tfrac{1}{2})^3]/(J+\tfrac{1}{2}) = 4B^*_{v,\Sigma}.$$

This quantity is nearly independent of J, and extrapolation to $J=0$ gives the $B^*_{v,\Sigma}$ values represented by Eq. (4). The mean of $B^*_{v,+1/2}$ and $B^*_{v,-1/2}{}^*$ then gives the true value of B_v. The evaluation was carried out graphically, as illustrated in Fig. 5. Strictly, the extrapolation should have been carried out to

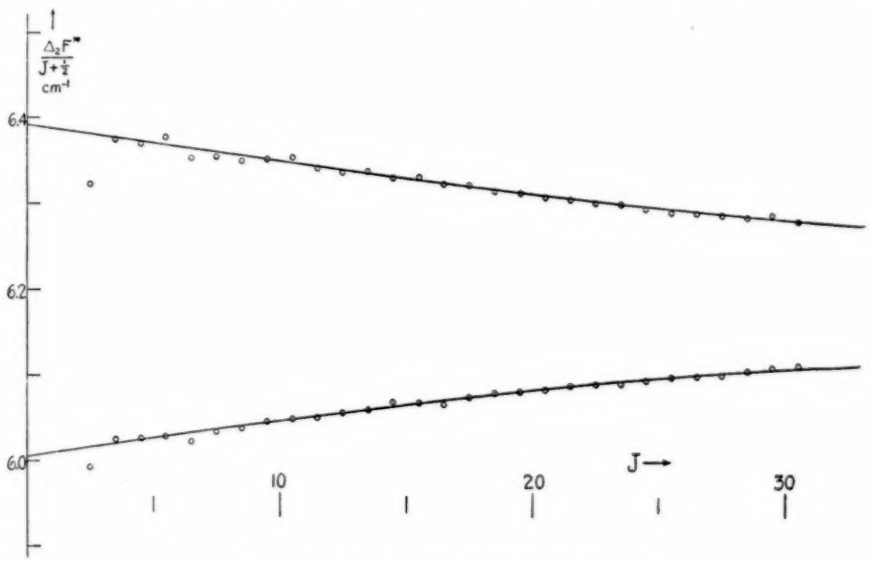

Fig. 5. Illustrating the graphical determination of $B^*_{v,\Sigma}$.

zero rotation, rather than to $J=0$. The difference, especially in B_v, is, however, slight, and unfortunately not exactly determinable. The resulting constants are given in Table IV, in which are also included the constants of the lower state, and the molecular constants derived from these.

TABLE IV. *Constants of the band structure.* All quantities are in cm^{-1} units, except I_e and r_e. Strictly speaking, the B^* values apply only to the d rotational levels.

v'	$B^*_{v,+\frac{1}{2}}$	$B^*_{v,-\frac{1}{2}}$	$B^*_{v,+\frac{1}{2}}-B^*_{v,-\frac{1}{2}}$	B_v'	$-D_v'\times10^6$	p_0	$-q_0$	$-A$	$2B_v^2/A$
4	1.5705	1.6727	−.1022	1.6215	6.140	0.00621	0.000252	52.14	−.1009
5	1.5490	1.6522	−.1032	1.6005	6.153	0.00853	0.000365	52.33	−.0979
6	1.5360	1.6352	−.0992	1.5855	6.166	—	—	52.52	−.0957
7	1.5140	1.6237	−.1097	1.5687	6.178	—	—	50.89	−.0967
8	1.5017	1.5990	−.0973	1.5502	6.191	0.01872	0.000435	51.65	−.0931

v''	B_v''	$-D_v''\times10^6$	γ_0		B_e	α	D_e	β	I_e	r_e
1	1.8731	6.415	—	$^2\Pi$	1.6990	0.01746	−6.133	−1.27	16.28	1.236
					±0.001	±0.002	$\times10^{-6}$	$\times10^{-5}$	$\times10^{-40}$ g cm	$\times10^{-8}$ cm
2	1.8558	6.425	0.0082	($A=-52.2$)						
					1.8991	0.01735	−6.401	−0.949	14.56	1.169
3	1.8384	6.435	0.0071	$^2\Sigma$	±0.0005	±0.001	$\times10^{-6}$	$\times10^{-5}$	$\times10^{-40}$ g cm	$\times10^{-8}$ cm

The column headed $-A$ gives the experimental values of the electronic separation in the $^2\Pi$ state. They were determined from the relation[26]

$$|A| = T_2'(\tfrac{1}{2}) - T_1'(1\tfrac{1}{2}) + B_v' - 3B_v'^2/|A| .$$

The variation in A for the different vibrational states is regarded as real, since independent results for this constant from different bands with the same upper state agreed closely. Thus the 6,2 and 6,1 bands gave 52.50 and 52.55, respectively, while the 7,3 and 7,2 bands gave 50.97 and 50.81. The high value for $v'=6$, and the low value for $v'=7$ are undoubtdely connected with the perturbation effects described below.

We have adopted $A=-52.20$ as the most probable value of the coupling constant. In Table IV the differences $B^*_{v,+1/2}-B^*_{v,-1/2}$* are compared with their theoretical values from Eq. (4), namely $2B_v^2/A$. The agreement is satisfactory, both in their magnitude and in their decrease with v', but the perturbations in A invalidate any more quantitative conclusions. The slight discrepancies between observed and calculated values can be attributed, at least partly, to the uncertainty already noted in connection with the extrapolations to get the B_v* values. The constants B_v are represented within experimental error by the equation

$$B_v = B_e - \alpha(v+\tfrac{1}{2}).$$

The results for B_e and α are included in Table IV, as well as the moment of inertia, I_e, and the internuclear distance r_e in the equilibrium position. As a rigorous test of the term-equations (1), we have computed the terms and observed frequencies for the 8,3 band, using the constants given in Table IV. As expected, slight systematic discrepancies are found at high values of K, which can be further reduced by slight adjustments of the constants. They are of the order of 0.2 cm^{-1} at $K=30$, and entirely negligible on the scale to which the Fortrat diagram of Fig. 3 is drawn.

[26] R. S. Mulliken, Phys. Rev. **33,** 747 (1929).

Λ-doubling in the $^2\Pi$ state

The term $\Phi_i(J)$ in the energy formulas (1) is double-valued for each component of the $^2\Pi$ state. This gives rise to four series of terms T_{1c}, T_{1d}, T_{2c} and T_{2d}, the subscripts c and d having the theoretical significance assigned to them by Mulliken.[27] The separation of T_{1c} from T_{1d}, and of T_{2c} from T_{2d} is small and represents the Λ-doubling. It is defined as the difference

$$\Delta\nu_{dc} = T_d(J) - T_c(J).$$

In the present case we can evaluate it from the relations

$$[R_2(J) - Q_2(J)] - [Q_2(J+1) - P_2(J+1)] \sim 2\Delta\nu_{2dc}(J+\tfrac{1}{2}) \text{ for } {}^2\Pi_{1/2};$$
$$[R_1(J) - Q_1(J)] - [Q_1(J+1) - P_1(J+1)] \sim 2\Delta\nu_{1dc}(J+\tfrac{1}{2}) \text{ for } {}^2\Pi_{3/2}.$$

Fig. 6 shows graphically the observed $\Delta\nu_{dc}$ in the initial states $v'=4$ to 8. For $v'=4$, 5, and 8 it takes the form known to be characteristic of $^2\Pi$ states intermediate between case (*a*) and case (*b*). As has been shown by Mulliken and

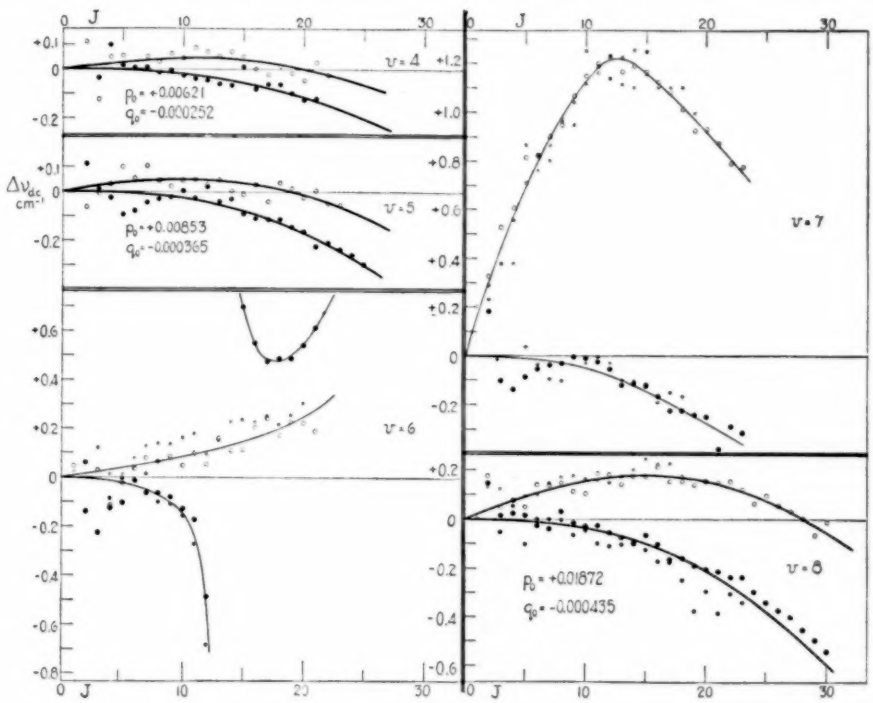

Fig. 6. Λ-doubling in the $^2\Pi$ state. The heavy curves in the cases $v'=4$, 5 and 8 are the theoretical curves, with the coefficients given. For the perturbed states $v'=6$ and 7, the curves are empirically drawn. Large dots and large circles are values of $\Delta\nu_{1dc}$ ($^2\Pi_{3/2}$) and $\Delta\nu_{2dc}$ ($^2\Pi_{1/2}$) obtained from the main branches. Small dots and circles are values whose determination involved the fainter branches $^SR_{21}$ and $^OP_{12}$. In the $v'=7$ figure, crosses are data from the 7,3 band, dots and circles from the 7,2 band. All data for $v'=6$ are from the 6,2 band.

[27] R. S. Mulliken, Rev. Mod. Phys. **3**, 94 (1931).

Christy,[17] the theoretical work of Van Vleck on Λ-doubling leads to the following expressions:

$$\Delta\nu_{2dc} = [(\tfrac{1}{2}p_0 + q_0)(1 + 2X^{-1} - YX^{-1}) + 2q_0X^{-1}(J - \tfrac{1}{2})(J + 1\tfrac{1}{2})](J + \tfrac{1}{2})$$
$$\Delta\nu_{1dc} = [(\tfrac{1}{2}p_0 + q_0)(-1 + 2X^{-1} - YX^{-1}) + 2q_0X^{-1}(J - \tfrac{1}{2})(J + 1\tfrac{1}{2})](J + \tfrac{1}{2}).$$

Here $Y = A/B_v$, $X = |Y[(Y-4)+(J+\frac{1}{2})^2]^{1/2}|$, and p_0 and q_0 are coefficients independent of J which are characteristic of the particular electronic and vibrational state. To determine these constants, the following relations are used:

$$\Delta\nu_{2dc}(J) - \Delta\nu_{1dc}(J) = (p_0 + 2q_0)(J + \tfrac{1}{2})$$
$$\Delta\nu_{2dc}(J) + \Delta\nu_{1dc}(J) = [(p_0 + 2q_0)(2 - Y)(J + \tfrac{1}{2}) + 4q_0(J - \tfrac{1}{2})(J + \tfrac{1}{2})(J + 1\tfrac{1}{2})]X^{-1}.$$

The theoretical curves are shown in Fig. 6, for the states $v' = 4$, 5 and 8, drawn according to the p_0 and q_0 values indicated. The agreement is good for $v' = 4$ and 5, but for $v' = 8$ a slight trend in the $\Delta\nu_{1dc}$ points is observed for high J. This is analogous to certain of the results of Mulliken and Christy, and is almost certainly due to the rotational stretching of the molecule.

In the case $v' = 7$, $\Delta\nu_{2dc}$ takes on exceptionally large values, and the experimental points cannot be fitted by curves involving only the two parameters p_0 and q_0. We regard this unusual doubling as having an origin similar to that of the perturbations in $v' = 6$, where quite evidently no simple equations like the above will hold. This will be discussed in the following section.

Perturbations

In the theoretical calculation of Λ-doubling, for a $^2\Pi$ state, certain terms enter which involve a summation over all of the $^2\Sigma$ and $^2\Delta$ states of the molecule. As shown by Mulliken and Christy, however, in many cases the effect is due predominantly to a certain $^2\Sigma$ state, which stands in the relation of "pure precession" to the $^2\Pi$ state and usually contributes a term much greater than the rest. In the present case, judging from the size of the observed p_0 values, this $^2\Sigma$ state is probably a high excited level not yet known experimentally (cf. the analogous case of BO, reference 17, pp. 99, 118). But in the present case a particularly large interaction also occurs for certain values of v and J, in spite of the absence of a relation of pure precession, between the $^2\Pi$ and the lower $^2\Sigma$ ($a^2\Sigma$) states when their rotational levels have nearly the same energy.[27a] According to Kronig[28] this is the cause of the perturbations, or irregularities in the term-series, which have been found in the terms of $a^2\Sigma^{(11)}(J)$ from a study of the CN tail bands.[29] (The superscript in parentheses is used to designate the vibrational quantum number, v). Kronig's theory predicted a corresponding perturbation in the $^2\Pi$ terms for each of those in $a^2\Sigma$. This was partially verified by Rosenthal and Jenkins,[12] who discovered a marked perturbation in the terms near $^2\Pi_{3/2}{}^{(6)}$ ($13\frac{1}{2}$), corresponding to that

[27a] Cf. reference 17, expecially pp. 110, 113–4, for a discussion of the relation between Λ-doubling and perturbations.

[28] R. de L. Kronig, Zeits. f. Physik **50**, 347 (1928).

[29] F. A. Jenkins, Phys. Rev. **31**, 539 (1928).

previously known near $a^2\Sigma^{(11)}(13\frac{1}{2})$. For this work, an analysis of the 6,2 band of the red system was made, from the same plates as those used in the present investigation. Rosenthal and Jenkins also showed that the $a^2\Sigma^{(11)}(J)$ terms undergo further perturbations at $J=25\frac{1}{2}$ and $27\frac{1}{2}$.

Since the existence of perturbations depends on the near coincidence of levels of the same J in two different electronic states, it is necessary to find the relative positions of the rotational levels in the two states. If the crossing is to occur at a relatively small value of J, it is obvious that the vibrational levels must also approach each other closely. In Fig. 7a we have drawn to scale the vibrational terms for the four states $a^2\Sigma$, $^2\Pi_{3/2}$, $^2\Pi_{1/2}$ and $b^2\Sigma$. The

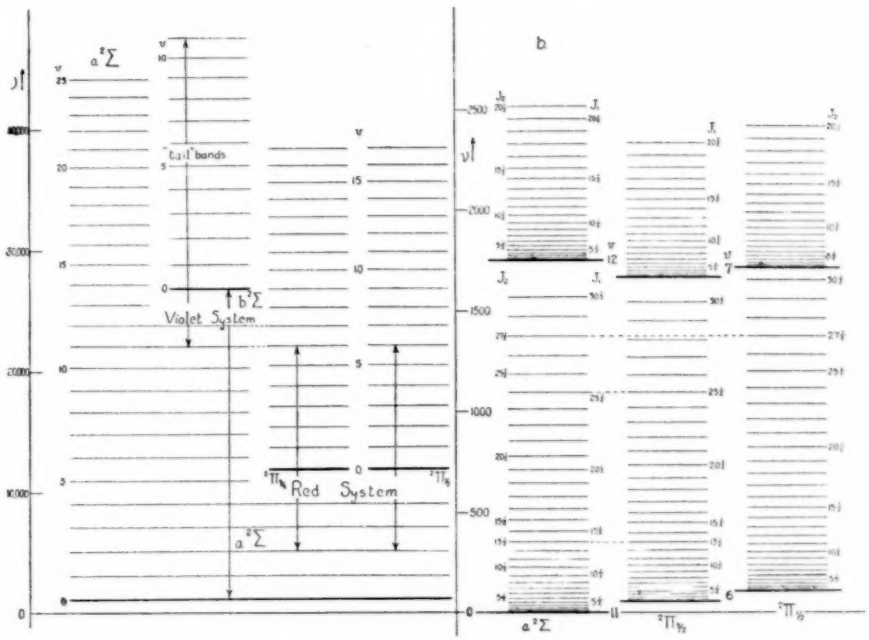

Fig. 7. (*a*) Electronic and vibrational terms of CN. The levels drawn to scale, with the vibrationaless condition of $a^2\Sigma$ as the zero of energy. Transitions are indicated giving one of the strongest bands of the red system, the violet system, and the tail bands, which are part of the violet system.

(*b*) Vibrational levels $a^2\Sigma^{(11)}$, $a^2\Sigma^{(12)}$, $^2\Pi^{(6)}$ and $^2\Pi^{(7)}$ with the associated rotational levels. The scale is magnified $16\frac{2}{3}$ times over *a*, and measured from $a^2\Sigma^{(11)}$ (0) as zero. Displacements of the rotational levels are found at the perturbations (but not shown in the figure), which occur where levels in $a^2\Sigma$ cross those in $^2\Pi$ with the same J value. These points are designated by the horizontal dashed lines.

$^2\Pi$ terms were found from the observed ΔG_v values for the range in which they are available from the red bands, ($\Delta G_{41/2}$ to $\Delta G_{101/2}$) and the remainder extrapolated by the vibrational equation deduced below. The terms for $a^2\Sigma$ and $b_2\Sigma$ are values derived by Birge from a study of the existing data on the violet system, and kindly made available to us in advance of publication. The ΔG_v values of $a^2\Sigma$ are known experimentally only for low v (0 to 3) from the ordinary violet CN bands, and for a range of high v (9 to 15) from the tail bands.

Nevertheless, Birge finds that they both fit a linear $\Delta G_v : v$ curve accurately, and so the absolute magnitudes of the higher G_v terms can be computed with some precision. The numerical values used in Fig. 7a are given in Table V. It will be seen that $a^2\Sigma^{(11)}$ and $a^2\Sigma^{(12)}$ lie very close to $^2\Pi^{(6)}$ and $^2\Pi^{(7)}$ respectively. This accounts for the fact that the only anomalies such as perturbations and unusual Λ-doubling observed in the red system occur in the initial states $v' = 6$ and 7. It accounts equally well for the fact that the only anomalies connected with the *final* state of the tail bands[29] are the perturbations in $v'' = 11$, and the unusually large spin doubling in $v'' = 12$.

To examine the situation in more detail, we consider the relative positions of the rotational levels associated with the above-mentioned vibrational states. These are plotted to scale in Fig. 7b, from the numerical values given in Table V. Since the absolute values of the vibrational terms are not known with great exactness for the $a^2\Sigma$ state in this range of v, their positions relative to $^2\Pi$ are best determined by the perturbations. These show that the terms T_{1c} in $^2\Pi_{3/2}{}^{(6)}$ are crossed by the T_2 terms of $^2\Sigma^{(11)}$ between $J = 12\frac{1}{2}$ and $13\frac{1}{2}$. In the article by Rosenthal and Jenkins,[12] it was assumed from theoretical grounds that the T_{1c} terms could only be perturbed by T_1 terms in the $^2\Sigma$ state. That this is not necessarily true, and that the displacements of the

TABLE V. *Term values of the CN molecule.*
a. Vibrational terms, $G_v + T_e$.

v	$a^2\Sigma$	$^2\Pi_{3/2}$	$^2\Pi_{1/2}$	$b^2\Sigma$
0	1,031.16	11,908.43	11,960.63	28,828.99
1	3,073.55	13,671.32	13,723.52	28,952.49
2	5,089.46	15,408.45	15,460.65	31,035.59
3	7,078.87	17,119.81	17,172.01	33,076.59
4	9,041.80	18,805.40	18,857.61	35,072.69
5	10,978.23	20,465.09	20,517.30	37,030.79
6	12,888.18	22,099.00	22,151.52	38,917.39
			p	
7	14,771.63	23,707.50	23,758.39	40,759.49
8	16,628.60	25,290.10	25,341.75	42,544.59
9	18,549.07	26,846.97	26,898.62	44,270.69
10	20,263.06	28,377.83	28,429.48	45,936.00
11	22,040.55	29,883.09	29,934.74	47,538.76
12	23,791.56	31,362.56	31,414.20	49,081.18
13	25,516.07	32,816.26	32,867.91	50.564.76
14	27,214.10	34,244.19	34,295.84	51,993.04
15	28,885.63	35,646.36	35,698.01	53,369.53
16	30,530.67	37,022.76	37,074.41	
17	32,149.23	38,373.40	38,425.05	
18	33,741.29			
19	35,306.87			
20	36,845.95			
21	38,358.55			
22	39,844.65			
23	41,304.27			
24	42,737.39			
25	44,144.03			

TABLE V. (*Continued*).
*Term values of the CN molecule.**
b. Rotational terms (Smoothed in perturbed regions)

J_1	J_2	$^2\Sigma^{(11)}$	$^2\Pi_{3/2}{}^{(6)}$	$^2\Pi_{1/2}{}^{(6)}$	$^2\Sigma^{(12)}$	$^2\Pi_{1/2}{}^{(7)}$	$^2\Pi_{3/2}{}^{(7)}$	$^2\Sigma^{(12)}(J) - {}^2\Pi_{1/2}{}^{(7)}(J)$
$\frac{1}{2}$		0			1752.51			37.62
$1\frac{1}{2}$	$\frac{1}{2}$	3.39	57.35	108.36	1755.86	1714.89	1665.45	36.10
$2\frac{1}{2}$	$1\frac{1}{2}$	10.19	64.97	113.28	1762.58	1719.76	1673.02	34.70
$3\frac{1}{2}$	$2\frac{1}{2}$	20.39	75.81	121.30	1772.61	1727.88	1683.50	33.39
$4\frac{1}{2}$	$3\frac{1}{2}$	33.97	89.80	132.79	1786.04	1739.22	1697.32	32.22
$5\frac{1}{2}$	$4\frac{1}{2}$	50.90	106.68	147.29	1802.81	1753.82	1713.86	31.22
$6\frac{1}{2}$	$5\frac{1}{2}$	71.26	126.75	165.50	1822.96	1771.59	1733.85	30.25
$7\frac{1}{2}$	$6\frac{1}{2}$	94.97	149.67	186.36	1846.37	1792.71	1756.46	29.63
$8\frac{1}{2}$	$7\frac{1}{2}$	122.09	176.12	211.09	1873.25	1816.74	1782.58	29.25
$9\frac{1}{2}$	$8\frac{1}{2}$	152.55	205.25	238.39	1903.35	1844.00	1811.48	28.71
$10\frac{1}{2}$	$9\frac{1}{2}$	186.40	237.93	269.58	1936.93	1874.64	1843.68	28.52
$11\frac{1}{2}$	$10\frac{1}{2}$	223.65	273.36	303.36	1973.69	1908.41	1878.73	28.43
$12\frac{1}{2}$	$11\frac{1}{2}$	264.31	312.29	340.99	2013.99	1945.26	1917.02	28.67
			p					
$13\frac{1}{2}$	$12\frac{1}{2}$	308.33	353.84	381.04	2057.40	1985.32	1958.18	28.88
$14\frac{1}{2}$	$13\frac{1}{2}$	355.82	399.02	425.17	2104.40	2028.52	2002.68	29.45
$15\frac{1}{2}$	$14\frac{1}{2}$	406.51	446.86	471.70	2154.56	2074.95	2050.01	30.07
$16\frac{1}{2}$	$15\frac{1}{2}$	460.70	498.15	522.27	2208.14	2124.49	2100.65	31.01
$17\frac{1}{2}$	$16\frac{1}{2}$	518.15	552.40	575.13	2264.90	2177.13	2154.11	31.84
$18\frac{1}{2}$	$17\frac{1}{2}$	579.02	609.81	631.95	2324.86	2233.06	2210.93	32.81
$19\frac{1}{2}$	$18\frac{1}{2}$	643.15	670.34	691.04	2388.02	2292.05	2270.51	33.89
$20\frac{1}{2}$	$19\frac{1}{2}$	710.72	733.85	754.37	2454.38	2354.13		34.96
$21\frac{1}{2}$	$20\frac{1}{2}$	781.55	800.58	819.81		2419.42		
$22\frac{1}{2}$	$21\frac{1}{2}$	855.82	870.29	889.55				
$23\frac{1}{2}$	$22\frac{1}{2}$	933.35	943.22	961.29				
$24\frac{1}{2}$	$23\frac{1}{2}$	1014.32	1019.13	1037.33				
$25\frac{1}{2}$	$24\frac{1}{2}$	1098.55	1098.26	1115.37				
			p					
$26\frac{1}{2}$	$25\frac{1}{2}$	1186.22	1180.37	1197.71				
$27\frac{1}{2}$	$26\frac{1}{2}$	1277.15	1265.70	1282.05				
				p				
$28\frac{1}{2}$	$27\frac{1}{2}$	1371.52	1354.01	1370.69				
$29\frac{1}{2}$	$28\frac{1}{2}$	1469.15	1445.54	1461.33				
$30\frac{1}{2}$	$29\frac{1}{2}$	1570.22		1556.27				
$31\frac{1}{2}$	$30\frac{1}{2}$			1653.21				

* *Notes:* For the $^2\Sigma$ terms, both J_1 and J_2 apply. For the $^2\Pi_{3/2}$ terms, J_1 alone applies. For the $^2\Pi_{1/2}$ terms, J_2 alone applies.

levels are more symmetrical if it is the T_2 $^2\Sigma$ terms which are perturbed, has been pointed out by Ittmann[30] in a discussion of these perturbations in CN. This change is definitely required by our other results. In Table V we have taken the crossing to occur about $\frac{2}{3}$ of the way between $J = 12\frac{1}{2}$ and $13\frac{1}{2}$. The positions of the remaining terms were then calculated by summing the experimental values of $\Delta_2 F_d$. This places the lowest level of $^2\Pi_{3/2}{}^{(6)}$ 57.3 cm^{-1} above the lowest level of $^2\Sigma^{(11)}$. This figure is probably correct to within 1 or 2 cm^{-1}, and is substantiated by the fact that the two *vibrational* terms given in Table

[30] G. T. Ittmann, Zeits. f. Physik **71**, 616 (1931). We wish to thank Dr. Ittmann and Prof. H. A. Kramers for sending us the manuscript of this paper.

IV differ by 59.4 cm^{-1}. The agreement is remarkable, considering the long extrapolation used by Birge in calculating the high $^2\Sigma$ vibrational terms.

In the analysis of the 6,2 band, it was found that besides the perturbation mentioned above, which affects the Q_1 and $^OP_{12}$ branches in the neighborhood of $J'=13\frac{1}{2}$, the R_1 and R_2 branches are also perturbed at the highest observed values of J. The displacements in the R_1 branch exceed 1 cm^{-1} beyond $J'=22\frac{1}{2}$ and in the R_2 branch beyond $J'=24\frac{1}{2}$. These perturbations evidently correspond to the very large ones found by Rosenthal and Jenkins in the T_1 terms (revised notation) of $^2\Sigma^{(11)}$ at $J=25\frac{1}{2}$ and in the T_2 terms at $J=27\frac{1}{2}$. They are predicted by Ittmann as due to the crossing of these terms by T_{1d} and T_{2d}, respectively. These perturbations are much more violent than that at $J=13\frac{1}{2}$, a fact which probably accounts for our failure to observe lines in the perturbed branches above $J'=22\frac{1}{2}$ and $24\frac{1}{2}$, respectively. One would expect a very strong interaction of T_{1d} of $^2\Pi$ with T_1 of $^2\Sigma$, since at high values of J we have essentially case (b) spin coupling in both, the spins being parallel to K in both of the two states which perturb each other. Similarly, it should also be strong between T_{2d} and T_2, where the spins are anti-parallel to their K's. In Table V, the terms as far as $J=30\frac{1}{2}$ have been computed by extrapolation beyond $J=20\frac{1}{2}$. Very satisfactory evidence for the above-mentioned coincidences is obtained, as will be seen by reference either to the table, or to Fig. 7b.

The interpretation of the unusually large Λ-doubling in $^2\Pi_{1/2}{}^{(7)}$ and of the corresponding spin doubling in $^2\Sigma^{(12)}$ follows from the relative positions and spacings of the associated rotational levels. The level $^2\Pi_{1/2}{}^{(7)}(\frac{1}{2})$ lies only 37.6 cm^{-1} below the lowest T_1 level, $^2\Sigma^{(12)}(\frac{1}{2})$. Further, the $^2\Pi_1{}'_2{}^{(7)}$ levels start off with a spacing which slightly exceeds that in the $^2\Sigma^{(12)}$ state. Levels of the same J in the two states therefore approach each other at first, and, as is evident from the last column of Table V, reach a minimum separation at about $J=11\frac{1}{2}$. It is known that the interaction of two levels becomes greater as their separation decreases, and we should therefore expect a maximum in the Λ- and spin-doubling at $J=11\frac{1}{2}$. This is in accord with observation; the curve of Λ-doubling for $v'=7$ shown in Fig. 6 has a maximum at about $J=11\frac{1}{2}$, and is remarkably similar in form and magnitude to the spin doubling curve for $^2\Sigma^{(12)}$, which also reaches a maximum at the same J value.[31]

The near equality of the constant B_v in the two perturbing state ($B_v=1.5855$ in $^2\Pi^{(6)}$, 1.6945 in $a\ ^2\Sigma^{(11)}$) is of some importance in permitting the large interactions here observed. The unperturbed rotational levels cross each other gradually in this case, with the result that some come into very close coincidence.

Another important factor in causing the relatively large interaction observed is the fact that the $U(r)$ curve of the $^2\Pi$ state approaches that of the $a\ ^2\Sigma$ state very closely for moderate and large v values. According to Morse curves constructed by one of the writers, the outer branch ($r>r_e$) of the $U(r)$ curves of the $^2\Pi$ state crosses that of the $a\ ^2\Sigma$ state at an almost grazing angle in the neighborhood of $v=14$ of the $^2\Pi$ state. The two curves then remain nearly in coincidence for higher v values. According to this, the observed per-

[31] Fig. 2 of reference 29.

turbations at $v = 6$ or 7 come below the crossing point, but the two $U(r)$ curves are already very near together. This is important because it means that the vibrational part of any $^2\Pi$ wave-function has a pronounced maximum at nearly the same value of r as that of any $^2\Sigma$ wave-function which has nearly the same energy. This tends to make the two wave-functions interact strongly.

Although the near approach of the $U(r)$ curves and of certain rotational levels of the $^2\Sigma$ and $^2\Pi$ states favor large interactions and large perturbations, it is probable that in respect to the electronic parts of their wave-functions, these two states are very unfavorable for interaction. Hence as a net result the observed perturbations are not very large.

In the 6,2 band, the Q_1 branch, as recorded in Table I, has two lines representing each of the J' values $12\frac{1}{2}$ and $13\frac{1}{2}$. This duplicity results from the fact that when the states interact very strongly, their wave-functions become "mixed," in such a way that $^2\Pi$ receives some of the characteristics of $a\ ^2\Sigma$, and vice versa. As a result, transitions become possible which have partially the character of transitions from $a\ ^2\Sigma^{(11)}$ to $a\ ^2\Sigma^{(2)}$, and this accounts for the extra lines. In a similar way, extra lines were observed in the tail band $b\ ^2\Sigma^{(11)} \rightarrow a\ ^2\Sigma^{(11)}$, for the same J values. These lines really could equally well be designated $b\ ^2\Sigma^{(11)} \rightarrow {}^2\Pi^{(6)}$. The microphotometer curve of Fig. 2d illustrates the intensity relations near the perturbation in the 6,1 band.

TABLE VI. *Intensities, band heads and band origins.*

v'	$v''=0$	1	2	3	4	5	6	
0	(10,937)							
1	(12,697)	(10,654)						
2	**1** (14,431)	(12,393)						
3	**1** 16,136.57 16,132.43	(14,098)	(12,086)					
4	**2** (17,828)	**6** 15,788.04 15,784.10	(13,772)	(11,782)				$\Delta G'$ 1659.69
5	**1** 19,489.54 19,486.22	**7** 17,447.33 17,443.79	**10** 15,431.55 15,427.75	(13,446)	(11,480)			1634.22
6	**2** (21,121)	**5** 19,081.27 19,078.00	**9** 17,065.46 17,061.98	**7** 15,075.87 15,072.14				1606.87
7		**4** 20,688.02 20,684.92	**6** 18,672.09 18,668.80	**6** 16,682.51 16,679.00	**3** 14,719.39 14,715.61			1583.35
8		**0** 22,271.19 22,268.40	**3** 20,255.07 20,252.13	**5** 18,265.49 18,262.37	**3** 16,302.27 16,298.95	**1** (14,361)		1556.87
9				**1** 19,822.15 19,819.25	**4** 17,858.89 17,855.82	**2** 15,922.08 15,918.81		1530.86
10				**2** 21,352.79 21,350.07	**1** 19,389.55 19,386.68	**1** 17,452.72 17,449.67	**1** (15,540)	1505.26
11				**0** 22,857.87 22,855.29	**1** 20,894.72 20,892.01		**0** (17,041)	
	$\Delta G''$ 2042.43	2016.06	1989.80	1963.38	1937.01			

Vibrational Structure

In addition to the rotational structure of the seven bands given in Table I. we have measured the R_2 head of every band appearing with any intensity, in order to derive equations for the vibrational energy. The results are given in Table VI, the frequency of the head in vacuum being the upper of the two frequencies given for each band. Frequencies given in parentheses are those of bands which were too weak to measure on our plates. The frequencies given are from measurements of Fowler and Shaw, and Asundi and Ryde. They were not used in our analysis, because not very accurate.

Each R_2 head is very near the origin ν_2 of a $^2\Pi_{1/2} \rightarrow {}^2\Sigma$ band. The corrections necessary to convert heads to origins are easily made from our data, as follows. From the term-formulas (3) we find

$$\nu_h - \nu_2 = (\tfrac{1}{4})B_v'' - B^{*2}_{v,-1/2}/4(B^*_{v,-1/2} - B_v'').$$

The origin ν_0 of the complete band is $(\nu_h - \nu_2 - A/2)$ cm^{-1} from the R_2 head. Applying the correction $\nu_h - \nu_2$ to the head frequencies eliminates the rotational energy, and yields the values ν_2, which are also given in Table VI. The combination principle applied to vibrational term differences obtained from our data gives values of ΔG which are consistent to a few hundredths cm^{-1} in all cases where the measurement was reliable. The data for the (3,0), (5,0), (8,1) and (10,3) bands may be somewhat in error, because of the indistinctness of the heads. The R_{21}, R_1, and Q_1 heads were in general more difficult to measure than R_2, and the data are omitted.

The vibrational differences for the lower state fit the equation

$$\Delta G_v'' = 2068.792 - 26.352(v'' + \tfrac{1}{2})$$

with a mean deviation of 0.02 cm^{-1}. This agrees very well with Heurlinger's expression[6] from the violet bands, which gave $\omega_e = 2068.89$, $2x_e\omega_e = 26.50$.[32] The upper state differences are not nearly as regular. In deriving the equation, we were obliged to omit the experimental values of $\Delta G_{61/2}$ and $\Delta G_{71/2}$, as they obviously did not fit in with the others. The equation adopted is

$$\Delta G_v' = 1788.659 - 25.766\,(v' + \tfrac{1}{2})$$

with deviations (obs.-calc.) for $\Delta G_{41/2}$ to $\Delta G_{101/2}$ of -0.13, $+0.16$, -1.35, $+0.82$, $+0.10$, -0.14, $+0.13$ cm^{-1}, in order. It will be noticed that $\Delta G_{61/2}$ is smaller than expected, and $\Delta G_{71/2}$ larger. This would be explained if the vibrational terms of two electronic states in coming close together "repelled" each other, as do rotational states at a perturbation, for then the $^2\Pi^{(6)}$ level would be shifted up, and $^2\Pi^{(7)}$ down (see Fig. 7b). Support for this idea is found in the fact that the interval $\Delta G_{111/2}$ in $a\ ^2\Sigma$, as found from the tail bands,[29] is about 2 cm^{-1} larger than expected, and $\Delta G_{121/2}$ about 0.7 cm^{-1} smaller. That it is somewhat arbitrary to distinguish between a "vibrational" and a "rotational"

[32] As pointed out to us by Professor Birge, this value for $2x_e\omega_e$ was originally given by Heurlinger, misquoted as 27.50 by Kratzer (reference 8), and erroneously copied by Jevons (reference 7) and Birge (reference 9).

perturbation is indicated by the results of Rosenthal and Jenkins.[33] A "vibrational perturbation" occurs when a whole set of rotational levels is simultaneously perturbed. It is true, however, that in these cases one cannot represent all of the band origins by a smooth function. The abnormal values of A determined experimentally for $v'=6$ and 7 (see Table IV) probably are due to the above effect. The best representation of the band origins is, from the above results:

$$\nu_0 = 11{,}043.20 + 1788.66(v' + \tfrac{1}{2}) - 12.883(v' + \tfrac{1}{2})^2 - 2068.79(v'' + \tfrac{1}{2}) + 13.176(v'' + \tfrac{1}{2})^2.$$

The vibrational intensity distribution in this system is shown by the bold face numbers in Table VI, most of which are eye estimates from the work of Fowler and Shaw.[4] We have added the 8,1 and 11,3 bands, which appear faintly on our plates. For many of the infrared bands, intensity estimates are not available. In order to establish the hitherto uncertain vibrational numbering of the $^2\Pi$ states, we have drawn $U(r)$ curves for the $a\ ^2\Sigma$ and the $^2\Pi$ states, with Morse functions, and have determined the nature of the intensity distribution to be expected in the $^2\Pi \rightarrow a\ ^2\Sigma$ bands according to the method of Condon, using the wave mechanics.[34] Comparison with the observed intensities shows excellent agreement when the $U(r)$ curve of the $^2\Pi$ state is drawn corresponding to the v numbering used here, which is that first proposed by Asundi and Ryde.[5] Any other v numbering gives disagreement. These results make it evident that most of the spectrum must lie in the infrared, largely beyond the reach of photography.

[33] J. E. Rosenthal and F. A. Jenkins, Proc. Nat. Acad. Sci. **15,** 896 (1929).
[34] Cf. E. U. Condon, Proc. Nat. Acad. Sci. **13,** 462 (1927), and Phys. Rev. **32,** 858 (1928)

BROAD LINES IN THE ARC SPECTRUM OF COPPER

By C. W. Allen
Commonwealth Solar Observatory, Canberra, Australia

(Received November 11, 1931)

Abstract

Attention is called to the anomalous broadening behaviour of certain lines in the copper arc spectrum, particularly those arising from initial terms $c^4D_{2,3}$. Breadths of several lines have been measured with copper arc spectra and pressures up to eighty atmospheres. The following are the most essential conclusions drawn:—(a) broad lines with the same initial term have the same breadth, (b) all lines show a linear increase of breadth with increasing pressure, (c) lines arising from $c^4D_{2,3}$ terms have a considerable breadth at zero pressure. The intensity contours of λλ4378, 4539 and 4587 ($c^4D_{2,3}$ lines) at one atmosphere have been determined and found to have a form represented by the formula $a^2/[(\lambda-\lambda_0)^2+a^2]$. The discussion touches on the nature and cause of the breadth of some of the copper lines, it being concluded that the breadth is an inner property of the copper atom, i.e., not due to external disturbances. The effective diameter of the copper atom would need to be increased considerably by excitation if the pressure broadening is to be accounted for by the Lorentz collision effect.

1. Introduction

IT IS a fairly general result of spectral analysis that lines of a single multiplet are characterised by similar structures; but the rule is not invariable, and the classifications of Shenstone,[1] Beale,[2] and Sommer[3] for the copper spectrum all agree in ascribing lines of very different breadths to single multiplets. The copper quadruplets which exhibit this peculiarity most strikingly are associated with transitions from c^4D initial terms (Shenstone's notation[1] is adopted), and the lines are characterised by the following structure:

Initial term	Character of line
c^4D_1	sharp
c^4D_2	broad
c^4D_3	broad
c^4D_4	sharp

The object of the present work was to investigate the broadening phenomena presented by these and other multiplets in the copper spectrum. The broad lines in particular show some unusual features, and it was hoped that measurements of their breadth might lead the way to an explanation of their peculiarities.

As the breadth is generally governed by the initial term, repetition will be avoided by referring to lines by their initial terms—thus λ4509 ($a^4F_2-c^4D_1$) may be called a c^4D_1 line. The word "sharp" refers to the character of the line and not to the series.

[1] Shenstone, Phys. Rev. **28**, 449 (1926).
[2] Beale, Proc. Royal Soc. **111**, 168 (1926).
[3] Sommer, Zeits. f. Physik **39**, 711 (1926).

2. Line Breadths in Emission Spectra

The breath of an emission line is usually defined as the whole wave-length distance between the two points where the intensity is half that of the maximum; this is often called the half-value breadth, and the definition is adopted in the present paper.

The chief objection to the use of the emission spectra for studying line breadths is that reversals are frequently present. By reversal the central part of the spectrum line is weakened more than the wings, the effect being to make the half-value breadth greater than that of the original emission line. However, the lines with whch we are particularly concerned are not reversed to any appreciable extent, and the results obtained indicate that no noticeable discrepancy has been caused in this way.

3. The Spectrum at Atmospheric Pressure

An ordinary electric arc has been employed with currents from two to ten amperes. In most cases the poles were of pure copper, but an alloy (Cu, 20 percent Ag, 80 percent) has been used for some spectra.

The spectrograms were photographed with a three-prism Hilger spectrograph of focal length 25 feet, the dispersion in the region investigated ranging from 0.8 to 2.4 mm per angstroms. Austral "Orthochromatic" and Ilford "Panchromatic" plates have been used, and were developed with "Rodinal" one-in-twenty. A good flow of developer over the plate was assured in all cases. Some plates were developed in a dish, a baffle being moved to and fro about 2 mm above the plate. Others were developed in a tank similar to that described by Dobson, Griffith and Harrison.[4]

The optical system is shown in Fig. 1.

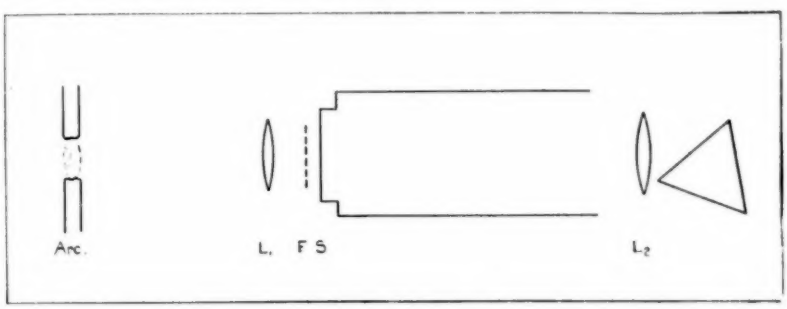

Fig. 1.

A step filter F[5,6] was mounted immediately in front of the slit S. By means of the lens L_1 the arc was focussed on to the collimating lens L_2, the image being of such size that the light from the incandescent poles could be excluded (though this made no difference). In this way it was found possible to obtain an even illumination of the slit, and the optical system was more economical

[4] Dobson, Griffith and Harrison, "Photographic Photometry" p. 77.

[5] Baly, Spectroscopy, Vol. 3, p. 157. Pannekoek and Minnaert, "Photometry of the Flash Spectrum" p. 10.

in light than that originally used by Dorgelo.[6] Times of exposure range from three minutes to two hours.

The step filter was prepared by exposing adjacent strips on a photographic plate and developing in the usual way. In order to determine the transmission coefficients for the various strips the filter was mounted as in Fig. 1, and a Pointolite spectrum photographed through it. On the same plate a series of Pointolite spectra with varying slit widths was photographed. It was assumed that the intensities of the members of this series were proportional to the slit widths; thus by measuring their densities with a Moll microphotometer at a certain point in the spectrum, it was possible to find the relation between intensity and density for that particular wave-length. In actual practice it is convenient to regard the galvanometer deflection of the microphotometer as a measure of plate density. (The plate density D is usually defined by the equation $D = \log_{10} U_0/U$, where U_0 equals deflection for clear glass, and U equals measured deflection.) The spectrum, when taken through the filter, becomes divided into a number of sections corresponding to the several filter steps. By measuring the densities of these sections, and by using the density-intensity relation just found, it is possible to derive the relative intensities for the sections, and hence the transmission coefficients of the filter steps. The calibration has been checked by comparison with a Zeiss platinum deposition filter that had been calibrated with an infrared spectrograph.

The arc spectrograms were photographed with the same optical system as shown in Fig. 1, and the microphotometer employed to trace the density curve for each section of the line. By plotting the central density for each section against intensity, as given by the filter calibrations, several points are obtained on the characteristic density-intensity curve for the wave-length region of the line being measured. From this curve one may determine the density which represents half the intensity of the line maximum, and thus the half-value breadth may be measured directly from the microphotograms. This method obviates all difficulties of uneven development and change of plate characteristic with wave-length.

The half-value breadths measured in the one atmosphere spectrum are given in Table I.

Each value in column 3 is the mean of from three to six measurements made in the different sections of the spectrum, and the variation in these values should indicate the accuracy to be expected. No instrumental correction has been applied; this will be referred to later, but it obviously cannot be greater than about ten percent for the broad lines, since λ4509 is quite sharp. Background corrections were frequently necessary; in one case the background intensity was forty percent of the intensity of the line maximum. Less reliable values are enclosed in brackets, the cause of the uncertainty being faintness of the line, or doubt about background correction.

In Table I lines with the same initial term have been grouped together, and it is apparent that within experimental error the breadth in wave-number units is the same for the lines in each group, There is, of course, a considerable change in breadth when angstrom units are employed.

[6] Dorgelo, Zeits. f. Physik **13**, 206 (1923). Dorgelo, Phys. Zeits. **26**, 756 (1925).

TABLE I.

λ	Designation	Breadth in cm^{-1}	Mean		Remarks
			cm^{-1}	A	
5857	$a^2P_2-c^4D_3$	2.9	2.9	1.0	
5432	$a^4D_2'-c^4D_3$	(3.0), 3.0, 3.05	3.02	0.89	
5391	$a^4D_3'-c^4D_3$	2.83, 2.94, 3.00, 2.97	2.93	0.85	
5201	$a^2F_3-c^4D_3$	2.97, 2.98, 2.95	2.97	0.80	
5144	$a^4D_4'-c^4D_3$	(3.2), 2.8, 3.1, 3.1	3.0	0.79	A broad line blended
4842	$a^4F_2-c^4D_3$	(3.0), (3.3)	3.2	0.75	Faint, heavy background.
4675	$a^4F_3-c^4D_3$	2.94, 2.90, 2.87, 2.92	2.91	0.64	
4587	$a^4F_4-c^4D_3$	2.90, 2.79, 2.78, 2.86, 2.85, 2.82, 2.98, 2.91, 2.84, 2.94, 2.96, 2.98	2.87	0.60	
4378	$a^4P_2-c^4D_3$	2.71, 2.90, 2.74, 2.95, 2.92, 3.0, 2.88	2.87	0.55	
4177	$a^4P_3-c^4D_3$	2.95	2.95	0.52	
5355	$a^4D_1'-c^4D_2$	(5.0), (4.4.4), 4.7, 4.4	4.6	1.3	?? Blended line
5250	$a^4D_2'-c^4D_2$	4.75, 4.64	4.70	1.3	
5212	$a^4D_3'-c^4D_2$	(4.8)	4.8	1.3	In wings of λ5218
5034	$a^2F_3-c^4D_2$	(4.6), 4.8, 4.65	4.7	1.2	
4697	$a^4F_2-c^4D_2$	(4.7), (4.6), 4.7	4.7	1.04	
4539	$a^4F_3-c^4D_2$	5.04, 4.88, 4.94, 4.75, (5.0), 4.82, 4.78, 4.9	4.87	1.00	
4416	$a^4P_1-c^4D_2$	5.01 (5.1), 4.73, 4.88	4.87	0.95	
4259	$a^4P_2-c^4D_2$	4.95	4.95	0.90	
4069	$a^4P_3-c^4D_2$	(4.7)	4.7	0.78	In wings of λ4063
5535	$a^2D_3'-c^2D_3$	4.2	4.2	1.3	
5408	$a^2D_2'-c^2D_3$	4.2, 3.91, 4.14	4.05	1.2	
5076	$a^2F_4-c^2D_3$	3.73, 3.88, 3.95	3.85	0.99	
4776	$s^2F_3-c^2D_3$	(3.9)	3.9	0.89	Heavy background.
4253	$a^4F_4-c^2D_3$	(4.0)	4.0	0.72	Faint.
4073	$a^4P_2-c^2D_3$	3.66, 4.0	3.8	0.63	
4513	$a^2P_1-b_2$	(2.5), (2.6)	2.6	0.53	Faint.
4242	$a^4D_3'-b_2$	2.29	2.29	0.41	
4123	$a^2F_3-b_2$	2.33, 2.14, 2.16	2.21	0.38	
4866	$a^2D_3'-a_3$	9.3, 8.63	8.9	2.1	
4767	$a^2D_2'-a_3$	9.1	9.1	2.1	
4507	$a^2F_4-a_3$	9.1, (8.0), 9.06, (9.3)	9.1	1.85	
4121	$a^2D_3'-d^1S_2$	0.92, 1.04, 1.03	1.00	0.17	
4080	$a^2D_3'-d_3$	1.77, 1.82	1.80	0.30	
4075	$a^2D_3'-c^2G_4$	0.64, 0.64	0.64	0.11	
5360	$a^2P_1-c^4D_1$	0.51, 0.50, 0.56, 0.47	0.51	0.15	
4509	$a^4F_2-c^4D_1$	0.37, 0.37, 0.46, 0.39, 0.38, 0.37	0.39	0.08	
4104	$a^4P_2-c^4D_1$	0.66, 0.66, 0.67	0.66	0.11	
5352	$a^2F_3-c^4D_4$	0.98, 0.85. 0.90, 0.85	0.90	0.26	
4797	$a^4F_3-c^4D_4$	0.92, 0.93, 0.92	0.92	0.21	

From the casual inspection of the copper spectrum all c^4D_1 and c^4D_4 lines would be classified as sharp, but there is actually a considerable difference between them. In general the c^4D_1 lines are sharper than c^4D_4, but apparently

exceptions to this rule exist; further refinement in measurement would be required to deal quantitatively with these lines, and for the present the chief purpose in observing them is to correct for the broader ones.

It seems obvious that there is a broadening factor present in the $c^4D_{2,3}$ and other broad lines which is definitely associated with the initial term. This will be referred to as the natural term breadth. In estimating the magnitude of this factor, which is the unusual feature of the lines in question, it is noted that all lines, broad and sharp, are influenced by instrumental breadth, pressure effect, Doppler effect, and radiation damping. I shall assume that the breadth of λ4509 (this being about the sharpest, and lying in proximity to the strongest broad lines) is entirely due to these causes. The natural term breadth can then be found by subtracting the breadth of λ4509 from the breadth of a line with the required initial term. The results of this operation are given in Table II.

TABLE II.

Term designation		Line breadth cm^{-1}	Natural term breadth cm^{-1}
Shenstone	Sommer		
c^4D_3	$^4D_3$	2.89	2.50
c^4D_2	$^4D_2$	4.87	4.48
c^2D_2	$^2D_3{}^1$	3.90	3.51
b_2	$^2D_2{}^1$	2.25	1.86
a_3	$^2D_3{}^2$	9.1	8.7
d^4S_2	$^2D_2{}^3$	1.00	0.61
d_3	$^2D_3{}^3$	1.80	1.41

We are justified in simply subtracting the breadth of λ4509, since the intensity contours of both broad and sharp lines are approximately of the form $a^2/[(\lambda-\lambda_0)^2+a^2]$ (see Section 6). When two primary broadening factors act independently, whether one be an instrumental effect, or whether both are spectroscopic, the resulting breadth may be obtained by combining together the two primary breadths; but not necessarily by simply adding them. The relation between Δ_1 and Δ_2 the primary breadths, and Δ the resultant breadth may be derived from the formula[7]

$$J(x) = \int_{-\infty}^{+\infty} L(u) \cdot S(x-u)du$$

where $L(x)$ and $S(x)$ represent the intensity contour of the primary factors, and $J(x)$ is that of the resulting line. x is the wave-length distance from the center of the contour. It is found that the relation between Δ_1, Δ_2 and Δ depends on the nature of the contours, and particularly on the intensity in the wings. Four types of contours are considered: (a) When there are no wings at all in the functions $L(x)$ and $S(x)$ (i.e., when they are of the form $L(x)=m$, from $x=-\Delta_1/2$ to $+\Delta_1/2$ and $L(x)=0$ for other values of x) then the relation becomes $\Delta=\Delta_1$ (supposing Δ_1 greater than Δ_2). (b) When small wings are

[7] Ornstein and Minnaert, Zeits. f. Physik **43**, 404 (1927).

present, as in the case of the errors curve $L(x)=e^{-ax^2}$, we have the relation $\Delta=(\Delta_1^2+\Delta_2^2)^{1/2}$ and the resulting contour is also an errors curve. (c) Passing to a contour with more prominent wings, namely $a^2/[x^2+a^2]$, we find the relation $\Delta=\Delta_1+\Delta_2$, and here again the resulting contour is similar to that of the primaries. (d) At the other extreme when the wings are very prominent as for the contour $e^{-a|x|}$ no simple relation exists, but $\Delta>\Delta_1+\Delta_2$.

From the $a^2/[x^2+a^2]$ contours in the present case it is apparent that the breadths may be simply added and subtracted.

As mentioned before the current strengths ranged from two to ten amperes. All measurements have been collected in Table I regardless of arc conditions. In order to examine whether there is any appreciable change of breadth with current strength the various values under different arc conditions are shown in Table III. Neglecting λ4509 (a sharp line) it will be seen that the measurements do not show any change of breadth with current strength, and also that the Cu-Ag alloy (20 percent copper) gives the same

TABLE III. *Breadth in* cm^{-1}.

λ	Pure copper arc					Alloy Cu 20% Ag 80%	
	2 amps.	3 amps.	4 amps.	6 amps.	10 amps.	3 amps.	10 amps.
4674		2.94		2.90, 2.87	2.92		
4587	2.94	2.78, 2.86, 2.84	2.79	2.85, 2.82. 2.78, 2.91, 2.96	2.98	2.90	
4539	(5.0)	5.04, (4.9)	4.88	4.75, 4.78	4.82	4.94	
4416			5.01	(5.1), 4.88	4.73		
4378		2.95	2.71, 2.92	2.90, 2.74, 3.00			2.88
4509	0.38			0.37, 0.39	0.46		0.37

results as pure copper; it is not unlikely that there is a slight increase of breadth with current strength of the same order as that exhibited (visually) by the sharper lines, but of course the effect is too small to detect in the broader lines. This constancy of breadth is perhaps the more significant in view of the considerable intensity changes for the same current variation. (See following paper.)

4. THE SPECTRUM AT HIGHER PRESSURES

The plates employed for determining the breadth of lines at higher pressures are grating spectrograms exposed some years ago by the late Dr. W. G. Duffield, and already described by him.[8] The source of light was a copper arc with a current of about thirteen amperes, and increase of pressure was obtained by forcing air into a cylinder enclosing the arc. It was not possible to deduce the characteristic curve separately for each plate, but the curve for the one-atmosphere plate was derived in a manner to be described, and it was assumed that other plates, which had been developed under similar conditions, had the same characteristics.

To find the relation between density (or galvanometer deflection of the microphotometer) and intensity for the one atmosphere plate, use was made of the two to one sum-rule intensity-ratio for the lines λ4531 and λ4480 ($2^2P_{2,1}-3^2S$). This value has been confirmed for arc spectra in this labora-

[8] Duffield, Phil. Trans. **A209**, 205 (1908).

tory, whence it appears that reversals, if present, have not appreciably affected the intensity ratio. A small difference of breadth was observed, the ratio for λ4531:λ4480 being 1.14:1. If it be assumed that the total intensity of each of these lines is proportional to the product of the breadth and the intensity of the maximum, then the relative intensity of the line maxima for λ4531:λ4480 must be $2/1.14 = 1.76$. This value is required for determining the characteristic curve. The lines on the grating spectrogram are drawn out by astigmatism, and spectra of the different intensities can be measured by

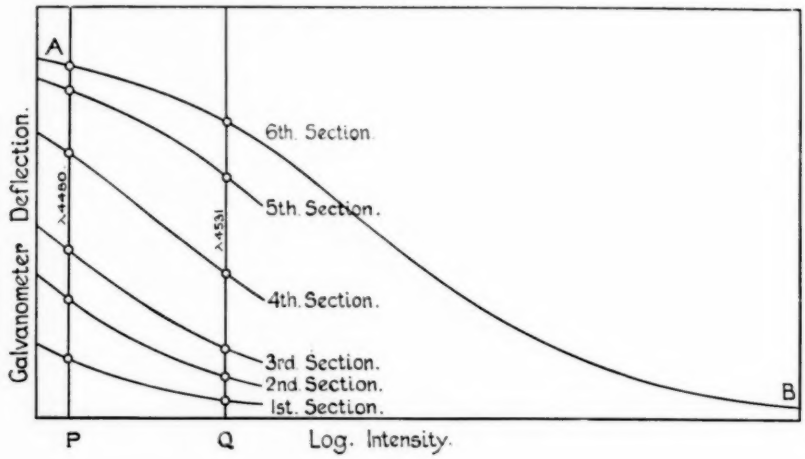

Fig. 2.

running the microphotometer at different sections normal to the lines. For each section the deflections for the maxima can be plotted against log intensity, as shown on the left of Fig. 2. Here the distance PQ equals the known log of the intensity ratio (i.e., log 1.76). The position of P is chosen arbitrarily. There are only two points to fix each curve, but the curves could be drawn, nevertheless, by use of the assumption that they are parallel to each other in the sense that for any pair the horizontal distance between them is constant. The final characteristic curve, AB in Fig. 2, is drawn by moving the

TABLE IV. *Breadth in wave-number units.*

λ	Designation	Pressure in atmospheres							Rate per atmosphere
		1	6	21	41	61	71	81	
4587	$a^4F_4-c^4D_3$	2.84	—	—	16.0	25.5	—	28.5	0.33
4539	$a^4F_3-c^4D_2$	4.4	6.9	11.4	19.2	28.6	—	36.0	0.38
4531	$2^2P_2-3^2S$	1.16	6.2	18.0	—	—	—	—	0.85
4509	$a^4F_2-c^4D_1$	0.64	2.5	6.7	—	—	—	—	
4507	$a^2F_4-a_3$	9.1*	10.6	—	—	—	—	—	
4378	$a^4P_2-c^4D_3$	2.71	4.95	9.2	15.2	19.8	26.5	30.2	0.33
4275	$a^4P_3-c^4D_4$	0.55	2.9	6.5	11.9	17.3	23.2	25.7	0.31
3530	$m^2D_2-a^4F_3$	0.6	—	2.3	4.4	6	—.	—	0.10

* Measured on prism spectrograms.

[9] Payne and Hogg, Harvard College Observatory Circular No. 301. 1927.

shorter curves horizontally to the right until they come into contact with each other. A similar graphical method has been employed by Payne and Hogg[9] for stellar spectra. By means of the characteristic curve the galvanometer deflections may be converted into intensities. The half-value breadths may then be measured on the microphotograms. The results are shown in Table IV and Fig. 3.

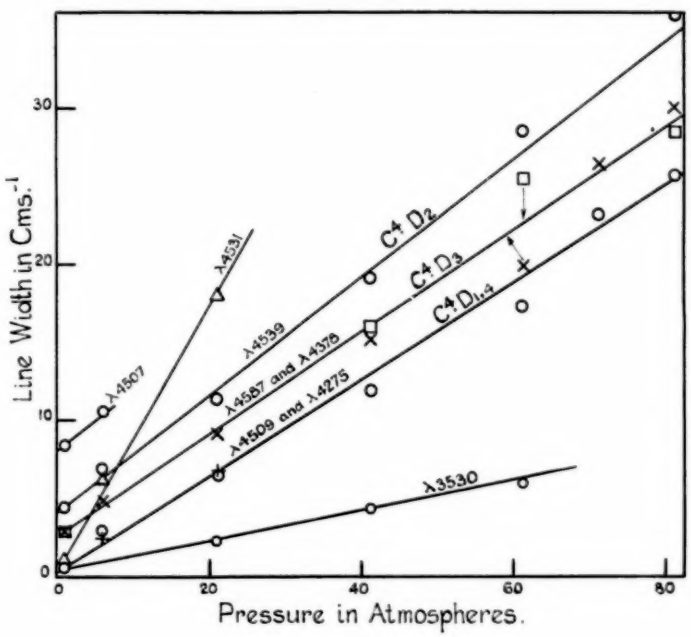

Fig. 3.

The deviations from a linear relation between breadth and pressure are probably due to the inaccuracy of the assumption that all plates have the same characteristic. It was found, in fact, that to give consistent results it was necessary to measure breadths on lines whose central density had a certain selected value. This introduces a certain amount of arbitrariness, and perhaps a considerable error into the absolute magnitude of the measurements, but it is not at all likely to affect any of the conclusions I have drawn, which are as follows:

(a) There is a linear relation between breadth and pressure for all the lines measured.

(b) For the c^4D lines the rate of increased broadening with pressure is almost the same; the variation of the rate is practically within experimental error.

(c) The line λ3530, whose initial term is at a much lower level (and therefore less likely to be disturbed by atomic collisions), is broadened much less rapidly than the other lines.

(d) The series line λ4531 is broadened much more rapidly than the non-series lines.

(e) The rule that lines with the same initial term have equal breadths still holds as the pressure increases.

(f) Extrapolating to zero pressure it would seem that all the $c^4D_{2,3}$ lines have a considerable breadth apart from any pressure effect.

(g) The broadening of λ4507, (and presumably all lines with the initial terms a_3, b_2, c^2D_3, and perhaps some others), if of the same nature as that associated with the $c^4D_{2,3}$ lines.

5. The Vacuum Arc Spectrum

From the foregoing results it appears likely that the $c^4D_{2,3}$ lines would remain broad when produced under low arc pressures, and consequently a few vacuum arc spectra have been secured in order to ascertain whether this is

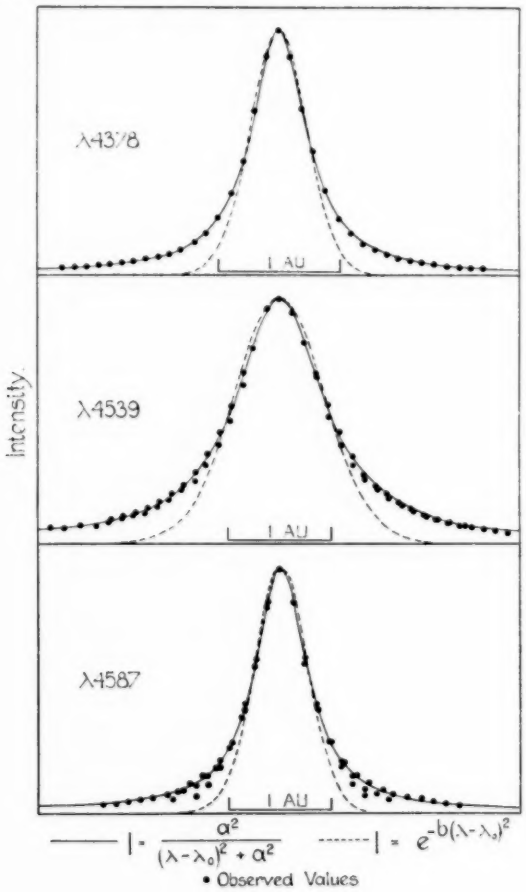

Fig. 4.

actually the case. These lines, however, become particularly faint at low pressures,[10] and at a pressure of 3 cm with a current of 11 amperes they were only just visible. The breadths of the $c^4D_{2,3}$ lines, λ4587 and λ4539, at this pressure, are practically the same as at atmospheric pressure.

[10] J. Barnes, Astrophys. J. **34,** 159 (1911); G. Wolfsohn, Ann. d. Physik **80,** 415 (1926).

6. Intensity Contours

Intensity contours of λ4587, λ4539 and λ4378 at one atmosphere (prism-spectra) have been derived from the microphotograms, using the intensity-density curve previously determined.

In Fig. 4 the experimental values are plotted against two empirical contours of the form $a^2/[(\lambda-\lambda_0)^2+a^2]$ and $e^{-b(\lambda-\lambda_0)^2}$ respectively, the constants a and b having been so adjusted that all the curves have the same half-value breadth. Fig. 4 shows that the lines are symmetrical and that they approximate more closely to the form $a^2/[(\lambda-\lambda_0)^2+a^2]$ then $e^{-b(\lambda-\lambda_0)^2}$. There are some differences among the contours of the sharp lines, but λ4509 approximates closely to the same form $a^2/[(\lambda-\lambda_0)^2+a^2]$.

It has not been possible as yet to plot intensity contours for lines at higher pressures. Many of them are unsymmetrical, and the shape of the contour is often different on the two sides. The ratios between the breadth of the red and the violet side $\Delta_r:\Delta_b$ are summarised briefly in Table V.

Table V.

λ	Type of line	Δ_r/Δ_v	
3530	$m^2D_2-a^4F_3$	1.0	Broadens symmetrically.
4539	$c^4D_{2,3}$ lines	1.0→2.0	1.0 at one atmosphere and approaches 2.0 as the pressure increases to about 80 atmospheres.
4275	$c^4D_{1,4}$ lines	2.0	Ratio does not change greatly with pressure.
4531	series line	2.7	Do Do

7. Discussion

The point to which it is desired to draw particular attention is that there still remains a considerable breadth to the $c^4D_{2,3}$ lines, (and probably other lines in the copper spectrum), when the arc pressure is reduced to zero. These lines therefore remain broad under conditions that in other spectra usually produce sharp lines, and one is faced with the question of the cause of their breadth. The factors usually considered to cause the broadening of lines[11] may be collected into three groups:

(a) The broadening consequent upon experimental conditions, including finite resolving power, Doppler effect, and reversals. These factors do not represent an actual range in emission frequency, and for study of atomic phenomena usually require to be eliminated.

(b) Broadening consequent upon emission conditions, including the effect of atomic collisions, coupling of atoms, electrical fields, and external disturbances of this kind.

(c) The natural breadth which remains when all external disturbances have been eliminated.

[11] Michelson, Astrophys. J. **2**, 251 (1895); Rayleigh, Phil. Mag. **29**, 274 (1915). Holtzmark and Trumpy, Zeits. f. Physik **31**, 803 (1925); Von Kluber, Zeits. f. Physik **44**, 481 (1927).

With reference to (a), the breadth of the $c^4D_{2,3}$ lines and other broad lines cannot be attributed to incomplete resolving power, since many much sharper lines are observed; nor to Doppler broadening, since its effect, when computed, is too small. Reversals are usually stronger for the more intense lines of a multiplet; and since the breadth under discussion is in no way a function of the intensity, this cannot be the cause; moreover the contours of the lines give no indication of reversals.

Concerning (b), one would expect to find the effect of atomic collisions the same for all lines of the multiplet, and proportional to pressure. This probably plays a considerable part in the broadening of lines under higher pressures, but cannot account for such broad lines at one atmosphere. The lines have not been reported as sensitive to electrical fields[12] as is the case with the much narrower 2^2P-3^2S lines, and therefore the breadth is not a Stark effect. Moreover, the effects of any such causes as these, which depend upon total pressure, should tend to vanish as the pressure decreases to zero, whereas there is quite a considerable residual breadth at zero pressure for the $c^4D_{2,3}$ lines quoted. On the other hand, any cause which depends on concentration of copper vapour such as coupling effect[13] and broadening due to the existence of molecular copper,[14] should be sensitive to change in current strength and composition of the poles of the arc, whereas no such variations have been found.

Apparently the phenomenon comes under group (c). The fact that the breadth is influenced so little by external conditions suggests that it is an internal property of the individual copper atom, depending on some peculiarity of the orbit. It is improbable that the broadening is due to unresolved satellites of nuclear origin since the lines are so wide and have an energy distribution of the form $a^2/[(\lambda-\lambda_0)^2+a^2]$ which is so fundamental in the theory of broadened lines. No sign of composite structure can be found from the spectra.

There are two possibilities which present themselves. (a) Normal spectrum lines are known to have a small natural breadth of the order 10^8 secs.$^{-1}$ (or 10^{-2} cm^{-1}) on account of radiation damping.[15] This has been explained in quantum language[16] by taking account of the finite length of time that an atom remains in a level before spontaneously radiating a spectrum line thereby falling to a lower level. In the normal case the mean life of a state is about 10^{-8} sec., giving as before a breadth of 10^8 sec.$^{-1}$. However, metastable levels are known whose mean length of life is considerably greater than 10^{-8} sec., and the possibility arises that particularly unstable levels may also exist for which the mean life is less than 10^{-8} sec. If such were the case presumably the lines produced from the unstable levels would have natural breadths

[12] Takamine, Astrophys. J. **50,** 23 (1919).

[13] Mensing, Zeits. f. Physik **34,** 611 (1925); Holtsmark, Zeits. f. Physik **34,** 722 (1925).

[14] Harrison and Slater, Phys. Rev. **26,** 176 (1925).

[15] Planck, Wied. Ann. **60,** 577 (1897).

[16] Van Vleck, Quantum Principles and Line Spectra, Bull. Nat. Res. Council, No. 54, p. 166, 1926.

greater than 10^8 sec.$^{-1}$, and a mean life of approximately 10^{-11} sec. would produce lines with widths of the same order as those of the $c^4D_{2,3}$ lines. Moreover, the intensity contours would be of the $a^2/[(\lambda-\lambda_0)^2+a^2]$ form as found (Section 6).

(b) On the other hand, the indefiniteness of the energy level may be due to aperiodicity of the electronic motion. A sharp quantization cannot be expected when the motion is not multiply periodic, or when the multiple Fourier series is only semi-convergent,[16] and broad lines would then be produced.

Whether due to instability or aperiodicity the breadth would be associated with the affected term, and all lines arising from one such term would have the same breadth as has been found in the present case. It is apparently rare to find wide lines of this type, but possibly the effect exists to a smaller degree in a number of sharper lines. It is however difficult to see why some lines should be affected, while others in the same multiplet are not. A study of the electron configuration has not, as yet, suggested any reason for the anomaly, nor have I been able to discover any regularity between breadth and term designation.

If the natural term breadth Δ_n is a purely inner atomic phenomenon, then the pressure broadening Δ_p of the lines concerned should be simply superimposed. In Section 3 was shown the manner in which the combination of the two broadening factors depends on their contours. In the present case the intensity contour of the natural term breadth is of the form $a^2/[(\lambda-\lambda_0)^2+a^2]$. I have not been able to determine the contour of the pressure broadening alone, (as exhibited by λ4275 ($a^4P_3-c^4D_4$) say), but the microphotograms give the impression that the wings are, if anything, more prominent than for $a^2/[(\lambda-\lambda_0)^2+a^2]$. Consequently the resultant breadth Δ should be equal to, or perhaps slightly greater than, $\Delta_n+\Delta_p$. If the pressure broadening for all the lines of the a^4F-c^4D multiplet is the same, then, as the pressure increases, we should expect the difference in the breadth to remain constant or to increase slightly. There is in fact a small increase shown in Fig. 3, though not more than could be accounted for by experimental error. The results are therefore consistent with the view that the natural term breadth and the pressure breadth act independently; that is to say, that the natural breadth is not affected by pressure.

It might be mentioned that the breadth of the pressure broadened lines is considerably greater than that produced by the Lorentz collision effect, if the ordinary gas kinetic atom radius is adopted. From the Lorentz collision theory the line breadth $2\nu'$ is given by $2\nu'=1/\pi T$ where T is the mean time between collisions.

From the kinetic theory of gases[17]

$$\frac{1}{T} = 2\cdot N\cdot S_{1s}{}^2\cdot\left(\frac{\pi}{h}\right)\left(\frac{1}{m_1}+\frac{1}{m_s}\right)^{1/2}$$

$$= \pi\cdot N\cdot S_{1s}{}^2\cdot\bar{C}\cdot\left(1+\frac{m_1}{m_s}\right)^{1/2}$$

[17] J. Jeans, The Dynamical Theory of Gases, 4th Edn., 1925, Equation 703.

and by using approximate values for the arc conditions (i.e., temperature $=3{,}000°K$; number of copper atoms in arc plasma small compared with other atoms; diameter of air molecule $=3.3\times10^{-8}$cm), and with the value of 2.7×10^{-8}cm for the diameter of the copper atom, calculation for a pressure of 61 atmospheres gives a breadth of

$$2.67 \times 10^{10} \text{ secs.}^{-1}.$$

The measured values are:

$$\text{for} \quad \lambda3530 \ (m^2D_2 - a^4F_3) \quad 18 \times 10^{10} \text{ secs.}^{-1}.$$

$$\text{for} \begin{cases} \lambda4509 & (a^4F_2 - c^4D_1) \\ \lambda4275 & (a^4P_3 - c^4D_4) \end{cases} \quad 57 \times 10^{10} \text{ secs.}^{-1}.$$

If the Lorentz collision effect is the chief cause of pressure broadening, it would be necessary to assume[18] that the effective diameter of the copper atom is about 12×10^{-8} cms when emitting λ3530 and 24×10^{-8} cm for λ4509 and λ4275. However, from the asymmetry of the lines it is clear that another factor is contributing towards the line breadth,[19] and consequently these values are likely to be an overestimate of the diameter of the excited atom. It is interesting to note, nevertheless, that the lines arising from the higher energy levels, such as c^4D, lead to greater atomic diameters than for the lower a^4F levels. This would be expected since the electronic orbits are greater in the higher levels.

[18] Stuart, Zeits. f. Physik **32,** 262 (1925).
[19] Minkowski, Zeits. f. Physik **55,** 16 (1929).

THE INTENSITY OF QUARTET LINES IN THE ARC SPECTRUM OF COPPER

By C. W. Allen
Commonwealth Solar Observatory, Canberra, Australia

(Received November 11, 1931)

Abstract

Intensity measurements in the arc spectrum of copper have been made for the quartets $a^4D^1-c^4D$, a^4F-c^4D, a^4P-c^4D, by using an electric arc at atmospheric pressure, and currents ranging from 1 to 19 amperes. It has been shown that the lines of these quartets may be divided into two groups, (a) those with initial terms $c^4D_{1,4}$ (sharp lines) and (b) those with initial terms $c^4D_{2,3}$ (broad lines), such that within each group the intensity relation of the lines remains practically constant for all current strengths. In comparison with group (a), however, the lines of group (b) increase their intensity rapidly with current strength up to about 12 amperes, beyond which they remain constant. The intensities approach nearer to the sum rule predictions for currents over 12 amperes, but even then there are some deviations. Nevertheless the similarity between the observed and calculated values supports the accuracy of the line classification.

IN THE preceding paper an investigation has been made of the abnormal breadth of certain quartet lines of the copper spectrum. The same lines are characterised by unusual intensity changes, which have been measured, and are discussed in the present paper. The lines observed belong to three quartets $a^4D'-c^4D$, a^4F-c^4D, a^4P-c^4D, which occur in the region λ4000–5600, and the designations are given for convenience in Table I, where the broad lines are marked "u".

Table I. *Wave-lengths of lines measured.*

Final terms	Initial terms c^4D_4	c^4D_3	c^4D_2	c^4D_1
a^4D_4'	5292	5144_u		
a^4D_3'	5555	5391_u	5212_u	
a^4D_2'		5432_u	5250_u	5016
a^4D_1'			5355_u	5111
a^4F_5	5641			
a^4F_4	4704	4587_u		
a^4F_3	4797	4675_u	4539_u	
a^4F_2		4842_u	4697_u	4509
a^4P_3	4275	4177_u	4069_u	
a^4P_2		4378_u	4259_u	4104
a^4P_1			4416_u	4249

Experimental Method

The method of measurement employed is similar to that developed by the Physical Institute of Utrecht, but with the optical system described in the

preceding paper, (see Fig. 1, p. 43). In the present case the light from the whole of the arc, including the poles, has been allowed to fall on to the spectrograph lens.

Two filters were employed (1) a photographic filter made in our own laboratory, and (2) a platinum deposit filter made by Zeiss. Both were calibrated by the method described in the previous paper, and about the same number of observations were made with each. An infrared spectrograph also was used to check the calibration of the Zeiss filter in the region λ5000–5600. The change of absorption with wave-length for the two filters was in the opposite sense, and there was no systematic difference between the results of each. The graphs should indicate the accuracy to be expected from the measurements.

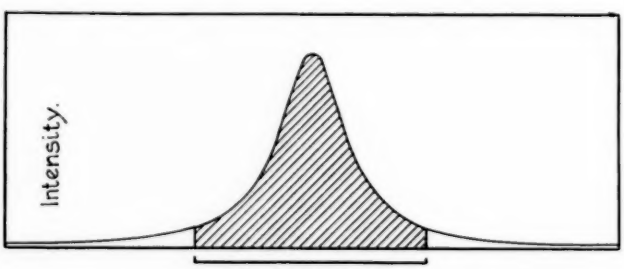

Fig. 1.

The color correction was made in the usual manner with (a) an a.c. Pointolite, and (b) a spiral filament lamp. The brightness temperature of the tungsten bead of the Pointolite was determined by means of an optical pyrometer, and from this the colour temperature was derived from the data of Hyde, Cady, and Forsythe.[1] The color temperature of the spiral lamp had been determined for a given voltage by the Nela Research Laboratory.

Most of the observations were made with a Hilger El quartz spectrograph using a slit whose width was equivalent to 27 cm^{-1} units on the plate at λ4500. Even with as wide a slit as this it was necessary to make a correction for the intensity of the broad lines relative to the sharp ones. In order to estimate the magnitude of this correction, use was made of the line contours determined in the previous paper. In making photometric observations the microphotometer deflection is determined for the center of the image only, and if the line is sharp the whole of its light energy contributes towards this central intesity. For a broad line however this is not so, since the central part of the image does not receive any of the light that lies outside the region whose wave-length distance from the center is greater than half the equivalent width of the slit. In the accompanying diagram (Fig. 1), which represents the intensity contour of the line, only the shaded part contributes towards the measured intensity, whereas it is desired to know the total intensity represented by the whole area; the values measured should therefore be increased in the ratio

[1] Hyde, Cady and Forsythe, Phys. Rev. **10**, 395 (1917).

$$\frac{\text{total area}}{\text{shaded area}}.$$

It has been shown in the preceding paper that the intensity distribution of the lines in question is of the form $a^2/[x^2+a^2]$ where for λ4587 "a" has the value 1.44 cm.$^{-1}$ Therefore for this line

$$\frac{\text{total area}}{\text{shaded area}} = \frac{\int_{-\infty}^{+\infty} \frac{(1\cdot44)^2}{x^2+(1\cdot44)^2}\cdot dx}{\int_{-13\cdot5}^{+13\cdot5} \frac{(1\cdot44)^2}{x^2+(1\cdot44)^2}\cdot dx} = 1\cdot07.$$

Consequently the intensity of λ4587 must be increased by 7 percent. Similar corrections were made for all c^4D_2 and c^4D_3 lines. It should be remarked that in adopting this procedure it is assumed that the $a^2/[x^2+a^2]$ form extends much further on either side of the line than has actually been measured. A similar assumption would have to be made whatever method was used to correct for the difference of breadth.

There was a certain amount of doubt about the intensity of some of the lines when the small resolution of the quartz spectrograph was used, on account of the proximity of other lines. In order to overcome this difficulty these lines were measured also with a large three-prism spectrograph, which gave more than sufficient resolution, but which had the disadvantage that only a small region of the spectrum could be photographed at one time; thus the intensity of lines measured with this instrument could be compared only with neighbouring lines. In order to determine the intensity of each line, the breadth was multiplied by the maximum ordinate of the intensity contour. The method of measuring line breadths has already been described.

Ilford Panchromatic plates have been employed, and developed with Rodinal in a tank similar to that described by Dobson, Griffith and Harrison.[2] Photograms of the plates were made with a Moll microphotometer, it being necessary to have a trace run off for each of the six sections of the spectrum produced by the filter steps.

The intensities were reduced graphically by the standard procedure. The background intensity, (which for the wide slit was considerable), was subtracted to give the true intensity of the line. No correction has been made for reversals, and it is believed that, if the effect is present at all, it is small because (a) in the broad lines there is no sign of reversal, which would be detected by a dip in the top of the microphotometer trace, (b) the change of relative intensity of sharp lines, (or alternatively broad lines), with current strength is small, if indeed it really exists. The small variation shown by λ4704, however, may possibly be due to a systematic diminution of the intensity of λ4651 by reversal with increased current. Reversals, then, may have modified the results slightly, but an allowance for them would not bring the results nearer the theoretical values.

[2] Dobson, Griffith, and Harrison, Photographic Photometry, p. 77.

Source of Light

An ordinary electric arc at atmospheric pressure was employed, the conditions being similar to those in the preceding work on line breadth. The distance between the poles was from 5 to 10 mm, and the current strength varied from 1 to 19 amperes.

Results

The results of the measurements are shown in the Figs. 2, 3 and 4.

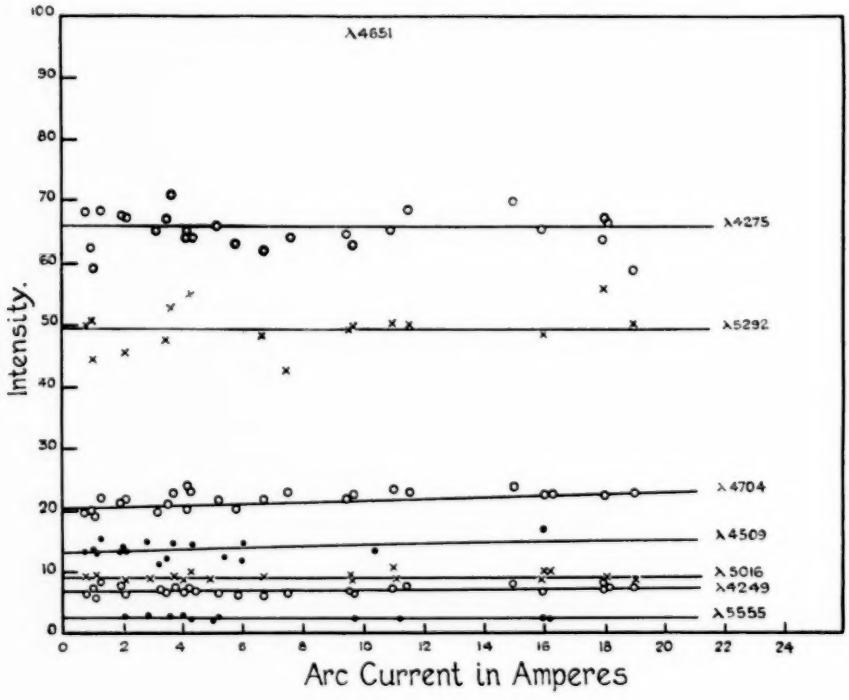

Fig. 2.

In Fig. 2 the line λ4651 ($a^4F_5 - c^4D_4$) has been taken as the standard, and for the various current strengths the relative intensities of other sharp lines, whose initial terms are either c^4D_1 or c^4D_4, are given. It will be noticed that there is practically no change of relative intensity with arc current.

In Fig. 3 the same line is taken as standard and the intensities of the broad lines, whose initial terms are either c^4D_2 or c^4D_3, are plotted. In this case a regular change of intensity is observed.

In Fig. 4 a broad line λ4587 ($a^4F_4 - c^4D_3$) is taken as standard, and the intensities of other broad lines, with initial terms c^4D_2 or c^4D_3, are compared with it. The results show no systematic change with current strength either for c^4D_2 or c^4D_3 lines. The increased irregularity of the values on the left of the diagram is due to the diminution of intensity for smaller currents.

The diagrams show that the lines of these quartets may be divided into two groups, (the $c^4D_{1,4}$ and the $c^4D_{2,3}$ groups), which are just as distinct as

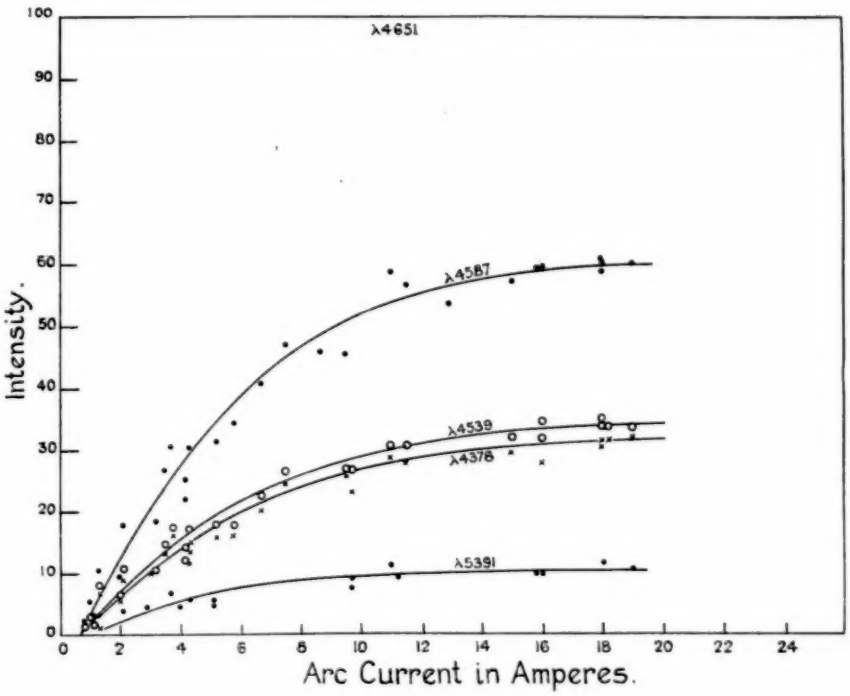
λ4651
λ4587
λ4539
λ4378
λ5391
Intensity.
Arc Current in Amperes.

Fig. 3.

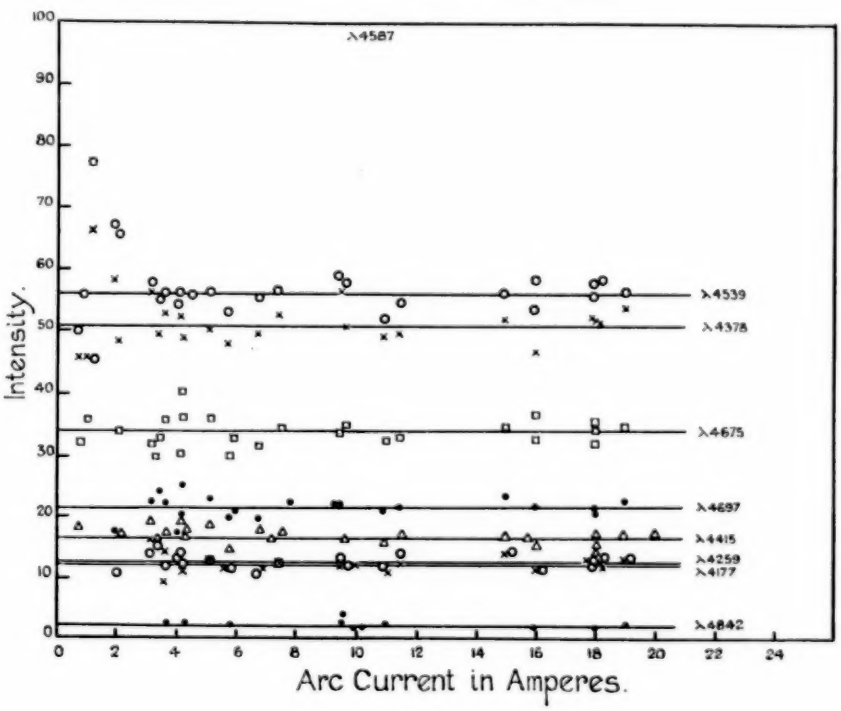
λ4587
λ4539
λ4378
λ4675
λ4697
λ4415
λ4259
λ4177
λ4842
Intensity.
Arc Current in Amperes.

Fig. 4.

regards their intensity behaviour as their breadth. Within each group the lines bear a constant intensity relation to one another, while, as a whole, the intensity of one group changes with respect to the other. In the preceding paper reasons were given for supposing that the breadth of the $c^4D_{2,3}$ lines

TABLE II.

Final terms	Initial Terms				Sums	I_m/I_e
	c^4D_4	c^4D_3	c^4D_2	c^4D_1		
a^4D_4'	82.9 68.8	(24) 11.2			106.9 80.0	1.34
a^4D_3'	4.9 11.2	19.0 34.6	5.2 14.2		29.1 60.0	0.48
a^4D_2'		11.0 14.2	17.8 15.8	12.2 10.0	41.0 40.0	1.02
a^4D_1'			9.8 10.0	8.1 10.0	17.9 20.0	0.90
Sums	87.8 80.0	54.0 60.0	32.8 40.0	20.3 20.0	194.9 200.0	0.97
a^4F_5	100.0 100.0				100.0 100.0	1.00
a^4F_4	22.0 11.6	56.7 68.4			78.7 80.0	0.98
a^4F_3	1.1 0.5	20.8 14.8	30.0 44.8		51.9 60.0	0.87
a^4F_2		1.6 0.8	12.6 11.2	11.9 28.0	26.1 40.0	0.65
Sums	123.1 112.0	79.1 84.0	42.6 56.0	11.9 28.0	256.7 280.0	0.91
a^4P_3	47.1 48.0	4.8 10.8	0.2 1.2		52.1 60.0	0.87
a^4P_2		24.0 25.2	5.3 12.8	0.7 2.0	30.0 40.0	0.75
a^4P_1			8.0 10.0	4.8 10.0	12.8 20.0	0.64
Sums	47.1 48.0	28.8 36.0	13.5 24.0	5.5 12.0	94.9 100.0	0.78
Total	258.0 240.0	161.9 180.0	88.9 120.0	37.7 60.0	546.5 600.0	
I_m/I_e	1.08	0.90	0.74	0.3	0.91	

was an inner atomic property, i.e., was not caused by external disturbances. It is therefore, now, rather surprising to find that the intensity of these lines is very much affected by external conditions (as, for example, arc current).

It might have been expected that, since the c^4D_2 lines are broader than the c^4D_3, the former would be more affected by arc current strength than the

latter. If this were so, a change of the relative intensity of λ4539: λ4378 should occur, but the results show this not to be the case (see Fig. 4).

Comparison with the Sum Rule Predictions

Since all lines with a common initial term have an intensity variation in the same sense, it is obvious that the sum rule cannot hold for all current strengths. However for currents above 12 amperes there is no great change of relative intensity, and it appears that the ratios reach a limiting value for high currents. It so happens that the intensities approach more nearly the sum rule predictions for this limiting value than for smaller currents.

In Table II the limiting intensities for high currents are divided by ν^4 and compared with the values predicted by the sum rule, as extended for individual intensities by H. N. Russell,[3]. and for intensities of triads by R. de L. Kronig.[4] The line λ4651 is given the intensity of 100 units for both measured and calculated values, and the measured value is placed above the calculated value. The ratios of the measured to the calculated sums I_m/I_c are also given. It will be noted that when the intensities are added vertically there is a gradual decrease of I_m/I_c from left to right. This may be due, to some extent, to the decrease of population of the higher initial energy levels on account of temperature equilibrium. Taking the two extremes c^4D_1 and c^4D_4, and by using the formula $\log_{10}R=0.625(\sigma_1-\sigma_2)/T$,[5] the derived temperature is about 5500°K. Although this is a considerably lower temperature than that found by Nottingham[6] for the electrons in the copper arc, his value being from 10,000° to 19,000°K, yet it is of interest to note that by adopting a tempera-

Table III. *Measured intensities corrected for temperature (5500°K).*

Final Terms	Initial Terms c^4D_4	c^4D_3	c^4D_2	c^4D_1	Sums	I_m/I_c
a^4D_4'	76.8	25.5			102.3	1.28
a^4D_3'	4.5	20.1	6.6		31.2	0.52
a^4D_2'		11.6	22.5	19.4	53.5	1.34
a^4D_1'			12.4	12.8	25.2	1.26
Sums	81.3	57.2	41.5	32.2		
a^4F_5	92.7				92.7	0.93
a^4F_4	20.4	60.2			80.6	1.01
a^4F_3	1.0	22.1	38.0		61.1	1.02
a^4F_2		1.7	16.0	18.9	36.6	0.92
Sums	114.1	84.0	54.0	18.9		
a^4P_3	43.6	5.1	0.3		49.0	0.82
a^4P_2		25.5	6.7	1.1	33.3	0.83
a^4P_1			10.1	7.6	17.7	0.88
Sums	43.6	30.6	17.1	8.7		
Grand sums	239.0	171.8	112.6	59.8		
I_m/I_c	1.00	0.96	0.94	1.00		

[3] Russell, Proc. Nat. Acad. **11,** 314 (1925).

[4] Kronig, Zeits. f. Physik **33,** 261 (1925). tide Harrison and Engwicht, J.O.S.A. **18,** 287 (1929).

[5] Harrison, J.O.S.A. **19,** 109 (1929).

[6] Nottingham, Bull. Amer. Phys. Soc. **3,** 11 (1928).

ture of 5500°K, and correcting the intensities to infinite temperature, there is a general improved agreement with the sum rule. The measured intensities corrected for a temperature of 5500°K are given in Table III. The vertical sums are, of course, considerably nearer the predicted values, since the temperature has been adjusted to make them so; but it will be noticed that there is an improvement in the horizontal sums also. With one exception (i.e., for a^4D_3') the values of I_m/I_c in the last column are now nearly constant within each multiplet. It cannot be assumed from this, with any certainty, that the effective emission temperature of the arc is actually 5500°K, since it is by no means certain that the line intensities approach so nearly the predicted values. There are still many wide discrepancies for the individual lines.

In view of the difference in nature of the $c^4D_{1,4}$ lines on the one hand, and the $c^4D_{2,3}$ lines on the other, one might be inclined to doubt the correctness of the term analysis, and the question arises whether the present intensity measurements support the classification that has been given. It should be remembered that the general agreement with the sum rule, described above, occurs only when high arc currents are employed, and that for low currents there is very little similarity between measured and predicted intensities. Nevertheless it is most improbable that there should be such agreement under any conditions, if the two groups of lines had no definite multiplet connection, and it is considered, therefore, that the intensities give strong support to the classification.

It has been shown that the intensity ratio of the broad $c^4D_{2,3}$ lines to the sharp $c^4D_{1,4}$ lines depends on the current flowing in the arc. This ratio depends also on other arc variables such as pressure; for it is found that at low arc pressures the $c^4D_{2,3}$ lines are very faint even for high currents. A further set of intensity observations has been made (not of great accuracy) to determine the manner in which this ratio depends on current strength when the poles of the arc are an alloy of copper and silver (10 percent copper). The result was approximately the same as for pure copper.

It is apparent that the variable factor in the arc, which controls the excitation of the $c^4D_{2,3}$ lines, increases with current strength, increases with pressure, and is not greatly affected by the composition of the poles. Nottingham's study of the copper arc[7] has shown that there is a significant increase of electron and ionic concentration with increase of arc current. Moreover these two factors would probably increase with pressure, and be independent of pole composition, and thus may be directly associated with the excitation of $c^4D_{2,3}$ lines, though there seems to be no explanation why such a connection should exist unless it is analogous to the production of forbidden lines in electric fields. A further point which is interesting, though not apparently significant, arises out of the variation of broad line intensity with pressure. Bowen[8] has shown that the intensity of lines from metastable levels (i.e., levels with long mean life) is increased at low pressures. On the other hand, the intensity of lines arising from the $c^4D_{2,3}$ levels, which I have suggested

[7] Nottingham, Jour. Frank. Inst. **207**, 299 (1929).

[8] Bowen, Astrophys. J. **67**, 1 (1928).

may be associated with a particularly short mean life (see previous paper, p. 000), is decreased at low pressure. A little consideration however shows that this decrease of intensity cannot be explained on Bowen's argument, and consequently the two phenomena are not to be ascribed to the same cause.

I have not been able to give a satisfactory explanation of the phenomena connected with the breadth and intensity of these lines, but it is hoped that the present measurements will be of some assistance in solving the problem.

Remarks on the two preceding papers by C. W. Allen on

1. Broad Lines in the Arc Spectrum of Copper.
2. Intensity of Quartet Lines in the Arc Spectrum of Copper.

The anomalous character of the Cu I quartet multiplets with which the above papers are concerned has long offered great theoretical difficulty, and I have, unsuccessfully, urged several specialists in the field of intensities to undertake quantitative measurements. Mr. Allen's papers cover the problem very effectively from the experimental standpoint but he is unable to offer any explanation for the fact that the diffuse lines still retain their great width at low pressures and that, relatively to the sharp lines, they all decrease in intensity with decreasing arc current and with pressure. The observations form the most complete confirmation of the theoretical explanation which I offered last spring (Phys. Rev. **37**, 1701A, 1931 and Phys. Rev. **38**, 873, 1931). Auto-ionization (Auger-effect) is undoubtedly responsible for these anomalies and Mr. Allen's paper offers the experimental basis for a further theoretical study of that effect. I hope to publish further observations on all of the negative terms of Cu I in the near future.

A. G. SHENSTONE

Princeton University,
November 20, 1931.

THE ABSORPTION OF INFRARED RADIATION BY SMALL PARTICLES

By A. H. Pfund and S. Silverman
Physical Laboratory, The Johns Hopkins University

(Received October 30, 1931)

Abstract

The absorption of infrared radiation by small particles of quartz, calcite and ammonium chloride has been studied. For this purpose a special radiometer was constructed, with its vanes coated with the material to be studied. Evidence is brought forth to show that the crystals, when sufficiently finely divided, do not reflect well in their regions of metallic reflection. This offers a simple method of studying the absorption spectra in these regions. In addition, a new type of selective filter employing a radiometer seems possible, with preliminary experiments in accord with expectations.

AN INVESTIGATION by one of us (S.S.)[1] on the fine structure reflection spectrum of polished calcite revealed a number of narrow reflection maxima whose positions agreed precisely with those of narrow transmission minima revealed by thin layers of powdered calcite. The question arose as to whether these minima were true absorption bands or whether they owed their existence to selective reflection, in virtue of which less energy would enter the powder film, thus decreasing the intensity of the transmitted radiation. To decide this matter, a study of the absorbing and reflecting properties of particles whose linear dimensions are small in comparison to the wave-length of radiation was undertaken.

The question might have been settled by using a hemispherical, silvered mirror of the Paschen[2] type. Such a mirror not being available it was decided to attack the problem by a method long used by one of us (A.H.P.). This procedure involves coating the receiving area of a thermopile or radiometer with a thin film of the powdered material to be studied. True absorption would cause an increased heating of the receiver while selective reflection would cause decreased heating.

For this work the radiometer was chosen in preference to the thermopile. The reason was that, since the sensitivity of the radiometer is primarily dependent upon the temperature difference between front and back of the vane, it was anticipated that, because of the high extinction coefficients of calcite, quartz, etc. in the regions of selective reflection, intense surface heating would be produced in case the powder particles acted as absorbers.[3] Two additional reasons which prompted the choice of the radiometer were: (1) ease of application of thin powder-films, (2) possibility of developing a "selective" radiometer, i.e., one which responds largely to a limited region of the spectrum.

[1] To be published shortly.

[2] W. W. Coblentz, Bur. Stan. Jour. Res. 9, 283 (1913).

[3] A detailed description dealing with the construction of radiometer vanes will appear shortly. A. H. P.

Apparatus and Method of Procedure

For such an investigation, on which slight demands are placed upon resolving power and sensitivity, it was found advisable to use a rock-salt prism spectrometer with an ordinary Wadsworth mounting. A single prism was used with mirrors of 30 cm focal length with slit-widths of approximately 0.5 mm. A Nernst glower, run at 0.2 amperes and 220 volts, was used as the source of radiation. The radiometer was very robust; the vanes were 1×7 mm and were mounted upon a quartz fiber of a length which gave a period of about 1 sec. The vanes were prepared by mounting lens-paper on thin films of nitrocellulose, and combined extreme lightness with great sturdiness. The vanes were mounted in pairs in the usual fashion; one was given an additional coat of gold-leaf which was then sooted with camphor-black, and the other was coated with the material to be studied. It was found that the precaution of adding gold-leaf enormously facilitated the deposition of an adequate layer of soot. The radiometer behaved admirably. It was very stable, being practically free of drifts and stray vibrations which render a lighter system of long period so difficult to operate; and it was possible to take all readings during the daytime.

The method of procedure was to mount the radiometer in place with a large bottle of some three liters capacity, containing some phosphorous pentoxide, placed in series with the tube; the system was then evacuated by means of an ordinary oil-pump. The large capacity served to prevent pressure fluctuations when the pump was shut off, and the pentoxide prevented water vapor from curling the vanes when the outfit was at atmospheric pressure. The system was evacuated until the radiometer became slightly ballistic; this is the optimum point obtainable as it provides good sensitivity with high speed of response and accuracy of readings. The radiometer at these pressures is an extremely good pressure gauge, so that it was rather easy to ascertain that the sensitivity of the radiometer remained constant throughout a run. In practice it was found that the sensitivity did not suffer any measurable change within 48 hours after turning off the pump. The radiometer gave readings of about 5–20 cm at a scale distance of 2 meters. The spectral runs covered a region from 3μ to about 11μ, at intervals of about 0.1μ. Readings were taken first with the blackened vane in place and immediately afterward a second run was taken with the powdered vane in position. The relative radiometric powers follow by simple ratios, for, with identical air-paths, atmospheric absorption is equal for both runs. Following this, a set of readings was taken to yield the transmission spectra of the various salts on nitrocellulose; the cellulose itself was so thin that it showed first order Newton's colors, and hence was almost perfectly transparent to the entire region covered. Inasmuch as NH_4Cl sublimes very readily, it was more feasible to fume the salt than to "paint" it. Powdered calcite and quartz were obtained in a state of fine subdivision and were mixed with water and a minute amount of gum arabic. These mixtures were well dispersed, and spread uniformly over the surface of nitrocellulose. The films were laid down to such a thickness that a bright tungsten filament could not be seen through them. The radiometer vanes, it might be

added, were coated in a similar fashion, except that the films were very much thinner, giving a smooth chalky surface which was gray against its dark background.

The reflection data for quartz and calcite were easily obtained from previous investigations.[4,5,6] However, for NH_4Cl, the best curve obtainable was that of Reinkober[7] which was taken on a plate of highly compressed powder. Although such a plate should approximate a smooth massive crystal, it was thought best to use a single slab of the salt, if possible. Fortunately a large crystal possessing a good surface of about 3×4 cm was found in a laboratory supply jar. The crystal was fairly clear and when ground and polished, it yielded a very creditable surface.

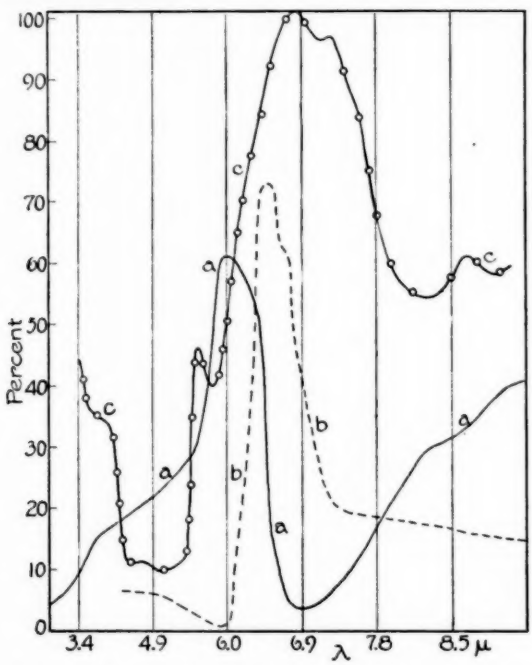

Fig. 1. Calcite (a, c powder, b, plate) a, transmission; b, reflection: c, radiometer.

Results

The reflection spectrum of calcite, Fig. 1b shows a strong maximum at $6.5-6.6\mu$ rising very sharply on the short wave side, and falling off less rapidly on the long wave side. The transmission of the thin powder, Fig. 1a, shows strong opacity at 2.9μ with a sharp rise in transparency, broken slightly at 3.5μ, to a maximum at 5.9μ of 60 percent. This is followed by a region of strong absorption whose center lies at about 6.8μ. The calcite again becomes transparent but never reaches a value much higher than 40 percent on the long wave side of this band. The radiometric curve Fig. 1c shows calcite to be

[4] Lecomte, "Le Spectra Infrarouge."
[5] Schaefer and Matossi, "Das Ultrarote Spektrum."
[6] Hardy and Silverman, Phys. Rev. **37**, 176 (1930).
[7] Reinkober, Zeits. f. Physik **3**, 1 (1920).

about 40 percent as good as soot at 3.5μ. This then falls with increasing wave-length to a minimum of 10 percent in the region of 5μ. Following this is a sharp, steady increase in radiometric power broken only by a small dip at 5.8μ. The curve rises again, increasing through the successive regions of strong reflection and absorption to a maximum value of nearly 100 percent between 6.7μ and 7.3μ. The curve then falls off to a fairly steady value of 60 percent as far out as 9.2μ. It might be pertinent to remark at this point that it is quite essential to provide a heavily sooted vane for comparison work of this sort. The first sooted vane which was used was prepared simply by depositing the soot directly on the paper vane; the second vane was prepared, as mentioned above, by depositing the black on goldleaf. It was found that at 10μ the second vane was nearly four times as sensitive as the first.

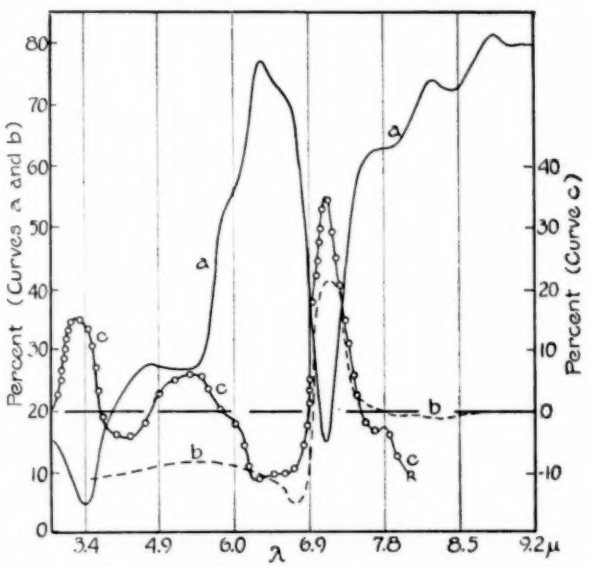

Fig. 2. Ammonium chloride (a, c, fumed; b, plate); a, transmission; b, reflection; c, radiometer.

Fig. 2b shows the reflection curve for NH_4Cl; the data taken for the large polished crystal were found to coincide very nicely with the results of Reinkober on a compressed plate of the same salt. There is relatively a strong maximum at 7.1μ, and a very weak one at 3.4μ. The transmission of the sublimed film is shown in Fig. 3, curve a. There is a minimum at 3.4μ and indications (which are not very pronounced) of another minium at 5.2μ; there follows a sharp maximum at 6.2μ with a precipitious minimum at 7.1μ. The absorption then falls off, and the material becomes increasingly transparent toward longer waves with slight fluctuations in percentage of transmission. The radiometric power (curve c) yields a trace which is a fine counterpart of the reflection and absorption curves; at 3.4μ and 5.2μ there are maxima, followed by a minimum at 6.2μ and a strong maximum at 7.1μ. Beyond this wave-length there is a sharp decrease. It will be noted here that there are recorded negative percentages, which correspond to a radiometer throw in the negative direction. Their significance is that at the wave-lengths where these

negative throws occur, the NH_4Cl is so transparent that the radiation penetrates to the back of the vane, which is in this case charred paper. This material is sufficiently black to create, upon heating, a "back radiometric" effect; and in these regions it is from this side of the vane that the radiometric action takes place; so that in this way a complete reversal of the direction of deflection may occur. Quite obviously this difficulty can be readily avoided by depositing a sufficiently heavy film of salt, or by employing some transparent material for the back of the vane.

Fig. 3, curve b, illustrates the reflection spectrum of quartz. It possesses a strong double maximum at 8.5 and 9μ as reported by previous investigators[4,5,6] Curve a of the same diagram represents the transmission spectrum of

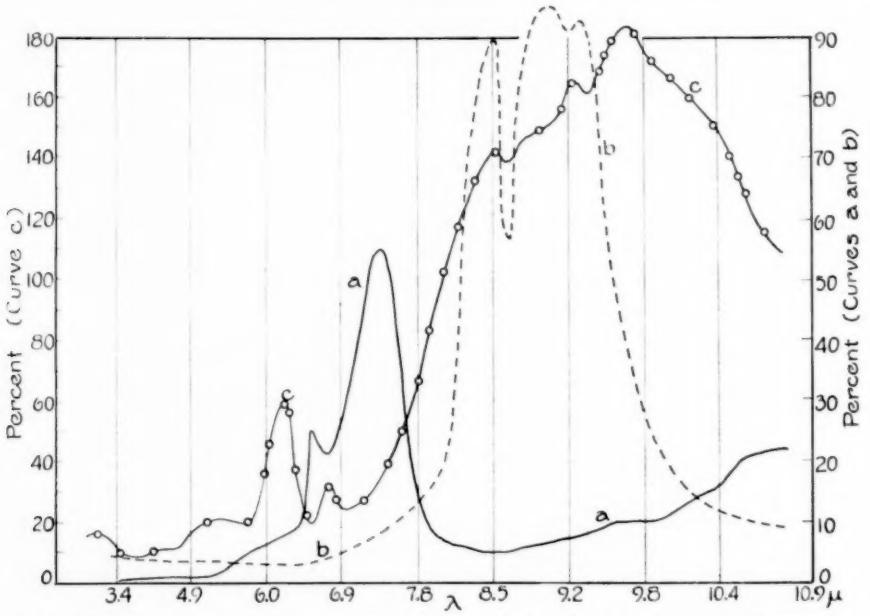

Fig. 3. Quartz (a, c powder; b, plate); a, transmission; b, reflection; c, radiometer.

the powdered crystal. There are maxima at 6.7 and 7.5μ and a minimum at 6.9μ; following the strong maximum at 7.5μ there is a region of opacity from 8.3μ to 10.4μ. Curve c is the radiometric curve. It shows small maxima at 6.2 and 6.9μ, rising to a high peak at about 9.5μ, where it is nearly twice as effective as soot; following, the radiometric power subsides with increasing wavelength to an efficiency of about 100 percent at 10.8μ.

Discussion

In all cases studied, it is to be noted that a strong radiometric effect is found both in the regions of selective absorption and selective reflection. In the case of calcite at 6.6μ where the reflection is over 70 percent and the transmission is about 25 percent, the radiometric effect is close to 100 percent. Again for NH_4Cl, at 7.1μ the reflection is 45 percent, the transmission is 15 percent and the radiometric effect is 35 percent. (It is to be noted here that

this is one of the few instances where the wave-lengths of the absorption and reflection bands have been reported to be identical. This question will be discussed later in connection with similar results obtained in connection with a study, by one of the writers,[8] of the 6.7μ band of calcite). In the case of quartz, we have a reflecting power of about 90 – 95 percent around 9μ, with a low transmission of only 10 percent. The radiometric power, despite the extremely high reflecting power, is better than that of soot. This may partly be due to the poor absorption of soot. Inasmuch as the greater portion of the radiometric effect is due to the heating in the superficial surface layer, the powdered salts are remarkably well adapted for use as radiometer coatings; since their absorption coefficients are high, most of the absorption will take place near the surface, which is advantageous for the production of a large radiometer effect. This means then, that in the study of the strong absorption or reflection bands of a particular solid, that the receiving device should be coated with the same material, when possible.

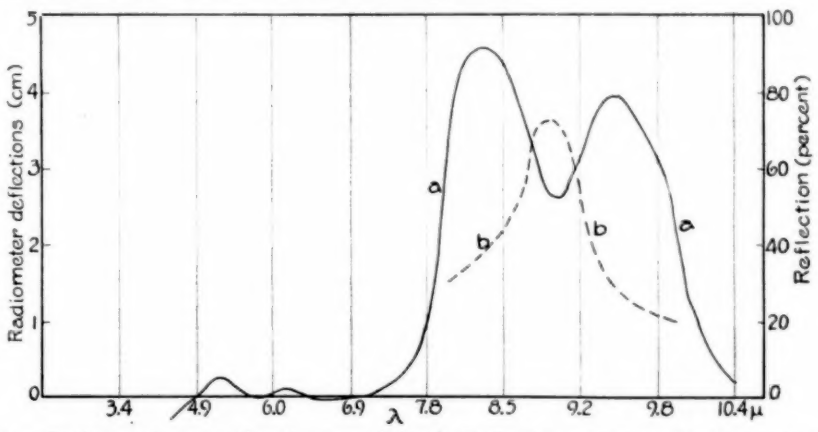

Fig. 4. a, Radiometric curve, fused quartz flake; b, Reflection spectrum, fused quartz plate.

Since the radiometric effect requires the phenomenon of absorption, these thin powders cannot reflect directly in their regions of selective reflection, for the possibility of such high reflection does not hold with the observed high radiometric power. This is illustrated in Fig. 4, curve a, which represents the energy curve for a vane made of a quartz film several μ thick. A strong minimum is perceived in the region of high reflection, (curve b). Since scattering is, for the same reason, not possible to any great extent, unless it leads to multiple reflections among the discreet particles within the powder, with ultimate absorption due to trapping, one is lead to the conclusion that the particles are too small to behave as reflectors, and absorb directly.

The particles are very fine: the quartz and calcite particles measure between 2.0 – 3.0μ and the ammonium chloride particles are considerably smaller, appearing reddish in transmitted light. This minuteness of particle and film seem to preclude possibility of trapping, and it appears that the logical explanation lies in a true absorption. This thesis has some support in a prob-

[8] S. Silverman, in print.

lem in the far infrared spectra of the carbonates which has been discussed briefly by Wood.[9] He arrives at the conclusion that particles, when too small to behave as resonators for reststrahlen, are unable to reflect, but absorb these radiations. It is quite likely that herein lies the explanation of the intense absorbing power of metallic substances such as bismuth black.

Use of the Radiometer as a Filtering Device

From an entirely different view-point, these results introduce interesting possibilities. In the ever important question of filters, it has always been desired to find a material which is transparent to the region to be studied and which is opaque to the shorter waves that lead to the contamination of higher orders in grating spectrometers. One of the writers has recently described one

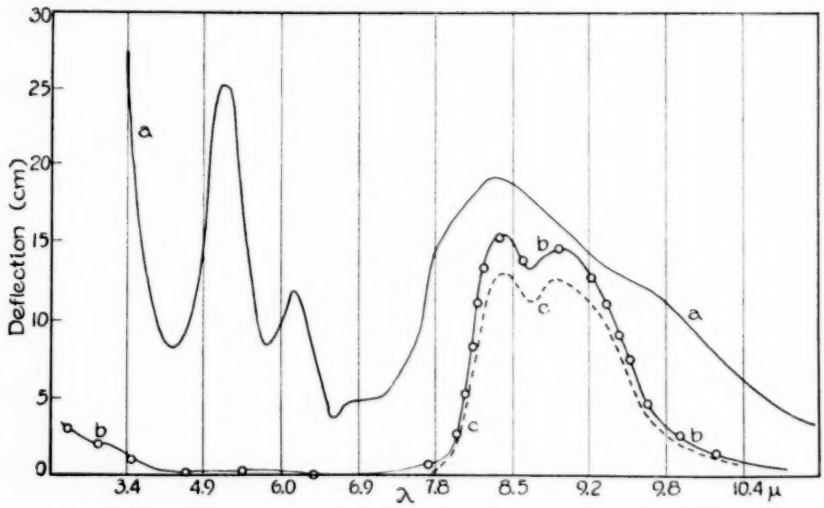

Fig. 5. Energy curves. a, Quartz coated vane: b, Quartz coated vane; radiation reflected from quartz mirror: c, Quartz coated vane with quartz mirror and MgO filter.

method by which this goal may be approached by using such powders as zinc oxide and magnesium oxide.[10] The reverse problem is much simpler: it is relatively easy to find a material which is opaque to a given region and which is transparent to shorter waves. A radiometer coated with a substance which fulfills these conditions should show a small sensitivity to the waves to which its coating is transparent, and a relatively large sensitivity to those radiations to which its coating is opaque. There is a possibility that such a filter might be very useful in the far infrared, where this difficulty has been very pronounced. For example, a vane covered with a thin film of one of the alkali-halides should be quite opaque to radiations longer than about 30μ, and shorter waves, due to the transparency of these halides in this region, should have a relatively small radiometric effect. Such a vane used with a transmission filter of quartz to deaden the enormously powerful region of 1.5μ might

[9] R. W. Wood, Physical Optics, p. 632 (Macmillan).
[10] A. H. Pfund, Phys. Rev. **36**, 71 (1930).

offer interesting possibilities in the long-wave region beyond 50μ where quartz again becomes transparent. Furthermore, by proper combinations, one could obtain a group of powders opaque to almost any given region. It is planned to attempt such an experiment in this laboratory in the near future. A preliminary attempt to construct a filter for the 9μ region is shown in Fig. 5. By a succession of combinations of a quartz-coated vane, a quartz mirror, and a film of magnesium oxide, a filter is produced which is opaque to radiations shorter than 8μ, and which is fairly transparent out to 9.5μ.

Conclusion

These investigations show that finely divided powders act as absorbers in the region of metallic reflection, and do not reflect. In a subsequent paper this is brought out to indicate that the coincidence of reflection maxima and transmission minima in calcite represents a true agreement between absorpton and reflection lines. This offers an extremely simple method of studying absorption spectra in regions of high reflection without having to allow for the loss of energy by reflection. The advantages of the radiometer over the thermocouple for this work are manifold. In addition to its superiority in speed and durability—a single suspension lasted throughout the entire experiment despite the many changes in vanes—it offers possibilities in filtering out radiations of lower wave-lengths. A preliminary combination has produced a radiometer vane and filter which is quite good for the region of 8μ to 9.5μ The general usefulness of such a filter is limited only by its transparency to shorter waves, and by the width and depth of its region of opacity. Since it has been shown that these finely divided materials become intensely black within the region of selective reflection and absorption, it is proposed to study the temperature emission of thin layers of such substances. It is anticipated that intense selective emission will occur within the region of great absorption.

The authors gratefully acknowledge a Grant-in-Aid of the National Research Council which has helped make this investigation possible.

CONCERNING THE ABSORPTION AND REFLECTION SPECTRA OF CALCITE IN THE INFRARED

By S. Silverman
Physical Laboratory, The Johns Hopkins University

(Received October 30, 1931)

Abstract

The reflection and absorption bands of calcite at 6.6–7.4μ have been studied with an echelette grating spectrometer of high resolving power, employing the resonance radiometer. A great deal of hitherto unobserved fine structure has been detected. It is to be noted: (1) that the maxima of the envelopes of the absorption and reflection bands differ widely in wave-length, as has been previously reported in the literature; (2) that within the bands, there is good agreement as to wave-length between the absorption and reflection lines. Possible explanations of this fine structure are offered, including that of combinations of reststrahlen and near infrared frequencies.

THE infrared absorption and reflection spectra of the carbonates have been studied over a long period of years. They are fairly easy to obtain in suitable form and are to be found in several interesting crystalline types. It was felt, after a previous paper[1] on the fine structure of quartz, that it would prove of value to study calcite more carefully, in view of its importance in optics, which is perhaps second only to quartz, among the uniaxial group.

The spectra of the carbonates, especially those of the uniaxial group such as calcite, have been found to be rather simple; and considerable work has been done in the exploration of their structure. Thus far there has been very good agreement between theory and experiment in depicting the form of the CO_3^{--} ion. X-ray evidence points to a plane structure for the CO_3 group, in which the oxygen-centers form the vertices of an equilateral triangle with the carbon situated at the centroid. Theoretical reasoning by Kornfeld,[2] Brester,[3] and others[4] predicts for such a model three active vibrations. The first of these lies at 7μ, and is due to a motion of the carbon in the plane of the group, either along or perpendicular to one of the medians; the relative positions of the oxygens remain fixed, or nearly so. The second vibration is to be found at 11μ, and is due to a vibrating membrane type of motion of the carbon perpendicular to the plane of the group. The third active vibration to be expected is at 15μ; it is due to a motion of an oxygen along a meridian, with an accompanying distortion of the remaining oxygen members. These predictions are well borne out, for in fact, in the near infrared there are three general regions of absorption and reflection: at 7μ, 11μ and 15μ. Moreover, the 7μ and 15μ bands are actually due solely to the ordinary ray, and the 11μ band is found only in the spectrum of the extraordinary ray.

[1] Hardy and Silverman, Phys. Rev. **37**, 176 (1931).

[2] Kornfeld, Zeits. f. Physik **26**, 205 (1924).

[3] Brester, Zeits. f. Physik **24**, 324 (1924).

[4] A full discussion, with complete references, is to be found in Schaefer and Matossi, "Das Ultrarote Spektrum," (Springer 1930) and in Rawlins and Taylor "Infrared Analysis of Molecular Structure" (Cambridge Univ. Press 1928).

Of these absorption bands, that at 7μ is very broad and deep, and it has defied complete resolution. The 11μ band is rather weak, and that at 15μ is sharper but not as strong as the band at 7μ. The reflection band at 7μ is sharp and narrow compared to the absorption at this wave-length; that at 11μ is much weaker than its predecessor, and the last band at 15μ is quite faint in comparison.

There are two outstanding features concerning the relationship between the absorption and reflection spectra. The first is the relative ease with which resolution of the reflection spectrum is obtained as compared to the absorption spectrum; the second is that the wave-lengths of the 7μ and 15μ reflection bands are shorter than the corresponding absorption wave-lengths, whilst the reflection at 11μ lies to the long wave side of the absorption band.

Now, a recent investigation of the reflection spectrum of quartz,[1] in which an unsuspected amount of fine structure was revealed, caused some doubt as to the simplicity of the reflection spectra of solids in this region. It was felt that this question and the question of disparity of wave-length between absorption and reflection ought to be reinvestigated with an instrument of high sensitivity and resolving power. The 7μ band was chosen for the first study because of its great strength, and because it is generally assumed to be the first eigenfrequency of the CO_3 group.

For this exploration, the spectrometer and resonance radiometer used by J. D. Hardy[1,5] and the author earlier this year in a similar investigation of quartz, proved to be adequate. The set-up was very much the same as that described in this paper. The same grating was employed with a different mounting so that its "blaze," or concentration of maximum energy, was cast into the region to be studied. Improvements in the resonance radiometer itself were made so that the sensitivity was doubled, and a mechanical adjustment of the grids was provided to compensate zero-drifts caused by rising temperatures in the room.

Magnesium oxide was found to be quite a good filter to eliminate the higher orders of radiations of shorter wave-lengths, when prepared under the proper conditions. As reported by Pfund,[6] this oxide is an excellent filter for wave-lengths of 6μ and longer. It was found that one could fume the powder at varying particle sizes simply by burning the metal at different distances from the mirror which was being coated; since the particle size is a function of the time of growth, which varies directly with the distance through which the particle rises. After a little experimentation, a filter was prepared (by the method of trial and error) which permitted only 10 percent contamination at 6.5μ. This filter was then mounted and made a permanent part of the apparatus.

The calibration of the instrument was made by observing the higher orders of the 5461 and the 5790 lines of the mercury arc. This calibration was then compared to the wave-lengths of prominent atmospheric absorption lines.[7]

[5] J. D. Hardy, Rev. Sci. Inst. **1,** 429 (1930).
[6] A. H. Pfund, Phys. Rev. **36,** 71 (1930).
[7] Plyler and Sleator, Phys. Rev. **37,** 1493 (1931).

The two methods checked very well, the average discrepancy being less than 10A. The slits were 0.10 mm wide, which gave an effective slit-width of 20A.

For the reflection spectrum, a large calcite crystal was cut and polished to produce a mirror-surface of 5×5 cm. The final polish was as good as plate glass, and the sheet produced an image completely free of distortion; this latter is an item of considerable importance, as it is necessary to be able to reproduce the image of the filament identically. The absorption spectrum was taken in the following manner. A piece of calcite was rubbed down against a wet piece of ground glass. The fine milky powder which resulted upon drying was collected and dispersed with water to the proper degree of pastiness. This

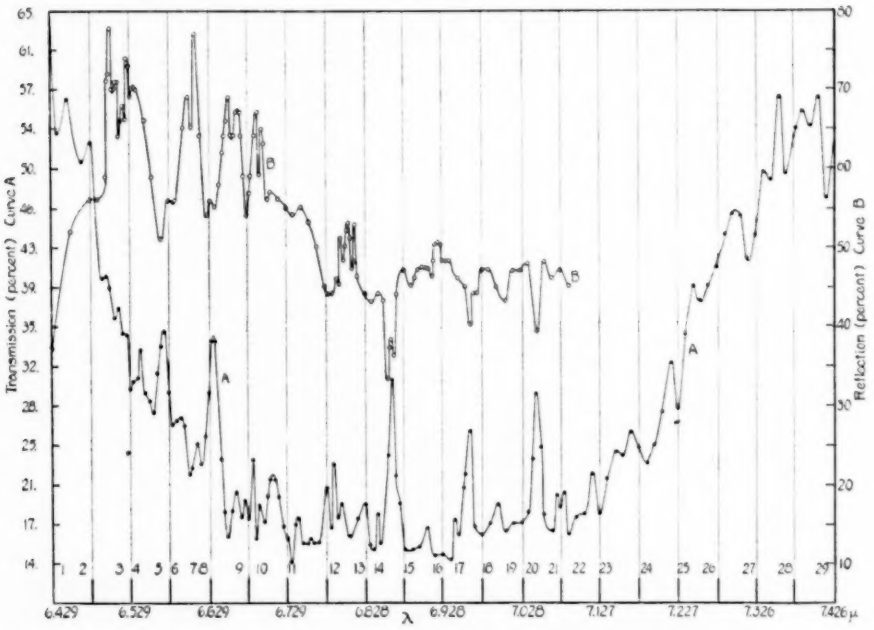

Fig. 1. *A*, Transmission of powdered calcite; *B*, Reflection from cleavage plane of calcite.

was then painted with a soft brush on a polished slab of rock-salt. Upon drying, the powder formed a thin, uniform white crust which appeared a golden brown against a bright background. In light of the previous paper, the transmission spectrum should yield, for such a powder, true absorption lines, as there is no contamination by reflection from these particles, which are small compared with the wave-length of light. The "cell" was so mounted that it could be removed from the path of the incident radiation without disturbing the calcite-coated surface. This film was thin enough to be some 14 percent transparent in the region of maximum absorption (a solid sheet 0.03–0.04 mm thick is about 2–3 percent transparent at this point). Because of the very strong and irregular atmospheric absorption in this region, it was necessary to take all readings with cell in and cell out in immediate succession. In the case of reflection, the calcite mirror was replaced by its gold counterpart for each new setting of the grating.

Results

The spectra are plotted in Fig. 1. The envelopes of the absorption and reflection curves are seen to be quite dissimilar, with the minimum of transmission lying to the longer wave-length side of the reflection maximum, in complete accord with the literature.[4] It is further seen that there is remarkably good correspondence between the wave-lengths of the absorption and reflection lines; as is shown in Table I.

Table I.

Wave-lengths of Reflection Maxima			Wave-lengths of Absorption Maxima (Transmission Minima)	
Line number	λ	$\tilde{\nu}$	λ	$\tilde{\nu}$
1			6.439	1551.6 ± 0.3
2			6.467 ± 0.0015μ	1546.3
3	6.507 ± 0.0015μ	1536.8 ± 0.3	6.505	1537.3
	6.512	1535.6		
	6.522	1533.3		
4	6.527	1532.1	6.529	1531.6
	6.537	1529.8		
5			6.559	1524.6
6			6.584	1518.8
7	6.604	1514.2	6.404	1514.2
8	6.614	1511.9	6.616	1511.4
	6.657	1502.2	6.655	1502.7
9	6.662	1501.0		
	6.669	1499.4	6.669	1499.4
			6.679	1497.1
10	6.691	1494.5	6.689	1494.8
	6.696	1493.4	6.699	1492.6
11			6.734	1484.9
12			6.783	1474.4
	6.798	1471.0	6.793	1472.1
13	6.808	1468.9	6.808	1468.9
	6.816	1467.1		
14			6.838	1462.4
	6.848	1460.3	6.848	1460.3
15	6.878	1453.9	6.878	1453.9
16	6.923	1444.4	6.928	1443.3
17			6.948	1439.2
18	6.986	1431.4	6.984	1430.9
19			7.008	1426.6
20	7.038	1420.9		
21	7.063	1415.8	7.068	1414.8
22			7.088	1410.8
23	observations not carried further		7.127	1403.1
24			7.187	1391.4
25			7.227	1383.7
26			7.257	1378.0
27			7.317	1366.7
28			7.366	1357.6
29			7.416	1348.4

It will be noted that a similar correspondence in wave-lengths of absorption and reflection lines is to be found in the case of ammonium chloride, although the agreement is not as striking as that presented here.

Discussion

A brief summary of the literature calls for a region of absorption and reflection at 7μ, Schaefer,[4] in a rather comprehensive treatment of the subject

concludes that there is a double absorption band at 7.14μ and 7.40μ respectively, corresponding to the double reflection maxima found at 6.68μ and 6.98μ. Recent results of Plyler[8] confirm the position and apparent doubling of the reflection band. In this present paper, it will be noticed that the envelopes of both the absorption and reflection bands agree admirably with the results of Plyler and Schaefer. In addition, however, a maze of fine structure, both in the absorption and reflection spectrum appears, which entirely escaped detection of less sensitive instruments. It is also to be remarked that there is actual identity in wave-length between many reflection and absorption lines, although the intensities are such as to preserve the general contours of the earlier bands. In light of the previous paper (A.H.P. and S.S.)[9] this indicates true coincidence of reflection and absorption; this means then, that it is possible to study the frequencies of crystals by either method. The theoretical side of this problem offers interesting ground, and it is hoped that such calculations will throw light upon this question.

There are two alternatives in explaining this fine structure, which in complexity rivals that of a gas. First, one might assume that there are crystal irregularities which greatly multiply the number of possible vibrations without disturbing the macroscopic symmetry of the crystal. Such an explanation has been previously offered to account for the "doubling" of this band. Secondly, one might assume that this fine structure is caused by a combination of far infrared frequencies with frequencies in the near infrared, similar to the combination of vibration and rotation frequencies in gaseous spectra. In support of this last assumption, it was noticed that there are 29 strong lines, or centers of absorption, in the band. Now, if we investigate the sequence of lines 1–16, 2–17, 3–18, $\cdots$, 14–29, we find that these transitions are all very close to 107 wave-numbers, with an average of 107.5$\bar{\nu}$. This agrees fairly well with the frequency of the far infrared reststrahlen of calcite which is at 106 wave-numbers. There are also other possible combinations to be located. For example, the set of lines 1–9, 9–15, 15–23, 23–29 are separated by approximately 50 wave-numbers. This explanation is so far only tentative, for these sets are merely the best in agreement out of several possibilities; in addition, it appears evident that complete resolution has not yet been reached. This has been acknowledged in the grouping of these lines in which two or three weak lines clustering a strong line have been merged as one frequency. However, in spite of this arbitrariness, the coincidence of these recurring frequencies is so striking that it is not possible entirely to neglect it. As a check, it is planned to pursue a similar investigation of the harmonics of this band, as well as the corresponding bands of the other carbonates of similar crystallographic structure.

The author wishes to acknowledge a Grant-in-Aid of the National Research Council which has materially aided this work. He also wishes to express his thanks to Professors Pfund and Herzfeld of this laboratory, with whom he has discussed this experiment in detail.

[8] E. K. Plyler, Phys. Rev. **33,** 948 (1929).

[9] A. H. Pfund and S. Silverman, Phys. Rev. **39, 64** (1932).

THE INFRARED ABSORPTION BANDS OF WATER VAPOR

By E. K. Plyler
University of North Carolina

(Received November 6, 1931)

Abstract

Further experimental work has been done on the near infrared absorption of water vapor in the regions of 1.40μ and 1.90μ. Forty-five lines have been listed for the region of 1.40μ. There is some difficulty in interpreting this band as to zero branch or double type. By using somewhat higher resolution the 1.87μ band has been shown to consist of more lines than previously observed. The region of 1.87μ has the appearance of a double type band when a small amount of water vapor was used. Calculations have been made as to the form of the water vapor molecule on the assumption that this is the third fundamental band of water vapor. Also, the intensities of the bands have been calculated and these are found to be in good agreement with the experiment values. A new classification has been made of the combination bands.

THE present work gives the results of the absorption of water vapor in the region of 1.40μ and 1.90μ and then a correlation is made with the other bands. The near infrared region has been studied by many observers[1] and each successive work has shown that with higher resolution more lines appeared. Plyler and Sleator[2] have recently made a study of the absorption bands of water vapor in the regions of 1.87μ, 2.67μ, 3.16μ, and 6.26μ, and this work was undertaken to make a study of the fainter bands with high resolution. It was found that the resolution in the band at 1.87μ could be increased and this region was measured again.

The apparatus was the same as that used by Plyler and Sleater[2] and will not be described here. A grating of 15,000 lines was employed in the region of 1.40μ and 1.90μ. The absorbing path was about 6 meters long and the pressure of the water vapor in the air was 2 cm for the absorption bands shown in Fig. 1 and 2, and 1.5 cm for absorption band represented in Fig. 3. The slits were 0.20 mm in width and the wave-length interval included in this slit width has been given in Table I as a function of the resolving power of the instrument.

Table I. *Resolving power of instrument.*

Region	Slit width A	Slit width cm^{-1}
1.40μ	3	1.6
1.90μ	3.5	0.99

[1] E. von Bohr, Phil. Mag. **28,** 71 (1914); G. Hettner, Ann. d. Physik **55,** 476 (1918); W. W. Sleator and E. R. Phelps, Astrophys. J. **62,** 28 (1925); E. R. McAlister and H. J. Unger, Phys. Rev. **37,** 1012 (1931).

[2] E. K. Plyler and W. W. Sleator, Phys. Rev. **37,** 1493 (1931).

In Fig. 1 a graph has been plotted to show the experimental results for the region of 1.40μ. The galvanometer deflections in mm have been plotted as the ordinate and the angle of the grating has been plotted as the abscissa. A large number of lines were found for this region.

TABLE II. *Region of 1.40μ. Intensity, wave-number and wave-length of lines.*

Line No.	Wave-length	Wave number	Rel. Int.	Line No.	Wave-length	Wave number	Rel. Int.
1	13461	7428.9	5	24	13767	7263.7	15
2	13474	7421.5	10	25	13783	7255.2	20
3	13484	7416.4	10	26	13803	7244.7	45
4	13499	7407.8	10	27	13824	7234.0	55
5	13519	7396.7	5	28	13833	7229.3	30
6	13526	7393.0	8	29	13846	7222.2	15
7	13545	7383.2	18	30	13853	7218.7	12
8	13554	7378.2	20	31	13868	7210.8	40
9	13572	7368.3	8	32	13901	7194.0	5
10	13583	7362.2	10	33	13920	7184.2	40
11	13590	7358.2	15	34	13950	7168.3	40
12	13603	7351.0	10	35	13959	7164.3	45
13	13619	7342.8	50	36	13968	7159.3	15
14	13643	7330.0	30	37	14001	7142.3	50
15	13649	7326.7	40	38	14008	7138.5	30
16	13664	7318.7	10	39	14053	7120.5	40
17	13673	7313.8	25	40	14069	7108.2	30
18	13682	7309.0	30	41	14093	7095.8	30
19	13693	7302.7	8	42	14142	7071.2	25
20	13704	7297.0	20	43	14171	7056.5	10
21	13717	7290.3	25	44	14189	7047.7	15
22	13743	7276.2	10	45	14233	7025.6	15
23	13754	7270.7	10				

In Table II the line number, intensity, wave number and wave-length for 45 of the more intense lines are listed. The values given in this table were obtained by taking the average values from two different curves. It was found that the wave-lengths of the two curves never varied over 2A for any line. This band has a region of about 40 waves per cm which has very little absorption. This is the spacing between the strong lines of the 6.26μ band and would indicate that this band is of the double type with its center at 13750A. This band is the first harmonic of the zero branch type band at 2.67μ and it would be expected to be also of the zero type. However, a change in the type of band from fundamental to harmonic has been observed in certain cases. If this band is of the zero branch type its center is probably located at 13840A.

The region of 1.90μ has been studied and the results obtained are given in Fig. 2 and Table III. The resolution used is somewhat greater than in the work of Plyler and Sleator[2] and has made it possible to separate some lines which formerly appeared as one. The curve given in this paper shows the lines as sharper and the intensities are probably more accurately represented. There are listed 68 of the more intense lines in Table III. Many of the wave-lengths check closely with the values found in the previous study, but in the first 25 lines the wave-lengths given in this paper are about 6A greater. It is believed that the values given here are more reliable than those in the previous paper and should replace them.

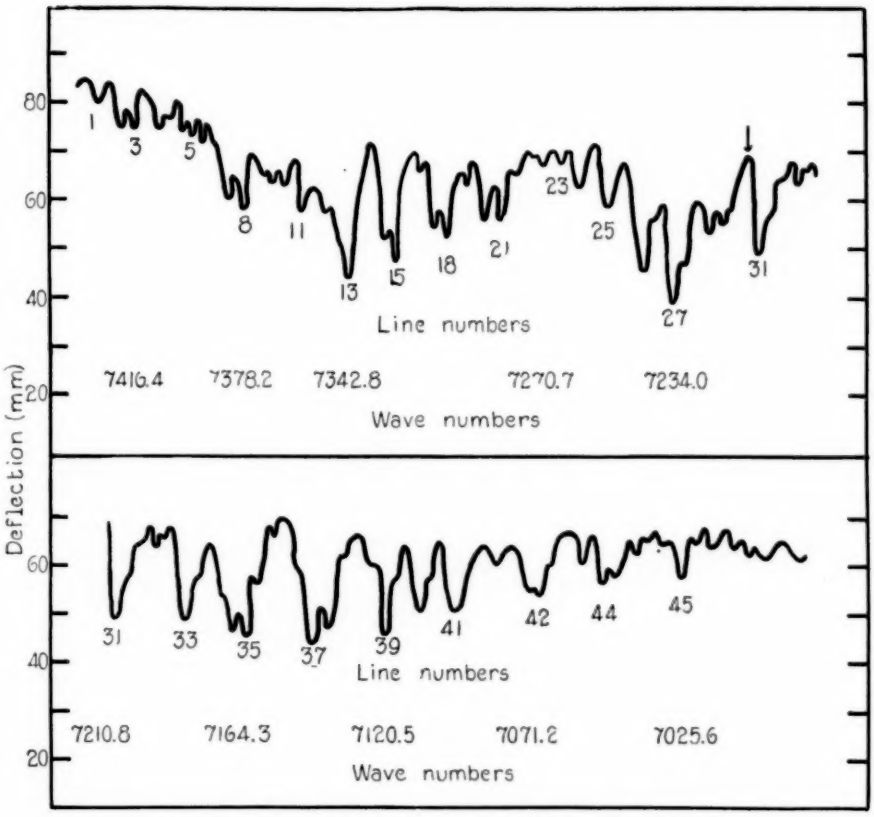

Fig. 1. Energy curve for the region of 1.40μ. Slit width 3A.

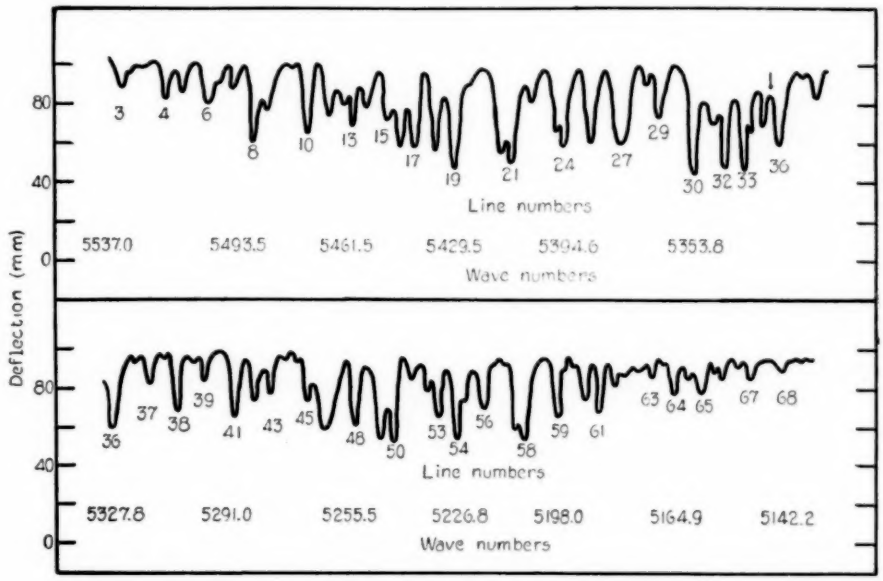

Fig. 2. Energy curve for region of 1.90μ. Slit width 3.5A.

TABLE III. *Region of 1.90μ. Intensity, wave number and wave-length of lines.*

Line No.	Wave-length	Wave number	Rel. Int.	Line No.	Wave-length	Wave number	Rel. Int.
1	18006	5553.3	5	35	18750	5333.4	20
2	18023	5549.4	5	36	18770	5327.8	40
3	18060	5537.0	10	37	18812	5315.8	15
4	18104	5523.6	15	38	18838	5308.3	20
5	18126	5517.0	12	39	18853	5304.2	10
6	18152	5509.0	20	40	18866	5300.6	15
7	18180	5500.6	10	41	18900	5291.0	40
8	18203	5493.5	45	42	18920	5285.4	25
9	18220	5488.5	20	43	18935	5281.2	15
10	18261	5476.1	40	44	18964	5273.2	10
11	18285	5467.7	25	45	18977	5269.6	15
12	18302	5463.9	15	46	18993	5265.4	45
13	18310	5461.5	25	47	19004	5262.0	10
14	18325	5457.0	15	48	19028	5255.5	40
15	18345	5451.0	25	49	19052	5248.8	45
16	18362	5446.0	40	50	19064	5245.7	45
17	18375	5442.1	40	51	19087	5240.0	15
18	18399	5435.1	40	52	19102	5235.0	15
19	18418	5429.5	50	53	19112	5232.3	40
20	18469	5414.5	45	54	19132	5226.8	45
21	18480	5411.3	45	55	19142	5224.1	20
22	18502	5404.8	15	56	19160	5219.1	30
23	18530	5396.7	20	57	19196	5209.4	40
24	18537	5394.6	40	58	19205	5207.0	45
25	18564	5386.2	40	59	19238	5198.0	35
26	18597	5377.4	50	60	19267	5190.2	20
27	18604	5375.5	35	61	19283	5186.0	25
28	18629	5368.0	10	62	19302	5180.8	15
29	18641	5364.5	25	63	19338	5171.1	10
30	18679	5353.8	60	64	19362	5164.9	15
31	18695	5349.0	20	65	19380	5159.9	15
32	18708	5345.3	50	66	19392	5156.8	10
33	18727	5339.8	50	67	19413	5151.4	10
34	18735	5337.6	15	68	19448	5142.2	5

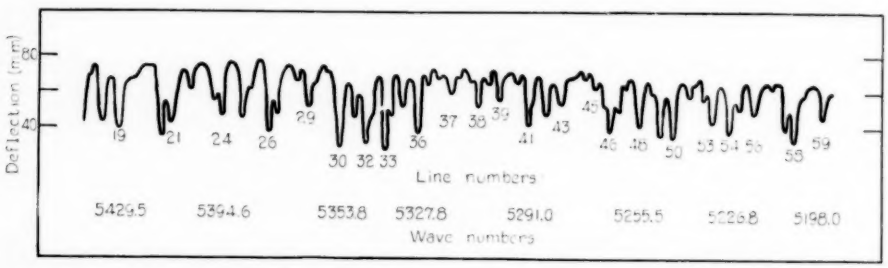

Fig. 3. Energy curve for region of 1.88μ with less water vapor present. Slit width 3.5A.

The part of this band at 1.8865μ appeared to have very few strong lines and it was studied again with less water vapor (1.5 cm pressure). It was found that the region then appeared more definitely as a separate band. The spacing between the two strong lines, numbers 36 and 41, is 37 waves per cm, which is of the order of that for the 6.26μ and 3.16μ bands, the spacing for the former band being 40 waves per cm and the latter 45 waves per cm. Lines number 41, 42, 43 on the longer wave-length side and numbers 34, 35 and 36 on

the shorter wave-length side have very much the same appearance as the first three lines on each side of the center as found in the 6.26μ band. This region is overlapped by the combination band $\nu_1+\nu_2$ and it is not possible to make a very complete correlation of lines, but the longer wave-length side has its stronger lines a considerable number of waves per cm from the center, as in the 6.26μ band. If this is a separate band overlapping the combination band at 1.87μ, it is probably the third fundamental band of water vapor. So far only the bands in the regions of 2.67μ and 6.26μ have been classified as fundamental bands.

By using the values of 5309, 1597, 3742 waves per cm as the fundamental frequencies of water vapor, the angle that the oxygen atom makes with the hydrogen atoms has been calculated by the use of the equation derived by Dennison.[3] The value obtained is 115° or the half angle, $\alpha=57.5°$. Also, the intensities have been calculated and found to be of the right order of magnitude. In Table IV are given the calculated and experimental intensities. The intensity of the 6.26μ band is set equal to 100 in the two cases by choosing the proper constants. It is difficult to determine the true intensity of a band and the experimental values should be considered as approximate.

TABLE IV. *Intensity of bands.*

Band	Frequency in waves per cm	Observed intensity	Calculated intensity
ν_1	3742	75	78.4
ν_2	1597	100	100
ν_3	5309	10	6.7

Also, if we consider 5309 waves per cm as the third fundamental of water vapor a complete classification of the near infrared bands of water vapor can be made. The theoretical frequency of the bands cannot be calculated for there is not known the correct frequency of a sufficient number of combination bands to determine the correction terms. However, the calculated frequency has been given in Table V without the correction terms to show that the assigned combinations are of the right order of magnitude.

TABLE V. *Combination bands. Calculated and observed values.*

Combination term	Experimental frequency	Calculated frequency
ν_1	3742	3742
ν_2	1597	1597
ν_3	5309	5309
$\nu_1+\nu_2$	5343	5339
$\nu_1+\nu_3$	8848	9095
$\nu_2+\nu_3$	6896	6906
$2\nu_1$	7224	7448
$2\nu_2$	3156	3194
$\nu_1+\nu_2+\nu_3$	10638	10648
$2\nu_3$		10618

[3] D. M. Dennison, Phil. Mag. **1**, 195 (1926).

The combination bands are given different designations from those given by Hettner.[4] The frequencies obtained by the present arrangement do not check better than those in Hettner's arrangement, but it is believed that the intensities of the observed bands may be more in accord with the probable intensities in the present combinations.

The experimental work of this paper was done in the Physical Laboratory of the University of Michigan and the writer wishes to express his appreciation to Professors Meyer and Barker for the use of their equipment.

[4] G. Hettner, Zeits. f. Physik 1, 345 (1920).

THE NEAR INFRARED ABSORPTION SPECTRUM OF METHANE

By J. G. Moorhead*
Northwestern University, Evanston, Ill.

(Received November 12, 1931)

Abstract

The infrared absorption spectrum of methane between 1.4μ and 2.6μ was obtained with an infrared spectrometer having a grating of 5000 lines to the inch. Strong bands were found in the 1.6μ and 2.3μ regions. The fine structure of the 2.3μ band was resolved in the first order spectrum. The fine structure of the 1.6μ band was resolved in the second order but not in the first order spectrum. Only at the 2.20μ and the 1.66μ bands could the fine structure be measured. The 2.20μ band has spacing of 10.7 cm^{-1}, giving for the value of the moment of inertia 5.17×10^{-40} c.g.s. units. The corresponding values for the 1.66μ band are 10.4 cm^{-1} and 5.32×10^{-40} c.g.s. units. These results are quite close to the values of 9.77 cm^{-1} and 5.66×10^{-40} c.g.s. units found for the 3.31μ band by Cooley.

Introduction

Cooley[1] has investigated the infrared absorption spectrum of methane. He resolved the rotational fine structure of the 3.3μ and the 7.7μ bands, but did not resolve the strong bands found in the 2.3μ region. Ellis[2] investigated the vibration bands of methane from 1μ to 3μ with apparatus of low dispersion. Easley, Fenner and Spence[3] found many bands between 1μ and 3μ in the spectra of the halogen derivatives of methane and ethane in the liquid form. It was thought worthwhile to investigate the absorption spectrum of methane in vapor form in the region from 1μ to 3μ with apparatus of high dispersion.

For a long time the model of the methane molecule almost universally accepted[4] was a regular tetrahedron with the carbon atom at the center and the four hydrogen atoms at the corners. More recently evidence has been brought forward in favor of a model in which the carbon atom forms the apex, and the four hydrogen atoms the base of a regular pyramid.[5] The fine structure of the bands measured by Cooley[1] at 3.3μ, 3.5μ, and 7.7μ have different spacings. On the quantum theory, this indicates different moments of inertia about different axes. The conflicting evidence for and against a symmetrical model has attracted much attention to the structure of the methane molecule. Several solutions have been given in an attempt to describe its vibrational and rotational motions.[6]

* At present teaching, at Westminster College, New Wilmington, Pennsylvania.

[1] Cooley, Astrophys. J. **62,** 73 (1925).

[2] Ellis, Proc. Nat. Acad. Sci. **13,** 202 (1927).

[3] Easley, Fenner and Spence, Astrophys. J. **67,** 3 (1928).

[4] Glockler, J.A.C.S. **48,** 2021 (1926). This summarizes the evidence in favor of the tetrahedral type of molecule.

[5] Henri, Chem. Rev. **4,** 189 (1927).

[6] Dennison, Astrophys. J. **62,** 84 (1925); Guillemin, Ann. d. Physik **81,** 176 (1926); Ruark and Urey, Atoms, Molecules and Quanta, p. 435 (1930).

Apparatus and Experimental Procedure

Radiation from the Nernst glower, passed through a Pyrex glass absorption cell 30 cm long, and was focused on the slit of an infrared grating spectrometer. The maximum slit width throughout the experiment was 0.025 cm. The grating of the spectrometer had a surface 16 cm long and 13 cm high ruled with 5000 lines per inch. The intensity of radiation of any particular wave-length was determined by a radiometer.[7] The slit width of 0.025 cm corresponded to wave-length interval of 12A. The smallest division on the dial of the spectrometer corresponded to approximately 10 angstroms.

Table I. *Methane 1.66μ band region, second order.*

Quantum number		Spectrometer setting	Wave-length μ	Frequency cm^{-1}	Frequency difference cm^{-1}
13		35.985	1.6292	6137.0	
12		36.04	1.6317	6128.0	9.
11		.10	1.6342	6119.0	9.
10		.145	1.6362	6111.6	7.4
9		.205	1.6388	6102.0	9.6
8		.265	1.6414	6092.2	9.8
7		.325	1.6441	6082.2	10.0
6		.39	1.6470	6071.6	10.6
5		.455	1.6498	6061.2	10.4
4		.505	1.6519	6053.4	7.8
3		.575	1.6550	6042.2	11.2
2		.65	1.6582	6030.4	11.8
1		.715	1.6611	6020.0	10.4
0	$2\nu_3$	.795	1.6645	6007.8	12.2
−2		.905	1.6692	5990.6	17.2
−3		.99	1.6729	5977.4	13.2
−4		37.06	1.6760	5966.4	11.0
−5		.13	1.6790	5956.0	10.4
−6		.205	1.6822	5944.4	11.6
−7		.28	1.6856	5932.4	12.0
−8		.35	1.6886	5921.8	10.6
−9		.445	1.6927	5907.6	14.2
−10		.52	1.6960	5896.2	11.4
−11		.59	1.6991	5885.2	11.0
−12		.64	1.7013	5877.8	7.4

The methane gas was generated by dropping water on magnesium carbide. The gas was then dried by passing it through a calcium chloride drying tube. Comparison was made with the water vapor bands described by Sleator and Phelps,[8] and with the bands of acetylene, ethylene, and ethane described by Levin and Meyer.[9] The bands found did not correspond to any of the gases named. Comparison of the bands with the results of Cooley[1] and Ellis[2] show conclusively that the bands described are all due to methane.

Readings in the important band regions were taken at intervals of about 10 angstroms. Readings were repeated over and over so that bands found are authentic beyond question. Most of the points of minimum transmission were read correctly to 5 angstroms or less.

[7] Spence, J.O.S.A. **6,** 625 (1922).
[8] Sleator and Phelps, Astrophys. J. **62,** 28 (1925).
[9] Levin and Meyer, J.O.S.A. **16,** 137 (1928).

Methane bands were found in the three regions, 1.6μ, 2.3μ, and 3.3μ. The first two are of the first order spectrum, the third is a second order spectrum of the 1.6μ region. This conclusion was reached by the following reasoning: Pyrex glass transmits very effectively to 2.5μ,[10] but the thickness used, 7 mm, would render it practically opaque to the radiation beyond that point. The radiation from the Nernst glower is very intense from 1.2μ to 2.5μ with a deep

TABLE II. *Methane 2.2μ band region.*

Quantum number	Spectrometer setting	Wave-length	Frequency cm^{-1}	Frequency difference cm^{-1}
7	23.63	2.1600	4629.6	
6	.70	2.1663	4616.1	13.5
5	.767	2.1728	4602.3	13.8
4	.83	2.1780	4591.3	11.0
3	.88	2.1825	4581.0	10.3
2	.95	2.1888	4568.6	12.4
0 ($\nu_2+\nu_3$)	24.07	2.1993	4547.0	21.6
−2	.19	2.2100	4524.9	22.1
−3	.25	2.2153	4514.0	10.1
−4	.30	2.2200	4504.5	9.5
−5	.365	2.2258	4492.8	11.7
−6	.42	2.2306	4483.1	9.7
−7	.48	2.2360	4472.3	10.8
−8	.53	2.2405	4463.3	9.0
−9	.59	2.2460	4452.4	10.9
($\nu_4^+ + \nu_3^+$)	.755	2.2608	4423.	
	.83	2.2678	4409.	
	.91	2.2750	4396.	
	.99	2.2820	4382.	
	25.06	2.2883	4370.	
	.11	2.2928	4361.	
	.17	2.2981	4351.	
	.21	2.3018	4344.	
($\nu_4+\nu_3$)	.37	2.3162	4317.	
	.57	2.3342	4284.	
	.64	2.3407	4272.	
	.71	2.3470	4261.	
	.75	2.3505	4254.	
ν_1	.97	2.3704	4219.	
	26.11	2.3829	4197.	
	.14	2.3857	4192.	
	.18	2.3892	4185.	
	.23	2.3935	4178.	
	.28	2.3980	4170.	
	.33	2.4025	4162.	
	.38	2.4068	4155.	
	.48	2.4158	4139.	
($\nu_2+2\nu_4$)	.57	2.4238	4126.	
	.70	2.4355	4106.	
	.78	2.4428	4094.	
	.83	2.4472	4086.	

minimum at 3μ to 4.5μ.[11] The second order of the 1.6μ region contains considerable energy, and lies in a region where the first order is cut off by the Pyrex glass. The bands of methane at 1.6μ and 2.3μ agree closely with those measured by Cooley and Ellis. The band at the 3.3μ region does not correspond

[10] Coblentz, Emerson and Long, U. S. Bur. Std. Bull. **14**, 653 (1918).
[11] Coblentz, U. S. Bur. Std. Bull. **4**, 533 (1908).

with those measured by Cooley, but has twice the wave-length of the band in the 1.6μ region. Similar consideration of the bands in the other compounds investigated make it certain that the bands at 3.3μ region are of the second order.

Results

Two groups of bands were found in the near infrared spectrum of methane, one in the region of 1.6μ, the other in the region of 2.3μ. The wave-lengths of the individual lines are shown in Tables I and II. The wave-

Table III. *Methane band centers.*

Designation	Moorhead Spectrometer setting	Moorhead Wave-length μ	Frequency cm^{-1}	Cooley Wave-length μ	Ellis Wave-length μ
$3\nu_3$					1.15
$\nu_4+2\nu_3$					1.37
$2\nu_3$	18.16	1.6645	6008.		1.66
	18.61	1.7055	5863.		
	18.84	1.7265	5785.		1.72
					1.80
$\nu_2+\nu_3$	24.07	2.1993	4547.	2.2008	2.20
$\nu_4^+ + \nu_3^+$	.755	2.2608	4423.		2.26
$\nu_4+\nu_3$	25.37	2.3162	4317.	2.3178	2.32
	.71	2.3470	4261.		
ν_1	.97	2.3704	4219.	2.3714	2.37
	26.23	2.3935	4178.		
$\nu_2+2\nu_4$	26.57	2.4238	4126.	2.4262	2.42
ν_3				3.3185	
ν_4				7.87	

lengths of the band centers are given in Table III, along with the wave-lengths as measured by Cooley[1] and Ellis.[2] In the latter table are also shown the classification given by Dennison[6] of the bands measured by Cooley and the classification made by Ellis of the bands which he had measured. The symbols indicate whether the bands are fundamental frequencies, harmonics of the fundamental frequencies, or some combination of the fundamentals or harmonics.

The 2.3μ region is shown in Fig. 1A to consist of a number of overlapping vibration-rotation bands. The four stronger ones are the bands observed by Cooley and Ellis. There appear to be three weaker ones, one of which was observed by Ellis. The 2.2μ band is the only one sufficiently separated from the neighboring bands to exhibit unconfused fine structure. The symmetry of the P and R branches is destroyed by the general increase of absorption with increase of wave-length. The Q branch is deep and sharp. It does not appear to spread out more to one side than to the other which indicates absence of perturbation between the rotation and vibration giving rise to the band. Perturbation, if present, would cause convergence of the P and R branches; that is, it would cause the frequency difference of the lines to become smaller in the direction of decreasing wave-length. Not enough lines are available for measurement to apply this test of convergence to this band. Quantum numbers are assigned to the lines from $m=5$ to $m=-9$, the num-

ber m referring to the initial state giving rise to the line. The average value of $\Delta\nu$ for these lines has the value $\Delta\nu = 10.7$ cm^{-1}. The moment of inertia computed from the equation $I = h/4\pi^2\Delta\nu$ gives $I = 5.17 \times 10^{-40}$ c.g.s. units.

At the 2.316μ band and the 2.370μ band, the Q branches are very sharp on the short wave side but shade off in the direction of increasing wave-length. This is very definite evidence of perturbation between the vibration and rotation to which the bands are due. All these bands overlap with so much confusion that it is impossible to assign quantum numbers to the lines or to determine the average frequency difference.

A number of bands were found in the first order spectrum of the 1.6μ region. The band at 1.665μ is strong and sharp, as can be seen in Fig. 1B. The

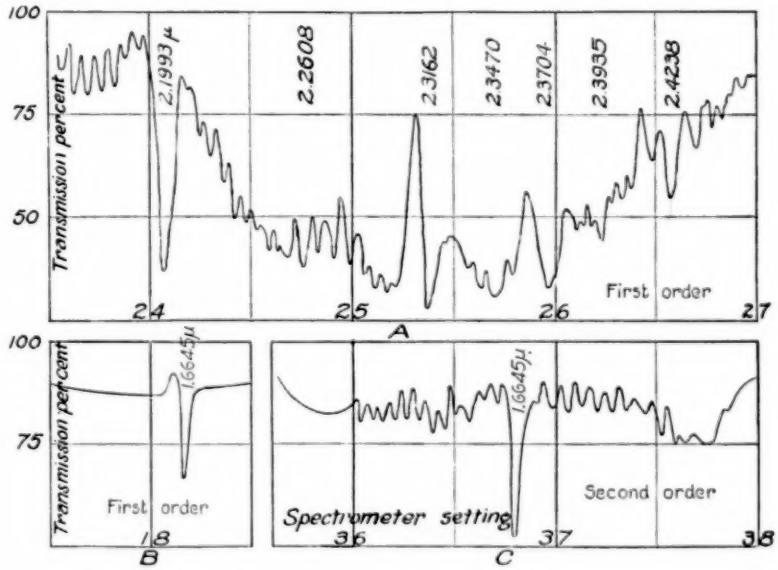

Fig. 1. Methane bands.

other bands of the first order are not very intense, but repeated observations proved them to be genuine. The fine structure was not resolved in the first order spectrum. In Fig. 1C is shown the second order spectrum of the 1.665μ band. The Q branch is very steep on the shorter wave-length side, but shades off on the long wave-length side, overlapping and concealing the first rotation band. This overlapping indicates perturbation. The irregularity in the shape of the band is due to the overlapping of other methane bands and of water vapor bands. The lines are in the main evenly spaced. The average frequency difference gives a value of $\Delta\nu = 10.4$ cm^{-1}. The moment of inertia computed from this, by the formula already given, is $I = 5.32 \times 10^{-40}$ c.g.s. units.

Table IV gives the average frequency difference and the resulting moments of inertia for the two bands measured by the author, and also the results given by Cooley for the three bands measured by him. The bands at 1.66μ, 2.2μ, and at 3.31μ give values for the moment of inertia all of the same

order of magnitude. It is not probable that experimental errors account for all the variation in these values, but that they indicate slightly different moments of inertia, due either to lack of symmetry of the molecule, or to displacement of the atoms by vibration. Dennison[6] proposed an explanation of

TABLE IV. *Methane bands. Frequency difference and moment of inertia.*

Band μ	Cooley Frequency cm^{-1}	Moment of inertia c.g.s. units	Moorhead Frequency difference cm^{-1}	Moment of inertia c.g.s units
1.66			10.4	5.32×10^{-40}
2.20			10.7	5.17
3.31	9.77	5.66×10^{-40}		
3.5	15.3	3.61		
7.67	5.41	10.2		

the fact that the spacing of the 7.7μ band is about half that of the 3.3μ band, by assuming the overlapping of two bands, each having spacing equal to that of the 3.3μ band. Guillemin[6] considered Dennison's explanation improbable, since twice the frequency difference of the 7.7μ band differs from the frequency difference of the 3.3μ band by more than the probable experimental error. Also the entirely different spacing of the weak band at 3.5μ has not been accounted for on the basis of the symmetrical methane molecule. While the question of the three entirely different moments of inertia indicated by the three different spacings remain unsolved, it is significant that the spacing of the two bands measured by the author is close to the value measured by Cooley at the 3.3μ band.

The author acknowledges his indebtedness to Northwestern University for the use of its facilities and to Professor B. J. Spence, who suggested the problem.

MAGNETIC ROTATION SPECTRUM AND HEAT OF DISSOCIATION OF THE POTASSIUM MOLECULE

By F. W. Loomis and R. E. Nusbaum

University of Illinois

(Received November 20, 1931)

Abstract

The magnetic rotation spectrum of the near red, $^1\Pi$-$^1\Sigma$ band system of K_2 has been photographed with the apparatus previously used for Li_2. In this way the series of upper vibrational levels has been extended from the 16th, the last one observed by Crane and Christy, to the 27th. This permits an accurate extrapolation to convergence, which is estimated to occur at $v'=31.6$, the corresponding energy being $17160\ cm^{-1}=2.12$ volts. It follows that the heat of dissociation of the normal molecule is 0.51 ± 0.02 volt. From this and other data the percentage of molecules in the vapor at various temperatures is calculated. An improved Franck-Condon diagram for the red and infrared systems of K_2 has been constructed. It gives a good representation of the observed distribution of bands and predicts the existence of an infrared edge. This is confirmed by observation. Magnetic rotation spectra have been found in the regions of the infrared and blue $^1\Sigma$-$^1\Sigma$ systems. They are probably analogous to the red magnetic rotation spectrum of sodium, and like it, are not yet understood.

THE apparatus which we constructed[1] and used to study the magnetic rotation spectrum of Li_2 has now been used on that of K_2 with the same object, that is, to measure the vibrational levels which come nearest to dissociation and to extrapolate them to find the energy of dissociation of the molecule. The apparatus, with a long column of vapor inside a solenoid, was designed to bring out the weak lines corresponding to these levels, and was successful in doing so in the case of lithium.

The spectrum obtained in the region of the red ($^1\Pi\leftarrow{}^1\Sigma$) system of potassium is shown in Fig. 1. In this figure the values of the quantum number v'' which have been assigned to the bands are indicated above them and the changes of quantum number, $v'-v''$, for the various sequences are indicated below. The spectrum was photographed with sunlight as a source. The comparison spectrum is neon. The continuum on the short-wave side is due to the magnetic rotation of the D lines of sodium which was present as an impurity. In the region where this comes near to the short wave end of the potassium rotation spectrum the absorption bands of potassium can be seen against it. The very strong line between the -5 and -6 sequences is the resonance doublet of atomic lithium which was also present as an impurity. The resonance doublet of potassium is far off the plate to the right. It will be seen that, as was the case with lithium, our method of observation brings out not only the heads of the bands but also a little structure on the long wave-length side of the stronger bands.

[1] Loomis and Nusbaum, Phys. Rev. **38**, 1447 (1931).

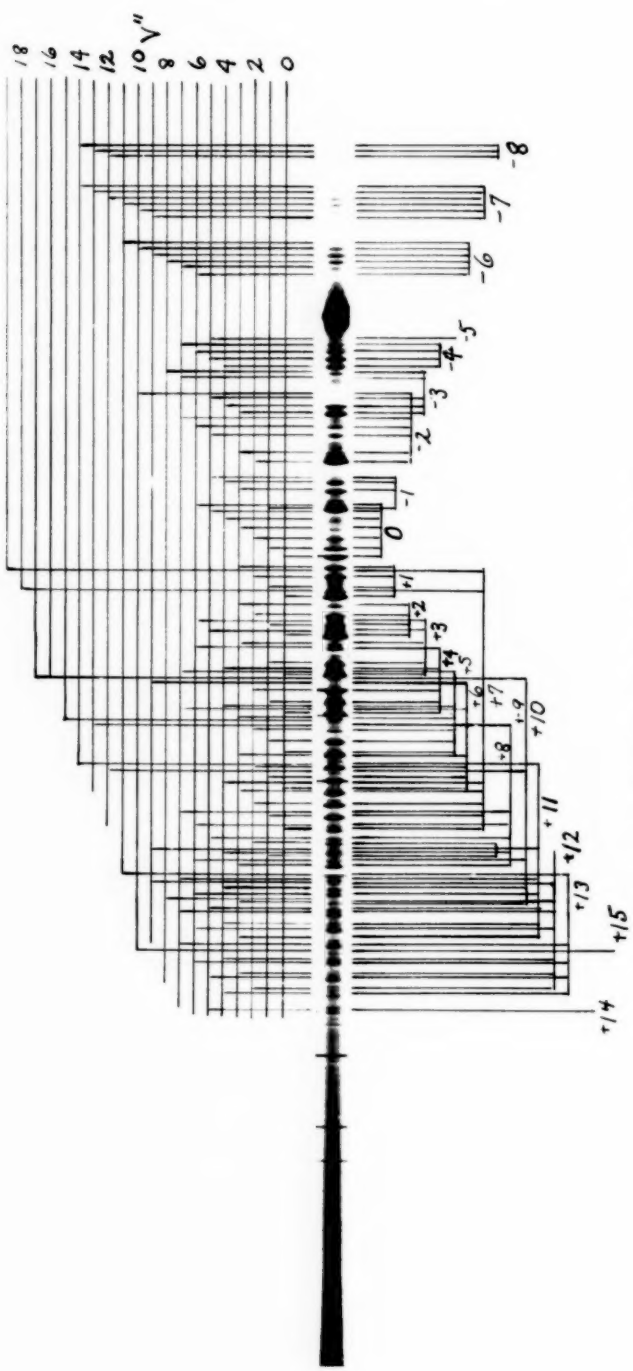

Fig. 1. The magnetic-rotation spectrum of K_2.

Table I gives the frequencies of all measured band heads with the exception of a very few weak ones and perhaps one or two that could not be distinguished from structural lines of strong bands. In many cases the frequen-

TABLE I

v'	v''	Intensity	Observed	Calculated	Observed-Calculated
22	6	0	16285.86	16283.61	+2.25
18	4	0	16227.84	16228.58	−0.74
21	6	0	16227.84	16227.28	+0.56
24	8	0	16217.69	16217.61	+0.08
19	5	2	16198.34	16199.35	−1.01
17	4	2	16168.31	16167.68	+0.63
14	2	2	16159.97	16159.46	+0.51
18	5	3	16139.80	16139.48	+0.32
21	7	3	16139.80	16139.60	+0.20
15	3	1	16131.91	16132.71	−0.80
24	9	1	16131.91	16131.33	+0.58
19	6	4	16111.70	16110.95	+0.75
16	4	3	16105.48	16105.76	−0.28
25	10	1	16091.96	16097.95	−5.99
20	7	2	16082.46	16082.02	+0.44
14	3	2	16069.39	16068.94	+0.45
18	6	4	16051.15	16051.08	+0.07
15	4	2	16042.88	16042.89	−0.01
19	7	4	16023.48	16023.27	+0.21
22	9	4	16023.48	16022.67	+1.81
16	5	4	16016.56	16016.66	−0.10
13	3	2	16003.24	16004.30	−1.06
20	8	0	15996.50	15995.04	+1.46
17	6	2	15990.10	15990.18	−0.08
14	4	3	15978.54	15979.12	−0.58
21	9	2	15968.35	15966.34	+2.01
18	7	2	15962.21	15963.40	−1.19
24	11	2	15960.08	15960.91	−0.83
12	3	7	15937.81	15938.83	−1.02
22	10	7	15937.81	15937.11	+0.70
19	8	7	15937.81	15936.29	+1.52
16	6	3	15928.30	15928.26	+0.04
25	12	1	15923.61	15928.95	−5.34
27	13	1	15923.61	15945.11	−21.50
13	4	3	15914.61	15914.48	+0.13
20	9	1	15908.83	15908.76	+0.07
23	11	1	15908.83	15907.28	+1.55
10	2	6	15896.26	15896.04	+0.22
14	5	4	15888.47	15890.02	−1.55
7	0	5	15873.22	15873.66	−0.44
11	3	5	15873.22	15872.56	+0.66
15	6	3	15865.99	15865.39	+0.60
8	1	11	15849.43	15850.95	−1.52
12	4	11	15849.43	15849.01	+0.42
19	9	11	15849.43	15850.01	−0.58
16	7	0	15841.91	15840.58	+1.33
9	2	12	15827.27	15828.25	−0.98
13	5	12	15827.27	15825.38	+1.89
6	0	10	15804.41	15803.71	+0.70
10	3	10	15804.41	15805.52	−1.11
26	14	1	15799.49	15813.39	−13.90
14	6	1	15799.49	15801.62	−2.13
24	13	1	15793.61	15793.33	+0.28
22	12	2	15768.63	15768.11	+0.52
8	2	4	15760.06	15759.73	+0.33
25	14	3	15755.80	15762.77	−6.97
9	3	4	15737.03	15737.73	−0.70
13	6	4	15737.03	15736.98	+0.05
5	0	4	15732.46	15733.07	−0.61
10	4	0	15717.63	15715.70	+1.93
26	15	0	15717.63	15731.37	−13.74
6	1	4	15711.86	15711.77	+0.09
7	2	4	15690.78	15690.50	+0.28
25	15	1	15674.44	15680.75	−6.31
8	3	2	15669.19	15669.21	−0.02
4	0	7	15660.70	15661.72	−1.02
13	7	0	15650.80	15649.30	+0.50
9	4	1	15647.23	15647.91	−0.68
5	1	5	15641.04	15641.13	−0.09
6	2	3	15619.57	15620.55	−0.98
15	9	1	15603.82	15604.45	−0.63
27	17	1	15597.04	15618.43	−21.39
3	0	10	15589.28	15589.68	−0.40
12	7	3	15582.92	15583.83	−0.91
8	4	3	15578.94	15579.39	−0.45
4	1	4	15569.09	15569.78	−0.69
10	6	4	15538.84	15538.20	+0.64
6	3	2	15529.68	15530.03	−0.35
2	0	15	15516.43	15516.90	−0.47
7	4	5	15511.01	15510.16	+0.85
3	1	4	15496.71	15497.74	−1.03
12	8	4	15496.71	15496.85	−0.14
8	5	2	15490.32	15490.29	+0.03
4	2	7	15478.29	15478.56	−0.27
5	3	3	15459.80	15459.39	+0.41
1	0	10	15443.15	15443.41	−0.26
25	18	4	15433.34	15438.93	−5.59
2	1	2	15426.18	15424.96	+1.22
3	2	8	15405.26	15406.52	−1.26
26	19	1	15397.29	15409.95	−12.66
4	3	8	15388.44	15388.04	+0.40
0	0	7	15369.04	15369.18	−0.14
5	4	7	15369.04	15369.57	−0.53
1	1	10	15351.59	15351.47	+0.12
6	5	10	15351.59	15351.11	+0.48
2	2	3	15333.18	15333.74	−0.56
3	3	2	15315.38	15316.00	−0.62
4	4	1	15297.82	15298.22	−0.40
5	5	1	15281.37	15280.47	+0.90
0	1	15	15276.96	15277.24	−0.28
6	6	2	15261.82	15262.71	−0.89
2	3	10	15243.54	15243.22	+0.32
3	4	4	15226.28	15226.18	+0.10
4	5	0	15209.65	15209.12	+0.53
0	2	20	15186.02	15186.02	0.00
1	3	5	15170.54	15169.73	+0.81
3	5	3	15136.67	15137.08	−0.41
4	6	4	15119.99	15120.72	−0.73
5	7	0	15105.14	15104.39	+0.75
10	11	0	15105.14	15106.84	−1.70
0	3	10	15095.90	15095.50	+0.40
1	4	10	15080.12	15079.91	+0.21
2	5	1	15064.63	15064.30	+0.33
8	10	0	15055.06	15055.39	−0.33
4	7	0	15032.28	15033.04	−0.76
5	8	2	15017.09	15017.41	−0.32
0	4	6	15004.91	15005.68	−0.77
1	5	8	14989.90	14990.81	−0.91
2	6	5	14975.82	14975.90	−0.08
3	7	4	14962.04	14961.00	+1.04

TABLE I (*Continued*)

v'	v''	Intensity	Observed	Calculated	Observed-Calculated	v'	v''	Intensity	Observed	Calculated	Observed-Calculated
3	8	2	14873.67	14874.02	−0.35	3	10	2	14702.57	14702.18	+0.39
4	9	1	14858.41	14859.78	−1.37	4	11	2	14689.71	14689.36	+0.35
0	6	0	14827.49	14828.18	−0.69	5	12	2	14676.74	14676.57	+0.17
1	7	2	14813.87	14814.73	−0.86	6	13	1	14663.24	14663.77	−0.53
2	8	4	14801.63	14801.24	+0.39	7	14	1	14651.23	14650.98	+0.25
3	9	5	14788.86	14787.74	+1.12	3	11	0	14617.43	14617.30	+0.13
4	10	3	14774.80	14774.22	+0.58	4	12	0	14604.86	14605.22	−0.36
5	11	2	14761.70	14759.77	+1.93	6	14	0	14581.46	14581.03	+0.43
6	12	1	14746.63	14747.21	−0.58	7	15	0	14567.87	14568.96	−1.09
2	9	1	14715.62	14714.96	+0.66						

cies are approximately the same as those of absorption bands reported by Crane and Christy,[2] but our measurements extend considerably further toward the short wave-lengths and also much further toward high quantum numbers. The highest value of v' reported by Crane and Christy is 16, whereas we have identified bands up to $v' = 27$, which according to our estimate below, comes within 5 levels of convergence. The quantum numbers which we have assigned to the bands measured by Crane and Christy are the same as theirs in all but one or two cases. The extension of the assignment to the higher numbered bands was carried out by a process of extrapolation by differences and was checked by the combination relation.

We were not able to identify any bands due to the isotopic molecule $K^{39}K^{41}$. This was doubtless due to the comparative scarcity of such molecules and to the smallness of the isotopic displacement.

The extension of the spectrum to higher values of v' made necessary a revision of Crane and Christy's formula. It was found that their formula for the v'' terms is adequate, but that for the v' terms had to be changed. It was found impossible to represent all the upper level terms by a polynomial of reasonably low degree. Eq. (1)

$$\begin{aligned}\nu = {} & 15378.01 + 75.00(v' + \tfrac{1}{2}) - 0.3876(v' + \tfrac{1}{2})^2 \\ & + 0.004366(v' + \tfrac{1}{2})^3 - 0.0001830(v' + \tfrac{1}{2})^4 - 92.64(v'' + \tfrac{1}{2}) \\ & + 0.354(v'' + \tfrac{1}{2})^2\end{aligned} \qquad (1)$$

however, was found to be satisfactory for all bands with v' less than 25, and the values in the fifth column of Table I are calculated on the basis of Eq. (1), as are also the residuals in the sixth column. It will be seen, however, from column 6 and also from Fig. 2, in which the residuals from Eq. (1) are plotted against v', that Eq. (1) is completely inadequate to represent the terms with $v' \geqq 25$. Eq. (2)

$$\begin{aligned}\nu = {} & 15379.44 + 72.870(v' + \tfrac{1}{2}) + 0.2535(v' + \tfrac{1}{2})^2 \\ & - 0.06916(v' + \tfrac{1}{2})^3 + 0.0033472(v' + \tfrac{1}{2})^4 - 0.00005986(v' + \tfrac{1}{2})^5 \\ & - 92.64(v'' + \tfrac{1}{2}) + 0.354(v'' + \tfrac{1}{2})^2\end{aligned} \qquad (2)$$

[2] Crane and Christy, Phys. Rev. **36**, 421 (1930).

is a least squares representation of the whole series of measured v' levels. It is represented by the curve in Fig. 2. It will be seen that it represents the levels 25–27 adequately and, indeed, represents all levels fairly well, but that it is inferior to Eq. (1) as a representation of the levels 0–24. Eq. (1) may, therefore, be considered as the best available representation of the constants of the molecule near the equilibrium point, whereas the extrapolation to dissociation can best be based on Eq. (2).

The extrapolation of the upper levels to convergence is shown in Fig. 3, wherein $\Delta\nu$, the difference between successive vibrational levels of the upper state, is plotted against T' the energy corresponding to the average of the two levels. The curve represents Eq. (2) which, as has just been pointed out,

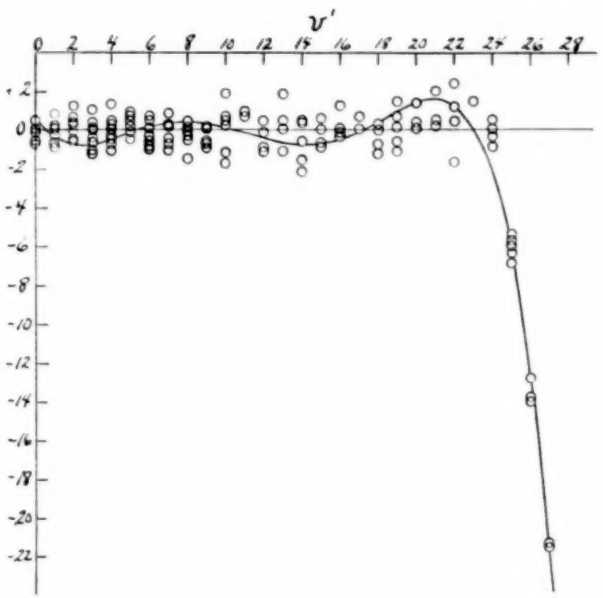

Fig. 2. Residuals of observed frequencies from Eq. (1). The curve represents Eq. (2).

is superior to Eq. (1) for high quantum numbers and for the extrapolation and which, for lower quantum numbers does not differ from Eq. (1) by enough to show on the scale of Fig. 3. It will be noted that the highest observed level lies within 0.02 volt of the estimated convergence and also that it would be difficult to make a reasonable extrapolation which would lie more than 0.02 volt above the estimated convergence, so that it may be said that the value of the energy of dissociation estimated by extrapolation according to Eq. (2) may be relied upon to within 0.02 volt.

According to Eq. (2) convergence occurs at $v' = 31.6$ and the corresponding maximum of T', that is the energy of the atoms into which the upper level dissociates, is 17160 cm^{-1}.

The energies of an excited potassium atom in the lowest ^2P states are 12985 and 13043 cm^{-1}. Since it is uncertain into which of these the excited

molecule dissociates and since the difference between them is somewhat less than the probable error of the extrapolation, it is sufficient to take the energy of the excited atom as the average, namely, 13014 cm^{-1}. The resulting value for the energy of dissociation of the normal molecule is 4146 $cm^{-1} = 0.51$ volt.

The value for the heat of dissociation calculated by Crane and Christy from their much shorter series of levels was 0.81 volt. It seems to be a general fact that too long an extrapolation is likely to lead to too high a value of the energy of dissociation.

Several other estimates of the energy of dissociation of the normal K_2 molecule have been published. Carelli and Pringsheim,[3] as the results of two

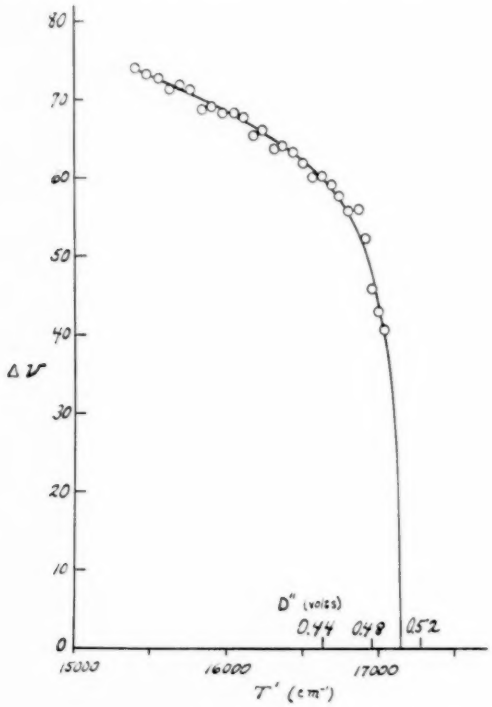

Fig. 3. $\Delta\nu$ vs. T' plotted and extrapolated to dissociation following Eq. (2). Upper scale of abscissae represents values of D_0'' which would be deduced from corresponding T' intercepts.

somewhat different experiments, find the values 0.63 volt and 0.53 volt. However, Crane and Christy[2] have made a critical study of Carelli and Pringsheim's experiments and conclude that they may be in error by as much as 0.3 volt. Dichtburn[4] and Walter and Barratt[5] make the assumption that certain diffuse bands in the spectra of Na_2, K_2, Rb_2, Cs_2, etc., are similar to the iodine continuum at 5000A and are to be interpreted as due to transitions from the lower state to the dissociated upper state. They deduce the values

[3] Carelli and Pringsheim, Zeits. f. Physik **55,** 643 (1927).
[4] Dichtburn, Proc. Roy. Soc. **A117,** 486 (1928).
[5] Walter and Barratt, Proc. Roy. Soc. **A119,** 257 (1928).

0.14, 0.53, 1.02 and 0.91 or 1.17 volts for the heats of dissociation of Na_2, K_2, Rb_2 and Cs_2, respectively. However, these values for the Na_2, Rb_2 and Cs_2 molecules are absurdly far from the true ones. Moreover, they tacitly assume that the transitions accompanying the continua start from the 0 vibrational level of the lower states as they do in iodine, whereas Fig. 5 shows that they must start from a lower vibrational state having, in the case of K_2, some 0.3 volt vibrational energy. It may reasonably be concluded that their agreement

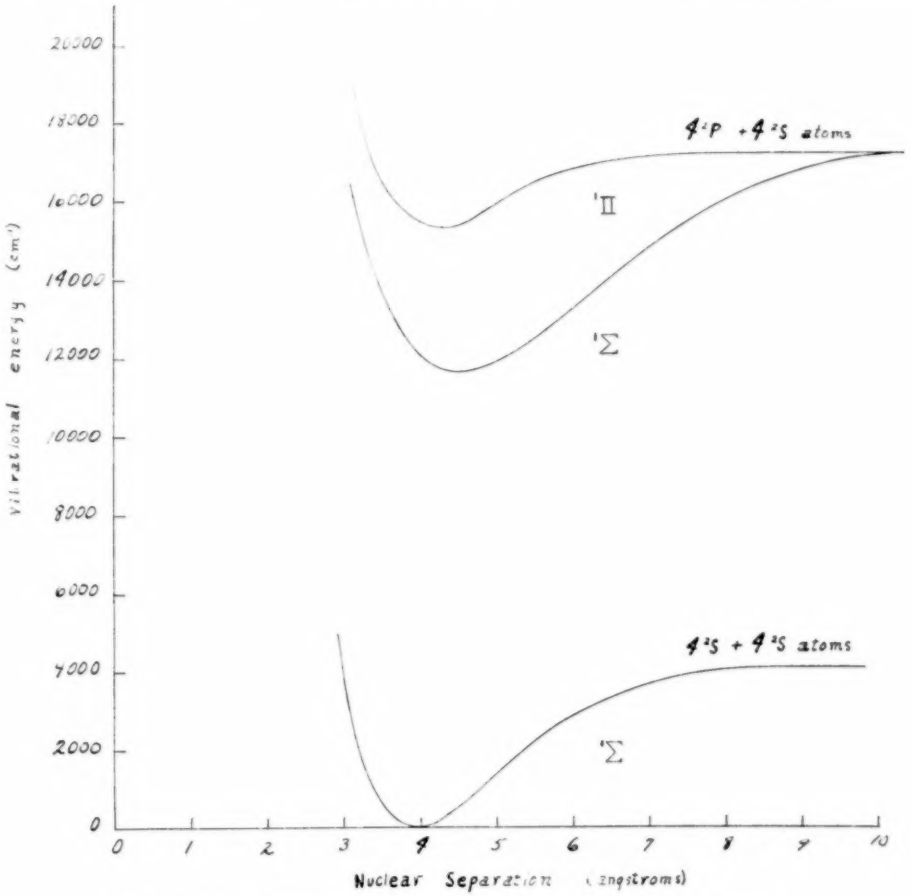

Fig. 4. Potential energy curves for the lowest three known levels of K_2.

with our value in the case of K_2 is wholly fortuitous. The significance of the observed continua remains obscure.

Probably the best chemical determination of the heat of dissociation of potassium is that of Lewis[6] who measured the ratio of molecules to atoms in a molecular beam and found that the value of the heat of dissociation which, when put into Gibson and Heitler's formula,[7] gave the best representation of his data, was 0.62 ± 0.04 volt. Unfortunately he took for the moment of

[6] Lewis, Zeits. f. Physik **69**, 786 (1931).
[7] Gibson and Heitler, Zeits. f. Physik **49**, 465 (1928).

inertia the value 184×10^{-40} g · cm² which is from the old discredited[8] work of Smith.[9] The true value[10] is 492×10^{-40} g · cm². We have recalculated his data, with the correct value of the moment of inertia, and find for the energy of dissociation 0.56 volt which differs from ours by very little more than the 0.04 volt which he claims as his probable error.

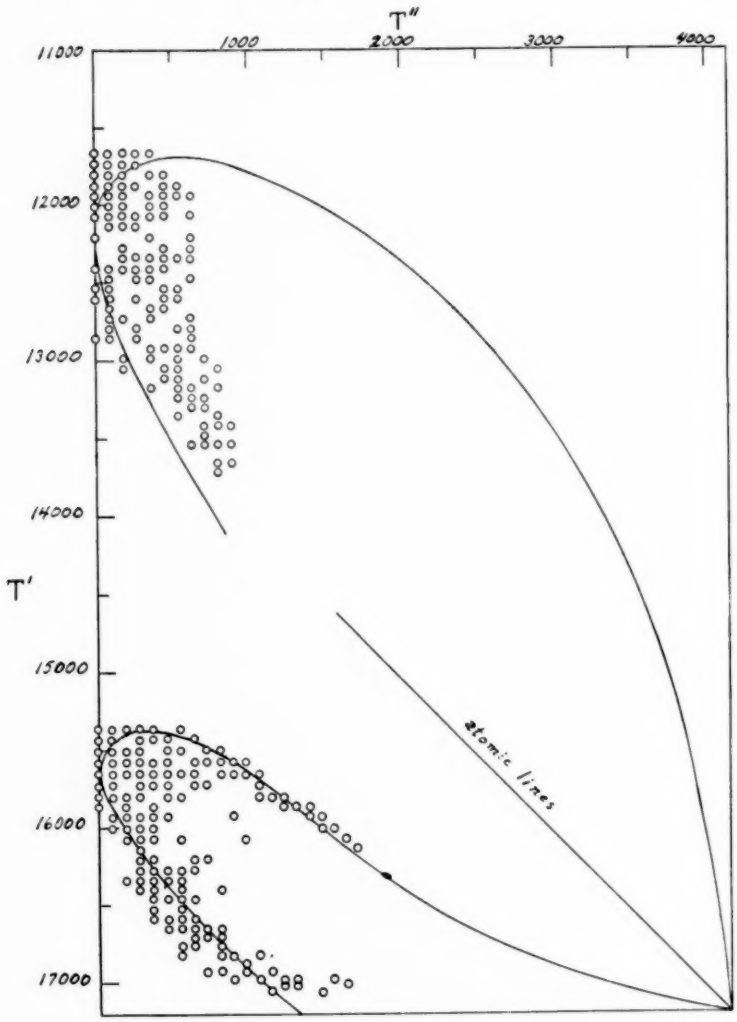

Fig. 5. Improved Franck-Condon diagram for the red and infrared systems. Lines of constant frequency have 45° slope.

The heat of dissociation has also been estimated by Ootuka[11], on the basis of experiments with low pressure flames, as 0.53 volt, which is an average of a selection of a number of values ranging from 0.51 to 0.66 volt.

[8] Loomis and Wood, Phys. Rev. **32,** 223 (1928).
[9] Smith, Proc. Roy. Soc. **A106,** 400 (1924).
[10] Loomis, Phys. Rev., in press.
[11] Ootuka, Zeits. f. phys. Chemic **B7,** 422 (1930).

Fig. 4 shows the potential energy curves of the three lowest states of K_2 as based on our value, 0.51 volt, for the energy of dissociation and on the constants of the molecule deduced by Loomis[10] in his rotational analysis of the spectrum.

Fig. 5 is a Franck-Condon diagram, in the improved form described in our paper on lithium,[1] for the red and infrared band systems of potassium. The circles in the case of the red system represent the magnetic rotation bands as observed by us. In the case of the infrared system they represent the absorption bands reported by Crane and Christy. The curves deduced from Fig. 4 give a good representation of the intensity distribution, which is a confirmation of the correctness of the rotational analysis and of our value of the energy of dissociation.

It will be noted that there should be a sharp edge to the infrared band system at about 10,300 cm^{-1} = 9700A. To check this point the absorption spectrum was photographed in this region. A rather sharp edge was found at 10600A = 9450 cm^{-1}. The difference between this and the calculated location is probably partly due to inaccuracy of the parts of the potential energy curves which are connected with the edge and partly to the fact that the edge may be beyond the maximum of intensity.

In column 3 of Table II are the values of the mass action coefficient, in millimeters of mercury, for the dissociation, calculated according to the equa- of Gibson and Heitler,[7] with the data in this paper and Loomis' value, $492\times$

TABLE II.

T°C	P in mm of Hg	K	α	T°C	P in mm of Hg	K	α
100°C	0.0000183	0.3013	0.999878	500	28.07	1709.	0.9687
150	0.000490	2.138	0.99954	600	127.4	4374.	0.9464
200	0.00655	10.08	0.9987	700	423.6	9325.	0.9199
300	0.290	115.1	0.9950	757.3	760.0	13439.	0.9031
400	3.95	506.9	0.9848				

10^{-40}, for the moment of inertia of the normal K_2 molecule. The corresponding vapor pressures of potassium, taken from the data as reported by Fiock and Rodebush[12] and by Edmondson and Edgerton,[13] are given in column 2. In column 4 are given the corresponding values of α, the degree of dissociation of the molecules into atoms. The relation between K and α is

$$K = \frac{4\alpha^2}{1-\alpha^2}\, p. \tag{3}$$

An attempt was made to settle the question as to whether the $^1\Sigma - {}^1\Sigma$ band system actually gives a magnetic rotation spectrum, as it appears to do in the case of sodium, although present theories indicate that it should not. By a long exposure with a rather wide slit, with a neocyanine plate, we suc-

[12] Fiock and Rodebush, Jour. Am. Chem. Soc. **48,** 2522 (1926).
[13] Edmondson and Edgerton, Proc. Roy. Soc. **A113,** 520 (1927).

ceeded in photographing what appears to be a magnetic rotation spectrum in the neighborhood of the infrared ($^1\Sigma - {}^1\Sigma$) system of K_2. As in the case of sodium, it has no simple relation to the absorption spectrum; at least, the magnetic rotation lines do not coincide with the absorption heads as they do in the $^1\Pi - {}^1\Sigma$ system. Another magnetic rotation spectrum, which likewise has no simple relation to the absorption spectrum, was found in the region of the blue system which lies on the long-wave side of the second line of the principal series and is probably also a $^1\Sigma - {}^1\Sigma$ transition.

PHOTOELECTRIC AND THERMIONIC PROPERTIES OF PALLADIUM

By Lee A. DuBridge and W. W. Roehr
Washington University, St. Louis, Missouri

(Received November 12, 1931)

Abstract

The photoelectric and thermionic properties of pure palladium were studied during an extended outgassing in high vacuum. The *threshold*, obtained by extrapolation of spectral sensitivity curves, shifted from below 2300A to above 3000A and then back to a *final* value of 2486A as outgassing progressed. In the final state the photocurrents excited by monochromatic light *increase with temperature*, the relative increase being greater for the longer wave-lengths. At the higher temperatures the spectral sensitivity curves approach the axis asymptotically. The results are shown to be in excellent agreement with Fowler's recent theory and his method of analysis yields the value 4.97 ± 0.01 volts for the true work function (2486A). The *thermionic work function* for the clean specimen was found to be 4.99 ± 0.04 volts, and the value of the constant A is very close to 60 amp./cm^2 deg^2.

I. Introduction

ALTHOUGH it was only a few years ago that it could be said that there was not a single metal for which the photoelectric threshold for the thoroughly outgassed state was accurately known, there are today no less then 12 metals for which the photoelectric properties have been carefully investigated under modern high vacuum conditions.[1] One is now justified in examining the existing data for general relationships between the photoelectric and other properties of the elements. In particular, it is well known that there is a definite relation between the photoelectric work function and the position of the element in the periodic table, for we find that the metals at the beginning of each period—the alkalis and alkaline earths—have very low work functions and there is a general tendency toward higher values at the end of each period. In 1927 one of the authors[2] reported a study of platinum (the last element in the third long period) in which it was found that its work function when thoroughly outgassed was approximately 6.3 volts, the highest value yet reported for any clean metal. This at once raised the question as to whether the elements palladium and nickel which occupy corresponding positions in the previous periods would also show unusually high work functions when clean. Accordingly the authors undertook a study of palladium, the results of which show that the work function of this metal, while considerably lower than that of platinum, is nevertheless definitely higher than for any other element in its period. A recently reported study by Glasoe[3] shows the

[1] The measurements have been summarized in Chap. III of "Photoelectric Phenomena" by Hughes and DuBridge (McGraw-Hill Book Co., in press). There are only three metals for which *both* the thermionic and photoelectric work functions are accurately known.

[2] L. A. DuBridge, Phys. Rev. **29**, 451 (1927); **32**, 961 (1928).

[3] G. N. Glasoe, Phys. Rev. **38**, 1490 (1931).

same thing is true of nickel. As more data are obtained it may be expected that we will find a still more definite relation between photoelectric threshold and atomic number and this should be of considerable assistance in formulating our theories of surface work functions.

Although the present study was undertaken merely for the purpose of determining the photoelectric and thermionic work functions of palladium, while the work was in progress an important paper was published by R. H. Fowler[4] in which he proposed a new theory of photoelectric emission. It seemed highly desirable, therefore, to obtain the additional data required to put the theory to an experimental test. This was done and the results, as will be seen, furnish a valuable quantitative verification of the theory.

II. Apparatus and Methods

Tube and vacuum system

The experimental tube was very similar to that used by DuBridge[2] in his study of platinum. It consisted of a Pyrex tube, with a strip of Pd foil suspended along the axis of three coaxial nickel cylinders, the two outer ones acting as guard rings and being connected to ground. The central collecting cylinder was connected to the electrometer through a well insulated seal at the side of the tube. A quartz window, attached by means of a graded quartz-to-Pyrex seal just opposite a circular opening in the collecting cylinder, served to admit the light when photoelectric readings were being taken, and to allow focussing of the optical pyrometer during temperature measurements. A magnetically operated shutter protected the window from deposits of vaporized palladium during the long outgassing process.

The vacuum system consisted of an air-cooled mercury diffusion pump in series with a Cenco-Hyvac pump, these being separated from the experimental tube by means of a mercury cut-off and liquid air trap. The system contained no waxed seals and all stopcocks were restricted to the low-vacuum side. Pressures below the range of the McLeod gauge were measured by an ionization gauge, and were below 10^{-7} mm Hg in the final stages.

Filament outgassing

After a thorough cleaning of the tube and foil, the tube was sealed to the pumps and baked at temperatures as high as 485°C for from 20 to 30 hours, the filament being kept at a dull red heat by means of an electric current from a low voltage transformer. All metal parts were thoroughly outgassed by means of a high frequency induction furnace. During the initial outgassing the liquid air level was kept fairly low to condense vapors in the bottom of the trap, and was later raised to prevent their escape into the system.

The specimen to be examined consisted of a ribbon of very pure palladium $120\times4.5\times0.01$ mm, bent in the form of a loop and suspended inside the collecting cylinders by means of heavy tungsten leads. There was great difficulty in getting the filament to survive the complete outgassing treatment. Most of the specimens developed hot spots after 75 to 300 hours of treatment at

[4] R. H. Fowler, Phys. Rev. **38**, 45 (1931).

1300°K and broke at these points, although this temperature is several hundred degrees below the melting point of palladium. The broken filaments showed a very marked crystallization near the break and under the microscope had an appearance very similar to micro-photographs of aged palladium foils published by Utterback.[5] The breaks seemed to occur along the crystal boundaries. This early failure of the filaments was finally overcome by beginning the outgassing process at much lower temperatures (<900°K), and, after 500 or 600 hours of heating, raising the temperature slowly to 1300°K with an occasional flashing at 1400°K. This greatly reduced the rate of evaporation and of crystallization and allowed the specimens to survive for 1000 hours or more, during which time the photoelectric behavior reached a steady state which could not be changed by further treatment. During most of the heating the filament was maintained 200 volts positive with respect to the cylinders, to assist the positive-ion emission (presumably gas ions) from the filament. The positive-ion currents were very large at first but decreased rapidly during outgassing, although they never completely disappeared.

Photocurrents were measured by means of a Compton electrometer whose sensitivity was varied from 5000 to 16,000 mm per volt depending on the emission to be measured. The rate-of-charge method was used. For thermionic currents, the electrometer was shunted to ground through one of several high resistances (10^7 to 10^9 ohms) and through a resistance-box potentiometer. It thus became a steady-deflection instrument, a null method of measurement being used. Dr. L. C. Van Atta of this laboratory made the high resistances used.[6]

In order to obtain steady heating currents while runs were being taken, a 24-volt bank of large storage cells was connected in series with a set of fixed wire resistances of negligible temperature coefficient. In this manner heating currents could be kept constant to about 0.001 amp.

Temperature measurements

At incandescent heat the temperature of the palladium was measured with a disappearing-filament type of optical pyrometer, which had previously been calibrated against a standard tungsten lamp supplied to this department by Dr. Forsythe of the Nela Park Laboratories. The true temperature was obtained from the brightness temperature using published tables for platinum,[7] the emissivities of palladium and platinum being the same. The lower temperatures were determined by measuring the resistance of the filament.

Source of light

The source of illumination was a vertical air-cooled quartz mercury arc operated at 90 volts and 2.0 amperes. The light was resolved by a Hilger,

[5] C. L. Utterback, Rev. Sci. Inst. **1**, 39 (1930).

[6] The method of making these resistances has been described in Rev. Sci. Inst. **1**, 687 (1930).

[7] International Critical Tables, Vol. V, p. 245.

quartz-prism, constant-deviation, monochromatic illuminator and focussed on the filament by a quartz lens. Relative intensities of the spectral lines were obtained from the response of a quartz sodium photoelectric cell connected to a direct-current amplifier, the cell having been previously calibrated by means of a tungsten lamp. This method will be described in detail elsewhere.

III. Photoelectric Results

The general trend of the photoelectric threshold during outgassing is shown in Fig. 1, in which the longest wave-length at which an emission was detected at room temperature is plotted as a function of the degassing time. The general shape of this curve is characteristic of all specimens examined. In all cases thresholds below 2300A were observed for fresh specimens. The

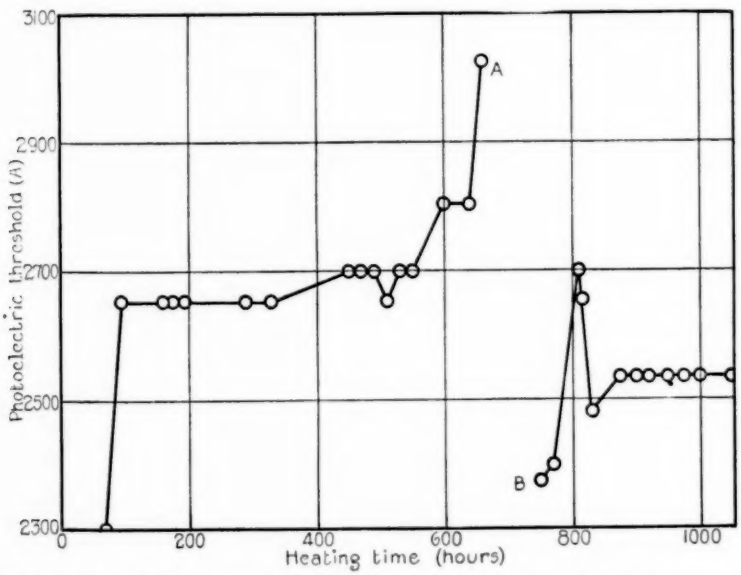

Fig. 1. Behavior of the photoelectric threshold for Pd during outgassing. The discontinuity *AB* was caused by rebaking the tube.

speed with which the long wave limit increased during the initial stages depended very greatly on the outgassing temperature. For example, for the specimen represented in Fig. 1 the threshold did not reach its maximum value (3022A) until after 600 hours of treatment at 900°K, while for other specimens a threshold of approximately 3300A was reached after only 25 hours at 1400°K. The severe initial treatment resorted to in the latter case, although it seemed to speed up the process, so weakened the specimen by evaporation and crystallization that it invariably failed to withstand further treatment long enough to reach a final stage. In Fig. 1 the sudden drop in threshold value from *A* to *B* at 660 hours is the result of rebaking the experimental tube. Exposing the filament to air for a short time at a pressure of several cm Hg resulted in the temporary increase in λ_0 shown at 800 hours. The long wave-length limit then decreased to 2536A at room temperature and

did not change for the last 200 hours. A hot spot which developed during the last 100 hours made further treatment at higher temperatures impossible. The final value of the surface work function for this specimen was 4.95 volts as calculated from extrapolation of $f(\lambda)$ curves for room temperature and 4.93 volts when the Fowler method of plotting was used. More reliable readings were obtained from another specimen which had been treated in a manner similar to that described above but which withstood over 1000 hours of outgassing treatment. The final value of the threshold for this specimen, obtained from the $f(\lambda)$ curve for room temperature (shown in Fig. 3 below), was

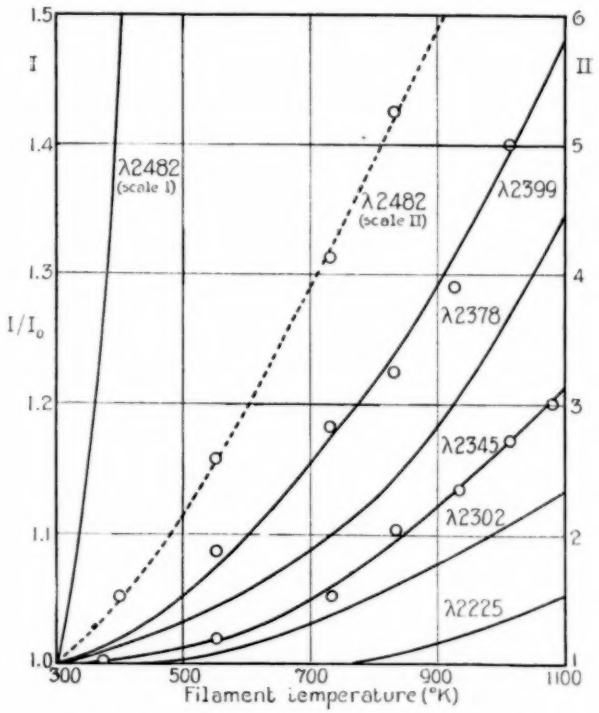

Fig. 2. Temperature variation of photo-currents.

2486A (4.97 volts). When the Fowler method of analysis was employed (see Fig. 4) the same value of the work function was obtained, and this may therefore be taken as the best value for the photoelectric work function of thoroughly outgassed palladium.

IV. Temperature Variation[8]

The variation with temperature of the photoelectric current from clean Pd excited by light is shown in Fig. 2, in which the ratio (I/I_0) of the photocurrent at a given temperature T to that at room temperature is plotted as a function of T. When the specimen had reached its steady state these curves were completely reproducible. It is seen that for wave-lengths far from the

[8] This problem is further discussed in the next paper in this issue of the Physical Review.

threshold (λ2225) the effect of temperature is almost negligible, while near the threshold (e.g., λ2482) the current increases very rapidly with temperature. (The curve for λ2482 is represented by the dotted line when the vertical scale is contracted ten-fold.)

The ordinary spectral distribution curves for three temperatures are shown in Fig. 3. The pronounced feet of these curves, especially at higher temperatures, are not due to scattered light. The curves do not cut the axis at any definite wave-length, but approach it asymptotically, the approach being more gradual for the higher temperatures. All of these curves are quite similar to those obtained by Winch,[9] Morris,[10] and Cardwell[11] for Ag, Au, and Ta surfaces respectively. It is seen from Fig. 3 that in the temperature range

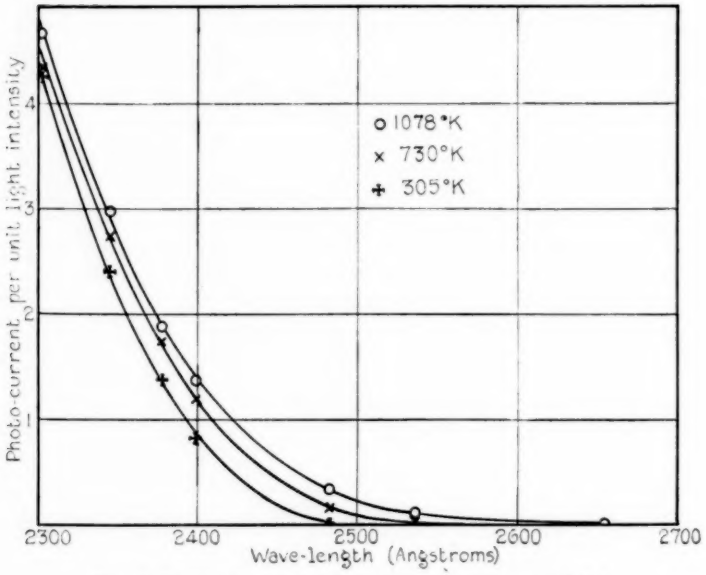

Fig. 3. Spectral distribution curves for outgassed Pd.

used, 305° to 1078°K, the threshold seemed to shift from about 2490A to 2660A corresponding to a change in work function from 4.95 to 4.64 volts. If, however, the approach is asymptotic, as predicted by R. H. Fowler,[4] and as indicated by Fig. 3, then the longest wave-length at which an effect is observed is limited only by the sensitivity of the measuring instruments used.[12] Thus the so-called "shift" in threshold has lost its meaning. Fowler has

[9] R. P. Winch, Phys. Rev. **37,** 1269 (1931).

[10] L. W. Morris, Phys. Rev. **37,** 1263 (1931).

[11] A. B. Cardwell, unpublished data quoted by R. H. Fowler (reference 4).

[12] The asymptotic approach of these curves to the axis is due to the thermal energies of the electrons. Suhrmann (Zeits. f. Physik **33,** 63 (1925)) pointed out that, on the basis of the *classical* electron theory of metals, the curves should be of this form, and he found this to be the case experimentally. Lawrence and Linford (Phys. Rev. **36,** 482 (1930)) obtained similar curves for K layers on W and stated that they could be accounted for by thermal energies of the electrons as given by the Fermi-Dirac statistics. The first quantitative treatment of this problem is that given by Fowler.

pointed out that the method of extrapolating the $f(\lambda)$ curves to zero current, hitherto employed to obtain the threshold, is no longer valid, and he has given a new method for evaluating this constant. It will be shown in the following section that Fowler's theory completely accounts for the temperature variation represented in Figs. 2 and 3.

V. Comparison with Fowler's Theory[8]

Fowler's theory leads to the result that the photoelectric current I excited in a metal surface at the temperature T by unit intensity of light of frequency ν is given by the relation

$$\log I/T^2 = \Phi(\mu) + \text{const.}$$

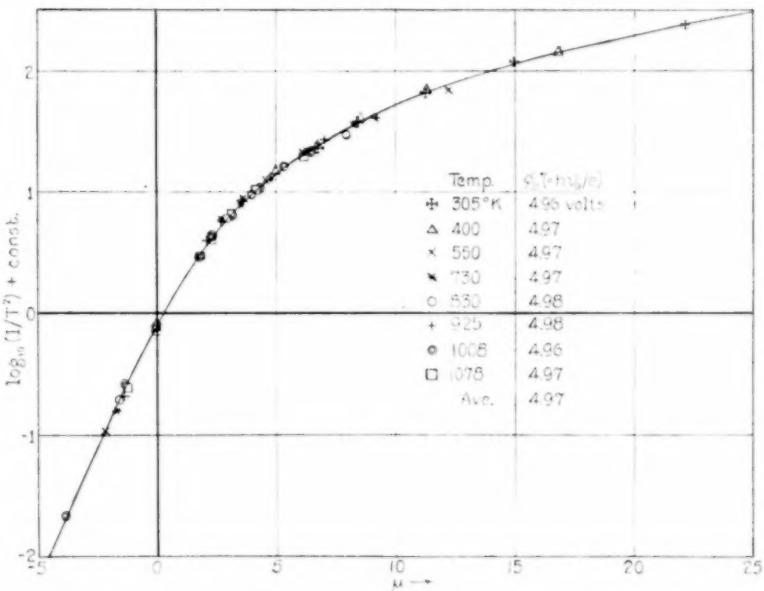

Fig. 4. Analysis of photoelectric observations by Fowler's method.

where $\mu = h(\nu - \nu_0)/kT$ and $\Phi(\mu)$ is a universal function of μ. ν_0 is the threshold at 0°K. If $\Phi(\mu)$ is plotted against μ the curve shown in Fig. 4 is obtained. To obtain ν_0 for a given surface the photoelectric observations at a given temperature are plotted in the form $\log I/T^2$ against $h\nu/kT$, and the horizontal component of the shift required to make this curve fit the theoretical curve is equal to $h\nu_0/kT$. Fowler showed that his theory was in good agreement with the results of Winch,[9] Morris,[10] and Cardwell,[11] but it is highly desirable to make further experimental tests.

An analysis by Fowler's method of the data for clean Pd is also shown in Fig. 4, in which the experimental points are plotted after they have been shifted by the proper amounts. Observations of I as a function of ν were taken for 8 different temperatures in the range 305°K to 1078°K, yielding 8 observed curves. The *vertical* shifts required to bring these curves into coincidence with the theoretical curve were the same for all temperatures, as de-

manded by Fowler's theory. From the *horizontal* shifts the work functions shown in the figure were computed. The individual values show an excellent agreement among themselves, yielding an average value of 4.97 ± 0.01 volts (2486A). This happens to be in good agreement with the value obtained by extrapolating the $f(\lambda)$ curve taken at room temperature (Fig. 3). Fowler's method, however, gives the *true* or absolute zero value of the work function which is not affected by an arbitrary extrapolation of a curve which really approaches the axis asymptotically.

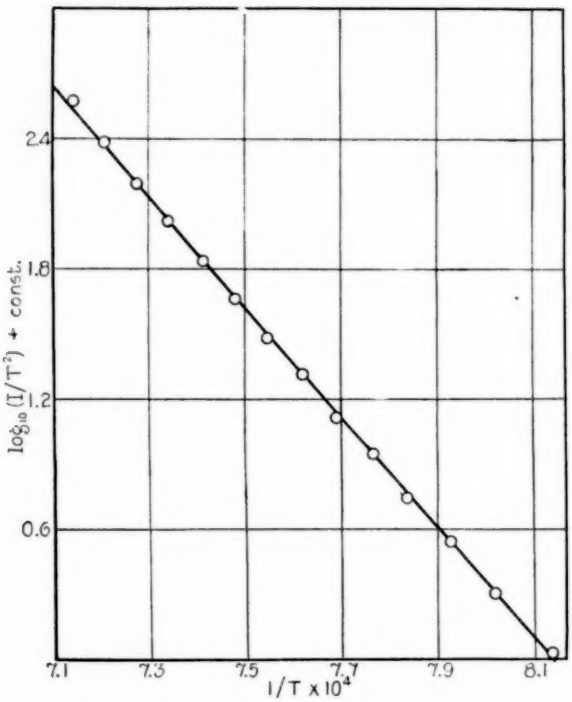

Fig. 5. Thermionic curve for outgassed Pd.

Application of Fowler's method to observations made before the specimen had reached a final state also gave a good fit, as well as good agreement in the values of ϕ_0 for various temperatures. It is to be concluded, therefore, that Fowler's theory is applicable not only to surfaces entirely free from gases but also to all surfaces in a state sufficiently stable to prevent any appreciable change during the course of the observations.

VI. Thermionic Measurements

In taking thermionic measurements, simultaneous readings were taken of the thermionic current and filament temperature. The true temperature, as determined from the average of several pyrometer settings, was plotted as a function of the filament heating current and the final temperatures were read from a smooth curve drawn through the experimental points.

After repeated attempts it was found that no systematic study of the behavior of the thermionic work function during the outgassing process could be made, since the temperatures required for thermionic measurements were higher than the temperatures at which the filament could be heated safely during the initial stages. It was found, however, that the thermionic work function decreased from high initial values down to values as low as 2.0 volts, and this was followed by a subsequent rise, in line with the corresponding photoelectric changes. Satisfactory thermionic measurements after the final state was reached were obtained for only a single specimen (the one for which the curves of Figs. 2, 3, and 4 are plotted), and this specimen developed a hot spot and burned out before the run could be repeated. The data for this run are shown in Fig. 5, plotted in the usual form for determining the work function in Richardson's equation,

$$I = AT^2e^{-b/T}.$$

The value of b is 57,950°K corresponding to a work function of 4.99 volts, with a possible error of about 1 percent.

Fowler's theory predicts that the value of the thermionic work function should be equal to the *true* photoelectric work function ϕ_0, determined by the method outlined in the previous section. It is seen that this prediction is verified within the limits of experimental error, the values being 4.99 ± 0.04 volts and 4.97 ± 0.01 volts, respectively. This point is of interest since it has not been previously tested directly and since it has occasionally been suggested that the thermionic and photoelectric work functions, in order to agree, should be measured at the *same* temperature. In the present experiments, however, if the photoelectric threshold is determined at high temperatures by the usual extrapolation methods, a work function is obtained (4.64 volts) which differs by 7 percent from the thermionic value. This furnishes further striking evidence in favor of Fowler's theory.

The average value of the thermionic coefficient A, although it could not be determined with high accuracy in these experiments, came out very close to the theoretical value of 60 amp/deg^2. cm^2, with a maximum deviation of about 30 percent from this value. This is in interesting contrast to the results for Pt which yielded very high values of A, although the two metals, since they occupy similar positions in the periodic table, would be expected to show a similar thermionic behavior. However, this result confirms the suggestion[13] that high values of A occur only with unusually high values of b.

The experimental work described in the present paper was assisted by a grant to the senior author from the Science Research Fund of Washington University.

[13] L. A. DuBridge, Proc. Nat. Acad. Sci. 14, **78** (1928).

A FURTHER EXPERIMENTAL TEST OF FOWLER'S THEORY OF PHOTOELECTRIC EMISSION

By Lee A. DuBridge
Washington University, St. Louis, Missouri
(Received November 12, 1931)

Abstract

Fowler's theory of photoelectric emission is discussed from the viewpoint of the experimental physicist and several significant consequences of the theory in analyzing experimental data pointed out. A new graphical method of testing the theory is suggested. This method makes it possible to determine the "true" photoelectric threshold of a surface from photocurrent-temperature curves taken at a single incident frequency, eliminating the necessity of measuring relative intensities of spectral lines. The method is applied to new experimental data on palladium and to Morris' data on gold and found to be completely successful, thus furnishing additional verification of Fowler's theory.

R. H. FOWLER[1] has recently made an important contribution to the theory of the photoelectric effect in metals by deriving an equation for the specific photoelectric emission from a metal surface as a function of the frequency of the incident light and the temperature of the surface. He has devised an ingenious graphical method of testing the theory and has shown that it is in excellent agreement with the best experimental results. The same graphical method is also used to determine from experimental results the true photoelectric threshold of the metal. The purpose of the present paper is to discuss some of the experimental implications of Fowler's theory and to suggest another method of testing the theory and determining the threshold. The method is an obvious variation of the one proposed by Fowler, but it is of considerable interest in itself and has been found by the author to be extremely useful in analyzing experimental data.

I. Discussion of Fowler's Theory

Fowler's assumptions are: (1) that the electrons within a metal obey the Fermi-Dirac statistics and (2) that the number which will be ejected by unit energy of absorbed light of any frequency ν is proportional to the number within the metal which have energies normal to the surface such that, when augmented by the energy $h\nu$, they are sufficient to surmount the surface potential step χ_0. Fowler was able greatly to simplify the theory by considering only the effects of incident frequencies which do not differ greatly from the threshold frequency ν_0. This restriction eliminates the necessity of considering such uncertain quantities as transition probabilities of electrons through surface potential barriers, for these introduce terms which can be considered essentially constant over small frequency ranges. On the other

[1] R. H. Fowler, Phys. Rev. **38**, 45 (1931).

hand the restriction is not a serious one from the experimental viewpoint for, except for the alkali metals, the frequencies available experimentally lie as a rule within 30 percent of the threshold, and over this range the theory is reasonably exact. The final equation obtained for the photoelectric current I excited in a metal surface at the temperature T by unit intensity of absorbed light of frequency ν is

$$\log_{10} I/T^2 = B + \Phi(\mu), \tag{1}$$

where B = constant, independent of ν and T,

$$\mu \equiv h(\nu - \nu_0)/kT,$$

and $\Phi(\mu)$ is a universal function of μ given by

$$\Phi(\mu) = \log_{10}(e^{\mu} - e^{2\mu}/2^2 + e^{3\mu}/3^2 - \cdots) \text{ for } \mu \leqq 0, \tag{2}$$

$$\Phi(\mu) = \log_{10}(\pi^2/6 + \tfrac{1}{2}\mu^2 - [e^{-\mu} - e^{-2\mu}/2^2 + e^{-3\mu}/3^2 - \cdots]) \text{ for } \mu \geqq 0, \tag{3}$$

Values of $\Phi(\mu)$ for a series of values of μ are listed in Table I, and these are plotted in the curve shown in Fig. 1.

TABLE I. *Values of Fowler's function* $\Phi(\mu)$.

μ	$\log_{10}\lvert\mu\rvert$	$\Phi(\mu)$	μ	$\log_{10}\lvert\mu\rvert$	$\Phi(\mu)$
−8.0	+0.903	−3.475	+2.0	+0.301	+0.546
−6.0	0.778	−2.606	3.0	0.477	0.785
−5.0	0.699	−2.171	4.0	0.602	0.983
−4.0	0.602	−1.739	5.0	0.699	1.150
−3.0	0.477	−1.308	6.0	0.778	1.293
−2.5	0.398	−1.095	8.0	0.903	1.527
−2.0	0.301	−0.884	10.0	1.000	1.713
−1.5	0.176	−0.674	12.0	1.079	1.866
−1.0	0.000	−0.469	14.0	1.146	1.998
−0.5	−0.301	−0.268	16.0	1.204	2.113
−0.2	−0.699	−0.160	20.0	1.301	2.305
0.0	$-\infty$	−0.085	25.0	1.398	2.497
+0.2	−0.699	−0.015	30.0	1.477	2.655
0.4	−0.398	+0.055	35.0	1.544	2.788
0.6	−0.222	0.125	40.0	1.602	2.904
1.0	0.000	0.249	50.0	1.699	3.097
1.5	+0.176	0.400			

Fowler's method of testing Eq. (1) is as follows: Observations are taken of the photoelectric current per unit intensity as a function of frequency, for a metal surface at a fixed temperature T. A plot is made of $\log I/T^2$ as a function of $h\nu/kT$. This observed curve should be of the form of the theoretical curve of Fig. 1, and should, after a shift parallel to itself, coincide with it. The vertical component of this shift is unimportant, since it involves only the constant B and will depend on the units in which the current and light intensity are measured. The horizontal component, however, should be equal to $h\nu_0/kT$, from which ν_0 may be determined. Fowler showed in this way that the theory was in excellent agreement with the observations of Winch,[2] Morris[3] and Cardwell[4] on Ag, Au, and Ta, respectively, while it has been

[2] R. P. Winch, Phys. Rev. **37**, 1269 (1931).
[3] L. W. Morris, Phys. Rev. **37**, 1263 (1931).
[4] A. B. Cardwell, unpublished.

shown in the previous paper in this issue of the Physical Review[5] that it is also in good agreement with the results of DuBridge and Roehr on palladium.[6]

The success of Fowler's theory makes it imperative to inquire further into its significance and its consequences. We find at once that, while it introduces no radically new ideas as to the nature of the photoelectric process itself, it nevertheless gives a quantitative interpretation of many experimental facts in the field of photoelectricity which have been a puzzle for many years. At the same time, because of its simplicity in form, it is exceedingly useful in analyzing and coordinating experimental data, and in serving as a guide to further research. There are several features of the theory which are of par-

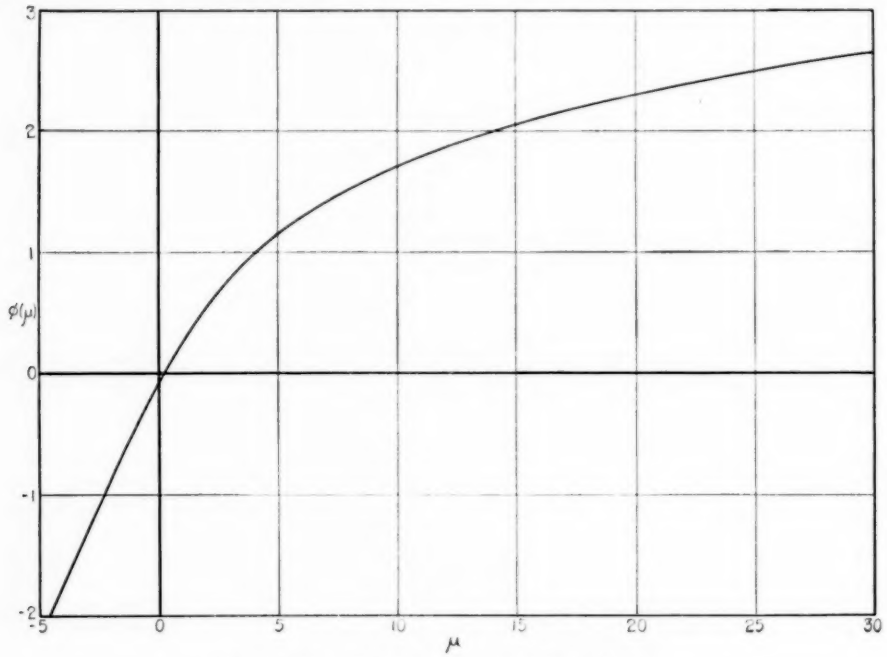

Fig. 1. Fowler's theoretical curve, $\Phi(\mu)$ vs. μ.

ticular interest to the experimentalist, and which therefore deserve further discussion.

1. The fact that the quantity $\log I/T^2$ turns out to be a *universal* function of μ is in itself of considerable interest since it will very greatly simplify the analysis and comparison of experimental results. In view of the wide variety in the forms of ordinary spectral distribution curves (I *vs.* ν) it is a result which would scarcely have been expected.

2. The threshold frequency ν_0 is defined by Fowler from the equation,

$$h\nu_0 = \phi_0 e = \chi_0 - \epsilon^* \tag{4}$$

where ϵ^* is the maximum kinetic energy of the electrons at absolute zero on

[5] L. A. DuBridge and W. W. Roehr, Phys. Rev. **39,** 99 (1932).

[6] G. N. Glasoe (Phys. Rev. **38,** 1490 (1931)) also finds an agreement with his results (for a single temperature) on Fe and Ni. See also A. H. Warner, Phys. Rev. **38,** 1871 (1931).

the Fermi statistics, and ϕ_0 is the surface work function. It is evident that ν_0 is *not* the threshold obtained by the ordinary method of extrapolating spectral distribution curves to the axis, for, as can be seen from Eq. (3), for $T > 0°K$ the current I does not fall to zero at $\nu = \nu_0$, but approaches zero asymptotically as ν decreases. *Hence there is no such thing as a sharply defined threshold at any temperature above* 0°K. At this temperature, however, I is proportional to $(\nu - \nu_0)^2$ so that ν_0 is the threshold at absolute zero. Since ν_0 is a real characteristic of the surface it may be called the *true* threshold, while ϕ_0 is the *true* work function. (ϕ_0 should be equal to the thermionic work function, since this is also defined by Eq. (4).) Fowler's theory gives a method by which the true threshold ν_0 may be determined from measurements made at ordinary temperatures.

3. Fowler's theory has greatly clarified the question of the temperature variation of the photoelectric effect, a problem which has been extensively investigated. It is evident that it is now meaningless to speak of the "temperature variation of the photoelectric threshold," for the *true* threshold is not temperature dependent, while the *apparent* thresholds obtained by extrapolation methods do not have sufficient quantitative significance to permit of exact discussion.[7] The question as to the temperature variation of photocurrents due to monochromatic light has, however, taken on added interest. It is well known that the early experiments showed that, over small temperature ranges, the photoelectric currents excited by *unresolved* light were nearly independent of temperature, while in a number of more recent experiments, taken over a wider temperature range, a definite increase of photocurrent with temperature has been observed. Ives[8] was the first to show that the increase is greater for light of longer wave-length. The only quantitative experiments with monochromatic light are those of Winch,[2] Morris,[3] and DuBridge and Roehr,[5] and these, as will be shown, are in complete agreement with Fowler's theory. According to this theory the temperature variation depends greatly on the incident frequency. Thus for $\nu = \nu_0$, I is proportional to T^2. For larger frequencies the variation is much slower and becomes almost inappreciable for light which is 200A or more on the short wave-length side of the threshold. For ν less than ν_0, on the other hand, the variation is extremely rapid, due to the exponential terms in Eq. (2). It is significant that *the temperature changes observed experimentally are entirely accounted for by the increase in thermal energy of the electrons*, without the necessity of attributing them to changes in the surface itself, such as thermal expansion, etc.

4. The lack of sharpness in the threshold at temperatures above 0°K in-

[7] This is of particular interest in connection with the recent discussion on the relation of the temperature variation of the threshold to the value of the thermionic coefficient A. (See L. A. DuBridge, Proc. Nat. Acad. Sci. **14,** 788 (1928); P. W. Bridgman, Phys. Rev. **31,** 90 (1928); K. F. Herzfeld, Phys. Rev. **35,** 248 (1930); J. A. Becker and W. H. Brattain, Phys. Rev. **37,** 462 (1931)). Evidently abnormal values of A can *not* be ascribed to a temperature coefficient of ν_0, since the *apparent* changes in ν_0 are due only to the thermal energies of the electrons and not to a real change in work function.

[8] H. E. Ives, J. O. S. A. **8,** 551 (1924); H. E. Ives and A. L. Johnsrud, J. O. S. A. **11,** 565 (1925).

volves also a lack of sharpness in the *maximum velocity* of the emitted electrons. And this means that the Einstein equation can be expected to hold exactly only at very low temperatures. This is an exceedingly important result, and one which requires further theoretical and experimental examination. It is a matter of good fortune that at room temperature the lack of sharpness in the threshold is not sufficiently marked to produce *serious* errors in the determinations of ν_0 by extrapolation. The lack of sharpness is *appreciable*, however, and *does* become serious at high temperatures. It remains to be seen how great are the errors involved in the usual method of determining *maximum velocities* of emission.

5. Finally it should be mentioned that the variation of the photocurrent with frequency and temperature predicted by Fowler's theory are due directly to the characteristics of the Fermi distribution of velocities among the electrons, and to nothing else. The success of the theory thus constitutes one of the most direct and most convincing tests yet obtained of the applicability of the Fermi-Dirac statistics to electrons in metals.

II. Another Method of Determining ν_0

Fowler's method of analyzing photoelectric observations consists in measuring I as a function of ν for a fixed value of T, and then plotting $\log I/T^2$ against $h\nu/kT$. By taking observations at other values of T one obtains a series of "isothermal" curves, and from the horizontal shifts required to make these curves fall on the theoretical curve, ν_0 is determined. There is, however, another obvious method of using Fowler's equation for the analysis of photoelectric observations, which, besides being of interest in itself, offers a number of advantages over Fowler's own method. By making use of this new method it is possible to determine ν_0 from measurements made at a *single frequency* of incident light, and this eliminates the necessity of measuring the relative intensities of spectral lines.

The method is as follows: Instead of plotting Fowler's function $\Phi(\mu)$ against μ, plot it as a function of $\log |\mu|$. The necessary data are given in Table I and the curve obtained is shown in Fig. 2. This curve consists of two branches, one for positive and one for negative values of μ. We will confine our attention for the present to the positive branch. Now suppose that for incident light of a fixed frequency ($\nu > \nu_0$) we observe the photoelectric current I as a function of the temperature of the emitting surface. We thus obtain an "isochromatic" instead of an "isothermal" run. If the observations are plotted in the form $\log I/T^2$ against $\log 1/T$ ($= -\log T$) we obtain a curve which, after a shift parallel to itself, should coincide with the theoretical curve shown in Fig. 2. The vertical component of the shift is again unimportant. It will involve the constant B, and will depend on the units in which I is measured. It will depend also on the intensity of the incident light, since in this case it is not necessary to reduce I to unit intensity. The horizontal component of the shift, however, is equal to $\log h(\nu-\nu_0)/k$, because $\log \mu = \log[h(\nu-\nu_0)/k] - \log T$. Hence, knowing ν, we may determine ν_0 at once. It is evident that this process is quite analogous to that of determining the

"characteristic temperature" of a substance from specific heat data by plotting c_v against $\log T$. The quantity $h(\nu-\nu_0)/k$ in the present case is, in fact, a sort of characteristic temperature for the particular surface and the particular frequency of light used.

Let Δ be the horizontal shift required to bring the observed and theoretical curves into coincidence, and set $\log \theta = \Delta$. Then we should have,

$$h(\nu - \nu_0)/k = \theta.$$

In actual practice we usually desire to determine the work function ϕ_0 of the surface in volts. Then $\phi_0 e = 300h\nu_0$. Let V be the voltage-equivalent of the frequency used, so that $Ve = 300h\nu$. Then we should have

$$e(V - \phi_0)/300k = \theta.$$

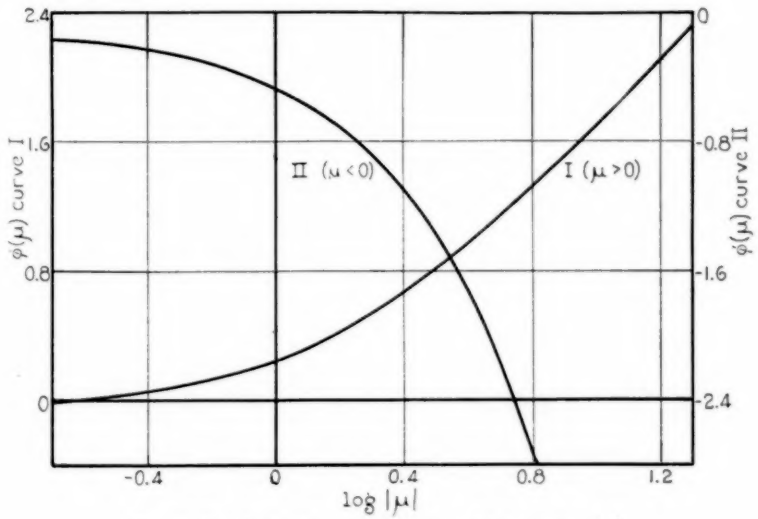

Fig. 2. Fowler's theoretical curve, $\Phi(\mu)$ vs. $\log |\mu|$.

Whence,

$$\begin{aligned} \phi_0 &= V - 300k\theta/e \\ &= V - (8.61 \times 10^{-5})\theta. \end{aligned} \tag{5}$$

The results of analyzing the experimental data in this way will be presented below, and it is shown that the method is completely successful. It is evident that this method of determining ϕ_0 has a number of distinct advantages over the previous one. In the first place, as has been pointed out, it makes possible for the first time the determination of ϕ_0 from measurements made at a single frequency. By taking several isochromatic curves at different frequencies, several determinations of ϕ_0 can be made, which, it has been found, agree within experimental error. Furthermore, in plotting these different curves it is not necessary to reduce I to unit intensity of absorbed light, for this factor would simply result in an additional vertical shift of each curve. (If I were reduced to unit intensity all curves would have the same vertical shift, but this does not assist materially in the "fitting" process.) It is

well known that measurements of the intensities of spectral lines are troublesome at best and for weak lines in the far ultraviolet are exceedingly difficult to obtain accurately. A method which eliminates the necessity of making such measurments will be of interest to every experimentalist in this field. It is only necessary to insure that the intensity of the light remains constant during each run.

Another advantage of this method lies in the fact that the quantity directly determined from experiment is not ν_0 but $(\nu-\nu_0)$. Hence, as can be seen from Eq. (5), an error in determining θ makes a much smaller error in ϕ_0, since the second term is much smaller than the first and since V is usually known with considerable accuracy. Theoretically, therefore, this method is capable of high precision in determining ϕ_0. In actual practice, however, it was found that the precision of the two methods was about the same, due to the fact that small errors in determining $\log \theta$ give much larger errors in θ itself.

Finally there should be mentioned several sources of error which must be guarded against in analyzing observations by either of the two methods. In the first place, it has been assumed that there is a fixed ratio between the amount of light absorbed by the surface and the amount incident upon it, so that we do not need to distinguish between incident and absorbed energy. This will not be true if the reflectivity of the surface varies either with the frequency or with the surface temperature. A variation with *temperature* will only introduce different vertical shifts in the *isothermal* curves but will change the shape of the *isochromatic* curves and thus introduce an error in determining ϕ_0. Changes with *frequency*, on the other hand, will only affect the vertical shift of the *isochromatic* curves, but will introduce an error in the *isothermals*. Fortunately, for the metals which have been studied, the reflectivity does not vary appreciably with either ν or T, but this possibility must be kept in mind, and if necessary corrected for. In this respect the isochromatic method of analysis has a slight advantage, since changes of reflectivity with temperature are more easily measured (by Winch's method[2]) than changes with frequency. (Care must be taken, of course, that the specimen does not warp or sag due to its thermal expansion so as to change the amount of light incident upon it.)

It will be noted that the lower end of the curve of Fig. 1 and the upper end of curve I of Fig. 2 are quite accurately linear. Hence if the range covered by the observations falls on one of the linear portions, no unique fit is possible and the threshold cannot be determined with certainty. The most accurate fitting of isothermal curves can thus be made in the region of low temperatures and high frequencies (i.e., ν considerably above ν_0), while for the isochromatic curves the most accurate results are obtained with high temperatures and low frequencies (ν near ν_0).

III. Experimental Tests

The new method of testing Fowler's theory and determining the true work function was applied to the data on palladium obtained by the author

and Mr. W. W. Roehr (see previous paper) and to the data on gold published by Morris.[3] The latter set of data is the only one previously published in a form sufficiently complete to enable the necessary calculations to be made. The results for clean palladium have been plotted in Fig. 3, in which the experimental points have already been shifted by the amount necessary to make the individual observed isochromatic curves fall on the theoretical curve. The details of experimental procedure have been described in the previous paper, and the observations used here are the same ones represented by the curves of Fig. 2 of that paper. Points are shown for six different mercury arc lines on the short wave-length side of the threshold, and the temperature range covered in each run was from 305°K to 1070°K. The mag-

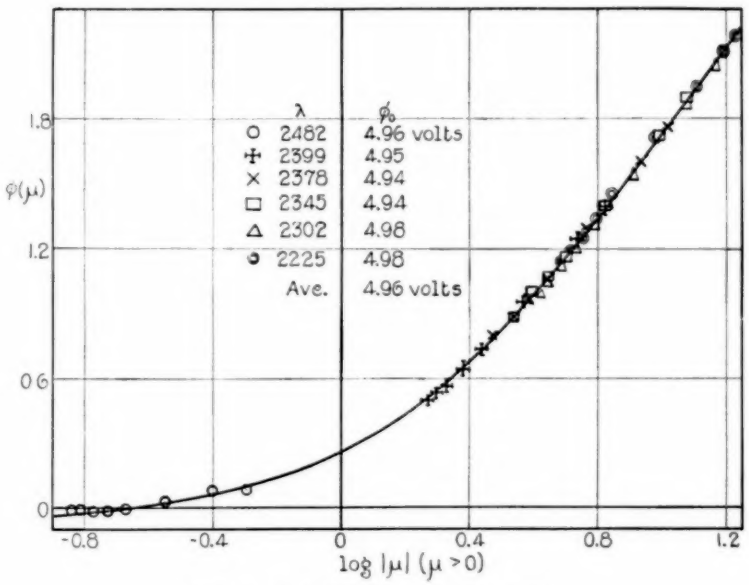

Fig. 3. Analysis of data for clean Pd.

nitudes of the horizontal shift ($\log \theta$) and of ϕ_0 for each wave-length are given in Table II. It is seen that the maximum deviation from the mean value of ϕ_0 is of the order of 0.5 percent, which is well within experimental error. The mean value is also in excellent agreement with the value 4.97 volts, obtained by analyzing data for the same specimen by Fowler's method.

TABLE II. *Analysis of data for clean palladium.*

λ(A)	V (volts)	$\log \theta$	ϕ_0 (volts)	λ_0 (A)
2225	5.549	3.75	4.98	2482
2302	5.363	3.65	4.98	2482
2345	5.265	3.56	4.94	2502
2378	5.192	3.47	4.94	2502
2399	5.146	3.36	4.95	2495
2482	4.972	2.19	4.96	2490
		Average	4.96	2491

A similar plot of the data for palladium which had not been thoroughly outgassed, but which was in a fairly stable state, is shown in Fig. 4, and Mor-

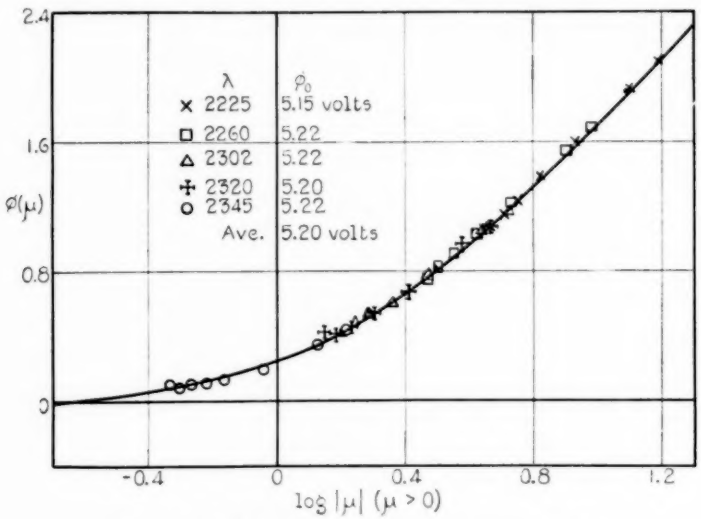

Fig. 4. Analysis of data for partially outgassed Pd.

ris' data for gold are shown in Fig. 5. It is seen that again an excellent fit with the theoretical curve is obtained and that the values of ϕ_0 are also in good

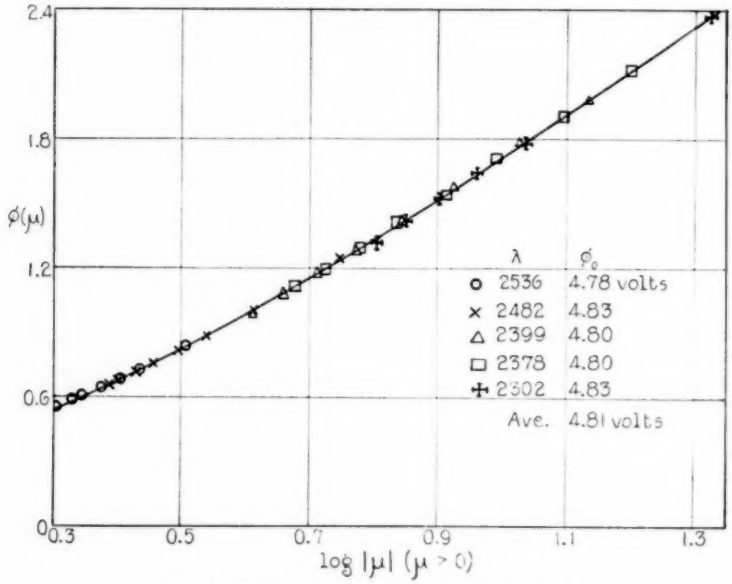

Fig. 5. Analysis of data for gold (Morris).

agreement. In the case of gold the average value of ϕ_0 obtained by this method (4.81 volts) is to be compared with the value 4.90 volts obtained by Fowler from his analysis of Morris' data. The discrepancy of about two percent might

easily be due to the errors involved in reading numerical values from the published curves. Also it was not certain that Morris' isochromatic runs were taken under exactly the same conditions as to freedom from gases as the isothermal curves used by Fowler.

Nothing has so far been said about the negative branch of the theoretical curve shown in Fig. 2. It is obvious that observations taken for a frequency which is on the long wave side of the true threshold ($\mu<0$) should fall on this branch. Measurements in this region, however, are difficult to obtain accurately, owing to the smallness of the currents themselves, and to the relatively large fraction of these currents which may be due to stray light of shorter wave-lengths. Nevertheless, in a few cases reliable runs were obtained

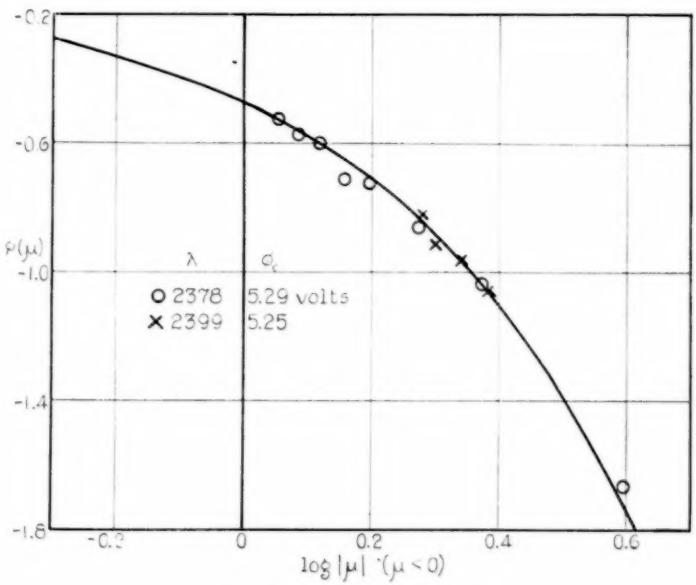

Fig. 6. Plot of data for $\nu<\nu_0$.

for one or two wave-lengths beyond the threshold, and the results are shown in Fig. 6. These runs were obtained at the same time as those shown in Fig. 4. The agreement, while not as good as before, is within experimental error, and the value of the work function agrees within about one percent with that obtained for shorter wave-lengths. While it is probably not practicable to use observations taken for $\nu<\nu_0$ in accurate determinations of ν_0, they nevertheless in this case furnish an additional experimental verification of the theory.

IV. Conclusion

It appears from the curves shown above and from those shown in Fowler's paper that Fowler's theory is in complete quantitative agreement with experiment, whether the isothermal or the isochromatic method of analysis be employed. His theory therefore marks a very great step forward in our understanding of photoelectric processes. It is particularly fortunate that Fow-

ler has put his theory in a form which is both understandable and useful to the experimental physicist in analyzing his data, and it may be expected to play an important role in future experimental studies.

In conclusion the author wishes to express his indebtedness to Mr. W. W. Roehr who assisted in the experimental work, in making the calculations, and plotting the curves, and also to acknowledge a grant from the Science Research Fund of Washington University which made the work possible.

TEMPERATURE VARIATION OF THE MAGNETIC SUSCEPTIBILITY, GYROMAGNETIC RATIO, AND HEAT CAPACITY IN Sm^{+++} AND Eu^{+++}

By Amelia Frank

Department of Physics, University of Wisconsin

(Received November 16, 1931)

Abstract

Calculations of the magnetic susceptibilities in Sm^{+++} and Eu^{+++} inclusive of second order Zeeman terms, previously made at $T=300°K$ only, are extended to include values over a temperature range 0°K–800°K. The value assigned to the screening constant used in computing the multiplet intervals is adjusted to make the theoretical susceptibilities agree as closely as possible with experimental data. This fixes the separation between the lowest two levels with less uncertainty than in existing spectroscopic estimates. The computations show that Sm^{+++} should exhibit an unusual behavior in that, whereas at low temperatures the susceptibility decreases rapidly with increasing temperature, a minimum is reached between 375°K and 450°K. The theoretical values of the temperature coefficients of susceptibility in Sm^{+++} and Eu^{+++} (both of which are much lower than the Curie value $1/T$) are in satisfactory agreement with experiment when the second order Zeeman terms are included. The other elements in the rare earth group do not deviate appreciably from the Curie law. The present computations show an increase in the gyromagnetic ratio in Sm^{+++} with increasing temperature, in contrast with the behavior in Eu^{+++} in which increasing temperature decreases this ratio. The temperature variation of the contribution of the multiplet levels to the heat capacity of Sm^{+++} and Eu^{+++} is also calculated.

Introduction

THE discrepancy between the theoretical and experimental values of the magnetic susceptibilities in the rare earth group was shown in a previous letter to the Editor[1] to be removed by the inclusion of the second order Zeeman terms, the effect of which is important only in Sm^{+++} and Eu^{+++}. A comparison of these theoretical results with those of Hund[2] is given in Fig. 1. In this figure, as well as throughout the rest of the paper, the three plus signs are omitted and every time the chemical symbol for an element is used, it stands for the triply charged ion of that element. Assuming infinite multiplet widths, Hund obtained an expression for the susceptibility

$$\chi = N\beta^2 g^2 J(J+1)/3kT \qquad (1)$$

which conforms to the classical Curie law ($\chi \propto 1/T$). In this expression, N is Avogadro's number, g the Landé factor $[3/2+(S^2+S-L^2-L)/2(J^2+J)]$, and β the Bohr magneton ($he/4\pi mc$). Here $\beta^2 g^2 J(J+1)$ is the square of the magnetic moment of the atom and is independent of the temperature. The solid line in Fig. 1 is obtained by plotting the values of $\mu = g[J+1]^{1/2}$ the

[1] J. H. Van Vleck and A. Frank, Phys. Rev. **34**, 1494, 1625 (1929).

[2] F. Hund, Zeits. f. Physik **33**, 855 (1925).

Bohr magneton number. The vertical lines show the range, obtained by various experimenters, of the effective Bohr magneton numbers at room temperature, defined as

$$\mu_{\text{eff}} = (3kT\chi/N\beta^2)^{1/2} \tag{2}$$

by analogy to Langevin's formula. As Curie's law does not always hold, μ_{eff} is not always independent of temperature and this comparison of theoretical and experimental values of μ_{eff} is merely a convenient way of comparing the susceptibilities at a given temperature. The dotted line shows the theoretical values of μ_{eff} at room temperature when allowance is made for the finite width of the multiplets and the second order Zeeman terms. These differ materially from the values of Hund in Sm and Eu, the values being raised from

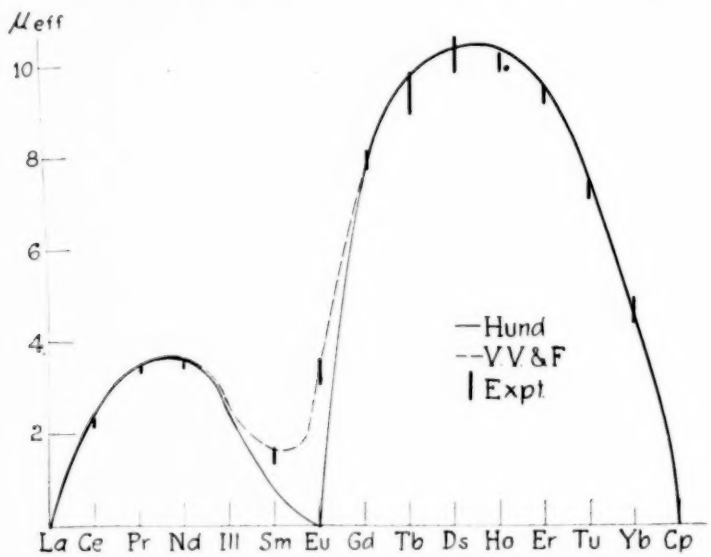

Fig. 1.

0.83 to 1.65 in the former and from 0.00 to 3.51 in the latter, the higher values agreeing with experiment.

In the cases of Sm and Eu, then, it is necessary to use the complete expression for the susceptibility

$$\chi = \frac{N\sum_J \{[\beta^2 g_J{}^2 J(J+1)/3kT] + \alpha(J)\}(2J+1)e^{-W_J^0/kT}}{\sum_J (2J+1)e^{-W_J^0/kT}} \tag{3}$$

Here $\alpha(J)$ is given[3] by

$$\frac{\beta^2}{6(2J+1)h}\left[\frac{f(J)}{\nu_{J-1;J}} + \frac{f(J+1)}{\nu_{J+1;J}}\right] \tag{4}$$

where

$$f(J) = J^{-1}[(S+L+1)^2 - J^2][J^2 - (S-L)^2].$$

[3] J. H. Van Vleck, Phys. Rev. **31**, 587 (1928).

The first bracket of (3) differs from the expression (1) given by Hund in that multiplet widths are no longer assumed infinite so that it becomes necessary to sum[4] over all values of J. The portion of (3) involving $\alpha(J)$, usually omitted, arises from the fact that the energy expression $W_J{}^0+g\beta MH$ is not always adequate. Instead the energy should be expanded to terms of the second order in the field strength,[5] in cases where the frequency intervals $\nu_{J-1;J}$ and $\nu_{J+1;J}$ occurring in the denominator of (4) are at all comparable with kT/h.

Fig. 2 is given to emphasize again the reason why $\alpha(J)$ is so important in Sm and Eu. These diagrams, giving the relative separation of components with different values of J, show that the interval between two consecutive components may be comparable with kT even though the overall-multiplet

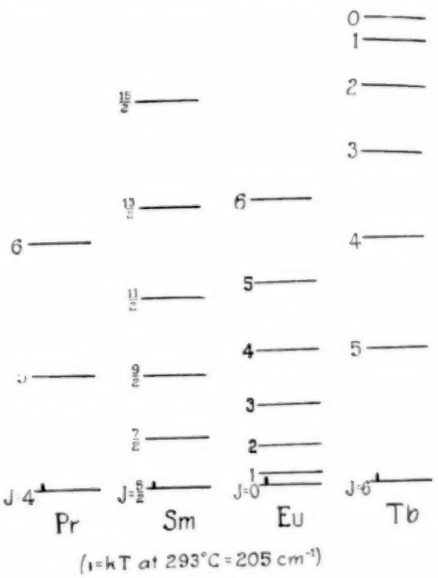

Fig. 2.

width is much larger. For instance with the Landé rule[6] $(W^0_{J+1}-W_J{}^0)\propto(J+1)$ which is assumed in Fig. 2 for the relative multiplet separations, the lowest interval in Sm is 7/55 and in Eu 1/21 of the overall multiplet widths, in contrast with the fractions 5/11 and 6/21 in Pr and Tb respectively. The latter is included to show why the effect of $\alpha(J)$ is negligible in the last half of the rare earth group. Here the interval between the states $J_{\min}$ and $J_{\min}+1$ is small but the multiplets are inverted so that $J_{\min}$ gives the state of highest

[4] Laporte took into account finite multiplet widths in his values for the susceptibilities in the iron group. In this case, however, taking into account finite multiplet widths and second order Zeeman terms improves the agreement with experiment for a few elements but there still remains a considerable difference not yet explained, especially in the last half of the iron group. Cf. O. Laporte, Zeits. f. Physik **47**, 761 (1928).

[5] This second order term represents an incipient Paschen-Back effect and was calculated in the old quantum theory by A. Landé, Zeits. f. Physik **30**, 329 (1924); and in the new quantum mechanics by E. Hill and J. H. Van Vleck, Phys. Rev. **31**, 715 (1928).

energy and that level is virtually unoccupied. The situation in which there may be a small interval between consecutive components arises when the multiplicity $(2S+1)$ is large but $J_{\min}$ $(=|L-S|)$ is small. This is the case with Sm and Eu, whose multiplet types, according to the Hund theory, are ^6H and ^7F. Then it becomes necessary to include not only the contribution of atoms not in the lowest state, but also the second order Zeeman terms, since the denominators $\nu_{J-1;J}$, $\nu_{J+1;J}$ are sufficiently small to make $\alpha(J)$ appreciable.

In computing the above separations quantitatively, the over-all multiplet width is obtained from Goudsmit's theory for the multiplet separation for equivalent electrons.[6] This gives

$$W^0_{J\max} - W^0_{J\min} = R\left(\frac{2\pi e^2}{hc}\right)^2 (Z-\sigma)^4(2L+1)/n^3l(l+1)(2l+1).$$

Where R is the Rydberg constant, $n=4$ and $l=3$ in the rare earth group, L is the resultant of all the l's, and σ is the screening constant. The screening constant for the rare earths is not obtained directly but is estimated from x-ray data for heavier atoms. In the previous work, Laporte's use of $\sigma=34$ was followed. Wentzel[7] gives $\sigma=34\pm4$ and Coster,[8] 33. In the present paper, the value assigned to σ has been adjusted to make the theoretical susceptibilities agree as closely as possible with experimental data.

Temperature Variation of the Susceptibility of Sm

Table I gives the value of the effective Bohr magneton number for Sm at

Table I. *Effective Bohr magneton numbers for Sm.*

	μ_{eff} (Theory)		μ_{eff} (Experiment)			
$T°K$	$\sigma=33$	$\sigma=34$	Williams[9] (oxide)	Freed[10] (hyd. sul.)	Cabrera & Duperier[11] (oxide)	(anh. sul.)
0	0.85	0.85				
20	0.91	0.92				
74	1.06	1.09		0.91		
85	1.09	1.12		0.96		
112	1.16	1.20		1.08		
123	1.18	1.23	1.08			
170	1.29	1.35		1.26		
205	1.37	1.43		1.35		
240	1.44	1.52		1.44		
293	1.55	1.65	1.58	1.57	1.50	1.58
375	1.73	1.85	1.77		1.69	
400	1.78	1.91			1.75	
500	2.00	2.15			1.97	
543	2.09	2.25	2.14		2.06	
600	2.20	2.38			2.17	
800	2.58	2.78				
1000	2.91	3.14				

[6] See e.g. Laporte, Handbuch der Astrophysik **3,** 634 ff. esp. Eqs. (50), (56).

[7] G. Wentzel, Zeits. f. Physik **33,** 849 (1925).

[8] D. Coster, in Müller-Poulliets' Handbuch der Physik, ii, 2057.

[9] E. H. Williams, Phys. Rev. **12,** 158 (1918); **14,** 348 (1919).

[10] S. Freed, J. Amer. Chem. Soc. **52,** 2702 (1930).

[11] These results are as yet unpublished but were kindly communicated to us by Professor Cabrera. Results of previous experiments of Cabrera and Duperier may be found in Comptes Rendus **188,** 1640 (1929).

various temperatures, using for the screening constant both 33 and 34, where μ_{eff} is given by (2) and χ by (3). Assuming the Landé interval rule, this takes the following explicit form in Sm

$$\chi_{mol}=\frac{0.1241}{xT}\left[\frac{2.14x+3.67+(42.9x+0.82)e^{-7x}+(142x-0.33)e^{-16x}+\cdots}{3+4e^{-7x}+5e^{-16x}+6e^{-27x}+\cdots}\right]$$

where x is 1/55 of the ratio of the overall multiplet width (expressed in ergs) to kT. If we take $\sigma=34$, then $x=191/T$ whereas with $\sigma=33$, $x=220/T$.

Figure 3 shows directly the variation of the susceptibility with temperature.[12] All of the experimental values given have been corrected for the diamagnetism of the cation but not for that of the anion since the latter is not known. The effect would be to raise the experimental points slightly.[13]

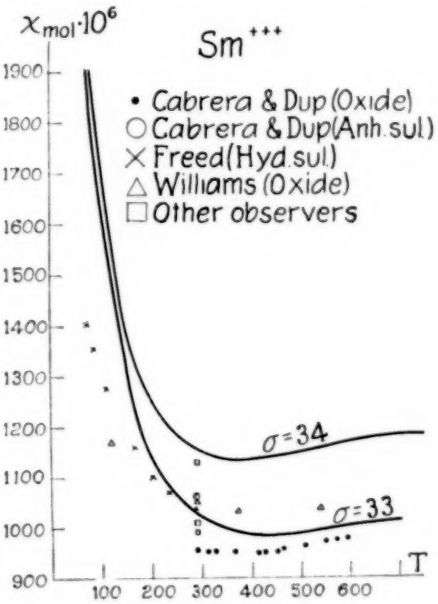

Fig. 3.

Table I and Fig. 3 show that better agreement with experiment is achieved when 33 is taken as the screening constant. Moreover, the agreement is as good as one may expect considering the differences of the experimentally determined susceptibilities among themselves and considering the fact that these determinations were made on solid compounds rather than upon the elements in the ideal gas state to which the theory applies. One may expect the oxide to deviate from theory even more than the sulphate, since

[12] W. Sucksmith recognized the importance of the second order Zeeman terms and made a qualitative comparison of the theoretical susceptibilities with Cabrera's measurements on Sm and Eu. Proc. Lond. Phys. Soc. **42**, 388 (1930).

[13] This diamagnetic correction has been estimated at about 30×10^{-6} using the method of obtaining screening constants given by L. Pauling, Proc. Roy. Soc. **114A**, 181 (1927) or J. C. Slater, Phys. Rev. **36**, 57 (1930).

the former is a firmer chemical combination. Freed's values at low temperatures show a departure from the theoretical curve, due no doubt to distortion by interatomic forces in the solid. In applying the theoretical expression for the susceptibility in gases to liquids or solids, the results are reliable only if "the work required to turn over an ion against interatomic forces is assumed small compared with kT".[14] This assumption is no longer valid at the low temperatures used by Freed.

Although at low temperatures, the susceptibility of Sm decreases quite rapidly with an increase in temperature, a minimum is soon reached and the susceptibility increases very slowly with further increase in temperature. This minimum is located at about $T_{min}=0.0628\ (Z-\sigma)^4$ which gives $T=386°K$ with $\sigma=34$ and $444°K$ with $\sigma=33$. If one could determine experimentally a more accurate value for the temperature at which this minimum occurs, the screening constant could be determined more accurately, but this would be difficult since the curve is so very flat in the region of the minimum. Such a minimum has been observed experimentally, however, by Cabrera and Duperier between about 350°K and 425°K in their recent work on Sm_2O_3. Williams also gives a lower value for the susceptibility at 375°K than at 543°K and 293°K although the difference is so small that he has interpreted his data as giving a value of the susceptibility of Sm which is independent of the temperature throughout that range.

This behavior in Sm is a decided departure from the usual Curie law in which the susceptibility continues to decrease with increasing temperature. The Curie value for the temperature coefficient ($\chi^{-1}d\chi/dT$) at room temperature is $1/293$ whereas the theoretical values are $1/2525$ for $\sigma=34$ and $1/1517$ for $\sigma=33$. The abnormally low value for the temperature coefficient is confirmed experimentally by the measurements of Williams (1/1600), Zernicke and James[15] (1/1700) and Freed (about 1/1600). Here again better agreement is obtained when the smaller value of the screening constant is used.

Comparison of theory and experiment then, indicates that the screening constant for Sm is apparently more nearly equal to 33 than to 34. Certainly values of the susceptibility using σ less than 32 or greater than 34.5 would definitely disagree with experimental results. Thus this comparison of theoretical and experimental magnetic data fixes the screening constant with less uncertainty than do the present spectroscopic estimates. Exception may be taken to this conclusion because Russell-Saunders coupling is used throughout as the basis for the g-factor and the multiplet separations, whereas it is quite probable that there is an appreciable departure from this type of coupling even for the lowest levels in elements of so high an atomic number. This objection may be partially met by considering σ as that screening constant which fixes the interval between the lowest two levels. It then becomes necessary to investigate the effect of the third level on the susceptibility. Reducing this level so that the second interval is only one half the value obtained when

[14] J. H. Van Vleck, Theory of Electric and Magnetic Susceptibilities, p. 193, or p. 254.

[15] Zernicke and James, J. Amer. Chem. Soc. **48**, 2827 (1926).

(In press.)

Russell-Saunders coupling is assumed makes no appreciable change in the susceptibility at room temperature, but the effect increases very rapidly with increasing temperature so that such a large change in this interval changes the shape of the curve. This would give a minimum at too low a temperature and then a rapid increase in χ at higher temperatures, whereas experimental results indicate a very slow increase in χ beyond the minimum. Thus the magnetic data not only fix the interval between the lowest two levels but also indicate that, when the lowest interval is thus fixed, the interval rule for Russell-Saunders coupling gives an approximately good value for the third level.

Comparison of the Above Results in Sm with Corresponding Calculations for Eu

Sm shows an unusual behavior in the variation of susceptibility with temperature because, as the temperature increases, the increasing concentration of ions in states with large J tends to compensate for the T in the denominator of the first bracket of Eq. (3). This is not true in Eu since, for the lowest state ($J=0$), the contribution of the second order terms is so great that increasing the concentration of ions in states of higher J is of less relative importance. For Eu, the temperature coefficient is nearer the Curie value, (1/293), the computed values being 1/525 and 1/542 for $\sigma=34$ and 33 respectively. Cabrera and Duperier give 1/500 for $Eu_2(SO_4)_3$ and 1/522 for Eu_2O_3.

The rest of the rare earths conform very closely to the Curie law in which the temperature coefficient is $1/T$. For example the computed value for Nd at room temperature when $\sigma=34$ is used is 1/304. Neither the second order term nor the change in screening constant to $\sigma=33$ has much effect here on the temperature coefficient. Changing the screening constant changes the temperature coefficient to 1/301 while the omission of the second order term yields 1/294. The departure of the other rare earths from the Curie law is still less.

Table II. *Effective Bohr magneton numbers for Eu.*

	μ_{eff} (Theory)		μ_{eff} (Experiment, Cabrera & Duperier[11])	
$T°K$	$\sigma=34$	$\sigma=33$	oxide	anh. sul.
0	0.00	0.00		
20	1.07	1.15		
70	2.01	2.14		
100	2.38	2.53		
200	3.09	3.20		
293	3.40	3.51	3.34	3.53
400	3.65	3.75	3.57	3.75
470	3.77	3.89	3.69	3.89
625	4.02	4.14		4.11

Table II and Fig. 4 show the effective Bohr magneton number and susceptibility of Eu as functions of temperature computed from the following expression obtained from (3).

$$\chi = \frac{0.1241}{yT}\left[\frac{24+(13.5y-1.5)e^{-y}+(67.5y-2.5)e^{-3y}+(189y-3.5)e^{-6y}+\cdots}{1+3e^{-y}+5e^{-3y}+7e^{-6y}+\cdots}\right]$$

where $y = 365/T$ with $\sigma = 34$ and $418/T$ with $\sigma = 33$.

Since we may expect the experimental data on sulphates to be more nearly in accord with the theory for gases, it is seen that probably 34 is a better estimate of the screening constant than 33. For Sm, on the other hand, values of the susceptibilities and the temperature coefficients agree better with experiment when 33 is assigned as the screening constant (although Cabrera gives as the temperature at which the minimum occurs in Sm_2O_3 a value more in agreement with that obtained with $\sigma = 34$). However, the screening constant increases with atomic number and may well be a little (perhaps 0.3)

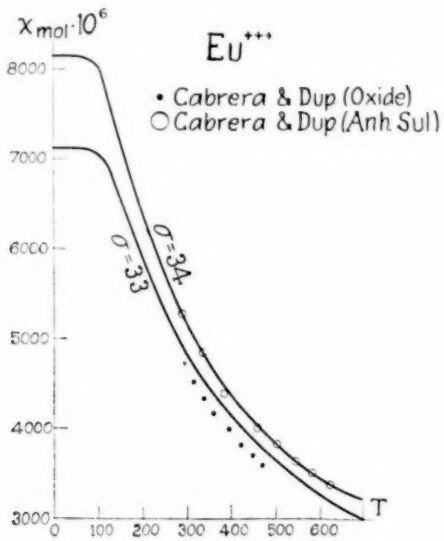

Fig. 4.

higher in Eu than in Sm. Whatever doubt there may be as to which of these two values is more nearly correct, it is quite clear that in Eu as well as in Sm, $\sigma = 32$ or $\sigma = 35$ would not fit the experimental data at all despite the fact that they come within the range 34 ± 4 allowed by the uncertainty in the estimates from x-ray data.

Temperature Variation of the Gyromagnetic Ratio in Sm and Eu

In order that a body be magnetized, angular momentum must be given to its atoms. This angular momentum Λ is supplied by the body as a whole, which consequently rotates with the angular momentum $-\Lambda$ if it was at rest before the field was applied (Einstein, Richardson, de Haas effect). The angular momentum supplied by the external field H itself is negligible as it is only a small fraction of the total angular momentum (of the order of magnitude of the diamagnetic correction to the paramagnetic susceptibility).[16] Table III

[16] J. H. Van Vleck, (reference 14) p. 255 ff.

TABLE III. *Theoretical values of the gyromagnetic ratios in Sm and Eu.*

Sm			Eu		
$T°K$	$\theta \times 2mc/e$		$T°K$	$\theta \times 2mc/e$	
	$\sigma = 34$	$\sigma = 33$		$\sigma = 34$	$\sigma = 33$
0	0.286	0.286	100	29.54	43.20
20	0.337	0.330	200	9.43	11.02
74	0.476	0.451	293	6.56	7.40
123	0.602	0.560	400	5.10	5.67
170	0.723	0.665	470	4.52	5.00
205	0.780	0.744	625	3.72	4.07
240	0.901	0.822			
293	1.026	0.937			
375	1.184	1.095			
500	1.335	1.268			
600	1.398	1.351			
800	1.448	1.430			

gives the theoretical values of the gyromagnetic ratio θ; i.e., the ratio of the magnetic moment χH to the angular momentum. This ratio can be shown to be the same as the ratio H/Ω in the converse experiment of magnetization by rotation[16] (Barnett effect) where H is the magnetic field which would produce the same magnetization as rotation of the solid with an angular velocity Ω.

The expression for the total angular momentum per cubic centimeter needed by the atoms to produce the magnetic moment is

$$\Lambda = \sum_{J\,M} \frac{Mh}{2\pi}\, e^{-W_J/kT} / \sum_{J\,M} e^{-W_J/kT}$$

where $Mh/2\pi$ is the free atom's angular momentum in the direction of the field. Here it is unnecessary to include second order terms since the angular momentum is only very slightly perturbed by the field.[17] This expression can be simplified by substituting $W_J = W_J{}^0 + Mg_J\beta H$, expanding the exponentials, and summing over M, which ranges from $-J$ to $+J$. Thus

$$\Lambda = \frac{\sum_{J\,M} \frac{Mh}{2\pi} e^{-W_J^0/kT}(1 - Mg_J\beta H + \cdots)}{\sum_{J\,M} e^{-W_J^0/kT}(1 - Mg_J\beta H + \cdots)} . \tag{5}$$

Now

$$\sum_{-J}^{+J} M = 0 \text{ and } \sum_{-J}^{+J} M^2 = \tfrac{1}{3}J(J+1)(2J+1)$$

so that, by using Eqs. (3) and (5), the complete expression for the gyromagnetic ratio becomes

$$\theta = \frac{\chi H}{\Lambda} = \frac{e \sum_J \{g_J{}^2 J(J+1) + 3kT\alpha(J)/\beta^2\}(2J+1)e^{-W_J^0/kT}}{2mc \sum_J g_J J(J+1)(2J+1)e^{-W_J^0/kT}} . \tag{6}$$

[17] The component of angular momentum in the direction of the field is a constant of the motion unperturbed by the field except for a small diamagnetic correction. See reference 16.

Eq. (6) reduces under the assumption of infinite multiplet widths to the usual expression $\theta = eg_J/2mc$ for the gyromagnetic ratio. In the case of Sm and Eu, however, θ is a function of T because we must add the contribution of atoms not in the lowest state, and because the terms involving $\alpha(J)$ are so important in their contribution to the magnetic moment. For example in Sm at room temperature, $\theta \times 2mc/e$ is 0.323 with $\sigma = 34$ and 0.305 with $\sigma = 33$ when the second order terms are neglected, while the table shows the much higher values, 1.026 and 0.937 at this temperature. These second order terms are particularly important in Eu for without them, the gyromagnetic ratio is independent of temperature, inasmuch as here g_J is independent of J. This situation arises in Eu since $S = L$ so that the g-factor reduces to $3/2$ ($J \neq 0$). Thus from (6) it is clear that $\theta = g_J e/2mc$ or $1.5\ e/2mc$ when the second order terms are omitted. When the second order terms are included, there is a decided change in θ with temperature. Unfortunately there are no precise experimental data available as yet although Sucksmith,[18] in a preliminary report on this very difficult experimental work which he is undertaking, indicates that the results at room temperatures favor the values found in the table, rather than $1.5e/2mc$. The great importance of the second order terms in Eu is particularly evident here since the gyromagnetic ratio decreases with increasing temperature, in striking contrast to the behavior in Sm. The explanation for this difference is again to be found in the fact that in Sm, increasing the temperature increases the concentration of atoms into states of higher J and higher g_J. Thus the numerator of (6) increases more rapidly than the denominator. In Eu, however, the term involving $\alpha(J)$ for the lowest state is so large that increasing the ions in states of higher J has less relative importance in the numerator than in the denominator where there are no $\alpha(J)$ terms.

The gyromagnetic ratio for the rest of the rare earths is very nearly equal to $g_{J\min} \times e/2mc$ and is almost independent of temperature. For instance, $g_{J\min}$ for Nd is 0.73. The gyromagnetic ratio ranges from $0.73e/2mc$ at 0°K to $0.79e/2mc$ at 600°K, with no appreciable difference whether σ is taken as 33 or 34. There is even less dependence on temperature for the rest of the rare earths.

Temperature Variation of the Heat Capacity in Sm and Eu

The contribution of the multiplet levels to the heat capacity of Sm and Eu, assuming the ideal gas state, is given by the expression

$$C = N \frac{d}{dT} \left(\frac{\sum_J (W_J^0 (2J+1) e^{-W_J^0/kT}}{\sum_J (2J+1) e^{-W_J^0/kT}} \right).$$

Table IV shows the variation of C with temperature for Sm and Eu, again assuming the Landé interval rule in obtaining W_J. This calculation illustrates again the difference between Sm and Eu, and the rest of the rare earth group.

[18] W. Sucksmith, Paper delivered at the British Association (1930).

TABLE IV.

T°K	Sm C (cal./mol.) $\sigma=34$	Sm C (cal./mol.) $\sigma=33$	T°K	Eu C (cal./mol.) $\sigma=34$	Eu C (cal./mol.) $\sigma=33$
0	0.00	0.00	0	0.00	0.00
170	0.06	0.03	50	0.21	0.10
205	0.17	0.08	70	0.85	0.54
240	0.31	0.18	100	1.79	1.46
293	0.57	0.38	200	2.10	1.94
400	1.04	0.83	293	2.02	2.05
500	1.34	1.16	400	2.00	2.02
600	1.52	1.38	470	1.99	2.01
800	1.73	1.64	625	1.99	2.00

In the other rare earths, all levels except the lowest are virtually unoccupied since $W_J \gg kT$. Fig. 2 shows that W_J is comparable with kT in Sm and Eu, especially for the lowest interval. Thus a change in temperature gives an appreciable change in the number of ions which occupy states other than that for which J is a minimum and hence a change in total energy. Eu shows a more rapid change in C than Sm for low temperatures, since the first interval is so much smaller that the total energy is even more sensitive to a change in temperature. Thus, whereas the values given for C in Table IV increases somewhat with temperature for Sm, for Eu it shows a much more rapid rate of increase for low temperatures, but reaches a maximum at room temperature or less.

I am very grateful to Professor J. H. Van Vleck, under whose direction these computations were made.

ON THE EVOLUTION OF A ROTATIONALLY UNSTABLE STAR

By Ross Gunn
Naval Research Laboratory

(Received November 13, 1931)

Abstract

The fission theory of binary star systems is reexamined and important objections to it are removed. The presence of a magnetic field in the atmosphere of a rotationally unstable star prevents loss of momentum through the loss of atmosphere at the star's equator. By interaction with the atmospheric electric and magnetic fields, the ions are constrained to move systematically in the direction of rotation and add angular momentum to the star proper. Eventually the star divides, and whereas the parent star was radially symmetrical the resulting components are highly asymmetrical and one-half of the star is at a much higher mean temperature than the other half. Tidal couples orient the components just after fission so that the newly exposed faces are oriented inward but are displaced through a small angle. The comparatively high temperatures of the hot faces cause the star to lose mass asymmetrically by radiation or by loss of atmosphere. The lost mass carries off momentum and the reacting forces add both angular momentum and kinetic energy to the massive components; the mechanism being analogous to that of a skyrocket or a pin wheel. When the excess mass lost from the hot face of the components amounts to roughly one five thousandth of the total mass, the added kinetic energy is sufficient to account for the evolution of any type of binary system and for the remarkable differences noted by Sears in his study of the kinetic energies of various types of stars. The relation of such a mechanism to Novae and Cepheid variables is considered. The introduction of reacting forces due to the asymmetrical loss of momentum removes the serious objections that heretofore faces the fission theory and it now seems probable that almost all stars have become rotationally unstable and divided sometime during their life. The magnitude of the radiation reaction forces makes it seem probable that many companion stars have been separated to infinity and that our sun is one star of such a pair. This conclusion has led to a new and more satisfactory theory of the origin of the solar system.

OBSERVATIONAL astronomy shows that at least one star out of four has associated with it a companion star of comparable mass. The chance of capture of one star by another seems far too small to account for the prevalence of star pairs and it seems necessary to assume that the pairs occur either as a result of condensation on two independent nuclei or that they originate by fission. The fission theory, developed by Poincaré, Darwin, Russell and others, suggests that a star becomes unstable as a result of rapid axial rotation and eventually breaks up into two components of nearly equal mass. The theory together with tidal evolution accounts fairly well in its present form for the occurrence and evolution of close binary systems but seems entirely inadequate to account for the visual pairs. While the detailed calculations of the stability of a rapidly rotating liquid star by Darwin yield considerable information regarding the mass ratios of the components, the figures of equilibrium, etc., they fail to describe the process of fission because

during this most interesting interval the equilibrium is essentially unstable and events proceed cataclysmally. The qualitative picture presented by the fission theory seems, however, essentially correct.[1] In the present paper we draw attention to certain additional physical processes which take place immediately after fission and show that the presence of these processes will enable us to account for the observed properties of all types of binary star systems.

The fission theory requires that a parent star shall rotate so rapidly on its axis that it becomes unstable. It was originally thought that this rapid rotation resulted from the original angular momentum of the parent nebula and that condensation of a star was sufficient to account for its presence. Moulton[2] has objected to this interpretation and shown that such a hypothesis leads to an improbably large ratio for the initial and final densities. His contention is further supported by Jeans[3] who has shown that a rotating and evolving star radiates angular momentum as well as mass. In a recent paper[4] we showed that the contraction hypothesis was not a necessary one and that sufficient angular momentum could be added to a star in the course of stellar time by purely electromagnetic means to make the star rotationally unstable. Another objection closely related to the foregoing has been raised by Chamberlin[5] who suggested that a rapidly spinning star will lose its atmosphere at the equator and that the lost particles will carry off angular momentum in such a manner as to stabilize it. This objection need no longer be considered, for these stars are observed not to lose their atmospheres[1] and we have shown that their retention is due to the presence of the star's magnetic field.[4]

A very serious limitation of the fission theory was discussed by Jeans[3] who showed that unless the mass ratio of the two components was less than three-tenths, the angular momentum of the critical Jacobian ellipsoidal configuration of the parent star was insufficient to separate the two resulting components to regions where they could be in stable equilibrium. That is to say, if the mass ratio of the two components is near unity (as is indicated by both observation and Darwin's calculations) each component will be inside the Roche limit of the other and hence it will disintegrate as a result of tidal and centrifugal forces. Such disintegration is not observed, and we are required to believe either that binary star systems are born with a low mass ratio and by unequal radiation of mass evolve into pairs of nearly equal mass, or that the fission theory is incomplete. Many actual cases are known, however, in which the mass ratios do approach unity, yet those systems must be so youthful that loss of mass by radiation could not be important. For this class of star pairs as well as for visual binaries the fission theory, in its present form at least, is inadequate.

Jeans[3] has already worked out the effect of radiation of mass on the orbits of the components and shown that a spectroscopic binary cannot well evolve

[1] H. N. Russell, Astrophys. J. **31,** 185 (1910).
[2] F. R. Moulton, Tidal and Other Problems, Carnegie Inst. Publication **107,** 79 (1909).
[3] Jeans, Astronomy and Cosmogony, Cambridge Press (1928).
[4] R. Gunn, Phys. Rev. **37,** 1129 (1931); **37,** 1573 (1931); **38,** 1052 (1931).
[5] Chamberlin, Carnegie Inst. Pub. **107,** 169 (1909).

into a visual pair by this simple means. Jeans' treatment has been criticised by Brown[6] who gave a substitute derivation yielding a different answer. Jeans[7] defended his treatment, and his result is in agreement with that obtained by the present author who employed the principle of adiabatic invariance in a modified form. The principle of adiabatic invariance, one of the fundamental principles of modern physics, seems well founded on observation and was developed to handle just the type of problem presented by the changing orbit of two stars which constantly radiate mass. The principle states that the mean value of the action integrated over a complete period is invariant. This form of the principle is incorrect if the mass varies, and in the degenerate case it is easy to see that the kinetic energy of a particle moving in a straight line and whose mass is changing cannot be conserved unless external forces act. A form of the principle, broader in application than the usual one and directly applicable to our problem, is

$$\int_0^T \frac{E_{\text{kin}}}{M}\, dt = \text{constant} \tag{1}$$

where E_{kin} is the kinetic energy of the system and M the mass function; and the integration is carried out over a complete period T. It does not appear necessary to carry out the complete calculation of our problem here for it leads directly to Jeans' result. The eccentricity of the orbits are unchanged as the masses dissolve into radiation, the major axis increases, varying as $(M+M)^{-1}$ and the period of the orbit increases, varying as $(M+M)^{-2}$. Thus, radiation of mass cannot help account for the observed differences in the orbits of binary stars and we must continue our search for other important mechanisms.

In case a star is gaseous instead of liquid it might appear that its expansion during the process of division would add considerable mechanical energy to the component stars and perhaps permit the stars to recede to positions of stability outside the Roche limit. By Poincaré's theorem the change in the internal thermal energies can be estimated, and it turns out that the energy converted is but a fraction of the original kinetic energy and is thus inadequate to account for the major observed discrepancies.

In light of the foregoing theoretical difficulties and available observational data it seems necessary either to abandon the fission theory entirely or to complete it by adding a physical mechanism capable of adding enough momentum and energy to the star to account for the observed mass ratio and orbits. In the following paragraphs a new mechanism is considered which seems quite adequate and is perhaps not unreasonable.

Relation of Rotational Evolution to a Star's Magnetic Field

We have seen in a series of earlier papers that most dwarf stars probably possess magnetic and electric fields and that these fields accounted well for many puzzling characteristics and properties of stellar atmospheres. It has

[6] E. W. Brown, Proc. Nat. Acad. **11**, 274 (1925).

[7] J. Jeans, Monthly Notices **85**, 904 (1924).

been shown that these fields impose systematic high velocity electromagnetic winds on the ions making up the stars atmosphere and that these winds transfer angular momentum to the star proper.[4] The calculations indicate that in the course of stellar time the angular momentum so communicated is ample to make the star rotationally unstable and it can break up. However, if the star could lose its atmosphere at the equator in the manner contemplated by Laplace in his nebular hypotheses, momentum would be lost at the equator as fast as it could be supplied, and the star could never quite accumulate angular momentum enough actually to divide. In a magnetized star this loss at the equator is never important because the magnetic field entraps the atmospheric ions[4] and to all intents and purposes the star behaves much as if it were liquid. Darwin's calculations therefore apply, in a degree at least, to a wholly gaseous star, but only if that star possesses a magnetic field. Thus a star's magnetic field is of paramount importance in bringing that star into such a condition that it can divide and form two companion stars. Because there is no clear-cut evidence that the interior of a star is other than effectively liquid, in the following we continue this usual assumption.

Tidal Effects

With the exception, perhaps, of tidal disintegration inside the Roche limit, the most important effect of tides on a rotating and evolving body is their ability to develop a torque about the axis of spin. These tidal couples play a major role in the transfer of angular momentum of axial rotation to that of orbital revolution in a recently divided star.

The magnitude of the angular acceleration due to tidal couples is readily evaluated if the two bodies are not too close. For example, Jeffries[8] shows that a uniform spinning sphere of density ρ_e, radius a and mass m changes its angular velocity Ω at a rate given by

$$-\frac{d\Omega}{dt} = \frac{18\pi\gamma\rho_e}{5}\left(\frac{M}{m}\right)^2\left(\frac{a}{R}\right)^6 \sin 2\delta \qquad (2)$$

where M is the mass of the tide generating body, R the separation of the two bodies, γ the gravitational constant and δ the angle of phase lag due to tides. Strictly the expression applies only to well separated bodies but calculations show that it applies roughly, even when the bodies are close, if the coefficient is modified somewhat and if $1/R^6$ is replaced by $R^2/(R^2-a^2)^4$. Thus when R becomes comparable to a the tides and tidal couples become tremendous. Unfortunately the angle δ cannot be estimated precisely by known methods; but it evidently increases in an unknown manner with increasing ratio of the relaxation time of the body to the tidal period. It is readily shown that the relaxation time is given very approximately by

$$\tau = \left(\frac{3\pi}{2\gamma\rho_e}\right)^{1/2} = 0.325\tau_e \qquad (3)$$

[8] Harold Jeffreys. The Earth, Cambridge Press.

and is thus comparable to τ_c the period of rotation of the body when it is ready to break up rotationally. In the case of the earth $\tau = 3000$ seconds and is small compared to the period of the earth's rotation. Thus in agreement with observation, the angle δ due to body deformation by the moon is very small. If, however, the period of rotation of the body should approach its critically unstable period the angle δ becomes quite large and tidal couples become large.

Two component stars immediately after fission are oriented in the manner shown in Fig. 1 and because they are each inside the other's Roche limit the tidal forces are tremendous. Precise calculations of the tidal couples are difficult, but the periods of rotation of the two component stars are initially close to their unstable value so that δ will be moderately large and rough

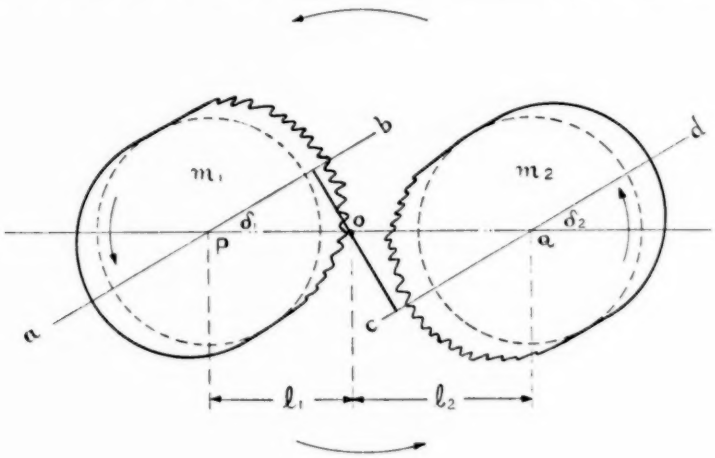

Fig. 1.

calculations show that *if the angle δ amounts to as much as a few degrees, the tidal couples are sufficient to cause the two components to separate to the Roche limit at least; with their internal faces always oriented nearly as shown.* Thus if the two components are of comparable size the process of fission is essentially a stabilizing mechanism. Tidal couples convert the axial rotation almost completely into orbital revolution and therefore there is no immediate tendency for the components to break up again. Electromagnetic mechanisms are probably operative in the components and these add angular momentum until, if the star is energetic enough, it breaks up again some 10^{12} years later. While the axial momentum is being transferred to momentum of revolution the value of δ is necessarily positive but after the transfer is complete it may change sign and even become periodic; however, by this time the initial evolution will be complete and we are no longer concerned with the mechanism.

Reaction Effects Due to Temperature Asymmetry

According to Darwin's calculations a rotationally unstable liquid star breaks up into two sections of substantially equal mass. The parent star is radially symmetrical but the components must necessarily be unsymmetri-

cal, for the hemisphere of each component, born from deep inside the parent star will be at a far higher mean temperature than the hemisphere born from the surface layers. The asymmetry is especially pronounced at the surface for one face of a component star is hardly disturbed by the cataclysm while the other, orginally deep in the interior of the parent star, suddenly becomes the surface. That the initial surface temperature of the inner face must be very high follows at once from the fact that the act of fission is cataclysmic. Thus the change is adiabatic and it seems legitimate to assume in our calculations that the initial temperatures of the inner faces are at an appreciable fraction of the original central temperature of the parent star. Obviously these surface temperatures are not maintained for long because radiation carries off the energy very rapidly as soon as the hot face is exposed to free space. On the other hand, a comparatively small fractional drop in the surface temperature of a hot face will set up large internal temperature gradients and energy will be rapidly transmitted to the surface either by radiation or by conduction. If the temperatures are unexpectedly high the process could, perhaps, be more accurately described by saying that the exposure of the hot face will give rise to a "radiation explosion" which is dynamically equivalent to the comparatively slow processes we use in the following calculations.

The asymmetrical loss of matter by radiation or by gaseous ions produces a reacting force on the star proper, and the reacting momentum is precisely equal and opposite to that carried away by radiation or by the lost atmosphere. Thus a recently divided component star with one face much hotter than the other behaves in a manner analogous to a skyrocket, and if there are two stars rotating about their center of mass and if the angle δ (see Fig. 1) is different from zero, the pair behaves like a pinwheel. When the hot face is at a sufficiently high temperature the mechanism has a profound and immediate effect on the orbit of the pair and may even operate to separate them to infinity. If the thermal asymmetry is not particularly pronounced the phenomena, of course, proceed at a slower rate but in the course of stellar time the asymmetrical loss of mass may greatly modify the original orbit.

A dividing star may lose momentum asymmetrically by the loss of its atmosphere. This loss will take place instantly when the thermal energy of the particles approaches that of the negative gravitational energy of the particle. The critical temperature corresponding to this condition is given by

$$T_c = \frac{2\gamma M m_1}{3kR} \tag{4}$$

where γ is the gravitational constant, M the mass of the star, R its radius, k the Boltzmann constant and m_1 the mass of the atmospheric particle. We have seen in an earlier paper that a star ordinarily does not lose its atmosphere because the star's magnetic field entraps the ions. Whether this mechanism is still operative in a star that has just divided cannot be stated, for one can only guess what actually happens to the magnetic field of a star on division. Experiments on superconductivity suggest that the magnetic field

may be maintained while other evidence[9] indicates that the magnetic field may be greatly reduced. Because of the high energies of the ions their curvature by a magnetic field is less than that at the surface of an ordinary star and it seems quite reasonable to expect a slight loss of atmosphere to result even if the star is magnetized. In Fig. 1 we assume that the lost ions on the average leave the stars in the direction Qc and Pb which are axes of thermal symmetry. If ΔM_i is the total loss of ponderable mass, u the mean thermal velocity of escape, ΔV the change in velocity of the star proper and M the mass of the star, we will have by aid of the principle of the conservation of momentum that

$$-\frac{\Delta M_i}{M} = \frac{\Delta V}{fu} \tag{5}$$

where u may be calculated from the mean value of

$$u = (3kT/m_1)^{1/2} \tag{6}$$

and f is a numerical factor somewhat less than unity whose value depends on the mean direction of emission of the mass elements with respect to the axis of thermal symmetry.

Radiation Reaction Forces and Couples

Perhaps the most important effects arise from the asymmetrical loss of mass by radiation. A star will lose radiation as long as it is a star irrespective of any local condition, such as a magnetic field, and a deep seated thermal asymmetry guarantees that the loss of mass by radiation will be asymmetrical whether the process is rapid or slow.

Momentum considerations lead immediately to

$$-\frac{\Delta M_r}{M} = \frac{\Delta V}{fc} \tag{7}$$

where c is the velocity of light. The relation is perhaps more useful in its differential form

$$\frac{dM}{dt} = \frac{-Ma}{fc} \tag{8}$$

where a is the reaction acceleration of the mass M. Now the rate at which the energy E is radiated is

$$\frac{dE}{dt} = c^2\frac{dM}{dt} = \sigma A T^4 \tag{9}$$

so that Eq. (8) can be written

$$Ma = \frac{fA\sigma T^4}{c} = F \tag{10}$$

where F is the reacting force on the star, A the effective radiating area, σ the constant in Stefan's law, and T the effective surface temperature.

[9] R. Gunn, Phys. Rev. **34**, 335, 1621 (1929).

In the case of a star pair we may write down entirely simi'ar expressions for the angu'ar momentum $\boldsymbol{M}$ and torque $\boldsymbol{T}$. If the two stars of the pair are separated by a distance l_1+l_2 and the distance from the center of gravity of each star to the center of the gravity of the system is l_1 and l_2 respectively, (see Fig. 1) we have that

$$\frac{d\boldsymbol{M}}{dt} = \boldsymbol{T} = \frac{\sigma}{c}[f_1 A_1 T_1^4 l_1 \sin \delta_1 + f_2 A_2 T_2^4 l_2 \sin \delta_2] \tag{11}$$

and the final total angular momentum of the system is

$$\boldsymbol{M} = \boldsymbol{M}_0 + \int_0^\infty \frac{d\boldsymbol{M}}{dt}\, dt \tag{12}$$

where $\boldsymbol{M}_o$ is the initial angular momentum. This quantity can be evaluated precisely when l, T and δ are specified as functions of the time. We can make estimates of the magnitudes of the forces and torques acting with sufficient precision to test the ideas here proposed if we assume that the quantities are constant over a relatively short period of time.

Very little really satisfactory information is available regarding the internal temperatures of stars and the estimates of the central temperature vary from 10^{11} degrees down to 4×10^7 degrees. The freshly exposed surface that has just emerged from the depths of the parent star may reasonably be assumed to be at a temperature of 4×10^7 degrees; it could well be much higher or even lower. We assume further that the component stars in size, mass and structure are not unlike the sun. The radiation from the cool side may be neglected in comparison to the hot face and we calculate the acceleration of the star by aid of Eq. (10) taking $T=4\times10^7$ degrees, $\sigma=5.71\times10^{-5}$, $A=1.5\times10^{22} cm^2$, $f=0.63$ and $M=2\times10^{33}$. We find that the acceleration of the component star amounts to 232 cm/sec.^{2} and represents an unbalanced acceleration since the original centrifugal and gravitational forces are precisely balanced. Even if the star were initially at rest such an acceleration would displace it a distance of 9×10^{11} cm or more than 10 solar radii in the course of a single day. The increase in angular momentum will also necessarily be large and the net result of the asymmetrical radiation process will be a cataclysmal increase in the kinetic energy of the system and its angular momentum.

Even if our estimate o' the surface temperatures has been much too high the mechanism is still effective and the evolution instead of being cataclysmic for the most part will be slow and persist throughout the life of the star. A star radiates an appreciable fraction of its mass in some 10^{12} years and it is clear that an initial deep seated thermal asymmetry of the star will guarantee that a small excess fraction of the total radiated mass will eventually be radiated from the hot side, even if the temperature differences between the hot and warm faces are relatively small. The internal temperatures are eventually equalized by radiation and conduction but this process will require some 10^8 years for the asymmetry to be reduced by half and at the same time the surface constantly cools off by radiation. For these reasons and evidence that

the interior of a star is effectively liquid we believe that the evolution of a binary pair is largely cataclymic, but this is not a necessary conclusion. It is interesting to contemplate what would happen to a Milne model star if it broke up. The internal temperatures of this model approach 10^{11} degrees and most of the internal mass is in the form of radiation. If one side of such a star was exposed to free space for a short time only, an appreciable fraction of the total mass of the star would certainly be lost and the reacting star, by Eq. (10), would shortly be shooting off through space at a velocity comparable to that of light! This, of course, is not observed and we must conclude that these stars do not break up by fission, do not have such excessively high temperatures or that the radiation from the surface so cools it that the radiation is almost immediately reduced to small values. Our calculations indicate that the asymmetrical loss of mass in a typical star seldom exceeds 1/10 percent of the total mass so that it is clear that powerful equilizing mechanisms are brought into play immediately after the star parts. If for some special reason a star breaks up so that the axis of symmetry of the reacting forces does not pass through the center of mass of the star the mechanism may produce axial rotation and destroy the organized kinetic energy and momentum imparted to the system. We neglect this relatively improbable type of asymmetry in the present discussion.

Stellar Equipartition of Energy

In a classical paper, Sears[10] has compiled statistical data on the masses and mean velocities of various classes of stars. His study shows that the mean kinetic energy for most types of stars is surprisingly close to a constant. However, the B type stars, many of which abundant evidence show to be well on the way to rotational instability, are notably deficient in energy of motion and on the average have only one-half the mean kinetic energy of other type stars.

The considerations of the foregoing paragraphs suggest that the type B stars are actually deficient, but the process of breakup releases energy by means of the reaction forces that we have considered and the mean kinetic energy of the resulting pair (which presumably evolves with great rapidity into a star of a later class) is actually greater than the original configuration.

The kinetic energy W added to a star by radiation reaction forces by aid of Eq. (7) is

$$W = \Delta M_r \left[fcV_0 + \frac{f^2c^2}{2} \frac{\Delta M_r}{M} \right] \tag{13}$$

where V_0 is the initial velocity of the star. By using Sear's numerical data it is found that the required kinetic energy will be added to a typical star if the star loses one five thousandth (0.02 percent) of its mass by radiation from one face. This amount of energy is evidently ample to change a close binary system to an open visual system or if the initial velocity has a moderate value, the parabolic velocity is exceeded and the component stars are separated to infinity.

[10] Sears, Astrophys. J. **55**, 165 (1922).

Our interpretation of Sear's statistical data suggests that the *O* and *B* type stars are the youthful members of our Universe and that the evolution toward the cooler types proceeds along both the main series and the giant branch. The matter deserves a closer inspection than can be given at the present time.

Orbital Development

It should be evident from the foregoing calculations that the radiation reaction forces must play an important part in the evolution of the orbits of a binary pair that originated by fission. In the absence of the foregoing mechanisms a star on division would form simply a very close spectroscopic binary of very low eccentricity, and if the mass ratios approached unity they probably would disintegrate.

The fundamental equation describing the relative orbit of a binary system is

$$1 - \epsilon^2 = \frac{-2Eh^2}{\gamma^2(M + m)Mm} \tag{14}$$

where ϵ is the eccentricity of the relative orbit, M and m the masses of the two components, h the areal velocity, and E the energy of the system defined by

$$E = \frac{-\gamma Mm}{2a_1} \tag{15}$$

in which a_1 is the semi-major axis. Logarithmic differentiation of Eq. (14) yields

$$\frac{1}{1 - \epsilon^2}\frac{d(1 - \epsilon^2)}{dt} = \frac{2}{h}\frac{dh}{dt} + \frac{1}{E}\frac{dE}{dt}. \tag{16}$$

The radiation reaction forces necessarily add kinetic energy to the system and thus by Eq. (16), the eccentricity of the orbit increases. An increase in the areal velocity h, on the other hand, which corresponds to the normal tidal angle δ, decreases the eccentricity. Thus, it appears that almost any shape or size of orbit can result from this process, for the relative values of the angular momentum and energy added by the mechanism will evidently depend on the magnitude of the angle δ and on the relation of the instantaneous surface temperatures to the instantaneous positions of the component stars. Evidently either close or visual pairs can result from one and the same mechanism. Moreover, if the surface temperatures actually approach the values assumed it seems not only possible, but quite probable, that certain pairs born of an energetic parent will be completely separated and spend the remainder of their life as isolated stars.

Curtailed Evolution and Cepheid Variables

In the foregoing we have assumed that the radiation or the atmosphere thrown off by the star receded to infinity. It seems probable that certain stars will break up and have such a surface temperature that an atmospheric atom

will have sufficient energy to get well away from the parent star but not enough to remove it to infinity, and the atom will describe gravitational orbits about the pair of stars. Thus under some conditions we might expect a recently formed pair to be surrounded by a close fitting veil or high density nebula. The presence of the veil which may be thought of as completely surrounding the binary pair, acts in a degree at least, as an absorber and reradiator of the radiant energy inside. Thus radiant energy from the hot surface no longer completely lost but a certain large fraction of it is returned and the radiation reaction forces are curtailed. Such a system will evolve into a true binary very slowly, the two components gradually separating while the pair rotates hot face to hot face with an outside protecting veil.

Such a rotating close pair may be thought of as a Cepheid Variable according to Jeans[3] who has shown that such systems fit in well with the mechanical properties of Cepheids. Jeans has apparently failed to note, however, that a surrounding radiating veil, light pressure and gravitational forces will account for the shape and phase relations of the luminosity-velocity curve, and will also account for the hitherto puzzling fact that the velocities of recession and approach are different for different elements. Reflection will show that the close binary pair at the center and the gravitational rotation of the veil will give rise to a rotation and a superposed radial pulsation having a period of one-half that of the close pair. An atom in the veil, if it were at rest, would be exposed to the hot faces of the pair twice a revolution and at such times would be blown outward by radiation pressure, the maximum outward velocity corresponding closely (but slightly later) to the maximum density of radiation. On the removal of the high temperature radiation the particles fall inward under gravity. The return of the particles under gravitational forces can be thought of as a relatively slower process than the outward blast due to radiation pressure. Since the outward motion is dependent on radiation pressure the velocity of different elements would be expected to differ. Qualitatively this type of star is almost equivalent to Shapley's pulsating model except that a definite mechanism is provided to account for the regular variation of the radiated energy.

Novae

The division of an energetic star exposes high temperature surfaces with a consequent loss of radiation and momentum. Such a cataclysm will certainly produce observable effects of the type we usually associate with Novae. Several Novae have increased in intensity 40,000 times, indicating that their surface temperatures must have increased tremendously, for, be it remembered, all radiation shorter than about 2900A is absorbed by our atmosphere and the maximum radiation for even 50,000 degrees falls in the extreme ultraviolet at 580A. Thus an observed increase in radiation by a factor of 40,000 certainly corresponds to a much larger true increase in radiation.

In spite of the comparatively small amount of light received from a Novae by an observer at the bottom of the atmosphere, the star might conceivably deliver sufficient radiation to the high atmosphere in the extreme ultraviolet

and soft x-ray region to ionize highly the earth's high atmosphere. The possibility that such a mechanism might produce effects on radio transmission or cause a magnetic storm has been examined by determining the correlation between magnetic storms of relatively long duration and the appearance of Novae. The correlation is no better (nor worse) than the agreement of magnetic storms with other supposedly related physical quantities and no definite conclusion can be drawn from available data.

Remarks

The addition of a mechanism which is capable of adding angular momentum and kinetic energy to a newly born binary components removes several of the most fundamental objections to the fission theory. The reaction forces readily account for the observed differences in the orbits of binary stars, wide pairs with moderate eccentricities being as readily produced as close pairs with zero eccentricity. Moreover, the restriction as to mass ratio is now removed, and Darwin's calculations for liquid stars apply, in a degree at least to actual stars which are probably largely gaseous. The requirement of an initial surface temperature approximating 10^7 degrees is by no means necessary for lower temperatures result only in a slowing up of the evolutionary process. A systematic asymmetric loss of mass amounting only to a few hundredths of a percent of the total mass is all that is required to account for the evolution of any type of binary system and such a loss not only seems possible but quite probable.

No attempt has been made to follow the variation of the orbit in great detail because the evolution depends, in an important manner, on the tidal angle δ and the manner in which this quantity changes with the separation of the components cannot now be calculated.

Close examination may show that radiation reaction forces are important in the evolution of spiral nebula, particularly if the arms of these systems are formed by any sort of a fission process.

Perhaps the most important result of our calculations, however, is the probability that certain very energetic parent stars will endow their offspring with sufficient energy by the process described to separate completely the two companions. Thus our own sun may well have had a companion star which was lost sometime immediately after the parent sun divided. This conclusion has a very important bearing on the origin of the solar system, for it has led to a consistent fission theory of the origin of the solar system. This matter will form the subject of a subsequent paper.

THE BANDS OF CH AND CN IN STELLAR SPECTRA

By P. Swings[1] and O. Struve
Yerkes Observatory, University of Chicago

(Received October 26, 1931)

Abstract

The upper limit of visibility in the spectral sequence of the CH band at λ4300 is found to be F8 (temperature about 6500°K). This value is considerably lower than has been adopted heretofore (classes F2 to A0; temperatures 7900° to 13000°K). The region occupied by the CH band is very rich in strong atomic lines and it is therefore not permissible to consider the general aspect of the Fraunhofer "G-band": the total intensity of the atomic lines greatly exceeds that of the molecular lines. The limit of visibility of the CN band at λ4200 is found to be at F8, in agreement with former estimates. The simultaneous disappearance of CH and CN, having heats of dissociation of 110 and 210 k cal/mol respectively, may be explained by the great abundance of H in stellar atmospheres.

1. CONSIDERABLE progress has been made, in recent years, in the application of the theory of ionization equilibria to the problem of line-intensities in various types of stellar spectra. Most of the work done thus far has dealt with lines of atomic origin. There exists, however, a similar problem in the case of molecular spectra. In principle, the changes in intensity of a molecular absorption band could be investigated by using the same general method that has proved to be of such value in the interpretation of atomic spectra. But in actual practice the molecular problem is far more complicated than that of the atomic lines: not only is it necessary to introduce into the equations the partial pressures of the various constituents, but, in addition to this, the constituent atoms may give rise to several different molecular combinations. Furthermore, since the energy of a molecule is the sum of three terms, *viz.*, its electronic energy, the vibrational energy of the nuclei and the energy of rotation of the whole system, the number of energy levels of a molecule greatly exceeds that of an atom.

Several investigators have discussed the intensity of the bands of CH and CN as function of spectral class. The band λ4315 of CH is observed in both branches of the spectral sequence: G–M and G–N. According to Rufus,[2] it reaches maximum intensity at R0 and at K0, respectively. Shane[3] placed the maximum of sequence G–N in class R3. Beginning at N3 and at Mb the band is very faint. For the bands of cyanogen Lindblad[4] found a maximum between G5 and K5, and Shane found another maximum near R5 in the secondary sequence G–N.

[1] Advanced Fellow of the C. R. B. Educational Foundation.
[2] W. C. Rufus, Publications of the Observatory, University of Michigan, **3**, 258 (1923).
[3] C. D. Shane, Lick Observatory Bulletins **10**, 79 (1919).
[4] B. Lindblad, Astrophys. J. **55**, 85 (1922).

With respect to the upper limits of temperature (or spectral class) at which the bands of CH and CN are at the limit of visibility, various estimates have been made, some of which are contradictory. In the case of CN the upper limit is usually[5] placed between F5 and G0; however, several investigators[6] believed that the band could be traced as far as A0. It seems certain that in stars of early spectral class the band near λ4200 is of instrumental origin, being caused by absorption in the glass of the optical train.[7] For the CH band a number of contradictory estimates have been made: some investigators[8] place the upper limit at A0; others[9] place it at F2.

It is generally believed[10] that the CH band persists at considerably higher temperatures than the CN band. If this were correct it would lead to difficulties, since the heat of dissociation of CH is appreciably less than that of CN.

We have undertaken a careful redetermination of the limiting temperatures and have found that the values heretofore adopted for CH are in error, the actual limit for both, CH and CN, being at F8. We have further investigated the equilibrium conditions for the molecules of CH and CN with their constituent atoms, and have attempted to explain why the two bands disappear in the same spectral class, notwithstanding the difference between their heats of dissociation.

2. The heat of dissociation of the CH molecule has not been determined spectroscopically, since no formula for the band- heads is available. We shall therefore use values determined chemically. According to Fajans,[11] the work required for separating the components of a CH molecule is in the neighborhood of 90 k cal/mol. More recent determinations give slightly higher values: Mecke[12] found for the C − H bond the following energies: 107 k cal in formaldehyde, 93 k cal in acetaldehyde, 110 k cal in benzaldehyde, 115 k cal in methane. Ellis[13] found 97 k cal/mol in hexane, and various values up to 117 k cal for other molecules. We shall adopt here as approximate energy of dissociation of CH, 110 k cal/mol.

The heat of dissociation of CN has been determined spectroscopically at 220 k cal—in good agreement with the thermo-chemical methods, which give 210 k cal. We shall use this latter value in our computations.

[5] B. Lindblad, reference 4; R. Wildt, Zeits. f. Physik **54,** 856 (1929).

[6] H. Shapley, Harvard Observatory Bulletin No. 805, 1924; A. V. Douglas, Monthly Notices of the Royal Astronomical Society **90,** 798 (1930); C. H. Payne, Stellar Atmospheres p. 168, 1925.

[7] H. Shapley, Harvard Observatory Bulletin, No. 862, 1928; C. T. Elvey and R. Zug, Astrophys. J. **70,** 243 (1929).

[8] S. Rosseland, Astrophysik p. 181, 1931; C. H. Payne, Stellar Atmospheres pp. 63, 168, 1925.

[9] W. C. Rufus, reference 2; A. J. Cannon, Harvard Annals **91,** 7 (1918); R. Wildt, reference 5.

[10] S. Rosseland, reference 8; R. Wildt, reference 5.

[11] K. Fajans, Ber. d. Deutsch. Chem. Gesell. **53,** 643 (1920).

[12] R. Mecke, Nature **125,** 526 (1930).

[13] J. W. Ellis, Phys. Rev. **33,** 27 (1929).

3. The molecule CH gives rise, in stellar spectra, to two bands situated roughly at λ4300 and λ3900A. The first of these is superposed over a region containing many strong atomic lines, and the blend of all these lines, atomic and molecular, constitutes the "G-band" of Fraunhofer, prominently seen in the spectrum of the Sun. We have investigated this band in stars of classes F and G. It results from the transition $^2\Delta - {}^2\Pi$; the lower level $^2\Delta$ of the band at λ4300 is probably the ground-level of the CH molecule.

The identification of the stellar band with CH was made by Newall, Baxandall and Butler.[14] It extends from about λ4250 to λ4320[15]—a region which is especially rich in strong atomic lines [Various strong lines of Fe, Ti, Ca, Cr, Mn, Sc II etc.]. These atomic lines, superposed over the rotational lines of the CH band, produce numerous blends distributed over the whole region.

Table I gives the number of lines of various Rowland intensities (greater than 2) in the region λ4250 to λ4320.[15] It is obvious that in the solar spectrum (class G0, dwarf) the contribution of the CH lines to Fraunhofer's "G-band" is much inferior to that of the atomic lines. Consequently, on plates taken with small dispersion, and especially with objective-prisms, the blended appearance of the region near λ4300 is almost entirely due to atomic lines.

TABLE I

Rowland intensity	15	8	7	6	5	4	3	2	3-blends	2-blends
No. of atomic lines	1	3	1	2	3	8	18	48	—	—
No. of CH lines	—	—	—	—	—	1	3	16	3	12

The observable bands of CN lie in two different spectral regions: those corresponding to the electronic transition $^2\Sigma - {}^2\Sigma$ fall between λ3590 and λ4606; the others, corresponding to the transition $^2\Sigma - {}^2\Pi$, are in the red,[16] near λ7000. The lower level of the two transitions ($^2\Sigma$) is the same for both band-systems. Little is known at present concerning the bands in the red. Those of shorter wave-length are listed in Table II. In stellar spectra these bands have been

TABLE II

n'' / n'	0	1	2	3	4	5	6	7
0	3883	4216	4606					
1	3590		4197	4578				
2				4181	4553			
3						4532		
4							4515	
5								4503

[14] H. F. Newall, F. E. Baxandall and C. P. Butler, Monthly Notices of the Royal Astronomical Society **76**, 640 (1916).

[15] C. E. St. John, C. E. Moore, L. M. Ware, E. F. Adams, H. D. Babcock, Revision of Rowland's Preliminary Table of Solar Wave-Lengths, 96, 1928.

[16] P. W. Merrill, Scientific Papers of the Bureau of Standards, No. 318, 1918.

observed by Shane,[17] Hale, Ellermann and Parkhurst,[18] and by Rufus.[19] The bands most convenient for study with the Bruce spectrograph (used with the 40-inch refractor of the Yerkes Observatory) are the ones near λ4216 (0−1), and λ4197 (1−2). There are, as in the case of CH, numerous blends with atomic lines, and the contribution of the CN lines is relatively insignificant, as Table III shows.

TABLE III. *Region λ4190 to λ4210.*

Rowland intensity	8	6	5	4	3	2	1	0
No. of atomic lines	1	1	2	5	8	7	17	17
No. of CN lines (certain)	—	—	—	—	—	1	1	2
No. of CN lines (uncertain)	—	—	—	—	—	1	1	5

4. In view of the great predominance of atomic lines in both regions, it is useless to investigate the appearance of the whole band on plates of small dispersion. The obvious method is to find, within the region considered, one or more individual lines of CH which are unblended with atomic lines. The linear dispersion of our spectrograph is 30A/mm at λ4500.

For the CH band we examined the wave-lengths λ4310.4 to λ4312.7. Here the rotational lines of the band appear almost pure, as we see in Table IV (in which the lines fainter than Rowland's int. 0 have been omitted). We have

TABLE IV.

CH Lines	Int.	Atomic lines		Int.
4310.38	2	4310.47	?	1
10.56	0	10.71	?	2N
10.99	1	10.90	?	1
11.17	2	11.51	Fe CH	2
11.45	2	12.20	?	2
11.72	2	12.56	Mn	1 N
12.09	2			
12.15	1			
12.71	0			

also used the line λ4293.12 of CH, intensity 3; but its proximity to λ4292.3 (Fe, int. 2), λ4294.1 (Ti II, Fe, int. 2+5) and λ4293.04 (?, int. 2) makes it less suitable than the region at λ4311. The line λ4303.942 (CH, int. 4) although blended with λ4303.84 (?, int. 2), λ4303.6 (Nd II, int. 1), λ4304.4 (CH, int. 1) and λ4304.57 (CH, Fe, int. 2), is mostly due to the band, and has therefore been used in the estimates.

For the CN band we have used the line λ4192.574 (CN, int. 2), which lies between λ4195.342 (Fe, int. 5) and λ4191.5 (Fe, int. 6+3). We have also examined λ4197.102 (CN, int. 2), lying between λ4196.7 (Fe, int. 1) and λ4198.06 (Fe, int. 2).

In order to be certain of the faint band-lines, we have used for most of our spectrograms Eastman Process high-contrast plates. The actual esti-

[17] C. D. Shane, Lick Observatory Bulletin **10**, 79 (1919).

[18] G. E. Hale, F. Ellermann and J. A. Parkhurst, Publications of the Yerkes Observatory **2**, 251 (1903).

[19] W. C. Rufus, Publications of the Observatory, University of Michigan **3**, 258 (1923).

mates, recorded in Tables V and VI, were made with the aid of a comparator fitted with a Bausch and Lomb wide-angle microscope. A half-silvered optical beam-divider made it possible to compare (or measure) two spectrograms simultaneously. In all estimates the solar spectrum was used as standard. Tables V and VI show that the bands of CH and of CN disappear at about

TABLE V. *CH band.*

Star	Absolute magnitudes[20]	Description of CH band
	Spectral class G5	
ϵ Gem	−1.4	Stronger than in the Sun
α UMa	+0.4	Stronger than in the Sun
η Dra	+0.7	Stronger than in the Sun
μ Her	+3.7	Stronger than in the Sun
	Spectral class G0	
α Aqr	−2.8	Fainter than in the Sun
ϵ Leo	−0.9	About the same intensity as in Sun
α Aur	+0.1	About the same intensity as in Sun
5 Ser	+3.5	A little less strong than in Sun
13 Cet	+3.8	Same as in Sun
η Cor	+4.3	Same as in Sun
	Spectral class F8	
γ Cyg	−3.0	Very uncertain. Hardly visible[21]
α UMi	−3.0	Extremely faint
δ CMa	−2.9	Extremely faint
ϵ Hya	+2.1	Faint
26 Dra	+4.0	Faint
99 Her	+4.4	Faint
	Spectral class F5	
ρ Pup	−2.1	No trace
ϵ Aur	−2.0	No trace
α Per	−1.3	No trace
41 Cyg	−1.1	No trace
α CMi	+3.2	Perhaps very faint
10 UMa	+3.2	No trace
θ Cyg	+3.4	No trace
γ Ser	+4.3	No trace
	Spectral Class F2	
π Sgr	−0.8	No trace
	Spectral class F0	
20 CVn	−1.4	No trace
γ Cap	−0.7	No trace
20 Per	+2.5	No trace

the same place in the spectral sequence, in class F8. There seems to be a definite indication that the CH band is stronger in dwarfs than in giants (cf. Sun and α Aquarii). This agrees well with theory. It is surprising, however, that the intensity of both bands, especially that of CH, decreases so rapidly as we pass from G0 (temperature[22] about 6200°K) to F5 (temperature 7200°K). This effect is very strikingly shown in Fig. 1: in the solar spectrum the band is very strong, while in Procyon (α Canis Minoris), a dwarf of class F5, it can hardly be seen.

[20] W. S. Adams, A. H. Joy, G. Strömberg and C. G. Burwell, Astrophys. J. **53,** 13 (1921).

[21] This agrees with: Lockyer and Baxandall, Philosophical Transactions of the Royal Society, (A), **201,** 205 (1903), whose list of lines in α Cygni does not contain 4303.9 (CH, int. 4) and 4293.1 (CH, int. 3).

[22] We have adopted here the temperature scale of Brill, in agreement with Wildt (reference 5), although a slightly lower scale would probably have been preferable.

5. It is clear from the foregoing that it is not possible to consider all of Fraunhofer's G-band as being caused by CH. Even in the solar spectrum the total intensity of the molecular lines is relatively small. In the past the distinction between molecular and atomic lines has not always been made. In-

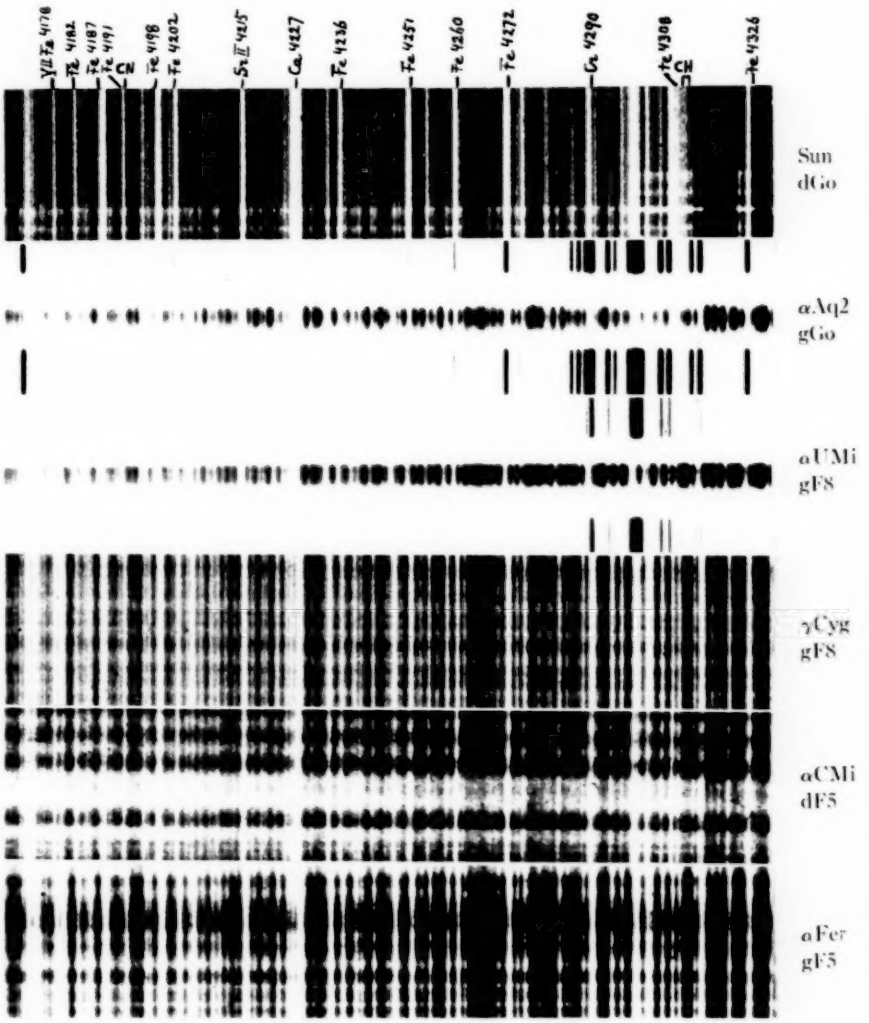

Fig. 1. Spectra of Sun and five stars, showing the region λ4170 to λ4330. The lines of CH and CN which were used in this investigation are marked on the upper margin. Two of the stellar spectra show the comparison lines of Ti and of Fe.

vestigations made prior to the work of Newall, Baxandall and Butler refer to the whole region of the G-band, and do not necessarily apply to the CH molecule. Thus, in the Henry Draper Catalogue[23] we read: "Class F0. Typical stars δ Geminorum and α Carinae. . . . The lines 4305.8, 4308.0 and 4309.9

[23] Harvard Annals **91**, 7 (1918).

TABLE VI. *CN band.*

Star		Absolute magnitudes	Description of CH band
α	Aqr	−2.8	About the same as in Sun
ϵ	Leo	−0.9	About the same as in Sun
α	Aur	+0.1	?
		Spectral class F8	
γ	Cyg	−3.0	Extremely faint
α	UMi	−3.0	Extremely faint
δ	CMa	−2.9	Extremely faint
		Spectral class F5	
ϵ	Aur	−2.0	No trace
α	Per	−1.3	No trace
α	CMi	+3.2	Perhaps very faint
		Spectral class F2	
π	Sgr	−0.8	No trace

and other lines, which form the absorption band called G by Fraunhofer, are faint and inconspicuous". It is certain[24] that the line λ4305.8 is Sc II 4305.715 (int. 2) and Ti 4305.92 (int. 4), rather than CH 4305.85 (int. 1); line λ4308.0 is identical with Ca 4307.75 (int. 3) and Fe 4307.91 (int. 6), rather than with CH 4308.05 (int. 0) and CH 4308.18 (int. 1); line 4309.6 is Fe 4309.38 (int. 3), λ4309.46 (? int. 1), *Y*4309.63 (int. 1) and Ce II 4309.72 (int. 1), rather than the faint CH lines λλ4309.38 and 4309.63. The band described in the Draper Catalogue is, accordingly, of atomic origin. The same is true of the Harvard descriptions for classes F2 (π Sagittarii),[25] F5 (α Canis Minoris,[26] ρ Puppis,[27] α Persei)[28] and F8 (γ Cygni and δ Canis Majoris).[29]

It may be noted in this connection that Dunham[30] found no lines definitely belonging to CH in the spectrum of α Persei, photographed with high dispersion at Mount Wilson.

In a recent paper Miss A. V. Douglas[31] has discussed the band near λ4200 in several Cepheid variables, and has attributed it to CN. Following is a list of lines taken from the "Revised Rowland",[32] within the range λ4198 to λ4202. The total intensity of the CN lines is seen to be negligible in comparison with that of the atomic lines (see also Table III). The latter are so closely packed that they are doubtless blended throughout the whole range. In particular, it is almost certain that the point at which Miss Douglas measured the microphotometer deflection corresponds to several atomic lines of Rowland intensity 1 and greater, while the strongest line of CN in the same interval is but 0.

[24] The intensities given in parentheses are from the Mount Wilson Revision of Rowland's Solar Wave-Length Tables.

[25] Harvard Annals **91,** introduction, 7 (1918); Harvard Annals **28,** 157 (1897).

[26] Harvard Annals **28,** 157 (1897).

[27] Harvard Annals **91,** introduction, 8 (1918).

[28] Harvard Annals **28,** 187, remark 178 (1897).

[29] Harvard Annals **28,** 188 (1897).

[30] Contributions from the Princeton University Observatory, No. 9, 1929.

[31] Monthly Notices of the Royal Astronomical Society **90,** 804 (1930).

[32] The average spectral class of the stars investigated by Miss Douglas is G0 for η Aquilae, F8 for α Ursae Minoris (Polaris), and F8 for RT Aurigae. All these are giants, and we should expect their band-lines of CN and of CH to be even fainter than those of the Sun, which is a dwarf of class G0.

TABLE VII.

Atomic lines		Int.	Lines of CN	Int.
4198.06	Fe	2		
.25	Fe	4	4199.67	−1
.34	Fe	4	4199.74	−2
.64	Fe	3	4200.70	0
99.11	Fe	5	4201.07	−1
.89	Ru	1		
.99	Fe	2		
4200.46	Ni	1		
.79	Ti	1		
.93	Fe	3		
1.71	Ni Fe	1		
2.04	Fe	8		

It is probable that her results for CH are also vitiated by the same effect of blending.

This effect of blending has doubtless influenced another investigation, one by P. ten Bruggencate,[33] on the spectra of δ Cephei variables. The linear dispersion of his objective-prism was about 100A/mm at Hγ. It seems, therefore, certain that the major portion of the microphotometer deflections attributed by him to CH, have in reality been caused by closely packed atomic lines.

6. We have seen in section 1, that the heat of dissociation of the CH molecule is appreciably lower than that of the CN molecule. It is therefore surprising, at first sight, that both bands disappear at the same temperature within the spectral sequence (F8, temperature about 6500°K). We shall show that this may be explained by the enormous abundance of H in the atmospheres of the stars, which causes a slowing down of the process of decomposition of CH.

In considering the equilibrium conditions of CH and CN, we shall follow the method of Wildt,[34] replacing in his formulae the heat of dissociation of CH by the more modern value, 110 k cal/mol, and using the same temperature of 6500°K for both molecules.

Consider a molecule AB; let p_A, p_B and p_{AB} be the partial pressures of the constituents of the gas: A, B and AB; and let K_p be the equilibrium coefficient at constant pressure, $p_A\, p_B/p_{AB}$. Then, following the formulae of Wildt, we have for

$$\mathrm{CN} \rightarrow \log K_p = -\frac{210000}{4.541T} + 1.5 \log T + \log (1 - e^{-2940/T}) + 0.07$$

and for

$$\mathrm{CH} \rightarrow \log K_p = \frac{110000}{4.541T} + 1.5 \log T + \log (1 - e^{-4000/T}) - 0.40.$$

Computation gives for $T = 6500°$

$$\log K_p{}^{\mathrm{CN}} = -1.7 \quad \log K_p{}^{\mathrm{CH}} = 1.3.$$

[33] Annalen v. d. Bosscha-Sterrenwacht, Lembang (Java) **5**, 1 (1931).

[34] R. Wildt, reference 5.

From the definition of the coefficient K_p, it follows that

$$\log \frac{p_{CH}}{p_{CN}} = \log \frac{K_p{}^{CN}}{K_p{}^{CH}} + \log \frac{p_H}{p_N}.$$

The ratio p_H/p_N is not accurately known; but H. N. Russell[35] has found that in the reversing layer of the Sun hydrogen is about 10^4 times more abundant (by number of atoms) than nitrogen. The total mass of the hydrogen atoms, per unit area, exceeds that of the nitrogen atoms by a factor of about 10^3. Since the partial pressure depends upon the concentration, it is probably not exaggerated to assume

$$\log \frac{p_H}{p_N} = 3.$$

This gives

$$p_{CH} = p_{CN} \qquad (\text{at } T = 6500°K).$$

The simultaneous disappearance of CN and CH may thus be explained.

It should be remembered in this connection that the coefficient of absorption of CH is probably greater than that of CN. The violet cyanogen bands result from an electronic transition of the type $^2\Sigma - {}^2\Sigma$, while the hydrocarbon band corresponds to $^2\Delta - {}^2\Pi$. The probability of the latter transition is greater than that of the former, which may be the reason why, in spectral classes G0 and F8, the band of CH is stronger than that of CN.

Professor H. N. Russell has called our attention to the fact that the CN band at 3883 (not investigated by us) is far stronger than that at 4216, and may perhaps persist higher up in the spectral sequence. However, T. Dunham Jr. found no trace of the 3883 band in the star Persei α (Contribution from the Princeton University Observatory **9**, 6 (1929)).

[35] H. N. Russell, Astrophys. J. **70**, 56 (1929). The author states that the values for H and N are uncertain, and they merely indicate the order of magnitude concerned.

THE EFFECT OF PRESSURE ON THE ELECTRICAL CONDUCTANCE OF SALT SOLUTIONS IN WATER*

By W. A. Zisman

Jefferson Physical Laboratory, Harvard University

(Received October 19, 1931)

Abstract

New data are presented for the change with pressure of the equivalent conductance of the following 1/100 normal salt solutions in water: at 30°C, HCl, LiCl, NaCl, KCl, RbCl, CsCl, NaF, NaBr, NaI, Na_2SO_4, $NaC_2H_3O_2$, $CaCl_2$, $BaCl_2$, $ThCl_4$, $K_3Fe(CN)_6$, $K_4Fe(CN)_6$; and at 75°C, all the above solutions excepting NaF and $ThCl_4$. The pressure range at 30°C is 1–10,000 kg/cm², and at 75°C it is 1–11,000 kg/cm². It is pointed out that the observed maxima in the equivalent conductance can not be entirely caused by a change in the degree of dissociation of the ions with pressure. By using a well-known expression for the equivalent conductance at infinite dilution, and also by using the Debye-Hücklel formula, it is shown in each case that there must be a large change in the diameters of the ions due to the pressure if the theory is to agree with the data.

THE influence of high pressure on the conductance of aqueous salt solutions was studied by Tamman and his pupil Körber[1] with pressures up to 3000 km/cm².

The experiments reported here were carried out to see if an extension of the pressure range to 12,000 kg/cm² would show anything striking. It was thought from consideration based on modern ideas of ion hydration that the ion diameter would decrease greatly at high pressures.

The conductance cell used in these experiments is shown in section in Fig. 1. The pressure transmitting fluid used throughout the high pressure apparatus was kerosene. A column of kerosene floating upon the salt solution served to transmit the pressure throughout the cell, thus eliminating sealed joints between glass and the metal electrical lead-in wires. This was very necessary because no combination of metal and glass was known where each substance had the same thermal expansion and compressibility as the other. The pressure was transmitted into the space between the electrodes through two $\frac{1}{4}''$ holes ground in the walls of the quartz tube used to space the two electrodes. The electrodes were of solid platinum and were 1.2 cm in outside diameter and 2 mm thick. The parts were maintained in alignment by grinding the ends of the quartz tube square and resting the bottom electrode upon a flat surface ground on the bottom of the inside of the Pyrex container, and finally by clamping the assembly together with a taunt piece of fishline wound once around the outside of the Pyrex container. A phosphor bronze spring

* This is a summary of the results obtained at the high pressure laboratory of the Jefferson Physical Laboratory of Harvard University during the academic year 1930–1931. The research problem was carried on as a Ph.D. thesis in Physics.

[1] F. Körber, Zeits. f. phys. Chemie **67**, 212 (1909).

maintained the tension. The electrical contact to the bottom electrode was made by a piece of platinum wire gold soldered to the edge of the electrode and insulated from the solution by means of a Pyrex capillary tube, not shown in the figure.

The usual sort of a.c. bridge was used. The fixed arms were two 1000 ohm Ayrton wound resistances made by the General Radio Company. The variable resistance was 10,000 ohms and was Ayrton wound, and made by the same company. A very carefully constructed General Radio condenser of 1500 micromicrofarads capacity was used in shunt with the variable resistance. The vacuum tube oscillator is a duplicate of the one described recently by G. Jones and R. Josephs.[2] In the same paper experiments showed that several

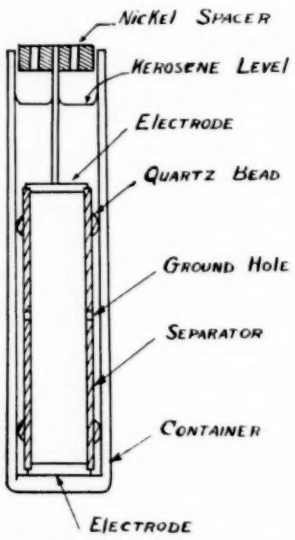

Fig. 1. Diagram of apparatus.

important grounding and shielding precautions had previously been neglected. These statements were very soon found true. The final arrangement used was found to give but 0.1 percent change in resistance of the cell when the oscillator frequency was altered from 2830 to 600 cycles. To the precision (0.2 percent) it was found unnecessary to use any earthing device such as a Wagner ground. The bridge balance was detected with a two-stage audio frequency amplifier and a pair of telephones. The bridge could easily be balanced to 0.1 percent.

A description of the pressure apparatus and gauge is unnecessary here; for details see Bridgman's papers.[3] The gauge is good to $\frac{1}{4}$ percent without special calibration.

The massive pressure cylinder which contained the conductivity cell was immersed in an insulating bath of kerosene at 30°C and in a mixture of kero-

[2] G. Jones and R. Josephs, Jour. Amer. Chem. Soc. **50,** 1049 (1928).
[3] P. W. Bridgman, Proc. Amer. Acad. Sci. **XLIX,** No. 11, Feb. (1914).

sene and vacuum pump oil at 75°C. A thermostat maintained the temperature at 30°C to 2/100° and at 75°C to 4/100°.

The procedure used in an experiment after placing the cell in the press was to take resistance measurements at atmospheric pressure, 500, 1000, 2000, 3000, 4500, 6000, 7500, 9000, 10500, 9800, 8200, 6800, 5300, 3800, 2500, 1500 kgm/cm, and back to atmospheric pressure. No hysteresis loop occurred, proving there was no relative motion in the parts of the cell, and no appreciable interaction between the kerosene and the salt solution that might be facilitated by a rise in pressure. The measurements at 30° C were made one day and at 75°C the following day. Several times after completing a 75° run the 30° readings were repeated and were found to check the first series of readings. A run at one temperature took from 6 to 8 hours because the changes of pressure caused heating or cooling effects that took 20 minutes to dissipate.

The distilled water for making up the salt solutions was made in a tin-lined still and it had a specific conductivity of about 1.0×10^{-6} mho. The salts were all chemically pure of the best grade obtainable from Kahlbaum, Merck and Company, and Eimer and Amend.

Several pressure runs were carried out at both temperatures by using distilled water in place of the salt solution. The water correction was found to be reproducible to around 2 percent. The correction was found to amount to from 0.5 to 1.5 percent depending upon pressure and temperature. The precise method for making this correction is debatable, however. In Table I,

TABLE I.

Pressure (k/cm²)	Resistance at 30°C	Resistance at 75°C
1	492,000 ohms	164,000 ohms
500	457,000	155,800
1,000	426,000	148,900
1,500	395,000	142,400
2,000	364,000	135,600
2,500	334,000	129,500
3,000	306,500	125,500
4,000	258,000	120,000
5,000	221,400	117,100
6,000	196,700	116,000
7,000	179,300	114,800
8,000	168,500	113,300
9,000	161,800	112,500
10,000	159,200	111,600
11,000	—	110,800

are given the cell resistances R for distilled water as a function of pressure. The resistance at atmospheric pressure varied with time for about 30 minutes after placing the cell in the press; the final resistance showed the specific conductance of water attained the value of 5×10^{-6} mho at 30°C and 15×10^{-6} mho at 75°C.

The water correction was made as follows: At pressure p the cell filled with salt solution had a resistance R, while filled with distilled water in equilibrium with the kerosene its resistance was R'. If the resistance of the cell when the water is nonconductive is R'', then

$$\frac{1}{R} = \frac{1}{R'} + \frac{1}{R''}.$$

The water correction increases with pressure. At 10,000 kg/cm² it is around 1.4 percent at 30°C, and 0.9 percent at 75°C. At 4000 kg/cm² it is around 0.3 percent.

A correction must be made because of the compressibility of the quartz separator. If the water corrected cell resistance is R and the resistivity of the salt solution is r, then at pressure p

$$r/r_0 = R/R_0(1 - pa/3).$$

Here "a" is the cubic compressibility of quartz which according to Bridgman[4] is 26.5×10^{-7} at 30° and 27.7×10^{-7} at 75°. At 11,000 kg/cm² this correction is 1.0 percent.

The minima of resistivity observed around 1,000 kg/cm² are partly caused by the compressibility of the solution. The effect due to a pressure change in ion-mobility is nicely shown by a calculation of the change of equivalent conductance with pressure. A solution of concentration C gram-equivalents per liter has an equivalent conductance Λ given by $\Lambda = 1000/cr$. Then using a zero subscript to denote values at atmospheric pressure $\Lambda/\Lambda_0 = C_0r_0/Cr$. If the volume of the salt solution used is V then obviously

$$C/C_0 = V_0/V.$$

Finally

$$\frac{\Lambda}{\Lambda_0} = \frac{V/V_0}{r/r_0}.$$

The ratio V/V_0 was computed as function of pressure from the data given by Bridgman[5] on the specific volume of water. To enable r/r_0 to be calculated from the equivalent conductance data presented here, the values of V/V_0 of Table II were computed by taking the mean of the values for 30° and

TABLE II.

Pressure in kg/cm²	V/V_0	Pressure in kg/cm²	V/V_0
1	1.0000	5,000	0.8691
500	0.9798	6,000	0.8547
1,000	0.9624	7,000	0.8399
1,500	0.9467	8,000	0.8275
2,000	0.9325	9,000	0.8175
2,500	0.9191	10,000	0.8075
3,000	0.9075	11,000	0.7984
4,000	0.8867		

75°C. This mean can be employed for either temperature with an accuracy of 0.2 percent. However, at 30° the water freezes around 10,500 kg/cm² and

[4] P. W. Bridgman, Amer. Journ. of Sci. **10**, Oct. (1925).
[5] P. W. Bridgman, Proc. Amer. Acad. Sci., **XLVIII**, No. 9, Sept. (1912).

therefore the value of V/V_0 in this table means nothing at 30°C and 11,000 kg/cm².

The resulting data on Λ/Λ_0 for the salts studied are presented in Table III–IV. The data are probably accurate to 0.3 percent.

TABLE III. Λ/Λ_0 *as function of pressure at 30°C. Pressure in kg/cm².*

Press.	HCl	LiCl	NaCl	KCl	RbCl	CsCl
1	1.0000	1.0000	1.0000	1.0000	1.0000	1.0000
500	1.0265	1.0135	1.0078	1.0098	1.0076	1.0050
1000	1.0464	1.0256	1.0100	1.0100	1.0042	1.0002
1500	1.0616	1.0240	1.0016	1.0039	0.9980	0.9904
2000	1.0715	1.0202	0.9924	0.9945	0.9850	0.9730
2500	1.0775	1.0070	—	0.9775	—	0.9544
3000	1.0812	0.9915	0.9545	0.9582	0.9493	0.9304
4000	1.0828	0.9520	0.9100	0.9150	0.9002	0.8794
5000	1.0780	0.9078	0.8618	0.8660	0.8517	0.8250
6000	1.0682	0.8601	0.8126	0.8178	0.7995	0.7725
7000	1.0545	0.8062	0.7578	0.7630	0.7478	0.7184
8000	1.0392	0.7545	0.7075	0.7129	0.6966	0.6654
9000	1.0218	0.7060	0.6598	0.6646	0.6474	0.6175
10000	1.0055	0.6600	0.6146	0.6168	0.5995	0.5705

Press.	NaF	NaBr	NaI	KI	Na_2SO_4	Na Acetate
1	1.0000	1.0000	1.0000	1.0000	1.0000	1.0000
500	1.0076	1.0034	0.9940	0.9980	1.0075	1.0010
1000	1.0116	1.0005	0.9722	0.9878	1.0080	0.9975
1500	1.0079	0.9915	0.9640	0.9728	1.0034	0.9820
2000	1.0020	0.9700	0.9400	0.9514	0.9945	0.9646
2500	—	0.9515	—	—	0.9798	0.9445
3000	0.9773	0.9294	0.8845	0.8965	0.9674	0.9230
4000	0.9434	0.8782	0.8272	0.8467	0.9285	0.8740
5000	0.9076	0.8250	0.7687	0.7926	0.8865	0.8250
6000	0.8724	0.7730	0.7150	0.7382	0.8395	0.7765
7000	0.8284	0.7196	0.6610	0.6845	0.7915	0.7238
8000	0.7910	0.6685	0.6120	0.6350	0.7455	0.6768
9000	0.7530	0.6225	0.5664	0.5910	0.7020	0.6330
10000	0.7170	0.5771	0.5233	0.5514	0.6586	0.5888

Press.	$CaCl_2$	$BaCl_2$	$K_4Fe(CN)_6$	$K_3Fe(CN)_6$	$ThCl_4$
1	1.0000	1.0000	1.0000	1.0000	1.0000
500	1.0114	1.0100	1.0230	1.0075	0.9934
1000	1.0153	1.0095	1.0338	1.0098	0.9825
1500	1.0100	1.0030	1.0460	0.9995	0.9703
2000	0.9980	0.9925	1.0275	0.9820	0.9525
2500	0.9800	0.9726	1.0160	0.9614	0.9348
3000	0.9625	0.9546	1.0005	0.9400	0.9150
4000	0.9186	0.9070	0.9655	0.8932	0.8710
5000	0.8668	0.8570	0.9200	0.8420	0.8260
6000	0.8154	0.8072	0.8735	0.7905	0.7750
7000	0.7595	0.7504	0.8170	0.7374	0.7248
8000	0.7025	0.6976	0.7640	0.6868	0.6755
9000	0.6496	0.6493	0.7148	0.6405	0.6278
10000	0.6000	0.6016	0.6670	0.5928	0.5797

DISCUSSION OF RESULTS

The ratio Λ/Λ_0 shows a linear decrease with pressure in the pressure range 3000–8000 kg/cm². The slope is the same at one temperature for all salt solutions tried. At 75°C the slope is less than at 30°C. The behavior in

TABLE IV. Λ/Λ_0 *as function of pressure at 75°C. Pressure in kg/cm².*

Press.	HCl	LiCl	NaCl	KCl	RbCl	CsCl
1	1.0000	1.0000	1.0000	1.0000	1.0000	1.0000
500	1.0125	0.9886	0.9875	0.9878	0.9870	0.9855
1000	1.0190	0.9815	0.9720	0.9755	0.9690	0.9678
1500	1.0218	0.9664	0.9570	0.9578	0.9530	0.9450
2000	1.0218	0.9514	0.9472	0.9418	0.9342	0.9258
2500	1.0225	—	—	0.9245	—	0.9024
3000	1.0229	0.9218	0.9018	0.9047	0.8952	0.8820
4000	1.0225	0.8845	0.8629	0.8670	0.8554	0.8378
5000	1.0171	0.8468	0.8238	0.8275	0.8121	0.7955
6000	1.0115	0.8120	0.7844	0.7900	0.7729	0.7537
7000	1.0040	0.7755	0.7472	0.7525	0.7317	0.7125
8000	0.9947	0.7400	0.7102	0.7150	0.6940	0.6720
9000	0.9866	0.7067	0.6764	0.6785	0.6575	0.6340
10000	0.9780	0.6722	0.6422	0.6445	0.6220	0.5980
11000	0.9680	0.6418	0.6097	0.6098	0.5900	0.5650

Press.	NaBr	NaI	KI	Na_2SO_4	Na Acetate
1	1.0000	1.0000	1.0000	1.0000	1.0000
500	0.9825	0.9726	0.9757	0.9884	0.9780
1000	0.9650	0.9497	0.9548	0.9747	0.9570
1500	—	0.9246	0.9310	0.9595	0.9345
2000	0.9228	0.8976	0.9037	0.9425	0.9120
2500	—	—	—	0.9280	0.8890
3000	0.8825	0.8470	0.8635	0.9111	0.8674
4000	0.8395	0.7998	0.8100	0.8787	0.8260
5000	0.7960	0.7525	0.7650	0.8470	0.7884
6000	0.7555	0.7086	0.7210	0.8150	0.7520
7000	0.7154	0.6690	0.6795	0.7827	0.7173
8000	0.6780	0.6307	0.6415	0.7505	0.6823
9000	0.6430	0.5965	0.6051	0.7215	0.6486
10000	0.6104	0.5633	0.5717	0.6920	0.6194
11000	0.5778	0.5334	0.5380	0.6625	0.5910

Press.	$CaCl_2$	$BaCl_2$	$K_4Fe(CN)_6$	$K_3Fe(CN)_6$
1	1.0000	1.0000	1.0000	1.0000
500	0.9900	0.9876	1.0020	0.9875
1000	0.9770	0.9730	1.0002	0.9715
1500	0.9615	0.9584	0.9950	0.9545
2000	0.9430	0.9405	0.9818	0.9340
2500	—	—	0.9684	0.9125
3000	0.9050	0.9040	0.9540	0.8930
4000	0.8663	0.8626	0.9225	0.8510
5000	0.8255	0.8205	0.8875	0.8084
6000	0.7844	0.7800	0.8504	0.7695
7000	0.7344	0.7417	0.8110	0.7312
8000	0.7050	0.7035	0.7735	0.6947
9000	0.6660	0.6668	0.7375	0 6624
10000	0.6292	0.6320	0.7021	0.6314
11000	0.5925	—	0.6683	0.6010

the range 1–3000 kg/cm² is typical of each salt. The equivalent conductance ratio Λ/Λ_0 shows either a maximum or else curvature in the same sense. The effect of raising the temperature is to decrease these maxima. The pressure at which the maxima occur is higher and the height of the maxima is greater the smaller the diameter of the ions as given by crystal lattice data, or the greater the valence of the ions concerned. The initial slope of the conductance curve is also greater the smaller the ion's lattice diameter and the greater its

valence. The effect of ion diameter is nicely shown by the family of alkali chlorides and by the family of sodium halides. The effect of valence is shown by $K_3Fe(CN)_6$ and $K_4Fe(CN)_6$, or by comparison of $CaCl_2$ with KCl and of $BaCl_2$ with CsCl. It is remarkable that the behavior of sodium acetate is so nearly like that of NaBr. The entire pressure data agree qualitatively with the behavior one would predict upon the basis of current ideas on ion-hydration. One would expect the most hydrated ions to show the greatest maxima and initial slopes. It is also not surprising to find such a complex ion as the acetate radical behaving so nearly like bromide ions. The ions in solution because of hydration are complex aggregates whether or not they are simple outside the solution.

In the high pressure range 8000–11000 kg/cm^2, the ratio Λ/Λ_0 begins to curve up again, and so the curve lies above the extension of the straight line portion of the curve. The difference in ordinate at 10,000 kg/cm^2 between the curve and the extended straight line part is variable with the nature of the salt and the temperature, and usually amounts to about 1 percent. This change of curvature can not be due to increase in the importance of the conductance contribution of the solvent because that has already been taken into account. In the cases of $ThCl_4$ and NaF hysteresis loops occurred in the pressure runs at 75°C. The loop for NaF was repeatable with different batches of solution, and its cause is not clear. The loop for $ThCl_1$ was not capable of repetition and a long series of runs showed the cause must reside in some sort of chemical reaction between the salt solution and the kerosene floating upon it. The same sort of behavior was found to occur in solutions of sodium hydroxide—at both temperatures. At 30° there was no sign of hysteresis in NaF but the slope of the straight line portion was distinctly less than for the other solutions.

The behavior of HCl under pressure is very distinctive. The initial slope of the conductance curve is the greatest for all solutions tried, and on the basis of the notions of ion hydration one would interpret that as proving that HCl fits nicely in the pressure data for the family of alkali chlorides, after assuming the hydrogen ion is smaller than the lithium ion and is even more hydrated. Yet at higher pressures the curve for HCl shows a very slow decrease after reaching a maximum, and at the highest pressure attained here the conductance ratio Λ/Λ_0 had not returned to its initial value of unity. The same thing occurs at 75°C. This apparently anomalous behavior of HCl is not unexpected, for it appears from a good many lines of research that the aqueous hydrogen ion is a proton actually buried within a molecule of water.

According to the Debye-Hückel theory of strong electrolytes the equivalent conductance Λ at concentration C, temperature T, of a uni-univalent salt whose ions have radii b_1 and b_2 in a solvent of dielectric constant D, is given by

$$\frac{\Lambda}{\Lambda_1} = 1 - \left[\frac{3.56 \times 10^9(b_1\xi_2 + b_2\xi_1)}{(DT)^{1/2}(\xi_1 + \xi_2)} - \frac{9.86 \times 10^5(\xi_1^2 + \xi_2^2)}{(DT)^{3/2}2\xi_1\xi_2}\right](2C)^{1/2}.$$

Here ξ_1 and ξ_2 are given by $\xi = 6\pi b\eta$ and η is the viscosity of the solution. Λ_1 is the equivalent conductance at infinite dilution, and it is given by $\Lambda_1 = Ne^2/9\times 10''(1/\zeta_1 + 1/\zeta_2)$, where N is Avogadro's number, and e is the electronic charge.

This relation cannot be tested at high pressures because b_1 and b_2 are not known as functions of pressure; yet the following calculations show b must vary with pressure very considerably.

Assuming this theory holds well enough for a 1/100 normal aqueous solution, we have sufficient data to test this theory by using the initial values of $d/dp(\Lambda/\Lambda_0)$, $d/dp(\eta/\eta_0)$, $d/dp(C/C_0)$, and the ion diameters at atmospheric pressure. At 30°C conductance data show the potassium and chlorine ions have mobilities differing less than 1 percent in water at infinite dilution. It is a fair approximation to take b_1 and b_2 and $db_1/dp = db_2/dp$ as equal for this salt. Now Λ_1 for KCl at 30° can be calculated, since at 18° it is 130 mho and its temperature coefficient is 0.0217. The result is 163 mho at 30°. The above relation leads to the value of 1.26×10^{-8} cm for b. Also the dielectric constant is 81.1 at 18° and its temperature coefficient is 0.0044; hence at 30° D is 85.3. Earlier experiments[6] showed $d/dp(D) = 0.0033$ at room temperature. Lastly $[d/dp(C)]/C$ is the same as the cubic compressibility of water, and its value as found by Bridgman is 4.47×10^{-5} at 30°.

Differentiating the Debye-Hückel relation we get

$$\frac{d}{dp}\left(\frac{\Lambda}{\Lambda_1}\right) = \frac{1.02\times 10^8 b}{D^{3/2}}(2C)^{1/2}\frac{dD}{dp} - \frac{281(2C)^{1/2}}{D^{5/2}}\frac{dD}{dp} - \frac{\left(\frac{2.04\times 10^8 b}{D^{1/2}} - \frac{187}{D^{3/2}}\right)}{(2C)^{1/2}}\frac{dc}{dp} - \frac{2.04\times 10^8 (2C)^{1/2}}{D^{1/2}}\frac{db}{dp}$$

$$= -1.33\times 10^{-6} - 0.312\times 10^7\frac{db}{dp}. \qquad \text{(A)}$$

But

$$\frac{d}{dp}\left(\frac{\Lambda}{\Lambda_1}\right) = \frac{1}{\Lambda_1}\frac{d\Lambda}{dp} - \left(\frac{\Lambda}{\Lambda_1}\right)\frac{1}{\Lambda_1}\frac{d\Lambda_1}{dp}$$

$$= 19\times 10^{-6} - 0.946\left[-\frac{1}{\eta}\frac{d\eta}{dp} - \frac{1}{b}\frac{db}{dp}\right].$$

According to Bridgman $(1/\eta)(d\eta/dp)$ for pure water is 23×10^{-6}. Hence experimental data show

$$\frac{d}{dp}\left(\frac{\Lambda}{\Lambda_1}\right) = 40.8\times 10^{-6} + 0.751\times 10^8\frac{db}{dp}. \qquad \text{(B)}$$

Comparing the result of theory, (A), with that of experiment, (B), we see that it would have been very incorrect to assume $d/dp(b) = 0$, for then theory

[6] S. Kyropoulis, Zeits. f. Physik. **40**, 507 (1926).

gives $d/dp(\Lambda/\Lambda_1) = -1.33\times10^{-6}$ while experiment then shows the same derivative must be $+40.8\times10^{-6}$. This difference is certainly far greater than inaccuracy of data could cause. Equating (A) and (B), and solving for $d/dp(b)$, we find $3(1/b)\ (db/dp) = -12.8\times10^{-5}$. This is the experimentally determined cubic compressibility of the ions of K and Cl. It is about 2.5 times greater than the cubic compressibility of water (4.47×10^{-5}).

The data of Körber[1] show the initial slope of the conductance-pressure curves varies very little in going from 1/10 to 1/1000 normal solutions of strong electrolytes. For instance, at 19° and 1000 kg/cm² the r/r_0 curve for 1/1000 normal KCl differs but 0.8 percent from the curve for a 1/10 normal solution. In the case of NaCl the same difference is 0.6 percent and in case of HCl it is only 0.2 percent. It is therefore not surprising that the compressibility of the ions can be shown to be the same as the above value simply by using the relation $\Lambda = Ne^2/6\pi\eta\ 9\times10^{11}(1/b_1+1/b_2)$ and calculating from it as in the above case.

We now have after one logarithmic differentiation:

$$\frac{1}{\Lambda}\left(\frac{d\Lambda}{dp}\right) = -\frac{1}{\eta}\left(\frac{d\eta}{dp}\right) - \frac{1}{b}\left(\frac{db}{dp}\right)$$

and our data give the result

$$\frac{3(1db)}{(bdp)} = -12.6\times10^{-5}$$

whereas the Debye-Hückel theory predicted the value -12.8×10^{-5}.

It is interesting to use this simple relation to calculate b as a function of high pressure. By using a zero subscript to denote values at atmospheric pressure we find

$$\frac{\Lambda}{\Lambda_0} = \frac{(\eta/\eta_0)}{(b/b_0)}.$$

This allows a calculation of b/b_0 as function of pressure. The result is given in Table V. The diameter decreases more slowly as the pressure rises. Of courses this calculation has only heuristic value, for it is questionable to use the macroscopically determined coefficient of viscosity η in place of the microscopic coefficient of ionic friction.

If incomplete ionization of salt molecules is assumed, and α is the degree of dissociation, then at sufficient dilution we can set

$$\Lambda = \frac{Ne^2}{9\times10''}\ \frac{\alpha}{6\pi\eta}\left(\frac{1}{b_1}+\frac{1}{b_2}\right).$$

It is very simple to show that change of α with pressure cannot alone explain the observed conductance data. Suppose b does not vary with pressure; then

$$\frac{\Lambda}{\Lambda_0} = \frac{(\eta/\eta_0)}{(\alpha_0/\alpha)}.$$

This permits a calculation of α as function of pressure. Evidently α/α_0 is simply the reciprocal of the ratio b/b_0 calculated for Table V. At high pressures then α_0/α must change by 25 percent. According to Arrhenius' theory

TABLE V. *Pressure in kg/cm². Temperature is 30°C*

Press.	η/η_0	Λ/Λ_0	b/b_0
250	0.988	1.0049	0.982
1250	0.937	1.0070	0.930
2250	0.872	0.986	0.885
3500	0.780	0.937	0.832
4500	0.710	0.891	0.797
5500	0.648	0.842	0.770
6500	0.595	0.790	0.753
7500	0.550	0.738	0.745
8500	0.512	0.689	0.744
9500	0.478	0.642	0.745
	Temperature is 75°C.		
250	0.983	0.994	0.989
1250	0.914	0.967	0.945
2250	0.845	0.933	0.905
3500	0.766	0.886	0.865
4500	0.700	0.847	0.826
5500	0.638	0.809	0.789
6500	0.577	0.771	0.748
7500	0.524	0.734	0.714
8500	0.473	0.697	0.679

a salt like 1/100 normal KCl is within 6 percent of being completely dissociated at atmospheric pressure; therefore, so great a pressure change on α is impossible. It is also obscure how one can explain why KCl has a maximum, while the less dissociated KI shows none.

A repetition of this series of measurements with other polar solvents would be very interesting; unfortunately the conductivity cell used here can not be employed with any of the interesting solvents due to their solubility in kerosene.

I wish to express my gratitude to Professor P. W. Bridgman for the use of his high pressure apparatus and for his valuable advice and interest. It is also a pleasure to acknowledge the many helpful suggestions on conductivity technique from Professor G. Jones of the Department of Chemistry.

LETTERS TO THE EDITOR

Prompt publication of brief reports of important discoveries in physics may be secured by addressing them to this department. Closing dates for this department are, for the first issue of the month, the twenty-eighth of the preceding month; for the second issue, the thirteenth of the month. The Board of Editors does not hold itself responsible for the opinions expressed by the correspondents.

Isotope Effects in Polyatomic Molecules

The isotope effects of the normal vibrations, of polyatomic molecules can be easily derived from Dennison's general non-central force treatment[1] of the vibrations. We find that the resulting expressions permit the evaluation of the molecular constants without appealing to intensity measurements and also furnish criteria for the assignment of particular spectral frequencies to particular modes of vibration.

For example, compare the symmetrical molecules YX_2 and $\bar{Y}X_2$, where mass of each X atom $=m$, mass of $Y=M$, mass of $\bar{Y}=\bar{M}$ $=M+\Delta M$. Then we find that the isotope effect $\Delta\omega_3/\omega_3$ of the frequency ω_3 (whose electric moment vibrates perpendicularly to the symmetry axis) depends only on the masses and the molecular angle, and once this latter is known from the isotope effect, one of the constants of the potential energy expression can be evaluated from ω_3 itself.

The other three force constants can be evaluated from the frequencies parallel to the symmetry axis and their isotope effects, each of which depends on the constants. But the *sum* of the parallel isotope effects depends only on the masses:

$$\frac{\Delta\omega_1}{\omega_1}+\frac{\Delta\omega_2}{\omega_2}=-\frac{m\Delta M}{\bar{M}(2m+M)},$$

which should prove useful in the analysis of spectra. For a collinear molecule, the isotope effect of the inactive frequency vanishes, the expression on the right becoming that for the active parallel isotope effect alone, say $\Delta\omega_2/\omega_2$, and we also have $\Delta\omega_2/\omega_2=\Delta\omega_3/\omega_3$.

These results are applicable to the electronic absorption bands of chlorine dioxide recently measured by Urey and Johnston.[2] Two frequencies in the normal state showed isotope effects $\Delta\omega/\omega$ whose sum is -0.0124; the value of $-[m\Delta M/\bar{M}(2m+M)]$ for $Cl^{35}O_2$ and $Cl^{37}O_2$ is -0.0129, and therefore those two frequencies represent the parallel vibrations. Since no single isotope effect in the excited or the normal state was even approximately -0.0129, the molecule can not be collinear in either state. Our assignment to parallel vibrations agrees with that of Urey and Johnston, who discuss the matter from the standpoint of valence forces.

For tetratomic molecules YX_3 and $\bar{Y}X_3$, the isotope effect of each normal vibration depends on the six molecular constants and so the frequencies and isotope effects suffice to determine the constants. Again, the sum of the isotope effects of the parallel frequencies depends only on the masses; the sum of the perpendicular effects depends only on the masses and on the ratio of the altitude of the pyramid to the length of side of the triangular base.

Relations for the effects of isotopy of the X atoms are somewhat different, of course. Possibly the most interesting case is the tetratomic molecule, where the small difference in mass of an X atom removes the degeneracy of the motion, so that while YCl_3^{35}, for example, would have four normal frequencies, $YCl_2^{35}Cl^{37}$ would have six.

The expressions upon which the above and other relevant conclusions are based will appear in detail. We take great pleasure in thanking Professor Dennison for advice at various stages of our work.

E. O. Salant
Jenny E. Rosenthal
Department of Physics,
Washington Square College,
New York University, N. Y.,
December 9, 1931.

[1] D. M. Dennison. Rev. Mod. Phys. **3**, 280 (1931).

[2] H. C. Urey and H. Johnston, Phys. Rev. **38**, 2131 (1931). We are greatly indebted to Professor Urey for the manuscript.

The Vibrational Constants of the ICl Molecule

The vibrational constants of the ICl molecule published hitherto have been determined from analysis of the absorption band spectrum in the visible region[1,2,3] which consists of portions of four progressions ($v''=0$, 1, 2 and 3). Of these, three have been analysed but the fourth ($v''=3$) is weak under normal conditions and no measurements of it are recorded. The absolute v' and v'' numeration now adopted is that determined from measurements of the isotopic separations by Patkowski and Curtis.[3] Measurements published by Wilson and by Patkowski and Curtis did not extend to the red below $v'=7$ ($\nu=15002.0$ cm^{-1}) for the $v''=0$ progression nor below $v'=6$ ($\nu=14445.2$ cm^{-1}) for the $v''=1$ progression. The extrapolation required to determine ω_0', the fundamental frequency referring to available vibrational energy in the excited state, was thus fairly long and in view of the non-linear variation of ω_v' with v' for higher v' observations somewhat unreliable.

The analysis of the absorption spectrum in the extreme red and near infrared thus seemed to be worthy of attention and the writer by raising the temperature of the ICl to 400°C and suitably increasing the vapour density has photographed portions of progressions for which $v''=3$, 4, 5, 6, and 7. The analysis of these progressions has made it possible to evaluate ω_v' to $v'=2$ and ω_v'' to $v''=6$. The fundamental frequencies ω_0' and ω_0'' are now deduced more accurately than was possible previously. ω_0' is given by a graphical extrapolation of two units of v' as 209.7 cm^{-1} and ω_0'' by a linear extrapolation of one unit of v'' as 383.0 cm^{-1}.

The frequency of the $v''=0$, $v'=0$ band head, ν^{00}, is 13655.3 cm^{-1} and the electronic frequency associated with the system, ν^{el}, is 13742 cm^{-1} or 1.70 volts.

Examination of the G', ω_v' data shows that a third parabola in addition to the two reported by Curtis and Darbyshire[4] is now required to represent the G', ω_v' curve over the whole range of observations now recorded. The slopes of the $dG'/d\omega_v'$, ω_v' lines corresponding to the three parabolas are -0.110, -0.260 and -0.351, the intersection of the first and second being at 109.1 cm^{-1} ($v'=17$) and that of the second and third at $\omega_v'=155.5$ cm^{-1} ($v'=10$). It is worthy of remark that the former "break" is in the neighbourhood of the $v''=0$, $v'=16$ band whose abnormal appearance was mentioned by Curtis and Darbyshire and is unexplained so far.

The convergence limit was re-determined from Wilson's values. Two different methods show that his value 17430 cm^{-1} is probably some 90 units too high. These are (1) extrapolation of the G', ω_v' curve to $\omega_v'=0$ which gives the value 17341 cm^{-1} for the limit, and (2) graphical evaluation of the area under the v', ω_v' curve between the limits $v'=0$ and the value of v' for which ω_v' vanishes which gives 17345 cm^{-1}. The mean value is 17343 cm^{-1} or 2.14 volts. The dissociation potential of the excited ICl molecule is thus 0.44 volt.

Within the limits of experimental error the ω_v'' values decrease linearly as v'' increases from 1 to 6 and by using the corresponding $\omega_0''x''$ value to extrapolate G'' to the value of v'' for which $\omega_v''=0$, the dissociation energy for the normal state is found to be 23260 cm^{-1} units, that is, 5917 units *greater* than the energy required to dissociate by excitation and further increase of vibrational energy in the excited state.

Bands of the $v''=3$, 4, 5 progressions in the ICl_{37} spectrum have been measured and for them the isotopic shifts are opposite in sign to that previously observed in the higher v' members of the $v''=0$ progression. In all cases agreement with the calculated values using the Mulliken formula is good.

It is hoped to publish detailed results in the near future.

ORRELL DARBYSHIRE

Physics Department,
Armstrong Castle,
Newcastle-on-Tyne,
England,
November 25, 1931.

[1] Gibson and Ramsperger, Phys. Rev., **30**, 598 (1927).

[2] Wilson, Phys. Rev. **32**, 611 (1928).

[3] Patkowski and Curtis, Trans. Faraday Soc. **25**, 725 (1929).

[4] Curtis and Darbyshire, Trans. Faraday Soc. 117, **77** (1931).

The Magnetic Properties of Nickel Colloids

The magnetic behavior of a colloidal suspension of ferromagnetic properties may be calculated on plausible assumptions if certain magnetic constants of the suspended material and its particle sizes are known.[1] The appropriate magnetic constants for metallic nickel are well known, and it appeared from a study of the literature that colloidal suspensions of pure metallic nickel should be easily obtainable. In an attempt to check the theory, however, such surprisingly unsatisfactory results were obtained that it seems desirable to record them here, since they appear to suggest new lines of attack on ferromagnetics and colloids.

Theory predicts approximate magnetic saturation for metallic nickel suspensions of usual particle sizes in a field of 3000 gauss. The intensity of magnetization of a sol of known concentration at this field value should therefore measure with fair accuracy the amount of nickel present in metallic form.

	Benzene carbonyl sol A	Benzene carbonyl sol B	Bredig hydrosol (Fresh)	Bredig isopropyl alcosol
Magnetic field (gauss)	3790	3500	3500	3500
Intensity of magnetization of sol	-2.58×10^{-3}	-2.14×10^{-3}	-2.01×10^{-3}	-2.35×10^{-3}
Intensity of magnetization of dispersing medium	-2.72×10^{-3}	-2.52×10^{-3}	-2.52×10^{-3}	-2.60×10^{-3}
Intensity of magnetization of nickel	$+0.14\times10^{-3}$	$+0.38\times10^{-3}$	$+0.51\times10^{-3}$	$+0.25\times10^{-3}$
Concentration of nickel	0.34 mg/g	0.11 mg/g	0.066 mg/g	0.074 mg/g
Percent of nickel uncombined	0.75%	6.3%	14.2%	6.2%
Approximate radii of particles			300 mμ	40 mμ

A small sample (0.2–0.4 grams) was placed on the beam of a Curie balance, previously described,[2] and the intensity of magnetization was measured, with distilled water as a standard substance. The nickel was suspended in the solution in such small quantities that most of the magnetization was due to the liquid phase. The amount of this had, of course, to be determined and subtracted from the values observed for the colloids. This impairs considerably the accuracy of a determination, but the data were sufficiently precise to give the desired information. Correction was also applied for the magnetic properties of the air. No correction is necessary for the combined nickel in the suspension since its mass susceptibility is negligible in comparison with that of metallic nickel.

Colloids were prepared by two methods: first, by dissociating nickel carbonyl[3] dissolved in benzene, toluene, and para-cymene, with rubber as a protective colloid and by the Bredig method with a high frequency arc in water and in isopropyl alcohol. The following table gives some typical results of the measurements. The values of the intensity of magnetization are expressed in electromagnetic units per gram of sol. The concentrations of nickel were determined after the magnetic measurement by weighing the precipitate obtained with dimethyl-glyoxime. The percentage of uncombined nickel is computed from the known saturation value of magnetization of nickel and the total concentration of nickel present. The probable error, as estimated from the mean deviation of five determinations, in the intensity of magnetization of a sol is about 0.02×10^{-3} per gram. The Bredig sols were prepared by arcing a current of about 2.5 amperes of frequency 1200 kilocycles between nickel electrodes immersed in the dispersion medium. The flask containing the medium and the electrodes was immersed in a cooling bath consisting of ice water for the hydrosols and a mixture of solid carbon dioxide and alcohol for the alcosols. A current

[1] C. G. Montgomery, Phys. Rev. [2] **38,** 1782 (1931).

[2] C. G. Montgomery, Phys. Rev. [2] **36,** 498–505 (1930).

[3] E. Hatshek and P. C. L. Thorne, Kolloid-Zeits. **33,** 1–8 (1923); **36,** 12–16 (1925).

of dried nitrogen was bubbled through the flask before and during the arcing. Around 500 cc of a sol with a concentration of nickel of the order given in the table was produced by about twenty minutes of arcing. The radii of the particles were determined by a rough count with a slit ultramicroscope. Measurements on the hydrosols were made as soon as possible after they were prepared as the value of the intensity of magnetization decreased with time as the nickel oxidized and in five or six days was indistinguishable from that of water.

The extremely small percentage of uncombined nickel determined by these measurements is rather surprising. Hatshek and Thorne[3] have published analyses of the material deposited on electrodes in a cataphoresis experiment on benzene-carbonyl sols of this type. They treated the material with hydrochloric acid in a nitrometer and measured the total amount of hydrogen evolved. From this they computed the proportion of uncombined nickel, and obtained values in the neighborhood of 80 percent of the total nickel. In no case have magnetic methods of measuring the purity given values over 7 percent.

Hatshek and Thorne report the only other impurity in their sols as a carbonate of nickel. In the above table, while sol A was prepared by the method used by these authors, sol B had any possible admixture of CO_2 removed from the gaseous mixture of CO and nickel carbonyl by absorption in soda lime just before the nickel carbonyl was dissociated. The percentage of metallic nickel of the sols was improved by this, but it still remained very low.

It is possible to explain this discrepancy otherwise than by contamination of the material used in the present experiments. It is now well recognized that the particles in metal sols obtain their charges by the adsorption of ions. The forces which hold these ions must be chemical in nature, since the adsorption is selective. Now it is quite reasonable to suppose that this weak binding is sufficient to destroy the ferromagnetic properties of nickel, and at the same time is so weak that chemical or mechanical manipulations will break it down.

It would be extremely desirable to obtain further information relative to the validity of this supposition, as it should throw light upon some of the well known, but poorly understood, phenomena of ferromagnetism and ion adsorption.

CAROL G. MONTGOMERY
Sloane Physics Laboratory,
Yale University,
December 12, 1931.

A Hydrogen Isotope of Mass 2

The proton-electron plot of known atomic nuclei shows some rather marked regularities among atoms of lower atomic number.[1] Up to O^{16} a simple step-wise figure appears into which the nuclear species H^2, H^3 and He^5 could be fitted very nicely. Birge and Menzel[2] have shown that the discrepancy between the chemical atomic weight of hydrogen and Aston's value by the mass spectrograph could be accounted for by the assumption of a hydrogen isotope of mass 2 present to the extent of 1 part in 4500 parts of hydrogen of mass 1.

It is possible to calculate with confidence the vapor pressures of the pure substances H^1H^1, H^1H^2, H^1H^3, in equilibrium with the pure solid phases. It is only necessary to assume that in the Debye theory of the solid state, Θ is inversely proportional to the square root of the masses of these molecules and that the rotational and vibrational energies of the molecules do not change in the process of vaporization. These assumptions are in accord with well-established experimental evidence. We find that the vapor pressures for these three molecules in equilibrium with their solids should be in the ratio of $p_{11}:p_{12}:p_{13}=1:0.37:0.29$. The theory of the liquid state is not so well understood but it seems reasonable to believe that the differences in vapor pressure of these molecules in equilibrium with their liquids should be rather large and should make possible a rapid concentration of the heavier isotopes, if they exist, in the residue from the simple evaporation of liquid hydrogen near its triple point.

Accordingly two samples of hydrogen were prepared by evaporating large quantities of liquid hydrogen and collecting the gas which evaporated from the last fraction of the last

[1] Urey, J. Am. Chem. Soc. **53,** 2872 (1931); Johnston, ibid., **53,** 2866 (1931).

[2] Birge and Menzel, Phys. Rev. **37,** 1669 (1931).

cubic centimeter. The first sample was collected from the end portion of six liters of liquid evaporated at atmospheric pressure, and the second sample from four liters evaporated at a pressure only a few millimeters above the triple point. The process of liquefaction has probably no effect in changing the concentration of the isotopes since no appreciable change was observed in the sample evaporated at atmospheric pressure.

These samples were investigated for the atomic spectra of H^2 and H^3 in a hydrogen discharge tube run in Wood's so-called "black stage" by using the second order of a 21 foot grating with a dispersion of 1.31A per mm. With the sample evaporated at the boiling point no concentration so high as had been estimated was detected. We then increased the exposures so that the ratio of the time of exposure to the minimum required to get the H^1 lines on our plates was about 4500:1. Under these conditions we found in this sample as well as in ordinary hydrogen faint lines at the calculated positions for the lines of H^2 accompanying H_β, H_γ, H_δ. These lines do not agree in wave-length with any molecular lines reported in the literature.[3] However they were so weak that it was difficult to be sure that they were not ghosts of the strongly overexposed atomic lines.

The sample of hydrogen evaporated near the triple point shows these lines greatly enhanced, relative to the lines of H^1, over both those of ordinary hydrogen and of the first sample. The relative intensities can be judged by the number and intensity of the symmetrical ghosts on the plates. The wave-lengths of the H^2 lines appearing on these plates could be easily measured within about 0.02A. The following table gives the mean of the observed displacements of these lines from those of H^1 and the calculated displacements:

Line	H_α	H_β	H_γ	H_δ
$\Delta\lambda$ calc.	1.793	1.326	1.185	1.119
$\Delta\lambda$ obs.				
Ordinary hydrogen	—	1.346	1.206	1.145
1st sample	—	1.330	1.199	1.103
2nd sample	1.820	1.315	1.176	—

The H^2 lines are broad, as is to be expected for close unresolved doublets, but they are not as broad and diffuse as the H^1 lines probably due to the smaller Döppler broadening. Although their intensities relative to the ghosts of the respective H^1 lines appear nearly constant for any one sample of hydrogen, they are not ghosts for their intensities relative to the known ghosts are not the same in the case of ordinary hydrogen and of the 1st sample as they are in the case of the second sample. They are not molecular lines for they do not appear on a plate taken with the discharge tube in the "white stage" with the molecular spectrum enhanced ($H^2{}_\gamma$ was found as a slight irregularity on a microphotometer curve of this plate). Finally the $H^2{}_\alpha$ line is resolved into a doublet with a separation of about 0.16A in agreement with the observed separation of the $H^1{}_\alpha$ line.

The relative abundance in ordinary hydrogen, judging from relative minimum exposure time is about 1:4000, or less, in agreement with Birge and Menzel's estimate. A similar estimate of the abundance in the second sample indicated a concentration of about 1 in 800. Thus an appreciable fractionation has been secured as expected from theory.[4]

No evidence for H^3 has been secured, but its lines would fall on regions of our plates where the halation is bad.

The distillation was carried out at the Bureau of Standards by one of us (F.G.B.), who is continuing the fractionation to secure more highly concentrated samples. The spectroscopic work was done at Columbia University by the other two (H.C.U. and G.M.M.) who are working on the molecular spectrum.

HAROLD C. UREY
F. G. BRICKWEDDE
G. M. MURPHY

Columbia University,
New York, N. Y.
Bureau of Standards,
Washington, D. C.
December 5, 1931.

[3] Gale, Monk and Lee, Astrophys. J. **57,** 89 (1928); Finkelnburg, Z. Physik **52,** 57 (1928); Connelly, Proc. Phys. Soc. **42,** 28 (1929).

[4] Keesom and van Dijk, Proc. Acad. Sci. Amsterdam **34,** 52 (1931).

Possible Narrowing of Compton Line Breadth by Preferentially Directed Electron Momenta in Ceylon Graphite

According to a theory of the author first published in Phys. Rev. **33,** 643 (1929), the considerable natural spectral breadth of the Compton modified line was ascribed to the initial momenta of electrons in the scattering body and as one consequence a mathematical expression was derived for the behavior of this breadth as a function of the primary wave-length and scattering angle (formula 23, page 657, above article). The breadth due to scattering by an assemblage of electrons all of the same speed βc but with perfectly random direction was given as

$$\Delta\lambda = 4\beta\lambda^* \qquad (1)$$

where $\lambda^* = \frac{1}{2}(\lambda_c^2 + \lambda_1^2 - 2\lambda_c\lambda_1 \cos\theta)^{1/2}$

θ = scattering angle

λ_1 = primary wave-length

$\lambda_c = \lambda_1 + 2(h/mc)\sin^2\frac{1}{2}\theta$

= Compton shifted wave-length for stationary electrons.

Since λ_c is nearly equal to λ_1, formula (1) is nearly expressed by

$$\Delta\lambda = 4\beta\lambda_1 \sin\tfrac{1}{2}\theta \qquad (2)$$

that is to say the breadth of the Compton line should be nearly proportional to primary wave-length on the one hand and nearly proportional to the sine of half the scattering angle on the other *provided initial electron momenta* are responsible for the breadth.

Both these predictions have since been verified by the author in collaboration with H. A. Kirkpatrick with the multicrystal spectrograph (Phys. Rev. **37,** 136 (1931) and Phys. Rev. **38,** 1094 (1931)). *This verification gives excellent support for the theory and hence for its basic assumption that the breadth of the Compton line is an effect of initial electron momenta.*

By an easy approximate analysis of the momentum balance for the case of an electron with initial momentum, mv, making an angle ψ with an axis of reference which bisects the angle formed by the incident and scattered x-ray momenta the author has shown that *only the component momentum* along this axis of reference contributes to the broadening of the Compton line (Phys. Rev. **38,** 1094 (1931)).

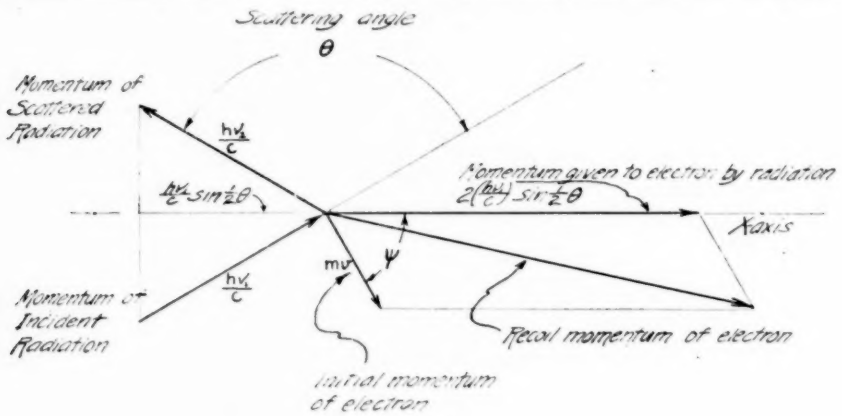

Fig. 1.

Referring to Fig. 1 it turns out that the shift of wave-length for one elementary, scattering process by an electron of initial momentum making angle ψ with the natural reference axis x, is given by

$$\lambda_2 - \lambda_1 = 2(h/mc)\sin^2\tfrac{1}{2}\theta + 2\lambda\left(\frac{v}{c}\cos\psi\right)\sin\tfrac{1}{2}\theta \qquad (3)$$

The first term in the right hand member of this equation is the Compton shift while the second term explains the breadth given in Eqs. (1) and (2) *when we consider the directions of electron momenta to be a random distribution.*

If, however, the directions of the initial electron momenta are not random it is evident that the Compton line may be narrower than the value given in Eqs. (1) and (2). In particular if the momenta for some fairly large and isolated class of electrons in the scattering body are all restricted very closely to a plane normal to the above natural axis of reference, then $\cos\psi$ in Eq. (3) will vanish and the contribution to the Compton line by these elec-

trons should be a sharp line—the sharper the more accurately the restriction to this normal plane is fulfilled.

Now it is possible that the outer electrons which may have very long orbits in some crystal lattices may be definitely related to the crystal structure. After considering a number of crystalline elements in the hope of selecting one which might conceivably have outer electron orbits restricted in some fairly definite plane, Dr. Alexander Goetz of this Institute suggested that Ceylon graphite might meet the requirement. Ceylon graphite, which crystallizes in small flat hexagonal plates, cleaves practically only along (0001), i.e., in a direction parallel to the flake. Also it is highly diamagnetically anisotropic.

Work was immediately started by Dr. Goetz and his collaborators to study Ceylon graphite and to prepare blocks of this material consisting of the tiny flakes stuck together with an adhesive

By a very ingenious method described in detail by Dr. Goetz in the same issue of this Journal the flakes are compelled to align themselves horizontally so that the whole block forms a sort of artificial single crystal. Dr. Goetz found that by taking special precautions (which he describes in his letter) amazing diamagnetic anisotropy ratios as high as twenty to one could be obtained for the blocks. This ratio can easily be acounted for by the assumption that the *anisotropy of each flake is complete* but that the flakes deviate by a "spread" of three or four degrees from mutual parallelism. This, together with the great disparity in cleavability parallel and perpendicular to the plate, lends hope that perhaps the orbits of the outer electrons in the flakes are fairly well restricted to one plane, though of course it is not absolute proof of this fact.

The author proposes to employ a curving scattering body made out of blocks of this especially prepared Ceylon graphite as a scatterer in the multicrystal spectrograph. If the outer electrons describe orbits which are nearly plane and parallel to the plane of the graphite flake then the flakes should be placed so that the normal to their flat faces bisects the angle between the primary and scattered x-ray beams. Under these conditions we may expect perhaps to get a very narrow spectral contribution to the Compton shifted line from the scattering by the outer electrons. This narrow peak will of course be superposed upon a broader base due to the contribution to shifted scattering of the remaining electrons in the graphite crystals.

The construction of the special graphite scatterer is now well advanced and the results should be obtained in a few weeks.

It is interesting to consider the bearings that either positive or negative results in this experiment may have in several fields of physics.

First, if the result is positive and a narrow shifted line appears:

1. This will be a tremendously convincing corroboration of the correctness of the author's explanation of Compton shifted line breadth as an effect of atomic electron velocities; for if the breadth can be shown to depend on the *orientation* of the crystalline scatterer the cause of the breadth must be some *vector quantity* (the electron momentum). If the breadth is to be explained in this way, its existence and amount are of the greatest importance since they furnish direct experimental evidence of the dynamic atom with electron velocities of the order of magnitude postulated by Bohr (still present with only slight modification in the more modern theory of quantum mechanics). All other spectral evidence for the dynamic atom must be considered as extremely indirect since such evidence is based on observations of *energy* effects. The observations on the breadth of the Compton line and its behavior constitute direct observations of atomic electron *momentum* in which respect they are unique. Energy may be either kinetic or potential but momentum can mean only one thing—*motion*.

2. Several reliable investigators, using the double crystal spectrometer, have reported much narrower Compton shifted lines than those obtained by the author and his coworkers. Some of these men, in particular P. A. Ross, in later investigations have obtained results which agree very satisfactorily with ours, however. Furthermore, those who obtained narrower line structures than ours disagree with each other to some extent as to the breadth. *All of these men used graphite scatterers.* If the author's guess proves correct and a positive result is obtained in the experiment now under discussion these perplexing disagreements may perhaps be completely explained. The author's broad line structures were the result of scattering from synthetic Acheson graphite, which is practically amor-

phous (or if it contains microcrystals, their orientation must be completely random). On the other hand, the investigators in disagreement with the author, and with each other in respect to line breadth, may have used *crystalline graphite more or less fortuitously orientated* so as to produce narrower Compton lines. In this connection it is interesting to note that on the author's theory *any departure from perfectly random electron momenta will have some narrowing effect.*

3. If the results are positive it may be possible from this experiment to obtain exceedingly valuable information as to the behavior of the outer electrons in crystalline graphite. If these electrons in preferentially orientated orbits form an isolated class well differentiated from the remainder, it may be possible to determine their number relative to the total number of electrons by comparing the area of the sharp peak they contribute with the area of the broader structure associated with the remainder. The interesting bearing of this experiment on the explanation of diamagnetism in crystals is also evident. The breadth of the narrow peak will give perhaps some evidence as to the degree of flatness of these preferentially orientated graphite crystal orbits. Many interesting considerations bearing on the nature of the solid state of matter and the mechanical properties of solid bodies may be closely connected with just such questions.

Second, if the results are negative and no narrow line appears:

1. This will decidedly *not* be negative evidence for the author's theory of Compton line breadth as an effect of atomic electron velocities. *That theory is the only one yet proposed which satisfactorily explains the observed behavior of the breadth as a function of scattering angle and primary wave-length* and this is the strongest possible argument for its correctness.

2. A negative result can be interpreted only as evidence that the outer *electron momenta* in the graphite crystals are not preferentially orientated as postulated above. It will not necessarily mean that the outer electron orbits are not conditioned geometrically by the crystal structure for they may each depart so far from flatness as to approximate an almost random distribution of direction. Or again they may be flat but have such a large number of quantized orientations as to approximate a random distribution to within the power of detection afforded by this method. Thus even a negative result will be to some extent information as to the dynamics of outer electrons in solids.

JESSE W. M. DUMOND

Norman Bridge Laboratory of Physics,
California Institute of Technology,
December 5, 1931.

The Production of Large Artificial Graphite Crystals

There are two problems brought into the focus of interest very recently which seem to make it desirable to obtain single crystals of graphite of several cm^3 size free from occlusions and chemical impurities.

One problem because of which possible methods of producing such crystals had to be considered is the investigation of the dependence of crystal diamagnetism on the size of crystals below certain "critical" dimensions as has been studied by Vaidyanathan,[1] Rao,[2] Mathur and Varma,[3] and in our laboratory in connection with other effects influencing crystal diamagnetism.[4]

The desirability of producing crystals of graphite was furthermore enhanced by the experiments on the Compton radiation from Acheson graphite by Dr. DuMond of this Institute, where the spectral breadth of the modified line has been interpreted by him[5] as due to the fact that the momenta of the electrons of the atoms of the scatterer are oriented at random in a microcrystalline material such as artificial graphite. These considerations led to the planning of the use of single crystalline scatterers as described by him in detail in a letter in this issue of the PHYSICAL REVIEW.

Since the occurrence of single crystals of graphite in nature, sufficiently large and perfect for the proposed types of experiments, is too scarce, (for DuMond's multicrystal spec-

[1] V. L. Vaidyanathan, Ind. Journ. of Phys. **5,** 559 (1930).

[2] S. R. Rao, Ind. Journ. of Phys. **6,** 241 (1931); Nature **128,** 153 (1931).

[3] R. N. Mathur and M. R. Varma, Ind. Journ. of Phys. **6,** 181 (1931).

[4] A. Goetz and A. B. Focke, Phys. Rev. **38,** 1569 (1931).

[5] J. W. M. DuMond, Phys. Rev. **33,** 643 (1929).

trograph not less than 50 equal crystals of ca. $10\times10\times30$ mm are needed) a method for artificial production had to be developed.

The usual ways of crystal growth by crystallization out of the liquid phase or by recrystallization however are unfeasible because of the high vapor pressure of graphite in these temperature regions. One way out of this difficulty is given by the abundant natural occurrence of almost single crystalline graphite powder, represented by the flake-like consistency of the Ceylon-mineral. The particles of this powder are thin plates, only a few microns thick and 3–0.01 mm in diameter; the planes of these plates coincide more or less with (0001) which is the principal cleavage plane. A system of lines on these planes indicates the existence of twinning or gliding planes of rhombohedral character.[6] The imperfection of these planes of the natural graphite is however very large and causes the thickness of the plates to be very irregular. A high powered microscope shows that this is due to adhering lamellae of other individuals, as shown in the microphotograph Fig. 1. In order to obtain large crystals it was planned to pile these flakes in such a way as to orient their principal axes all parallel and to fix them in this position by means of a neutral adhesive. Experiments however showed that this was not possible because of the mentioned imperfection of the (0001) planes.

Fig. 1. Microphotograph of the surface of a flake of untreated Ceylon graphite, $495\times$ magnified. It shows the inhomogeneity due to adhering crystal fragments.

The conjecture that the imperfections of the flakes were due to impurities proved to be right, since the measurements of the magnetic susceptibilities by Mr. Focke of this Institute on those crystal cakes showed large amounts of iron which necessitated the use of a thorough extraction method with HCl worked out by Dr. Faessler. Repeated magnetic and chemical tests proved the necessity of extracting for periods of several days after which time no ferromagnetic susceptibility could be traced. The microscopic observations however did not show much improvement of the cleavage planes but the presence of SiO_2 deposits on the (0001) planes was found with the polarization microscope. Therefore the graphite underwent first a treatment in HF before the iron was extracted. Now the cleavage planes were almost perfect although the size of the flakes had decreased considerably by the chemical process. Fig. 2 shows a microphotograph of such a plane which shows now only a pattern of small holes similar to etching figures.

Fig 2. Microphotograph of the surface of a flake from which SiO_2 and Fe were removed (0001) plane, $495\times$ magnified. The surface is much more uniform and shows a pattern indicating the crystallographic symmetry.

From the investigations of Honda and Soné[7] it is known that graphite crystals show an unusually large diamagnetic anisotropy, such that the susceptibility parallel to the axis [0001] is 7 times large than perpendicular to it, whereas the azimuthal variation of the susceptibility is apparently zero, a phenomenon

[6] P. Niggli, Spezielle Mineralogie Pag. 361.

[7] K. Honda and N. Soné, Sc. Rep. Tohoku Univ. **2, 1** (1913).

which now is almost to be expected from the knowledge of the lattice arrangement. This large anisotropy suggests immediately a method of lining up the perfected flakes: the purified flake powder was suspended in a solution of 3 percent gum Damar in benzene and was then allowed to settle within the inhomogeneous field of a strong electromagnet. After the flakes had settled, the benzene was evaporated and a cake was obtained which possessed considerable rigidity due to the adhesive qualities of the gum. It is obvious that it is very easy to produce such artificial crystals of any size desired. A large advantage of this method is the possibility of using the Gouy method for the exact determination of the magnetic qualities of the graphite crystals with respect to the orientation, which measurement can also serve as indicator of how well the flakes are lined up.

Mr. Focke performed these measurements which show the effect the perfection of the cleavage planes have on the anisotropy of the artificial crystals, being largely influenced by quartz deposits. Crystal blocks free from Fe, however, in presence of SiO_2 showed anisotropy $(\chi_\parallel/\chi_\perp)=4$ which is much less than Honda's observation on a natural crystal. If however the quartz is removed by HF *the anisotropy is increased to 13.2.* There can be little doubt that the line-up of the flakes is still imperfect and estimates of the possible variations seem to indicate that the true anisotropies may reach values up to 20, assuming the validity of the relation:

$$\chi_\perp = \chi_\parallel - (\chi_\parallel - \chi_\phi)/\sin^2\phi,$$

where ϕ designates the mean deviation of the flakes from the correct direction. Fig. 3 shows a photograph in almost natural size of such an artificial crystal broken so as to show the arrangement of the flakes. With the exception of the tin-alloyed Bi crystals[1] these crystals show by far the largest anisotropic diamagnetism known so far.

The method described can be modified in order to measure the oriented susceptibilities of very small crystals, as is essential for the investigation of the dependence of crystal diamagnetism on the dimensions of the particle. For this purpose the purified flakes are ground under special precautions and the powder obtained is settled in an agar solution in order to segregate in different sizes. As soon as the largest particles have settled, the agar solution is solidified, thus fixing each particle in its position. If the whole process is performed in an inhomogeneous magnetic field, all particles are forced into positions which are crystallographically parallel. Thus the agar block forms a kind of a graphite single crystal in which each horizontal layer consists of parallel particles of the same size, the susceptibility and anisotropy of which is easy to determine.

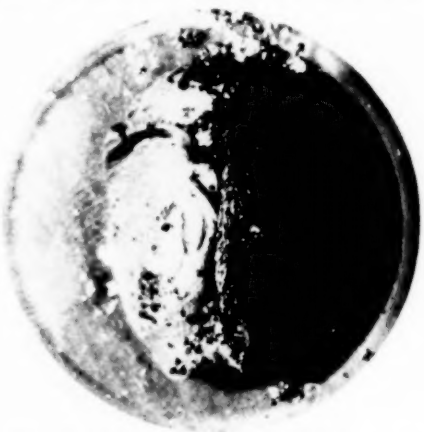

Fig. 3. Photograph of an artificial graphite crystal of approximately natural size. The crystal was broken to show the alignment of the flakes.

The results obtained from these "crystals" are thought to contribute an interesting addition to our knowledge of the nature of the crystal electrons.

ALEXANDER GOETZ
ALFRED B. FOCKE
ALFRED FAESSLER

California Institute of Technology,
Pasadena, California,
December 7, 1931.

Some Remarks on the Theory of Photoelectric Effect on Metals

In the July, 1931, issue of this Journal appeared a paper by Frenkel,[1] containing among other matters a criticism of a theory of photoelectric effect on metals, advanced recently by Mr. Schubin and me.[2] It is easy to see that

[1] J. Frenkel, Phys. Rev. **38,** 309 (1931).

[2] Ig. Tamm und S. Schubin, Zeits. f. Physik **68,** 97 (1931).

this criticism was largely based on misunderstanding.

One of the two main arguments advanced in Frenkel's criticism runs as follows. Frenkel says (reference 1, p. 317): "Tamm and Schubin actually made a hypothesis that (in metals) there are besides the absolutely free electrons another group of relatively bound (Bloch's) electrons, which enter into play at a threshold frequency $\nu_0' > \nu_0$," and proceeds to criticize this "hypothesis," which of course we never thought of advancing. The fact is, that having mentioned the well-known facts, that a completely free electron is not able to absorb a photon and that a conduction electron in the metal is not free, but bound (1) by the potential barrier at the surface of the metal and (2) by the periodic field of the metal lattice, we proceeded to discuss separately the influence of these two different modes of binding on the absorption of photons by electrons. As the first kind of binding can be accounted for even in the simple Sommerfeld theory of "free electrons," we used this first approximation to evaluate the corresponding part of the complete photoelectric action. But to account for the periodic field of the lattice it was of course necessary to use a better kind of approximation to actual conditions; i.e., to use Bloch's theory. In this manner we were able to establish that although of course *all* the conduction electrons in the metal are of one and the same kind, there are *two different mechanisms* of photoelectric action (the surface and the volume effect) with widely different characteristics. The only hypothesis actually made by us is, that *in the first approximation* these two mechanisms, corresponding to two modes of binding mentioned, may be treated separately.

As to the second argument of Frenkel (reference 1, p. 316): citing numerical data, used by us, Frenkel says, that Tamm and Schubin get for the potential energy jump across the surface of the metal C a value of "about 2 volts," whereas the evidence of cathode ray diffraction indicates that C varies between 12 and 20 volts for different metals. He concludes that the Fermi-Sommerfeld theory used by us is fallacious. Mentioning at last a theory proposed by himself in 1928,[3] Frenkel says that this theory enables one to calculate the values of C "in good agreement with experimental data," using only the data for the photoelectric threshold frequency.

The actual facts may be gathered from the following table, containing the values of C in volts for the metals K, Na, Ag and Au: (1) given by Rupp,[4] as derived from the evidence of cathode ray diffraction measurement (first line), (2) derived by summing up the energy $h\nu_0$ of the threshold frequency photon, as measured experimentally, with the zero point maximum electron energy

$$\epsilon_0 = \frac{mh^2}{2}\left(\frac{3n}{8\pi}\right)^{2/3}$$

calculated according to the Fermi-Sommerfeld theory of free electrons (these values were used by us in our paper) and (3) calculated according to the above mentioned Frenkel's theory of 1928 (third line).

TABLE I. *Potential jump* C *for different metals in volts.*

Method	K	Na	Ag	Au
1. Rupp (C_d)	7.3	?	14	14
2. Fermi (C_f)	4.02	4.95	9.6	10.3
3. Frenkel	11.9	10.9	24.7	28.9

It will be seen that the values of Rupp and of "Fermi" differ by a factor 1.4–1.8, and not by a factor 6 or 10, as one is apt to conclude from Frenkel's paper. Further the "Frenkel" values are by no means in better agreement with the values of Rupp, than the values of "Fermi"; if anything the reverse is the case.

Still, I am inclined to think that the difference of the values of C derived from the evidence of cathode ray diffraction (C_d) and those, calculated according to the theory of free electrons, (C_f) is a real one and can scarcely be completely accounted for by the fact, that the theory used in the calculations is an approximate one.[5] The explanation of this discrepancy seems to lie in the simple fact,

[3] Frenkel, Zeits. f. Physik **49**, 31 (1928).

[4] Rupp, Elektronen-Interferenzen (Leipziger Vorträge), Leipzig, 1930, p. 7.

[5] To bring the calculations into agreement with the cathode ray diffraction measurements, Rosenfeld and Witmer, Rupp and others suppose, that, e.g., in the case of Ag and Au, the number of free electrons in the lattice is not equal to the number of atoms, but is twice as large. This hypothesis seems very artificial, especially if applied to the case of potassium.

that C_d and C_f are actually two different physical quantities.

The energy spectrum of an electron in a crystal lattice consists of an succession of (practically) continuous bands of allowed levels, each band corresponding to an energy level of an isolated atom. The lower bands are occupied by the inner electrons of the atoms up to a certain band number n say, only half of which is occupied (at the temperature $T=0$) by the valency (i.e., conduction) electrons (we confine our attention to the metals of the first group, having one valency electron per atom).

To use the theory of free electrons means to ascribe to the lowest level of the band number n (i.e., to the valency electron of the least energy) the potential energy—C_f and the *kinetic energy zero* and to calculate the distribution of the energy levels lying higher than this particular level according to the Fermi statistics, disregarding the periodic field of the lattice and the fact, that the energy values, lying between successive allowed bands n, $n+1$, $n+2$ . . . are forbidden (if the bands do not overlap). Since all the electrons in a metal possess in reality both potential *and* kinetic energy, it follows, that *the "potential jump" C_f is actually an (approximate) measure of the whole (potential and kinetic) energy $W_0=U_0+T_0$ of the "bottom valency electron"*:

$$C_f \doteqdot -W_0 = -(U_0+T_0).$$

Since U_0 and T_0 have opposite signs, C_f is smaller than $-U_0$.

Actually one does adjust the value of C_f not to the least possible energy of an valency electron W_0, but to the work function $h\nu_0$, which can be measured experimentally. It means, that one ascribes to the uppermost level, occupied at the temperature $T=0$ by valency electrons, the energy $-h\nu_0$, and calculates C_f from the relation $C_f=\epsilon_0+h\nu_0$. Since the actual spreading of energy levels within an allowed band is smaller, than the spreading ϵ_0, calculated according to the theory of free electrons, this value of C_f will be somewhat larger, than W_0.

On the other hand the value C_d, as derived from the cathode ray diffraction measurements, is by definition numerically equal to the mean potential energy of an electron in the lattice.

When comparing C_f with C_d we have further to take in account, that "the mean potential energy" U_0 of the bottom valency electron is equal to

$$U_0 = \int U|\psi_0|^2 \cdot dV,$$

where ψ_0 is the wave function of this electron, whereas the quantity C_d, also designated as "the mean potential energy," is independent of ψ:[6]

$$C_d = -(1/V)\int U dV.$$

It follows, that if the valency electron is in an s-state, C_d must be somewhat smaller than $-U_0$, since $|\psi_0|^2$ increases when one approaches the positive nucleus.[7]

Thus the relation between C_f and C_d is somewhat complicated. Still, as $C_f \sim -(U_0+T_0)$ and $C_d \sim -U_0$, one may expect theoretically C_d to be greater than C_f and the difference between their values to be of the order of magnitude of several volts, as is actually the case.

I will not enter into a criticism of the theory of photoelectric effect in metals, proposed by Frenkel in the paper cited, because he has informed me that he no longer advocates this theory.

I may add, that Professor Frenkel has given me permission to state, that he now considers his criticism, advanced against our (Schubin's and Tamm's) theory, to have been based on a misunderstanding and withdraws the arguments mentioned above.

IG. TAMM

University of Moscow
November 30, 1931

[6] Bethe, Ann. d. Physik **87,** 55 (1928). According to the more elaborate theory of Morse, Phys. Rev. **35,** 1310 (1930) (cf. Eq. (24)) C_d seems to have a somewhat larger value. Both Bethe and Morse suppose the field of the lattice to end abruptly at the surface of the metal. This simplification can hardly be justified in the case of relatively slow cathode ray electrons, with which we are concerned here.

[7] Further, when calculating C_d one has to take in account the field of all the electrons in the metal, whereas when calculating U_0 one has to leave out the field of the valency electron considered.

BOOK REVIEWS

Constitution of Atomic Nuclei and Radioactivity. G. GAMOW. Pp. 114, figs., 40. Oxford University Press, 1931. Price, $3.50.

This is the second book to appear in the Oxford International Series of Monographs on Physics, which began with Dirac's well-known volume. Dr. Gamow here presents the first book, to the reviewer's knowledge, on what may be termed the quantum-mechanical in distinction from purely empirical study of nuclear structure. Some of the most exciting developments in theoretical physics in the past two or three years have been concerned with atomic nuclei. Consequently the appearance of Dr. Gamow's monograph is particularly timely and interesting.

It is now becoming quite widely known that the phenomenon of nuclear decay is to be attributed to the quantum-mechanical leaping of classically unsurmountable barriers. An alpha-particle which classically would be sentenced to abide for eternity in a crater of potential energy has in quantum mechanics a finite probability of passing the rim of the crater and coasting out to freedom. This phenomenon has been remarkably fruitful in clarifying theoretically the Geiger-Nuttall relation between the ranges of alpha-particles and radioactive decay constants. Passing to another field, information on nuclear spin is continually being deduced from hyperfine structure and band intensity measurements.

The topics mentioned in the preceding paragraph are all discussed in Dr. Gamow's book—also, however, still more recent and so more unfamiliar, though no less spectacular developments in the correlation of the velocities of alpha-particles with the frequencies of gamma-rays and with excited states of the nucleus. For instance, Rosenblum has observed anomalous alpha-particles with energies smaller than usual by a given amount x. Also, γ-rays have been measured having $\nu = x/h$. The obvious interpretation is that sometimes the nucleus is left in an excited rather than normal state after the alpha disintegration. In this case the escaping alpha-particles are the abnormally slow ones, while reversion of the nucleus to the normal state gives the gamma-rays. It has even been found possible to excite some of the gamma-rays artificially by alpha-ray bombardment, thus evidencing critical potentials of the nucleus. One can also now differentiate between various types of artificial disintegration whereby a proton is driven out of the nucleus. Sometimes the bombarding alpha-particle is captured by the nucleus, sometimes it is not, and sometimes, in accord with theory, there is a resonance phenomenon in which alpha-particles of certain particular velocities are abnormally effective in disintegrating the nucleus.

All phenomena such as those just mentioned show that alpha-particles and protons in the nucleus behave on the whole quite respectably and have many of the properties of ordinary quantum mechanical systems. Not so with electrons. There is even considerable evidence pointing to the conclusion that in the nucleus the electrons lose completely all their normal properties. In fact the law of conservation of energy fails unless one postulates the Pauli neutron, which incidentally is a hypothesis too recent for mention in Gamow's book. In the original manuscript, all paragraphs dealing with nuclear electrons were set off by skull and crossbones, but in the actual printing this has, alas, been changed to the rather colorless symbol $\sim$.

The style of writing is bright, concise, and lucid. Although the preface states that "the book is written from a theoretical point of view and no details of experimental methods are given," this should not be construed as meaning that the content is primarily mathematical. Quite the contrary, our existing nuclear models are so crude that only the most elementary quantum-mechanical methods are needed and mathematical polish is out of the question.

Perhaps the most serious criticism which can be made of the volume is the rather lackadaisical absence of all references to theoretical work. In the preface the author agrees to document with experimental but not with theoretical references. Consequently it is hard to know who has worked in the field, and where to go for supplementary reading. Not once, for instance, do the names of Gurney and Condon appear in the entire volume. A few references to the mathematical literature would also not have been amiss where questions of rigor (convergence, Stokes phenomenon, etc.) have very properly been omitted in the interest of simplicity.

J. H. VAN VLECK
University of Wisconsin

Rotation of a Rigid Body in Quantum Mechanics. H. B. G. CASIMIR, Diss. Leiden, 1931. Pp. 112. Published by J. B. Wolters, Groningen.

One of the most interesting problems in any system of mechanics is the rotation of a rigid body. The classical theory, the matrix mechanics and the wave mechanics all contribute some part to its solution and it is most illuminating to have the various methods of attack collected together in one small book. This has been attempted by Casimir and although his work is far from exhaustive, as indeed would be impossible in so few pages, some of the principal results have been very ably described. Perhaps a little too much space is given to the classical theory but it is done in such a way as to make clear the generalisations to the quantum theory. Again, little is said about the important work of Kramers and Ittmann, the reader being referred to the original papers. The first chapter is devoted to the classical theory. The second is very good and is a synopsis of the work of Klein and Wang, containing the results of earlier workers on the symmetrical top as special cases. It deals with the selection rules and transition probabilities of the symmetrical top and the four types of wave functions of the asymmetrical top, together with its selection rules. In the third and fourth chapters a sketch is given of the connection between the theory already developed and the theory of the group of three-dimensional rotations, and some interesting theorems on the eigenvalues and functions of differential operators are stated. The last chapter is concerned with the form of the Hamiltonian function for the motion of a polyatomic molecule. In general this proves too difficult a problem but it can be solved in two simpler cases, the superposition of which can be considered to give the general molecules. It yields the well-known result that the motion can be divided up into rotations and vibrations, together with some knowledge of the interaction terms.

The book will be found useful for giving a rapid insight into the work which has been done on the quantum theory of the top.

W. G. PENNEY
University of Wisconsin

Problems in Physics. WILLIAM D. HENDERSON. Pp. ix+245, Figs. 206, McGraw-Hill Book Company, New York, Second edition, 1931. Price $2.25.

One of the greatest difficulties in presenting problems in physics, is to get the student to visualize the conditions presented in the problem. To develop such a practice, if one can do nothing more than draw a line and make a few points for the simpler cases, eventually leads to a method which is of the utmost advantage in the more difficult examples.

Before each different group of the problems in this book is presented, the principles and basic formulas involved are discussed. There are also figures in each case showing the specific dimensions represented by the various factors used in the formulae. Before each of these groups a number of typical illustrative problems have been carefully analysed and worked. In this respect the text affords much assistance in the visualization of problems. There is a total of 835 problems, covering all the subjects in physics, including radiation examples in heat, light and electricity.

Another commendable feature is the use of both metric and British units. It is highly desirable to become as versatile in one system of units as in the other, and a clearer conception of a definition is obtained when it is interpreted in the different units.

Very few of the problems have the answers given. This is a much discussed subject among instructors. Which is the better system, probably depends on how the system is used.

The book is also quite self-contained in that it presents some thirty-seven tables of equivalents and physical constants. The grade of problems presented is such as can well accompany the general course in physics given in technical schools, colleges and universities.

L. F. MILLER
University of Minnesota

PROCEEDINGS
OF THE
AMERICAN PHYSICAL SOCIETY

MINUTES OF THE CHICAGO MEETING, NOVEMBER 27–28, 1931

The 173rd regular meeting of the American Physical Society was held in Chicago, Illinois, at the Ryerson Physical Laboratory and Eckhart Hall of the University of Chicago on Friday and Saturday, November 27 and 28, 1931. The presiding officers were Dr. W. F. G. Swann, President of the Society, and Dr. P. D. Foote, Vice-president.

On Friday evening the Physical Society had a dinner at the Hotel Windermere. There were eighty-five present. President Swann presided. The after dinner speakers were H. G. Gale, P. D. Foote, A. H. Compton and H. A. Barton.

Meeting of the Council. At its meeting held on Friday and Saturday, November 27–28, 1931, one person was elected to fellowship, three transferred from membership to fellowship, and thirty-two elected to membership. *Elected to Fellowship:* Willi M. Cohn. *Transferred from Membership to Fellowship:* James W. Broxon, R. A. Castleman Jr., and Louis Thompson. *Elected to Membership:* Hans Benndorf, Mark D. Butler, C. Hawley Cartwright, Merril Distad, Allice Hartley, Malcolm H. Hebb, Raymond G. Herb, Lyman B. Johnson, Shannon Jones, Louis C. Jordy, S. Kalandyk, Atusi Kobayasi, Henry N. Kozanowski, Mary Louise Kropp, Robert A. Merrill, Zen'emon Miduno, Henry J. Miller, Nubuo Motida, L. A. Murray Jr., Gladys I. Nason, Saizo Ohno, Gerald L. Pearson, Edith H. Quimby, Masaaki Sasao, Gordon B. B. M. Sutherland, D. C. Swanson, G. A. Van Lear Jr., I. Walerstein, Sinzi Watanabe, F. Lorraine Yost, Hughes M. Zenor and William A. Zisman.

The regular scientific program of the Society consisted of 57 papers, numbers 17, 19, 32, 33, 41, 49 and 52 were read by title. Paper number 33 as printed in Bulletin, Vol. 6, No. 5, was removed from the Proceedings at the request of the author. The abstracts of these papers are given in the following pages. An **Author Index** will be found at the end.

W. L. SEVERINGHAUS, *Secretary*

1. X-ray diffraction of ethyl ether at the critical temperature. WALDEMAR NOLL, *University of Iowa.*—X-ray diffraction ionization curves were obtained for ethyl ether at 43.16 kg/cm² pressure with temperatures in the range from 25°C to 210°C. Liquid and gas types of curves were obtained. In the former case, there is a broad peak at 7.5° at 25°C with a decrease in the direction of both smaller and larger angles. In the gas type, the curve from a point near 0° falls rapidly with increasing angle but with the slope decreasing in magnitude. Immediately below the critical temperature is a combination of the two types, falling rapidly near 0°, then rising to a distinct peak and again falling with increasing angle. Because of the accentuation of general radiation by transmission through the aluminum vessel, the position of the peak is not that caused by ether alone, about 8.5° Mo$K\alpha$. If the height of peak be plotted with temperature,

the curve has a course much similar to that of the latent heat of vaporization-temperature curve, decreasing more and more rapidly to the limiting value, zero, at the critical temperature. The experiments are in accord with the view of "cybotactic grouping" of the molecules occurring through the action of all the molecular forces including those which delineate the volume of a molecule.

2. X-ray diffraction with the two liquid phases of ethyl ether and nitrobenzene. G. W. STEWART, *University of Iowa.*—Wolfke and Mazur have found two liquid phases in ethyl ether and in nitrobenzene. The temperatures of transformation at atmospheric pressure are respectively -105.4°C and 9.5°C. The corresponding freezing points are -117.2°C and 5.7°C. The value of the latent heat of transformation for ethyl ether is 0.07 cal./gram and for nitrobenzene is unpublished. X-ray diffraction measurements, using Mo$K\alpha$ radiation, were made in the neighborhood of these transformation points with the result that distinctly rapid changes in the cybotactic groups were found for the ethyl ether and a noticeable change for the nitrobenzene. The x-ray diffraction measurements of liquids in general show a variation of "grouping" of the molecules with temperature. It becomes apparent that this variation may not always be continuous and when discontinuous may be accompanied by a latent heat of transformation. The statistical mechanism of the transformation is understood if explained in terms of the cybotactic groups.

3. A 600 k.v. x-ray plant. F. K. RICHTMYER, H. A. BARTON, AND M. T. JONES, *Cornell University.*—A 600 kv, two-section x-ray tube with an induction coil voltage source has been described in the General Electric Review by Dr. W. D. Coolidge. This tube has been loaned to Cornell University. The installation is in a separate building so situated that no lead housing for the tube is necessary. The walls of the building are of thick stone. Rays going through windows and roof will pass above all other structures. The distance to the latter is such that inverse square law provides ample protection from scattered rays. The door of the building is in the shadow of a lead house—to protect operator and instruments—of which the exposed wall is $\frac{1}{2}$ inch thick while sides, back and roof are $\frac{3}{8}$ inch thiick. All operations are carried out from the operator's house by remote control of a special power switchboard. Visual operation is provided by a periscope arrangement. Door switches, water switches, interlocking control relays, and other safety devices provide against accidents to persons or plant. The size of the focal spot is varied by means of a magnetic focusing coil and may be made as small as one centimeter diameter for a tube voltage of 500 kv.

4. Comparison of 700,000-volt x-rays and gamma-rays. G. FAILLA, *Memorial Hospital, New York.*—The cascade x-ray tube developed by Dr. Coolidge, of the General Electric Company, has been in operation at the Memorial Hospital since June. The tube is designed for a maximum voltage of 900,000 volts, and has been run at 850,000 volts for short intervals. It can be operated conservatively and for long periods of time at 700,000 volts and 5 milliamperes. The radiation output of the tube has been determined both as to intensity and quality, at different voltages. At 700,000 volts and 5 milliamperes the radiation emission, through a filter of 5 mm of copper, is equivalent to the gamma-ray emission of 400 to 600 grams of radium, depending on the criterion of equivalence chosen. This radiation can be measured by ionization after passing through 4 cm of lead. With the tube running several hours a day, the question of protection of personnel assumes great importance. The protective means employed will be illustrated. Absorption curves for different materials will be shown. These were determined under comparable conditions for x-rays at 200,000 to 725,000 volts and gamma-rays of radium.

5. Discrepancies in M-series absorption edges of heavy elements. CHARLES WHITMER, *Olivet College.*—The M_3, M_4, and M_5 absorption edges have been measured for tantalum. The theoretical positions of these edges as computed from the L_3 edge differ by 2.9 units (in terms of ν/R) for the M_4 and M_5 edges; the discrepancy for M_3 in within the experimental error. The M_1, and M_2 edges could not be measured. These results agree with other results obtained at Iowa and at Upsala, showing quite generally among the heavier elements discrepancies of several units for the M_4 and M_5 edges and comparatively small ones for the M_1, M_2 and M_3 edges. Siegbahn explains these discrepancies as due to line absorption by M_2 and M_3 electrons involv-

ing transitions to the $O_{4,5}$ levels which are known to be unfilled for the elements below gold. The explanation probably does lie in line absorption but the particular transitions postulated by Siegbahn scarcely account for the results. The M_5 level more nearly represents true ionization than does the L_3 and may well be used as a reference level.

6. Peripheral x-ray levels of the heavy elements. J. A. ELDRIDGE, *University of Iowa.*—The discrepancies found in x-ray absorption levels are accounted for if it is assumed that electrons can only be displaced in absorption from the $M_{4,5}$ levels to levels in the energy diagram above the Sommerfeld free electron layer but from levels of smaller eccentricity transitions to other lower postulated levels are permitted. Such results throw much light upon the arrangement of the outer electrons in the elements of high atomic number. For the heaviest elements, thorium and uranium the transitions are all within the free gas layer and the discrepancies consequently smaller.

7. Variation in the effective lattice constant of crystals with wave-length. J. M. CORK, *University of Michigan.*—This investigation is carried out in order to determine if x-ray wave-lengths as recorded, based upon angular measurements with a calcite crystal, possess an appreciable error with wave-length due to a variation in the refractive index of the crystal. To this end the reflection angles for particular emission wave-lengths up to 5.5A are observed using a quartz crystal. These angles are combined with the recorded measurements of these same wave-lengths obtained with a calcite crystal. The value for log $[\lambda_{\text{calcite}}/2 \text{ Sin } \theta_{\text{quartz}}]$ when plotted with wave-length yields a curve with a discontinuity at a wave-length corresponding to the K absorption edge of calcium. It is shown that the shift in value of this ratio at the absorption edge is in the opposite sense to what would be expected from the generally accepted theory of refraction. A similar conclusion follows regarding the results of Siegbahn and Hjalmar in comparing calcite and gypsum. The dispersion theories of Kallmann and Mark and Kronig account satisfactorily for the discontinuity as observed.

8. The thermal motions of atoms in crystals. B. D. HOLBROOK, *University of Chicago.* (*Introduced by A. H. Compton.*)—The theory of the effect upon reflection of x-rays by crystals of the thermal motions of the atoms is reexamined, and an expression obtained for the distribution of the atom-centers about their mean positions; this expression involves only quantities directly obtainable from measurements (1) of the reflecting power of crystals for x-rays, (2) of the scattering of x-rays by gases. The distribution function is evaluated for a particular case, using for (1) data on the reflecting power of KCl at two temperatures, and for (2) data on the scattering of x-rays from argon; the results show that the atoms possess considerably more translational energy than is predicted by the classical theory, thus indicating the presence of zero-point energy.

9. The distribution of x-ray reflecting power in quartz crystals. CHARLES S. BARRETT AND CARL E. HOWE, *Naval Research Laboratory, Washington, D. C.*—In the study of the phenomena recently observed by Fox and Carr in piezoelectric quartz oscillators, Nishikawa, Sakisaka and Sumoto and independently ourselves, observed that non-oscillating crystals yielded Laue spots that were doublets, oscillating crystals yielded solid spots. This indicated increased reflecting power of the entire crystal due to a reduced extinction of x-rays in the crystal lattice during oscillation. Further photographs with improved conditions indicate that in general Laue spots from oscillating crystals have a fine structure. The nature of the fine structure is such as to indicate that the increase of reflecting power of a given plane varies greatly from point to point in the crystal. At a given locality in the crystal the reflecting power of different planes is increased in different amounts with a resultant intensity distribution unlike that obtained from ground surfaces, but resembling that obtained from a non-oscillating crystal under elastic inhomogeneous strain. The intensity distribution from ground surfaces is explicable as the result of randomly directed strains in the surface. It may therefore be possible, with observations such as these (or similar ones taken stroboscopically), to analyze the distortions throughout the interior of quartz oscillators and resonators and other inhomogeneously strained crystals of suitable perfection.

10. Diffuse scattering of x-rays from sylvine at low temperature. G. E. M. JAUNCEY AND G. G. HARVEY, *Washington University, St. Louis, Mo.*—With a modification of the photographic method described by Claus the authors have compared the intensities of x-rays of wave-length 0.43A diffusely scattered from sylvine at angles in the range 25° to 90° at a temperature of 90°K with the intensities at these same angles at a temperature of 300°K. Jauncey and Harvey have shown that the intensity of the diffusely scattered rays should be given by

$$S = S' - F^2/Z,$$

where S' is independent of the temperature and F is the atomic structure factor containing the effect of thermal agitation. By using James and Brindley's F values at 90°K and 300°K theoretical values of S at 90°K have been calculated. The experimental values of S at 90°K are lower than the theoretical values. This result is in accord with that found by Claus for rocksalt. Plotting log $(S'-S_1)/(S'-S_2)$, where the subscripts refer to the two temperatures, against $(\sin^2 \phi/2)/\lambda^2$ a straight line is obtained whose slope agrees with that required by the Waller and not the Debye formula for the temperature effect. It is impossible by means of this experiment to show whether or not there is zero point energy. In order to do this an assumption concerning the electron distribution in the atom must be made.

11. Absorption of soft x-rays in air, oxygen, and argon. R. G. SPENCER, *The University of Chicago.* (*Introduced by Elmer Dershem.*)—A crystal spectrograph of high resolving power for measuring absorption coefficients of soft x-rays in gases has been constructed. Absorption measurements have been made for air, oxygen, and argon for four spectral lines of wave-lengths 1.537, 2.284, 4.145, and 6.973A. By using general radiation, absorption coefficients have been measured in the regions immediately adjacent to the K absorption limit of argon within 0.002A of the limit on each side of it. No departure from the ordinary absorption law greater than experimental error was found in these regions. The magnitude of the K absorption discontinuity of argon has been measured by a method which does not depend upon the extrapolation of curves to the limit. The following table gives the absorption coefficients obtained for both spectral lines and general radiation.

	1.537A	2.284A	3.716A	3.8637A	3.8677A	3.946A	4.145A	6.973A
Air	9.54	29.3					168.	747.
Oxygen	11.6	35.5					221.	971.
Argon	112.	344.	1320.	1465.	147.	151.	171.	762.

12. The effect of temperature on the absorption bands of benzene and some of its derivatives at low temperatures. A. H. CROUP, *University of Pittsburgh.*—The ultraviolet absorption spectra of benzene and the derivatives, ortho, meta, and para dichlorbenzene, were investigated throughout the temperature range from −190°C to 20°C. The behavior of the spectra of the four compounds is very similar. They all show a number of unresolved major and minor absorption bands. Both the frequency and the intensity of these bands increase with a decrease of temperature. The temperature-frequency curves are all approximately represented by parabolic equations, except in the neighborhood of their melting points. The frequency difference between the bands remain constant with temperature within the limits of the experiment and agree favorably with those found by other spectroscopic methods. If these frequency differences are due to the vibrational transitions within the molecule, this spectral shift due to temperature cannot be accounted for on the basis of a change in the inner vibrational terms, as has previously been suggested. A preliminary theoretical discussion based on a recent paper of Pauling, shows that this shift may be due partly to a perturbed rotational motion of the molecule.

13. Band spectrum of potassium hydride. G. M. ALMY AND C. D. HAUSE, *University of Illinois.*—The band spectrum of potassium hydride has been photographed with a glass-prism, E−1 Hilger spectrograph. The source was a 220-volt d.c. arc in hydrogen at a pressure of a few mm of mercury. The spectrum obtained extends from 4100A to 5100A and is similar to the $^1\Sigma \rightarrow {}^1\Sigma$ systems of LiH and NaH. A short-exposure plate on which the spectrum extends

from 4300A to 4900A has been analyzed. The spectrum consists of nine overlapping bands belonging to a single v' progression. The assignment of vibrational quantum numbers cannot be made from the present data. ω_x (where x is simply the number of the band and differs by a constant integer from the true $v'+\frac{1}{2}$) follows the relation:

$$\omega_x = 285.63 + 3.72x - 0.388x^2 - 0.0295x^3 + 0.0035x^4$$

ω_x rises to a maximum (as in LiH and NaH) before falling off in the conventional manner. The rotational analysis shows, (1) that the bands consist of P and R branches only so that the system is doubtless due to a $^1\Sigma \rightarrow {}^1\Sigma$ transition, (2) a great difference in the values of B and equilibrium distance (r_e) for the upper and lower states. The constants obtained are:

$$B_x' = 1.432 - 0.001x^2 \qquad B'' = 3.379$$
$$D' = -1.44 \times 10^{-4} \qquad D'' = -1.7 \times 10^{-4}$$
$$F' = 4.0 \times 10^{-8} \qquad F'' = 1.4 \times 10^{-8}$$
$$r_e' \cong 3.47 \times 10^{-8} \text{ cm} \qquad r_e'' \cong 2.26 \times 10^{-8} \text{ cm}.$$

14. Spectrum of strontium hydride. WILLIAM W. WATSON, *Yale University*, AND W. R. FREDRICKSON, *Syracuse University*.—A metallic strontium arc in a hydrogen atmosphere yields three groups of bands in the near infrared with main heads at 7020A, 7347A, and 7508A. Analysis shows that the latter two constitute a $^2\Pi \rightarrow {}^2\Sigma$ system with only the (0,0) and (1,1) bands, while the first group represents a transition from a higher $^2\Sigma$ to the same ground $^2\Sigma$ level. Analysis of the (0,0) bands shows that the $^2\Pi$, $^2\Sigma$ band is similar to that of BaH, the constants being $A=299$, $B_0''=3.620$, $D_0''=1.29\times10^{-4}$, $B_{0,+\frac{1}{2}}^{*}=3.6787$, $p_0=-3.92$, and $q_0=-0.40$, with all figures subject to slight correction. The very large negative p_0 and q_0 indicate interaction with the near higher-lying $^2\Sigma$ level, and the corresponding large doubling of this level is exhibited in the structure of the 7020A band. This is much the largest doubling yet found in a $^2\Sigma$ level. The relative positions of the $^2\Pi$ and $^2\Sigma$ levels in CaH, SrH, and BaH and the atomic levels of Ca, Sr, and Ba suggest $\cdots d\sigma$ for the upper $^2\Sigma$ level.

15. Spectrum of barium hydride. W. R. FREDRICKSON, *Syracuse University*, AND WILLIAM W. WATSON, *Yale University*.—High dispersion spectrograms have been obtained of a BaH band system in the region 6925–6380A, the source being a metallic barium arc in a hydrogen atmosphere. The (0,0), (1,1), and (2,2) bands only are present. Analysis of the (0,0) band shows the system to be the expected $^2\Pi \rightarrow {}^2\Sigma$ case a type with twelve branches in each band. The Λ-type doubling is large in the $^2\Pi_{1/2}$ state, but small and of opposite sign in the $^2\Pi_{1\frac{1}{2}}$ state, giving $p_0=+0.85$ and $q_0=+0.0067$. The spin doubling is regular and gives $\gamma_0=+0.186$. Evaluation of the molecular constants from the $2\Delta F$ term differences gives $B_0''=3.404$, $D_0''=-9.61\times10^{-5}$; $B_{0,+\frac{1}{2}}'=3.4468$, $D_{0,+\frac{1}{2}}'=-1.13\times10^{-4}$; $B_{0,-\frac{1}{2}}'=3.5156$, $D_{0,-\frac{1}{2}}'=-1.20\times10^{-4}$. The separation of the two $^2\Pi$ sublevels, calculated in the usual way, yields $A=462$, as compared with $A=832$ for the ^3P levels of Ba. A large perturbation in one of the $^2\Pi_{1\frac{1}{2}d}$ levels, and the sign and magnitude of the p_0 and q_0, indicate another lower-lying excited level for BaH.

16. Heats of dissociation of Na_2 and K_2. R. E. NUSBAUM AND F. W. LOOMIS, *University of Illinois*.—The apparatus constructed to produce the magnetic rotation spectrum of Li_2 has now been employed to study those of Na_2 and K_2, and in particular to extend the spectra to the high v' levels of the excited state which are used in extrapolating towards dissociation. As with lithium, it is found that, near the limit, convergence takes place more rapidly than any simple polynomial extrapolation would indicate. For this reason Loomis' previous estimate of the heat of dissociation of sodium (1.0 ± 0.1 volts) and Crane and Christy's estimate for potassium (0.81 volt) were too high. The present measurements extend much further, coming within 0.03 volt of the estimated dissociation in the case of sodium and within 0.02 volt in the case of potassium. The heats of dissociation measured from the zero level of the normal state are, for sodium 0.76 ± 0.02 volt, for potassium 0.51 ± 0.02 volt. The value for sodium agrees closely with the best evidence from chemical data. That for potassium is in accord with the fact that density measurements of potassium vapor do not show a measureable amount of molecules.

17. Absolute value of transition probabilities in band spectra. R. LADENBURG, S. LEVY AND G. WOLFSOHN, *Kaiser-Wilhem-Institut f. physik. Chemie, Berlin-Dahlem.*—By measuring anomalous dispersion near many lines of the red Li_2- bands we have determined the number of corresponding oscillators of the rotation lines. Calculating approximately the number of molecules in the rotational levels we find f-values of about 1/30–1/100 and transition probabilities (A-values of Einstein) of about 3×10^6. On the other hand we get no effect on the dispersion near the Schumann band lines of oxygen ($\simeq$. 1900A) at atmospheric pressure as measured with a fluorite interferometer. The transition probabilities of these lines are therefore relatively small (smaller than 10^3). The absolute determination of the dispersion over the region from the visible to 1900A shows that the main absorption band of oxygen with high transition probabilities lies below 900A, as one would expect from the spectra of oxygen atoms and molecules.

18. A new criterion for predissociation. JOSEPH KAPLAN, *University of California at Los Angeles.*—From time to time the writer has reported some striking deviations from the intensity distributions predicted by the Franck-Condon principle. This phenomenon has been convincingly shown in the experiments of Lord Rayleigh and others on the afterglow of nitrogen in rare gases and also in the present writer's experiments on the emission spectra of nitrogen-oxygen mixtures. An explanation of this phenomenon is of considerable importance because it provides an interpretation of the striking role of rare gases in many experiments on the excitation of molecular and atomic spectra. It is shown that the effect can be interpreted as a criterion for predissociation, which is especially valuable in cases in which the probability of predissociation is not high enough to quench the emission bands completely, or to produce diffuseness in the rotational structure of the absorption bands. Experiments have been performed which show that predissociation is sensitive to excitation conditions. As a result of these experiments an explanation is obtained for certain astrophysical spectra in which the deviations from the predictions of the Franck-Condon principle are so large as to make the identification of some of the bands difficult.

19. The dissociation of nitrous oxide by light, and the electronic levels of O_3, N_2O and NO_2. OLIVER R. WULF AND EUGENE H. MELVIN, *Bureau of Chemistry and Soils, Washington, D. C.*—Nitrous oxide in long paths has shown no absorption over the region 10,500A to about 2000A where the absorption previously observed by Leifson (Astrophys. J. **63,** 73 (1926)) occurs. In the present work this has been observed to as long wave-lengths as 2300A. The absorption of this radiation leads to the appearance of the gamma bands of NO in absorption in the gas, and it is shown that the elementary act accompanying the absorption of this radiation is very probably the dissociation of N_2O into NO and N. Certain rather striking similarities are pointed out between the electronic levels of O_2 and O_3, and with this in mind, the electronic levels of N_2O and NO_2 are discussed.

20. The enhancement of the iodine absorption spectrum by the admixture of oxygen. F. W. LOOMIS AND H. Q. FULLER, *University of Illinois.*—When oxygen at atmospheric pressure, or even a few centimeters, is added to a tube containing iodine, many of the iodine absorption bands are greatly enhanced. The effect is under certain circumstances so pronounced that a considerable change of color of the iodine is apparent. The enhancement is appreciable only for bands with $v'>12$ and begins at about this number in each of the progressions $v''=0$, 1, 2. It reaches a maximum at roughly $v'=25$ and thereafter decreases. The shape of this curve is very similar to that which Turner found for the quenching of iodine fluorescence by a magnetic field, and it is believed that the explanation of the effect is as follows: The oxygen, possibly by the magnetic fields of its $^3\Sigma$ molecules, relaxes the selection principle and allows the excited iodine molecules with $v'>12$ to predissociate. This shortens the lives of such molecular states and correspondingly broadens the absorption lines leading to them. The effect of broadening a very narrow absorption line, at the center of which nearly 100 percent of the light is being absorbed, is to increase the total amount of light absorbed. It is believed that this increase of absorption due to broadening offers a convenient means of locating and studying such induced predissociation effects. This phenomenon affords an explanation of Ramsauer's apparent observation that admixture of oxygen not only quenched iodine fluorescence, but that it weakened the various lines of a fluorescence series unequally. Actually the effect was due to reabsorption of the fluorescence lines while getting out of the iodine, this reabsorption being irregular along a fluorescence series, and being greater when oxygen was present.

21. Duration of afterglow in nitrogen. CHARLES. T. KNIPP, *University of Illinois.*—A 22-liter Pyrex flask was prepared with a stem about 2 meters long and about 70 mm diameter. On April 10, 1930, it was pumped out to free it of moisture, and then without further drying or outgassing it was primed with tank nitrogen and sealed off at a pressure which gave the best electrodeless discharge. The exciting coil was permanently wound round the stem about 20 cm from the bulb and consisted of 7 turns of heavy lamp cord (No. 10) taken double. The flask with its stem was energized by damped oscillations from a motor-generator high-voltage high-frequency set. The bulb thus prepared has been under observation over an extended length of time, and has been flashed (duration about 0.1 sec.) but *three times since* the initial flash, resulting in the following data:

Date	Total interval	Duration of afterglow
April 10, 1930	0 days	35 min
Aug. 12, 1930	122 "	110 "
March 4, 1931	324 "	187 "
Oct. 18, 1931	553 "	165 "

Apparently the duration of the afterglow reached a maximum in about a year. The observations are to be continued.

22. The Paschen-Back effect of hyperfine structure, I. Thallium II and thallium III. J. B. GREEN, *Ohio State University,* AND JOHN WULFF, *Massachusetts Institute of Technology.*—The Zeeman effect of thallium spark lines has been studied at field strengths of 14,700, 32,500, and 43,350 gauss with the 21-foot concave grating and large Weiss magnet of the University of Tübingen. In particular, λλ 3092, 2531, 2298 and 5950 of Tl II and 4110 of Tl III show exceptionally good agreement with Goudsmit and Bacher's theory of the Paschen-Back effect of hyperfine structure. λ3092 is especially suitable as a test of the theory since it is the simplest example of this effect, being a transition from $j=1$ to $j=0$ and involving a nuclear moment $i=1/2$, the smallest value yielding a hyperfine structure.

23. The Paschen-Back effect of hyperfine structure, II. Bismuth II and bismuth III. JOHN WULFF, *Massachusetts Institute of Technology,* AND J. B. GREEN, *Ohio State University.*—As a continuation of the work on the spark lines of thallium, the spark lines of bismuth were chosen. The Zeeman patterns of these lines are much more complicated, since the nuclear moment of bismuth is 9/2. In particular, the lines λλ5719 of Bi II and 4561 and 3695 of Bi III were investigated because of the rather large hyperfine structures involved in the transitions, and the sharpness of their magnetic patterns. An excellent agreement between theory and experiment was noted.

24. The polarization of mercury resonance radiation. L. LARRICK AND N. P. HEYDENBURG, *State University of Iowa.*—The polarization of the line λ2537A of mercury in resonance radiation is calculated on the assumption that isotopes 199 and 201 have nuclear moments of 1/2 and 3/2 respectively, while the even isotopes 198, 200, 202, and 204 have zero nuclear moment as Schüler and Keyston have suggested (Naturwiss. **31,** 676 (1931)). With "broad line" and "narrow line" sources respectively, resonance radiation excited by light polarized with the electric vector parallel to the magnetic field should be 85 percent and 89 percent polarized, in fair agreement with the observations of Olson 79 to 86 percent (Phys. Rev. **32,** 443 (1928)), and von Keussler, 79.5 percent (Phys. Zeits. **27,** 313 (1926)). Relative transition probabilities within a hyperfine multiplett are calculated on the assumption of *LJS* type coupling between *J*, *F* and *I*.

25. Polarization of cadmium resonance radiation. A. ELLETT AND L. LARRICK, *University of Iowa.*—The cadium resonance lines λλ2288 and 3261A excited by unpolarized radiation in a magnetic field parallel to the exciting light beam are found to be 76 percent and 85–86 percent polarized respectively. From spectroscopic evidence Schüler has assigned nuclear moments of 0 and 3/2 to the even and odd isotopes of Cd. Separations in 2288 are small compared to Doppler breadth, while in 3261 the strong component of the 3/2 isotope pattern merges with the 0 isotope line. If we suppose that the introduction of spin does not change the net transition

probabilities between the gross levels concerned these polarization values both yield 2.5 for the ratio of abundance of even and odd isotopes. A recent calculation of C. D. Mitchell leads to other results, but is based on the apparently incompatible assumptions that intensities in the source are proportional to isotope abundance but in absorption are determined by assigning equal weights to Zeeman levels making absorption by the spin isotope twice that by the non-spin isotope for equal abundance and uniform spectral distribution, conflicting with Kirchhoff's law.

26. A note on the origin of continuous cometary spectra. WILLI M. COHN, *A. D. Little, Inc. Cambridge, Mass.*—Different theories concerning the origin of the continuous spectra of comets are discussed. The "solar type spectrum" with a maximum at 4700A may be explained by the reflection from particles contained in the comets large in comparison to the wave-lengths of the incident light. Laboratory experiments show that continuous spectra may be produced by bombardment of ions of different materials with electrons in high vacuum. A theory is developed which assumes that electrons are emitted constantly from the sun. These electrons will give rise to the "violet type spectrum" (maximum at 4000A) and—in the tail at a great distance from the head—to the solar type continuous spectrum observed in comets. The polarization phenomena of the light emitted by comets are explained by the new theory. Continuous spectra of straight and curved tails are expected to differ in the shift of the maximum with growing distance from the head. Band and line spectra observed in comets are assumed to be mainly excited by electrons emitted constantly from the sun.

27. Inner vibrations in molecules from the Raman effect. WILLIAM D. HARKINS AND HAROLD E. BOWERS, *George Herbert Jones Laboratory, University of Chicago.*—The Raman frequency characteristic of a carbon-halogen bond is found in normal compounds to be independent of the length of the chain between two and five carbon atoms. This indicates that the characteristic frequency is related to an inner and not to an outer vibration. A comparison of the values with those for the methyl compounds seems to indicate that the group which vibrates is the $-CH_2$ group adjacent to the halogen atom. However this is affected by the constraints from and the vibrations of the other parts of the molecule. A not too distant branching of the chain reduces the frequency by about five percent. The force constants are calculated as 3.0 for the chlorice, 2.6 for the bromide, and 2.2 for the iodide, in 10^5 dynes per cm, which is much lower than the value of about 5.0 found for the single bonds C.C, C.O, and C.N.

28. Effect of the target on breakdown in cold emission. WILLARD H. BENNETT, *Ohio State University.*—A tube was used in which cold emission was drawn from a fine point to a plane. By means of a magnetic field, the electrons could be prevented from striking the anode in the vicinity of the cathode but the electrons could be forced to strike the anode in parts of the tube well removed from the cathode. After breakdown had been produced, by using unoutgassed electrodes, and the current had been made steady by reducing the electric field slightly, fresh ruptures of the cathode occurred whenever the magnetic field was changed to a value not previously used. The observations can be explained on the basis that breakdown is due to the rupture of the cathode surface by a highly concentrated stream of positive ions which is produced by an initial small electron emission from a point on the cathode near where breakdown occurs, but not directly at it.

29. A new method of determining thermionic work function by photoelectric cell. ROSCOE E. HARRIS, *Lake Forest College.*—A method of determining thermionic work function has been developed which uses a photoelectric cell to identify sameness of temperature. Change of filament wattage upon emission was measured with potentiometer accuracy while the filament was maintained at a constant brightness temperature as indicated by the photoelectric cell. Simultaneous data were obtained for determining the work function from saturation currents, and compared with this latent heat method. The sensitivity was such that one mil change in emission current caused up to 50 mm deflection upon a galvanometer. This method gave consistent values somewhat higher than those obtained by saturation current method, the latter values being similar to those usually accepted. Calculation of the resistance of the filament

indicates an increase of resistance upon emission without change in temperature. The assumption of constant resistance may account for different values obtained by others with the latent heat method. Recent statistical theories indicate that the usually accepted values of the work function may be too small. The working equation used in this method seems to be independent of the statistical theory employed.

30. The emission of positive ions from metals. H. B. WAHLIN, *University of Wisconsin.*—When a tungsten wire containing uranium dioxide was heated to a temperature of about 1800° C three types of ions were observed by a magnetic deflection method, U^+, W^+, and an ion of mass 254 ± 2. This is probably UO^+. Assuming this to be the case it seems more probable that an ion of mass 247 ± 2, which was observed when thoriated tungsten was heated and which has been reported earlier, is ThO^+. An investigation of the positive ions from Cu and Ag has shown that at a temperature just below and persisting above the melting point, ions of the metals themselves are emitted. This characteristic ion current is small compared with that due to alkaline impurities.

31. Spurious contact potentials and "trapped" electrons. W. B. NOTTINGHAM, *Massachusetts Institute of Technology.*—The contact potential between a thoriated filament and a nickel collector has been observed to depend on the "history" of the current flow to the collector. This experimental result can be explained by assuming a potential barrier near the nickel surface following the mirror image law from infinity to within about 3×10^{-7} cm, joining a potential function with a minimum and a maximum following the Fowler-Nordheim theories of composite surfaces, an experimental test of which was reported at the Schenectady Meeting. Electrons caught in the potential valley are assumed to run over the surface as a two dimensional gas producing a change (Δv) in the effective contact potential of approximately $\Delta v = 4\pi ned$ (n = number of electrons per cm²; d = width of potential hill separating electrons from metal). The valley is "populated" by allowing a large current to flow to the collector for a time assuming that a small number of electrons fall into the valley. Experimentally determined "mean lives" of electrons in the valley are $t_1 = 5{,}000$ sec. and $t_2 = 200$ sec. The formula,

$$t = 1/f \exp\left\{\frac{4\pi}{h} \int (2m(V - W))^{1/2} dx\right\},$$

where $(V-W)$ is the difference between the electron energy and the potential function depending on x, and f is the number of approaches to the potential hill made by an electron per sec., can be used to calculate t for any particular potential barrier. It has been found possible to construct a potential barrier of "atomic dimensions" for which the observed mean lives are the appropriate ones for the lowest and the next lowest "quantized" states in the valley. This theory explains certain changes in the current flowing in FP-54 pliotrons and many other results in experiments involving contact potentials.

32. Electric oscillations in ionized gases—some remarks on their present theories. J. KUNZ, *University of Illinois.*—The frequency of oscillations in ionized gases is given by

$$\cdots \omega^2 = 4\pi(e^2/m)N, \tag{1}$$

ω being the frequency per 2π seconds, N the number of electrons per cm³, e the charge, and m the mass of the electron. The theory of Sir J. J. Thomson and I. Langmuir and L. Tonks can be applied also to a gas containing mostly positive ions and finally to a gas containing positive and negative ions. Let E be the electric force acting in the gas, $E = E_0 \cos \omega t$, i be the current, $i = Neu$, where u is the velocity of the electrons, $u = [Ee/(\omega m)] \sin \omega t$, then $i = N(E_0e^2/\omega m) \sin \omega t = I \sin \omega t$, where the amplitude of the alternating current

$$I = NE_0e^2/(\omega m). \tag{2}$$

But from (1) and (2), $Ne^2/m = I\omega/E_0 = \omega^2/4\pi$, or

$$\omega = 4\pi I/E_0. \tag{3}$$

For a constant electric force E_0 we see that the frequency is proportional to the alternating current I. We next assume that the density ρ of negative ionization over a distance l shall be

constant. Then we can write, $\omega^2=4\pi\rho e/m$, and $E=-4\pi\rho\omega x=-dV/dx$ and the potential difference $V=2\pi\rho l^2$, or $\rho=V/2\pi l^2$ and $\omega^2=(2eV)/(ml^2)=(2\pi c/\lambda)^2$, hence

$$\lambda = 2\pi cl(m/2e)^{1/2}V^{-1/2}. \tag{4}$$

We compare this last result with the original wave-length determined by Barkhausen and Kurz for the short oscillations in three electrode tubes. They found that the oscillations could be explained by the assumption that individual electrons oscillate between the filament and the grid or the plate and that the corresponding wave-length λ is equal to

$$\lambda = 2cl(m/2e)^{1/2}V^{-1/2}. \tag{5}$$

Their formula differs from (4) by a factor π. In this paper, I hope to offer further considerations regarding the coupling of these oscillations with external circuits.

33. Electron oscillations in thermionic tubes. J. T. TYKOCINER AND A. E. ABEL, *University of Illinois.* (Abstract withdrawn.)

34. A thermionic frequency doubler. C. K. STEDMAN, *Purdue University.*—The output voltage of a thermionic tube operated over a suitable restricted range of grid voltages may be represented approximately by the parabola $e_p=b_0+b_1e_g+b_2e_g^2$. By adding in opposite phase the output of another tube, operated on the straight line portion of its curve, we may balance out entirely the term b_1e_g, so that the characteristic of the combination of tubes is $e_c=b_0+b_2e_g^2$. The system will then operate as a frequency doubler, for the output is proportional to e_g^2 alone. With a 201A tube an output of 0.175 volts of frequency $2f$ is obtained from an input of 1.0 volts of frequency f. It is found that when the characteristic of the system is plotted, the curve is never a symmetrical parabola $e_c=b_0+b_2e_g^2$ over a very wide range of grid voltages, because the coefficient of the cube term in the equation of the tube characteristic is not negligibly small, and the equation must be written $e_c=b_0+b_2e_g^2+b_3e_g^3$. It is shown how the coefficient b_3 may be determined by measuring the dissymmetry of the curve. Since b_2 governs the amount of desired second harmonic, and b_3 the amount of third harmonic distortion in the output, a good figure of merit for the frequency doubler is b_2/b_3. With the tubes tested this quantity varied from 45.0 to 6.0. In the case of the 201A tube mentioned above $b_2=0.35$ and $b_3=0.0085$.

35. Automatic voltage control by means of a photoelectric cell. H. T. CLARK AND W. KOHLHAGEN, *Purdue University.*—The method described by Lark-Horovitz and Sherman some time ago (Phys. Rev. **32,** 328 (1928)) for regulation of voltage by the use of a photoelectric cell in connection with a mechanical device has been modified by using electrical control throughout. The photoelectric current is amplified by two stages of screen grid amplification directly coupled and a last power stage consisting of four 250 tubes in parallel. The plate current is used as a variable shunt across an external resistance in series with the field of a 500 cycle generator; and the potential drop across this resistance furnishes the plate voltage for the power tubes. The maximum plate current, using 175 volts drop across the power tubes, is about 360 milliamperes—more than one third of the field current required for normal voltage output. The sensitivity reached is about 200 milliamperes for a change in light of 0.35 lumens.

36. A new Wilson apparatus for the photography of alpha and beta-ray tracks. DAVID M. GANS, WILLIAM D. HARKINS, AND D. A. WALLACE, *University of Chicago, Dept. of Chemistry.*—A large Wilson ionization chamber, 17 cm in diameter, has been constructed in this laboratory for operation at gas pressures from 4 cm of mercury to several atmospheres, in order to show the disintegration and synthesis of atomic nuclei and to give greater accuracy in the study of the quantum relations of the nucleus. In the design are included ideas developed by Wilson, Shimizu, Harkins and Ryan, Petrova, Hippel, and others. The action is entirely mechanical and periodic, and the principal feature is the fact that every important operation can be timed with considerable accuracy by a simple mechanism. The shutter which admits alpha-rays lies entirely within the chamber, and is operated accurately by two electromagnets that lie outside. This avoids surges in the gas, which have been the cause of considerable inaccuracy in earlier forms of apparatus that operated continuously. A pressure of one-half atmosphere is used to give greater accuracy in the measurement of angles than can be obtained at higher pressures. Still lower pressures may be used as easily, but lower the number of inelastic nuclear collisions obtained.

37. On the structure of vitreous oxides. W. H. ZACHARIASEN, *University of Chicago.*—Of all the different oxides X_mO_n only a limited number have been prepared in the vitreous form. This fact can be explained on the basis of the hypothesis that the atomic arrangement in vitreous solids is characterized by extended three-dimensional networds that differ from the crystalline networks by the absence of periodicity and symmetry. We consider the oxides to be built up of oxygen polyhedra which are formed around the atoms X. The periodicity and symmetry of crystals arise from the fact that the oxygen polyhedra share corners with each other in such a way that the polyhedra assume definite relative orientations. The formation of a vitreous solid thus will depend upon the nature of the polyhedra and the way in which they link together. In the case of individual oxides the conditions for the formation of glass can be expressed in the following simple rules: (1) Two polyhedra have not more than one corner in common, (2) An oxygen atom is linked to not more than two atoms X, (3) The number of corners in each polyhedron is small, probably less than six, (4) At least 3 corners in each polyhedron are shared with other polyhedra. Only the following oxides satisfy these requirements: B_2O_3, SiO_2, GeO_2, P_2O_5, As_2O_5. Some doubtful ones are P_2O_3, As_2O_3, V_2O_5, Sb_2O_5, Cb_2O_5, Ta_2O_5, Sb_2O_3. Vitreous modifications have been observed for B_2O_3, SiO_2, GeO_2, P_2O_5, As_2O_5, As_2O_3, in excellent agreement with the derivation. Many properties of glasses can be accounted for on the basis of the hypothesis proposed. Investigations on the composition and properties of general types of glasses are in progress.

38. On the detection of inhomogeneities in the magnetization of iron. FRANCIS BITTER, *Westinghouse Research Laboratory, East Pittsburgh, Pa.*—A method has been developed for detecting inhomogeneities in the magnetization of ferromagnetic materials. This consists of allowing small permanently magnetized particles of Fe_2O_3 (approximately 10^{-4} cm in diameter) suspended in alcohol to settle gently on a magnetized surface. At a certain critical magnetization the suspension settles in parallel straight lines whose direction varies from grain to grain. These lines are usually more or less perpendicular to the direction of magnetization. Within a single grain the spacing is regular and usually in the neighborhood of 0.1 mm. The lines do not turn when the direction of the field is changed, but gradually disappear and new sets of lines appear. It is improbable that they have anything to do with slip planes, first because they are not always perfectly straight, and secondly because they have been observed on the surface of a melted sample that was never subjected to any mechanical treatment whatever. For large magnetizations the lines degenerate into irregular spots elongated at right angles to the direction of magnetization and do not stop at grain boundaries. It is suggested that the observed patterns are due to a periodicity inherent in the nature of magnetization.

39. The Hall effect on induced currents in circular disks of bismuth and antimony. CARL A. BECK, *Northwestern University.*—Corbino (Phys. Zeits. **22,** 561 (1911)) found this induced effect in bismuth. According to his theory, the quantity of electricity which flows radially is $-(1/8\pi R)c_H SH^2$, where R is the resistance of the galvanometer circuit, and c corresponds to the final field, H. Thus the equivalent change of flux in this circuit is $N=(-c_H SH^2)/8\pi$. On the other hand, K. K. Smith deduced the formula, $N=-S/4\pi\int_0^H cHdH$. These expressions agree only if the coefficient c is independent of H. Experiments on bismuth show that the value of the coefficient in the first formula is always greater than that derived from the second. For the coefficient decreases as the field increases, and the value calculated from the first formula corresponds not to the final field but rather to a weaker field. By using rectangular plates cut from the circular disks, one finds, with steady currents and steady magnetic fields, that the ratio of Hall coefficient to resistivity agrees more nearly with the coefficient derived from the second formula than with that from the first. In antimony the induced effect has been found. It is small and opposite in sign to that in bismuth. The coefficient decreases only slightly as the field increases.

40. Supercooling liquid copper. J. J. HOPFIELD, *Chicago, Ill.*—A striking example of supercooling is provided by liquid copper. I know of no other case where this phenomenon is shown by the change in brightness of a body. The apparatus necessary is a glass rod (preferably Pyrex) with a globule of copper fused into it, and a blast lamp using oxygen. The demonstra-

tion is as follows: the glass containing the metal is heated until the copper is melted and then removed from the flame. If the copper sphere has a diameter of 2 mm or more it cools about 40°C below its melting point, and then flashes bright remaining so while solidification is taking place. Under suitable conditions this supercooling of copper may furnish a handy reference point in calibrating optical pyrometers. After the initial flash there may be a weak second flash, probably due to copper oxide. The supercooling is greater for smaller droplets, and the flashing time is shorter. Supercooling in copper does not depend primarily on pressure for it occurs even at atmospheric pressure. It depends upon the purity of copper. Copper alloyed with about ten percent of gold or silver does not show it. Under the conditions studied neither gold nor silver shows the effect.

41. Thermal expansion of electrolytic chromium. PETER HIDNERT, *Bureau of Standards.*—The linear thermal expansion of a 300 mm tube of electrolytic chromium prepared here by G. E. Renfro was investigated between 20 and 500°C. The composition determined by R. M. Fowler was as follows: Chromium 99.3, silicon 0.002, iron 0.002 percent, manganese, lead and copper not detected. Chromium produced here under similar conditions was found by H. C. Vacher to contain about 0.1 percent hydrogen. Further tests will be required to identify the remaining 0.6 percent in this material. During the first expansion test the chromium tube contracted considerably on heating to 500°C due to evolution of hydrogen. After cooling to 20°C, the tube was 1.1 percent shorter than before heating. The following coefficients of expansion were derived from the observations on heating in the second and third tests.

Temperature range (°C)	Average coefficients of expansion per degree centigrade	
	Test 2	Test 3
	$\times 10^{-6}$	$\times 10^{-6}$
20 to 60	6.2	5.9
20 to 100	6.8	6.7
20 to 200	7.5	7.5
20 to 300	8.1	8.1
20 to 400	8.5	8.6
20 to 500	8.6	8.8

E. L. Peffer found that the density of a duplicate tube of electrolytic chromium (before heating) was 6.93 g/cm³ at 25°C.

42. A gravitational explanation of the spectral shift of light from very distant stars. HERBERT J. BRENNEN, *Northwestern University.*—In recent years, it has been found that, for light from very distant stars, the spectral shift towards longer wave-lengths is greater, the greater the distance of the star from us. It has been assumed that this shift is due to a Doppler effect but this leaves unanswered the question why all of the very distant stars should be receding from us. However, by assuming nebulae of radii of hundreds of thousands of light years and having densities of the order of 10^{-21} gram per cubic centimeter, it is shown that the spectral shift can easily be explained as merely a gravitational effect and, moreover, equations are derived which show, as a first approximation, that the spectral shift is proportional to the distance of the star.

43. The beryllium molecule. W. H. FURRY AND J. H. BARTLETT, JR., *University of Illinois.*—The existence of a stable diatomic beryllium molecule has not yet been inferred either from band spectra or on theoretical grounds. By an application of the Heitler-London method, which gave good results for Li_2, the writers have previously shown that two normal beryllium atoms repel each other (Phys. Rev. **38**, 1615 (1931)). This work has been extended to the case in which a normal beryllium atom interacts with a beryllium atom having the configuration $2s2p$ (^1P and ^3P states). The K-shells have been neglected and a much more general notation than that hitherto used has been adopted. Even then however the calculation becomes so complicated that its extension to the problem of B_2, where six electrons interact, does not seem practical at the present time. It is found that of the eight molecular states two may give rise to a stable molecule. The lower is a $^1\Sigma$, the other a $^1\Pi$. The heat of dissociation for the $^1\Sigma$ is of the order of two volts.

44. Corpuscular description of electron diffraction phenomena. R. M. LANGER, *University of Minnesota.*—It is generally not sufficiently emphasized that the particle interpretation of experiments on diffraction of electron and atom beams is simpler and more straight forward than the customary wave interpretation. The argument originally given by Duane for x-ray reflection applies equally well for any particles, and the modern conception of a solid justifies the assumption of Duane that momentum can be transferred only in quanta. With this assumption the application of the conservation of energy and momentum leads directly to the Laue reflection formulae. No wave properties of the impinging beams are relevant in any of the experiments thus far performed. This description has the advantage of clarity over the wave formulation especially when the explanations of surface effects, ordinary ruled grating reflections and half order reflections are concerned. The patterns due to single molecules can also be treated without relying on any coherence or interference of the scattered electrons. Losses of small amounts of energy on reflection should occur with considerable probability but the question of their influence on the diffraction pattern has not yet been sufficiently studied.

45. A further generalization in the kinetic interpretation of the Kelvin relations. E. A. UEHLING, *University of Michigan.* (*Introduced by G. E. Uhlenbeck.*)—The derivation of the Kelvin relations for the reversible heat development and the thermoelectric force in anisotropic crystals is shown to depend only on the assumption of the principle of detailed balancing. Previous treatments have been less general. The work of Nordheim is valid only for isotropic materials, and that of Ehrenfest and Rutgers depends on the assumption of elastic collisions between the electrons and the atoms of the metal. These restrictions are shown to be unnecessary. These authors also use special methods of reducing the integral equation which determines the distribution function. In the general case these methods are impossible and prove to be unnecessary. Because of the principle of detailed balancing, the integral equation has essentially a symmetric kernel. By using the formal Fredhohn solution one can derive the electric and heat current equations and prove certain reciprocal relations, from which the Kelvin equations follow. These conclusions may be considered as a substantiation in a special case of the very general considerations of Onsager.

46. The impulse-energy tensor of the Dirac equations. O. LAPORTE AND G. E. UHLENBECK, *University of Michigan.*—Extending our considerations on the applications of the spinor analysis to Dirac equations (Phys. Rev. **37,** 1380 (1931)), we have translated the results of Tetrode on the impulse-energy tensor into the spinor language. Starting from the second order Dirac equations, one can derive

$$f^i = \partial T^{i\alpha}/\partial x^\alpha$$

when f^i is the four-force, and T^{ik} a tensor quadratic in the ψ and their derivatives. T^{ik} can now be split up in the symmetric S^{ik} and antisymmetric part A^{ik}, and for the latter one can prove:

$$A_{lm}{}^* = (\partial k_m/\partial x^l) - (\partial k_l/\partial x^m)$$

when $A_{lm}{}^*$ is the dual of A^{ik} and k_m the four vector, with components quadratic in ψ introduced by us (l.c. p. 1396). Thus we may write:

$$f^i = \partial S^{i\alpha}/\partial x^\alpha$$

when now S^{ik} is a symmetric tensor, but with the diagonal sum not zero. The application of the spinor analysis has the advantage, besides giving the equations in an automatically covariant form, that it is very easy to decompose any tensor T^{ik} into its irreducible parts.

47. A note on the uncertainty principle. E. L. HILL, *University of Minnesota.*—Frenkel has suggested that one can interpret the uncertainty principle for one electron by saying that the magnitude of the momentum has a definite (i.e. the *classical*) value, but there is an ambiguity in the direction of motion. It has been found possible to rewrite the wave equation for motion in one-dimension in such a way as to show that this interpretation seems in agreement with the wave mechanics (when $E \geq V$). The method lies in resolving the wave function into beams, one moving to the right and one to the left, each having the classical velocity. The electron

then moves with the classical velocity but it has a chance of being reflected at every point, thereby changing its direction of motion. The average drift of electrons is measured by the current which is the (vector) sum of the currents for the two beams, written in the classical form current = density × velocity. Application of the momentum operator yields the classical value for the magnitude of the momentum, the sign being opposite for the two beams.

48. Electricity as a natural element of Riemannian geometry. CORNELIUS LANCZOS. (*Introduced by K. Lark-Horovitz, Purdue University.*)—The gravitational equations $R_{ik}=0$, excluding singularities, give only a Euclidian geometry. For a more generalized geometry, according to the differential character of Riemann's geometry we have to expect field equations for the fundamental quantity R_{ik}. We can prove generally that if these field equations can be deduced from a Hamiltonian principle the integration of the field equations leads to the appearance of a free vectorial function ϕ_i. The mathematical reason for this fact is that the curvature tensor R_{ik} has to obey the conservation law div $(R_{ik}-\frac{1}{2}Rg_{ik})=0$, besides the field equations. This additional condition gives a determination for the free vectorial function ϕ_i. If we select the Hamiltonian function by the natural idea of "guage-invariance," this vectorial function ϕ_i seems to correspond in all its properties to the electromagnetic vector potential. The conservation law is strictly fulfilled, the potential equation in a first approximation, and for the action of the field on a material particle we obtain in first approximation the Lorentz ponderomotive force. The antisymmetric tensor of the electromagnetic field-strengths appearing in this force law has otherwise no fundamental significance.

49. β disintegration. ARTHUR BRAMLEY, *Bartol Research Foundation.*—The electrons in the nucleus are supposed to be either firmly bound to an α-particle or free to move about the α-particles similar to the bound and free electrons in a metal. The free electrons are prevented from leaving the nucleus by a potential barrier of height C and width d at distance a from the center of the nucleus. The energy of the electron E is supposed to be small compared with C. In β-particle disintegration, an excited α-particle gives its energy ϵ to the electrons by internal absorption. The electrons are distributed in the nucleus according to the Bose-Einstein law, that the number of particles with energy E, $N(E)$ is

$$N(E)dE \backsim \frac{E^2dE}{e^{E/A\epsilon}-1}.$$

The probability $P(E)$ of an electron of energy E leaving the nucleus is (Fowler and Wilson, Proc. Roy. Soc. **A124**),

$$P(E) \backsim \frac{E^{3/2}}{C^2}e^{-2K(C^{(a+d)^2})^{1/2}}$$

so that the distribution of β-particles after leaving the nucleus is

$$L(E)dE \backsim \frac{E^{7/2}\cdot dE}{e^{E/A\epsilon}-1}.$$

The probability of a β-particle emission is

$$\int_0^\infty L(E)dE \backsim (A\epsilon)^{4.5}.$$

Thus the reciprocal of the mean life should vary as the 4.5 power of the energy of the excited α-particle.

The assumption has been made in the derivation that the rest energy $m_0c^2 < E$. It makes no appreciable difference with the available data whether the Bose-Einstein or Fermi-Dirac statistics is used.

50. On the physical nature of ponderomotive forces between living cells.—N. RASHEVSKY, *Westinghouse Elect. & Mfg. Co., East Pittsburgh.*—It has been observed, that isolated living cells sometimes exert on each other forces of attraction or repulsion. It was also suggested that these forces are due to the action of certain substances whose concentration is non-uniform around the cell. According to Rhumbler, if a substance lowers the surface tension of the cell,

the cell tends to move in the direction of lower concentrations of the substance. In the present paper the problem is treated mathematically, from a more general point of view. An expression is derived for such forces, as would result on a small liquid drop, placed in a field of non-uniform concentration of a substance, which in general is assumed to be also soluble in the drop. This expression is composed of two terms, of which one represents the force, due to the influence of the dissolved substance on the surface tension of the drop. But the other term, which may even exceed the first, is independent on any surface phenomena, and represents a volume effect, due to the circumstance, that whenever the drop is brought from a region with one concentration into that with another, the concentration of the substance inside the drop changes also, and this is accompanied by a change in the free energy of the system. Some consequences of the formulae are discussed.

51. Rotational analysis of the red K_2 bands. F. W. Loomis, *University of Illinois.*—The plates taken by Loomis and Wood to determine whether or not the nuclear spin of K_2^{39} is zero have been measured and the (1,0) (1,1) (0,1) and (0,2) bands of the red K_2 system have been analyzed. As expected, the system is found to belong to a $^1\Pi \leftarrow {}^1\Sigma$ transition. The most important rotational constants are as follows:

$$B_0'' = 0.05611 \qquad r_e'' = 3.91 \times 10^{-8} \qquad \alpha'' = 0.000219$$
$$B_0' = 0.04812 \qquad r_e' = 4.22 \times 10^{-8} \qquad \alpha' = 0.000235.$$

The relationships between the molecular constants show that all rotational levels, with both even and odd J, are present. Lines with odd J'' are stronger than neighboring lines with J'' even. Hence the conclusion of Loomis and Wood, that the nuclear spin of potassium is definitely not zero, is confirmed and it is concluded that the K^{39} nucleus obeys the Fermi-Dirac statistics.

52. Oscillations in corona discharges. J. T. Tykociner and W. A. Laning, Jr., *University of Illinois.*—In continuation of the investigation reported at the Washington meeting May 1, 1931 (Abs. 49, Phys. Rev. **37**, 1689 (1931)) an oscillographic study was made of oscillations in corona discharges produced by constant potentials within the range of 600–1500 volts, 5–150μa and 2–30 mm Hg pressure. The discharge appeared mostly in form of beads on a wire at negative potential within a cylindrical anode. When the potential was gradually increased regions of regular oscillations (sine waves) followed in succession the regions of irregular oscillations (complex wave forms). The latter occurred during a state of transition of the discharge from a single bead to a double or multiple number of beads. By evaluating the oscillograms the following correlations were found for the frequency, superimposed corona current, pressure and amplitude in the region of regular oscillations. At constant pressure the frequency (3000–15000) is proportional to the d.c. corona current. The amplitude is a linear function of frequency, a linear function of superimposed corona current and a complex function of the pressure. At constant superimposed corona current the frequency increases with pressure. The rate of change $\Delta f/\Delta p$ increases linearly with pressure. At pressures below 2 mm Hg oscillations set in when the wire is at positive potential. Details of the investigation will be published in a bulletin of the Eng. Exp. Station, University of Illinois.

53. The method of least squares. Herbert J. Brennen, *Northwestern University.*—The ordinary method of least squares of finding the values of n of the $n+1$ coefficients (the $n+1$th coefficient being put equal to unity), of a linear equation in n variables, $x_1, x_2, \cdots, x_n$,

$$a_0 + a_1x_1 + a_2x_2 + \cdots + a_nx_n = 0 \qquad (1)$$

suffers from the fact that, in general, $n+1$ different solutions of the problem are obtained depending on which one of the $n+1$ coefficients is put equal to unity. Furthermore, the value of the sum of the squares of the so-called residuals is changed if the original equation is multiplied by a constant although the graph is unaltered; for this reason it is difficult to compare the different solutions obtained. If, however, we put:

$$F \equiv \Sigma E_i^2 - \lambda^2(a_1^2 + a_2^2 + \cdots + a_n^2) = 0 \qquad (2)$$

where ΣE_i^2 is the sum of the squares of the residuals and λ^2 is an undetermined multiplier; and carry out the minimization with respect to all the coefficients before assigning the value of unity to any one. This procedure gives us $n+1$ linear homogeneous equations in the $n+1$ unknown coefficients; the vanishing of the determinant of these equations permits the calculation

of the value of λ^2, the smallest (positive) value being chosen. Now we may equate to unity any coefficient we choose and solve any n of these equations for the other n coefficients. Furthermore, the value of λ^2 is unaltered when the original equation is multiplied by a constant.

54. Oriented molecules at the solid-liquid interface and the non-specific nature of ordinary adsorption. WILLIAM D. HARKINS, *George Herbert Jones Laboratory, University of Chicago.*—If a powder, whose grains have clean surfaces, is immersed in a liquid heat is evolved, about 1 calorie per gram for many fine powders. With titanic oxide the relative values with different liquids are (data of Harkins and Dahlstrom) water 1.00 (absolute value 1.15 calories per gram), butyric acid 0.77, ethyl acetate 0.70, butyl alcohol 0.67, acetone 0.58, carbon tetrachloride 0.47, and benzene 0.34. With other powders of the nature of stannic oxide, zinc oxide, silicon dioxide, and barium sulphate, the relative values are approximately the same, except in individual cases (as zinc oxide and an acid) in which it is known that a chemical reaction occurs. Thus the effect may be considered as due in general to non-specific or non-chemical forces. If an organic acid (or water) is added to benzene the heat of immersion of the powder rises rapidly until the heat evolved becomes almost as high as with the pure acid (or water) just as the monomolecular adsorbed film becomes tightly packed (Harkins and Gans). Thus when the amount of water present in the benzene is 0.03 percent the heat of immersion is increased by three times by this small quantity of water. Such monomolecular films produce very remarkable effects in connection with the settling of powders in liquids, often reducing the volume to one-fifth of that occupied by the suspension when the monomolecular film is not present. The great effect of polar groups in increasing the energy of immersion shows that the molecules at the interface are oriented with their polar groups toward the solid and the nonpolar groups toward the liquid.

55. Comparison of cosmic rays in the Alps and the Rockies. A. H. COMPTON, *University of Chicago.*—With a pressure ionization chamber built by R. D. Bennett and used by J. C. Stearns and the writer for cosmic-ray measurements on Mount Evans in Colorado, similar measurements have now been made at the high altitude research laboritory at Jungfraujoch, elevation 11,380 feet. The ionization due to the cosmic rays is found to be the same, within a probable experimental error of 2 or 3 percent, as that at the same altitude on Mt. Evans. At both locations the cosmic radiation was compared with the gamma-rays from a milligram of radium as a standard, and the effect of local radiation was determined by measuring the ionzation when the chamber was shielded successively by 2.5 cm of copper, an additional 2.5 cm of lead, and 5 cm of lead. The zero point of the chamber was determined at both locations by measurements in tunnels. The absolute value of the ionization is in close agreement with that reported by Millikan for similar altitudes.

56. Fine structure of the visible bromine bands. WELDON G. BROWN *National Research Fellow, University of Chicago.* (*Introduced by R. S. Mulliken*).—A group of bands (from $v'=7$ to $v'=13$, $v''=2$, 3 and 4) in the main absorption band system of bromine ($Br_2^{79,81}$) have been analyzed and found to consist of P and R branches only. Branches of the less abundant molecules, Br_2^{79} and Br_2^{81}, showing alternating intensities, have been recognized in several cases, thus permitting an accurate calculation of vibrational isotope shifts. This has confirmed the quantum numbering previously deduced by the writer from measurements of band heads. Values of the constants of the $Br_2^{79,81}$ molecule are as follows:

$B_e''=0.08091$	$B_e'=0.05956$
$\alpha''=0.00028$	$\alpha'=0.00063$
$I_e''=341.9\times10^{-40}$	$I_e'=464\times10^{-40}$
$r_e''=2.28\text{A}$	$r_e'=2.65\text{A}.$

57. The lens effect of pressure windows. THOMAS C. POULTER AND CARL BENZ, *Iowa Wesleyan College.*—The lens effect of high pressure optical systems involving glass or quartz windows has been studied and found to be due to four primary causes: 1st, pseudo lens effects due to temperature gradients following changes of pressure; 2nd, bulging of the outer surface of the pressure window; 3rd, pseudo lens effect due to unequal distribution of strain in the window; 4th, the difference in index of refraction of the material in the cylinder and that of the window combined with the bulging of the inside surface of the window. These effects are measured and methods for their correction outlined.

AUTHOR INDEX TO ABSTRACTS OF CHICAGO MEETING

Abel, A. E.—see Tykociner
Almy, G. M. and C. D. Hause—No. 13

Barrett, Charles S. and C. E. Howe—No. 9
Bartlett, J. H., Jr.—see Furry
Barton, H. A.—see Richtmyer
Beck, Carl A.—No. 39
Bennett, Willard H.—No. 28
Benz, Carl—see Poulter
Bitter, Francis—No. 38
Bowers, Harold E.—see Harkins
Bramley, Arthur—No. 49
Brennen, Herbert J.—Nos. 42, 53
Brown, Weldon G.—No. 56

Clark, H. T. and W. Kohlhagen—No. 35
Cohn, Willi M.—No. 26
Compton, A. H.—No. 55
Cork, J. M.—No. 7
Croup, A. H.—No. 12

Eldridge, J. A.—No. 6
Ellett, A. and L. Larrick—No. 25

Failla, G.—No. 4
Fredrickson, W. R. and William W. Watson—No. 15
——— see Watson
Fuller, H. Q.—see Loomis
Furry, W. H. and J. H. Bartlett, Jr.—No. 43

Gans, David M., William D. Harkins and D. A. Wallace—No. 36
Green, J. B. and John Wulff—No. 22
——— see Wulff

Harkins, William D. and Harold E. Bowers—No. 27
——— No. 54
——— see Gans
Harris, Roscoe E.—No. 29
Harvey, G. G.—see Jauncey
Hause, C. D.—see Almy
Heydenburg, N. P.—see Larrick
Hidnert, Peter—No. 41
Hill, E. L.—No. 47
Holbrook, B. D.—No. 8
Hopfield, J. J.—No. 40
Howe, C. E.—see Barrett

Jauncey, G. E. M. and G. G. Harvey—No. 10
Jones, M. T.—see Richtmyer

Kaplan, Joseph—No. 18
Knipp, Charles T.—No. 21
Kohlhagen, W.—see Clark
Kunz, J.—No. 32

Ladenburg, R., S. Levy and G. Wolfsohn—No. 17
Lanczos, Cornelius—No. 48
Langer, R. M.—No. 44
Laning, W. A., Jr.—see Tyckociner
Laporte, O. and G. E. Uhlenbeck—No. 46
Larrick, L. and N. P. Heydenburg—No. 24
——— see Ellett
Levy, S.—see Ladenburg
Loomis, F. W. and H. Q. Fuller—No. 20
——— No. 51
——— see Nusbaum

Melvin, Eugene H.—see Wulf

Noll, Waldemar—No. 1
Nottingham, W. B.—No. 31
Nusbaum, R. E. and F. W. Loomis—No. 16

Poulter, Thomas C. and Carl Benz—No. 57

Rashevsky, N.—No. 50
Richtmyer, F. K., H. A. Barton, and M. T. Jones—No. 3
Spencer, R. G.—No. 11
Stedman, C. K.—No. 34
Stewart, G. W.—No. 2
Tykociner, J. T. and A. E. Abel—No. 33
——— **and W. A. Laning Jr.**—No. 52

Uehling, E. A.—No. 45
Uhlenbeck, G. E.—see Laporte

Wahlin, H. B.—No. 30
Wallace, D. A.—see Gans
Watson, William W. and W. R. Fredrickson—No. 14
——— see Fredrickson
Whitmer, Charles—No. 5
Wolfsohn, G.—see Ladenburg
Wulf, Oliver R. and Eugene H. Melvin—No. 19
Wulff, John and J. B. Green—No. 23
——— see Green

Zachariasen, W. H.—No. 37

CURRENT LITERATURE OF PHYSICS

Extracts from the Tables of Contents of Some of our Contemporaries

MOST of us find it difficult to keep abreast of current literature in physics as thoroughly as we would like. Many of us would be encouraged to do so if we knew precisely what papers were appearing in the important journals of research.

As a new service to its readers the Physical Review will publish in each issue the titles of papers on physics which are appearing in some of our more important contemporaries. We hope to make this service a very prompt one. Many of the journals are now sending us advance proof sheets of their Tables of Contents so that they should appear in the Physical Review almost as soon as the journal itself.

PROCEEDINGS OF THE ROYAL SOCIETY

SERIES A, VOL. 134, NO. A823 — NOVEMBER 3, 1931

Combination of Hydrogen and Oxygen on the Surface of Silica and its Relation to the Propagation of Reaction Chains in the Gas. By **W. L. Garstang and C. N. Hinshelwood.** 1

Atomic Weight of Xenon. By **R. Whytlaw-Gray, H. S. Patterson and W. Cawood** 7

Diffusion of Colloidal Electrolytes and other Charged Colloids. By **G. S. Hartley and C. Robinson** 20

Arc Spectrum of Gold. By **J. C. McLennan and A. B. McLay** 35

Spark Spectrum of Mercury, Hg II. By **J. C. McLennan, A. B. McLay and M. F. Crawford.** 41

Steady Broadside Motion of an Anchor Ring in an Infinite Viscous Liquid. By **F. E. Relton** 47

Thermal Conductivities of Certain Approximately Pure Metals and Alloys at High Temperatures. By **L. C. Bailey** 57

Thermal Conductivities of the Saturated Hydrocarbons in the Gaseous State. By **W. B. Mann and B. G. Dickins** 77

Sorption Process in the Zeolite Chabazite. By **M. G. Evans** 97

Interaction Energy of Two α-Particles at Close Distances, Determined from the Anomalous Scattering in Helium. By **H. M. Taylor** 103

Mobility of Positive Ions in Helium. Part I.—Helium Ions. By **A. M. Tyndall and C. F. Powell** 125

Quantum Mechanics of Electrolysis. By **R. W. Gurney** 137

Scattering of α-Particles by Light Elements. By **W. Riezler** 154

Formation of Vortices from a Surface of Discontinuity. By **L. Rosenhead** 170

On Dirichlet's Divisor Problem. By **J. R. Wilton** 192

Electron Scattering in Helium. By **S. Werner** 202

Kinetics of the Decomposition, in Carbon Tetrachloride Solution, of Ozone and of Ozone-Chlorine Mixtures. By **E. J. Bowen, E. A. Moelwyn-Hughes and C. N. Hinshelwood** 211

Experimental Study of the Rate of Dissociation of Salt Hydrates. The Reaction $CuSO_4 \cdot 5H_2O = CuSO_4 \cdot H_2O + 4H_2O$. By **M. L. Smith and B. Topley** 224

Studies of Gas-Solid Equilibria. Part III.—Pressure-Concentration Equilibria between Silica Gel and (a) Water, (b) Ethyl Alcohol, Directly Determined under Isothermal Conditions. by **B. Lambert and A. G. Foster** 246

Normal Vibrations of Carbonate and Nitrate Ions. By **A. C. Menzies** 265

Theory of Electronic Semi-Conductors.—II. By **A. H. Wilson** 277

Measurement of the Viscosity of Gases at High Pressures.—The Viscosity of Nitrogen to 1000 Atms. By **A. Michels and R. O. Gibson** 288

Theory of Metallic Corrosion in the Light of Quantitative Measurements. Part V.—The Corrosion of Iron and Mild Steel. By **G. D. Bengough, A. R. Lee and F. Wormwell** 308
Effect of Frequency on the Condensed Discharge Ignition of Carbonic Oxide-Air Detonating Gas. By **G. I. Finch and H. H. Thompson** 343
Elastic Collisions. By **J. S. Townsend** 352

PHILOSOPHICAL MAGAZINE

SEVENTH SERIES, VOL. 12, NO. 80 — NOVEMBER, 1931

Solutions of the Boundary-layer Equations. By **V. M. Falkner and Miss S. W. Skan** 865
On an Estimation of the Height of the Heaviside Layer in Bengal. By **Hrishikesh Rakshit** 897
Adsorption at the Surface of a Solution. By **W. F. Kenrick Wynne-Jones** 907
Significance of the Compton Effect in Absolute Gamma-Ray Absorption Measurements. By **L. H. Clark** 913
Relation between Uranium and Radium.—Part IX. Period of Ionium. By **Frederick Soddy** 939
On the Refractivities and Optical Dispersions of Methane and of its Substituted Chlorine Derivatives. By **G. W. Brindley and H. Lowery** 945
Surface-Tension of Different Dilutions of Boys' Soap Solution. By **L. D. Mahajan** 954
Classical and Modern Gravitational Theories. By **Alexander Marcus** 959
Precise Experimental Determination of Energy of Excitation by Electron Impact in Helium. By **J. E. Roberts and R. Whiddington** 962
X-Ray Investigation of some Copper-Aluminium Alloys. By **G. D. Preston** 980
Steady Motion of Two Doublets. By **M. A. Higab** 993
Note on a Problem in the Conduction of Heat. By **C. E. Wright** 1015
Temperature Coefficient of the Dielectric Constant of Water. By **R. T. Lattey, O. Gatty, and W. G. Davies** 1019
On Curve-Fitting by Means of Least Squares. By **W. R. Cook** 1025
Balance Method of Measuring Sound Transmission. By **A. E. Knowler** 1039
Flame Temperatures. By **W. T. David, W. Davies, and J. Jordan** 1043
On the Analogy between the Electromagnetic Field and a Fluid containing a Large Number of Vortex Filaments. By **J. J. Thomson** 1057
Note on the Physical Significance of Second Order Terms in the Perturbation Theory. By **H. Jones** 1063

NATURE

VOL. 128, NO. 3240 — DECEMBER 5, 1931

Recent Developments in Optical Glass Manufacture. By **W. M. Hampton and W. N. Wheat** 926
Letters to the Editor:
Determination of the Yard in Terms of the Wave-length of Light. By **J. E. Sears, Jr.; Dr. A. E. H. Tutton** 965
Electron Exchange Phenomena in the Excited Atom. By **R. Whiddington and J. E. Roberts** 966
Atomic Weight of Fluorine. By **E. Moles** 966
Carbon Contacts. By **C. Turnbull and C. V. Boys** 968
Electrical Conditions in Stratified Clouds. By **Dr. Michael Grabham** 969
The Band Spectrum of AsH. By **George E. Kimball and John R. Bates** 969
Branching of Lightning. By **Major J. L. P. Macnair** 969

ZEITSCHRIFT FÜR PHYSIK

VOL. 73, NOS. 1 AND 2 — NOVEMBER 24, 1931

On the Question of Chemical Binding. By **F. Hund** 1
H_1 Discharge Tube. By **E. Lau and O. Reichenheim** 31
Method for the Determination of the Mobility of Inert Gas Ions with the Help of Negative Striae. By **M. J. Druyvesteyn** 33

Effect of Roentgen and Gamma-Rays on the Conductivity of Paraffin. By **F. Seidl** 45
On the Theory of Ferromagnetism. By **Tokutaro and Tadayosi Hikosaka** 62
Band Spectrum of Mercury Hydrite. By **R. Rydberg** 74
Resolution of the $K\beta_1$ and β_3 Lines of the Heavy Metals. By **H. Seemann** 87
Concept of the State of a System in Quantum Mechanics. By **Arthur March** 107
Theory of the Breakdown of Dielectrics. By **L. Rosenkewitsch and C. Sinelnikow** 118
On Relativistic Quantum Mechanics. By **G. Wataghin** 121
Specific Ionization of Cosmic Rays. By **W. Kolhörster and L. Tuwim** 130
Remarks on the Communication of Mr. Gr. Landsberg and L. Mandelstam "On the Selective Scattering of Light." By **W. Kapuscinski** 137

ZEITSCHRIFT FÜR PHYSIK

VOL. 73, NOS. 3 AND 4 DECEMBER 2, 1931

New Atmosphere Oxygen Band at λ7710. By **R. Mecke and W. Baumann** 139
Electromagnetism as a Natural Property of Riemannian Geometry. By **Cornell Lanczos** 147
Behavior of an Atom in a Rotating Magnetic Field. by **P. Güttinger** 169
Setting in of Direction Quantization. By **T. E. Phipps and O. Stern** 185
Displacement to the Red of the Photoionization of Alkali Atoms Adsorbed on Negative Salt Surfaces. By **J. H. de Boer and M. C. Teves** 192
Observations Concerning a Relation Between the Barkhausen and the Wiedemann Effects. By **Walter Brandt** 201
Continuous Spectra and "Forbidden" Series in the Sodium Arc Spectrum. By **Hans Bartels** 203
Refraction and Dispersion of Light in Gaseous Hydrocarbons. By **Sten Friberg** 216
Resonance Phenomena Connected with Frequency Dividing. By **L. Mandelstam and N. Papalexi** 223
Hansen's Stufenblendenkondensor. By **P. H. van Cittert** 249
Remarks on the Correspondence Principle Method of treating the Relativistic Problem of Several Bodies. By **L. Rosenfeld** 253
Magnetic Behavior of the Cobalt Atom. By **Hans Vatter** 260
Transmission Bands of Silver. By **S. Schubin** 273

DIE NATURWISSENSCHAFTEN

VOL. 19, NO. 49 DECEMBER 4, 1931

Heating by Electrical Induction without Iron Core. By **Wilhelm Fischer** 974
Short Original Contributions
On the Processes of Electrofiltering. By **R. Ladenburg** 987
Brief Reviews
Diffraction of Proton Waves. **R. Frisch** 991

DIE NATURWISSENSCHAFTEN

VOL. 19, NO. 50 DECEMBER 11, 1931

Emil Warburg, in Memoriam. By **James Franck** 993
Remarks on the History of the Development of Research on Electron Diffraction. By **H. Seemann** 1002
Nuclear Moment of Caesium. By **Wilhelm Schütz** 1007
The γ-Spectrum of Th C″ and the Gamow Theory of the α Fine Structure. By **Lise Meitner and Kurt Philipp** 1007

PHYSIKALISCHE ZEITSCHRIFT

VOL. 32, NO. 22 NOVEMBER 15, 1931

Wave Mechanical Discussion of Conduction and Photoelectric Effects. By **F. Bloch** 881
Electronic Conductivity of Solid Oxides of Various Valence Sequences. By **M. Le Blanc and H. Sachse** 887
New Results Concerning Sperrschicht Photo Cells. by **E. Perruca** 890
Structure Analysis of Photoelectric Surfaces by Means of Electron Interference. By **W. Kluge and E. Rupp** 890

Measurements of the Conductivity of Powders. By **P. Guillery** 891
On the Theory of Heat Conductivity and of Diffusion. By **K. Uller** 892
Collision Cross Section of Argon Atoms with Respect to A^+ Ions. By **F. Wolf** 897
New Measurements on the Aerodynamics of a Cylinder. By **W. Linke** 900
Scattering of X-Rays by Water. By **E. Amaldi** 914
Variation with Frequency of the Conductivity of Aqueous and Non-Aqueous Electrolytes. By **H. Goertner** 919

ANNALEN DER PHYSIK

VOL. 11, NO. 8 DECEMBER, 1931

Influence of Magnetization on the Modulus of Elasticity for Stretch-Vibrations of Ferromagnetic Rods. By **E. Giebe and E. Blechschmidt** 905
Hysteresis Phenomena in Magnetostriction. by **A. Schulze** 937
Sensitive Method for Measuring Small Ellipticities of Polarized Light. By **G. Szivessy and A. Dierkesmann** 949
History of the Discovery of the Critical State. By **Walter Konig** 985
Measurement of Ponderomotive Radiation Forces on Resonators in an Electromagnetic Field. by **Karl Fritz** 987

COMPTES RENDUS

VOL. 193, NO. 21 NOVEMBER 23, 1931

On the Uniqueness of the Solution of Problems of Friction. By **R. Mazet** 986
Lines of Slippage on a Cylinder. By **C. Woronetz** 989
Periodic Waves on the Surface of Water. By **J. Baurand** 992
Mechanism of the Photolysis of Alkyl Iodides By **G. Emschwiller** 1003
Calorimetric Study of the Absorption of γ-rays of Radium. By **D. K. Yovanovitch and P. Savitch** 1006

PHYSICA

VOL. 11, NO. 9 NOVEMBER, 1931

Effect of Light on the Photographic Plate. By **A. P. H. Trivelli** 289
Field in Ion Concentrations Near the Cathode of an Arc Discharge. By **W. de Groot** 307
Reality in Formation of Concepts. By **H. A. Kramers** 321

PROCEEDINGS OF THE NATIONAL ACADEMY OF SCIENCES

VOL. 17, NO. 11 NOVEMBER, 1931

Heating of Liquids by the Absorption of Sound, and its Relation to the Energy of Intense High Frequency Sound Waves. By **William T. Richards** 611
Crystal Lattice of Calcium Metaborate, $Ca\,B_2O_4$. By **W. H. Zachariasen** 617
Search for an Electrostatic Analog to the Gravitational Red Shift. By **Roy J. Kennedy and Edward M. Thorndike** 620

BUREAU OF STANDARDS JOURNAL OF RESEARCH

VOL. 8, NO. 1 JANUARY, 1932

International Comparison of X-Ray Standards. By **Lauriston S. Taylor** Research Paper No. 397
Method for Determining the Volume Changes Occurring in Metals during Casting. By **C. M. Saeger, Jr. and Eugene J. Ash** 399
Registration of Cathode Rays by Thin Films of Metals and Metal Compounds. By **Warren W. Nicholas and C. G. Malmberg** 400
Ultrasonic Measurements of the Compressibility of Solutions and of Solid Particles in Suspension. By **Chester R. Randell** 402
On Elimination of Liquid Potentials with Potassium Chloride and Ammonium Chloride. By **G. M. Kline, M. R. Meacham, and S. F. Acree** 403
Electrostatic Voltmeter. By **Warren W. Nicholas** 404
Heats of Combustion of Methyl and Ethyl Alcohols. By **Frederick D. Rossini** 405
Clock-Controlled Constant-Frequency Generator. By **A. B. Lewis** 406

JOURNAL OF THE FRANKLIN INSTITUTE

VOL. 212, NO. 6 — DECEMBER, 1931

Cathode-Ray Oscillograph. By **J. B. Johnson** 687
Report on the Work of the Bartol Research Foundation, 1930–31. By **W. F. G. Swann** ... 719
Paints for Reflecting Biologically-Important Ultraviolet Radiation. By **M. Luckeish and L. L. Holladay** 787

JOURNAL OF THE ACOUSTICAL SOCIETY OF AMERICA

VOL. III, NO. 2, PART I — OCTOBER, 1931

Reverberation Time Measurements in Coupled Rooms. By **Carl F. Eyring** 181
Planetary Reduction Gear System for Recording Turntables. By **A. V. Bedford** 207
Plane Sound Waves of Finite Amplitude. By **Leslie N. Leet** 242
Theory of Supersonic Interferometers. by **W. D. Hershberger** 263
Acoustic Insulation and the Cancellation Effect at the Basilar Membrane. By **A. G. Pohlman** 269
Differential Pitch Sensitivity of the Ear. By **E. G. Shower and R. Biddulph** 275
Regulating the Acoustics of Large Rooms. By **Ernst Petzold** 288
Minimizing Discrepancies of Intonation in Valve Instruments. By **John Redfield** 292
Further Studies of the Strike Note of Bells. By **Arthur Taber Jones and George W. Alderman** 297

THE JOURNAL OF THE ACOUSTICAL SOCIETY OF AMERICA

VOL. III, NO. 2, PART II — OCTOBER, 1931

Some Physical Characteristics of Speech and Music. By **Harvey Fletcher** 1

JOURNAL OF RHEOLOGY

VOL. II, NO. 4 — OCTOBER, 1931

Slippage in a Non-Newtonian Livuid. By **Markus Reiner** 337
Quasi-Laminar Capillary Flow. By **R. L. Peek, Jr., and W. R. Erickson** 351
Some Physical Concepts in Theories of Plastic Flow. By **R. L. Peek, Jr., and D. A. McLean** 370
Flow of Colloids Which Show Anomalous Viscosity. By **H. Kroepelin** 385
Notes on the Ring and Ball Method. By **Fred C. Eaton** 392
Flow of Dry Sand through Capillary Tubes. By **Eugene C. Bingham and Robert W. Wikoff** 395
International Comparison of Viscometers. By **S. Erk** (errata) 401
Notes on the Fluidity of Water in the Vicinity of 20 degrees. Report by the Committee on Viscosity Standards. By **Eugene C. Bingham,** Chairman 403

JOURNAL OF THE OPTICAL SOCIETY OF AMERICA

VOL. 21, NO. 12 — DECEMBER, 1931

Photographic Plates for Use in Spectroscopy and Astronomy. By **C. E. Kenneth Mees** ... 753
Measurement of Reflection-Factors in the Ultraviolet. By **A. H. Taylor** 776
Laminary Reflection Gratings for Infrared Investigation. By **C. Hawley Cartwright** 785
On the Spectra of Gases Appearing in the Early Stages of the Spark. By **E. Matuyama** ... 792

THE REVIEW OF SCIENTIFIC INSTRUMENTS

VOL. 2, NO. 12—New Series — DECEMBER, 1931

New High Vacuum System. By **J. A. Becker and E. K. Jaycox** 773
Acid Standard Cells of the Unsaturated Type. By **Yuichi Ishibashi and Tadashi Ishizaki.** 785
Optimum Outputs of Photo-Sensitive Devices. By **Earl D. Wilson** 797
Cylindrical Rotating Sector Photometer. By **F. Lowell Dunn** 807
Method for Measuring Very High Values of Resistance. by **G. M. Rose, Jr.** 810
Photoelectric Method for Testing Camera Shutters. By **Herbert J. Reich and Gordon S. Marvin** 814
Mounting of Thin Metallic Membranes Under Tension. By **C. K. Stedman** 818
200,000 Volt X-Ray Tube. By **William W. Hansen** 820

PHYSICS

VOL. 1, NO. 6 DECEMBER, 1931

Some Experiments with Gas-Filled Cs-O-Ag Photo Cells. By **K. H. Kingdon and H. E. Thomsen** 343

Use of Glycol-Phthalic Anhydride Resin as a High-Vacuum Cement. By **T. P. Sagur and R. G. Kennedy, Jr.** 352

Time Lag of the Electric Spark. By **John A. Tiedeman** 354

New Method of Dielectric Constant Measurement at Radio Frequencies. By **H. L. Andrews** 366

Charts for Transmission Line Problems. By **H. E. Hartig** 380

Magnetic Sharpener. By **L. W. McKeehan** 388

Thixotropy of Litharge and Glycerine. By **E. Karrer and P. Wasserman** 393

Thermo-Stromuhr Method of Measuring Blood Flow. By **J. F. Herrick and Edward J. Baldes** 407